Universidad de Valladolid

Escuela de Doctorado Universidad de Valladolid

PROGRAMA DE DOCTORADO EN CONSERVACIÓN Y USO SOSTENIBLE DE SISTEMAS FORESTALES

TESIS DOCTORAL:

SILENCIAMIENTO GÉNICO INDUCIDO POR PULVERIZACIÓN: UNA HERRAMIENTA BIOTECNOLÓGICA INNOVADORA PARA MITIGAR ENFERMEDADES FORESTALES CAUSADAS POR HONGOS Y OOMICETOS PATÓGENOS.

Presentada por Irene Teresa Bocos Asenjo para optar al grado de
Doctora por la Universidad de Valladolid

Dirigida por:
Dr. Julio Javier Diez Casero
Dr. Jonatan Niño Sánchez

Universidad de Valladolid

Escuela de Doctorado Universidad de Valladolid

PHD PROGRAM IN CONSERVATION AND SUSTAINABLE USE OF FOREST SYSTEMS

DOCTORAL THESIS:

SPRAY-INDUCED GENE SILENCING: AN INNOVATIVE BIOTECHNOLOGICAL TOOL FOR MITIGATING TREE DISEASES CAUSED BY FUNGAL AND OOMYCETE PATHOGENS

Submitted by Irene Teresa Bocos Asenjo in fulfilment of the requirements for the PhD degree by the Universidad de Valladolid

Dirigida por:
Dr. Julio Javier Diez Casero
Dr. Jonatan Niño Sánchez

Table of contents

Abbreviations

A: Absorbance

aa: amino acids

AGO: Argonaute

Amp_{100}: Ampicillin [100 µg/mL]

AV: Artificial Vesicle

BCA: Biocontrol agent

bp: base pairs

cDNA: complementary DNA

CD: Carbon Dot

CDS: Coding sequence

CHV-1: Cryphonectria hypovirus 1

CLSM: Confocal Laser Scanning Microscopy

Ct: Cycle threshold value

CTAB: Cetyl Trimethyl Ammonium Bromide

Cy3: Cyanine3

CYP51: Cytochrome P450 sterol 14α-demethylase

dsRNA: double-stranded RNA

DCL: Dicer-like

ddH_2O: double-distilled water

DED: Dutch Elm Disease

EDTA: Ethylenediaminetetraacetic acid

EF1α: elongation factor 1 alpha

EPPO: European and Mediterranean Plant Protection Organization

EtOH: Ethanol

FAO: Food and Agricultural Organization

GADPH: glyceraldehyde 3-phosphate dehydrogenase

GFP: Green Fluorescent Protein

HIGS: Host-Induced Gene Silencing

hpRNA: hairpin RNA

IQR: Interquartile range

LB: Luria-Bertani

MNase: Micrococcal Nuclease

mRNA: messenger RNA

NCBI: National Center for Biotechnology Information

nt: nucleotide

OD: Optical Density

OE-PCR: Overlap Extension Polymerase Chain Reaction

PCR: Polymerase Chain Reaction

PDA: Potato Dextrose Agar

PDB: Potato Dextrose Broth

PPC: Pine Pitch Canker

PVP: Polyvinylpyrrolidone

qPCR: quantitative Polymerase Chain Reaction

QDE1: Quelling Defective 1

RE: Restriction Enzymes

RdRp: RNA-dependent RNA polymerase

RMSD: Root Mean Square Deviation

RNAi: RNA interference

RPB2: RNA polymerase II subunit B

RQ: Relative quantification

rRNA: Ribosomal RNA

RT-PCR: Reverse Transcription-Polymerase Chain Reaction

SD: Standard Deviation

SE: Standard Error

SIGS: Spray-Induce Gene Silencing

siRNA: small interfering RNA

sRNA: small RNA

T_a: annealing temperature

TAE: Tris-Acetate-EDTA

T_m: melting temperature

UTP: uridine triphosphate

YFP: Yellow Fluorescent Protein

Figures

Tables

Abstract

Forest diseases seriously affect natural ecosystems and plantations, causing significant economic and ecological losses. Within the Mediterranean region, some forestry species are seriously threatened by pathogenic fungi and oomycetes. Chemical control of plant pathogens has been demonstrated to have a notable ecological impact, often resulting in incomplete efficacy in disease management, and may induce the development of resistance among certain pathogens. Furthermore, the utilization of such products is prohibited within forest environments, so although some preventive measures are used, there are currently no effective methods of controlling many forest diseases. Consequently, there is a current emphasis on exploring new sustainable alternatives in plant pathology. One such alternative is spray-induced gene silencing (SIGS), which is a plant protection method based on the ability of eukaryotic organisms to uptake small RNAs from the environment that induce silencing of genes through RNA interference (RNAi). This strategy offers an environmentally friendly and sustainable option for disease control compared to chemical methods. Our research focuses on investigating the potential of SIGS in treating forest diseases, particularly those caused by *Fusarium circinatum* and *Phytophthora cinnamomi*. Double stranded RNAs (dsRNAs) have been designed to target essential genes involved in critical pathways of these pathogens, such as vesicle trafficking, transduction of the signal, cell wall biogenesis and RNAi machinery. Gene silencing through these dsRNAs provided significant protection against both pathogens across different host plants and experimental conditions. The results show that SIGS effectively reduced the virulence of *F. circinatum* and *P. cinnamomi*, representing a promising step toward its implementation in forest pathology, a field where its potential remains largely unexplored.

Introduction

1. Forest diseases and their impact on ecosystems

1.1. Importance of forests and their role in ecosystems

According to the Food and Agricultural Organization (FAO) in 2020, the total area of forestry across the globe amounts to 4.06 billion hectares, constituting 31% of the planet's total land area (FAO, 2020). Forest ecosystems play a crucial role in preserving ecological stability and supporting human well-being. They serve as reservoirs of biodiversity, harboring a vast variety of plant, animal, fungal, and microbial species that collectively contribute to the complex dynamics of ecosystems (FAO 2024). Additionally, forests act as natural buffers, protecting soil from erosion, filtering water resources, and regulating hydrological cycles (Shvidenko *et al.*, 2005). Moreover, they play a critical role in climate change mitigation by absorbing and storing carbon, thus representing a key tool in the fight against global warming (McKinley *et al.,* 2011). The economic significance of forests cannot be overstated as they provide timber and a wide range of non-timber forest products, including cork, natural resins, mushrooms, medicinal plants, nuts, and berries. These resources support multiple industries, such as construction, paper production, pharmaceuticals, and energy. These ecosystem services have a significant impact on the economy of rural areas, many of which are experiencing depopulation and abandonment, leading to negative consequences for both local economies and ecosystem conservation (Gómez and Ortuño, 2022).

Forests face multiple disturbances from natural and human factors that negatively impact their health and sustainability. The main threats to forests include deforestation, forest fires, severe weather events, and pests and diseases, among others (van Lierop *et al.*, 2015). In Europe, these disturbances led to forest mortality averaging 56 million m^3 per year between 2000 and 2010, with an estimated potential loss of 33 billion tons of woody biomass (Forzieri *et al.,* 2021). Furthermore, the decline and degradation of forests due to these causes poses a serious

threat to biodiversity, reduce carbon storage capacity, and decrease the supply of many forest services, with significant negative impacts on rural communities (Watson *et al.,* 2018).

The occurrence of pests and diseases seriously endangers the health of forests. The spread of pests and diseases in forests has increased due to globalization and climate change. These two drivers of global change are among the most significant stressors impacting forest ecosystems today (Camarero and Gazol, 2022). They are likely to increase opportunities for the spread, establishment and impact of new pests and pathogens (Pautasso *et al.*, 2015; Sturrock *et al.*, 2011). Trees are susceptible to a wide range of pests and diseases, with the most significant causal agents including viruses, bacteria, fungi, oomycetes, and insect herbivores. While some forest diseases are caused by native organisms, many of the most severe threats arise from introduced species that infect trees outside their natural range (Boyd *et al.*, 2013). The effects of globalization, particularly the increasing international trade of plants, seeds, wood, and soil substrates, have facilitated the spread of these pathogens across borders, posing a growing risk to forest health (Ghelardini *et al.*, 2022). Climate change exacerbates this threat, by affecting both pathogen behavior and host tree vulnerability, as both are closely shaped by environmental conditions. Shifts in temperature, humidity, and precipitation patterns can weaken host defenses, making stressed trees more susceptible to infections. These changing abiotic factors not only enhance pathogen establishment but also alter the geographic distribution of forest diseases, leading to the emergence of new threats in previously unaffected areas (Sturrock *et al.*, 2011). Ultimately, climate change influences the dynamics between pathogens, hosts, and the environment, amplifying disease severity. Rising temperatures, prolonged droughts, and extreme weather events can trigger widespread tree mortality and extensive outbreaks of pests and pathogens, leading to devastating ecological and economic consequences (Guégan *et al.*, 2023).

1.2. Main diseases in forests

Over the past five decades, forests have experienced several large-scale pathogen outbreaks, leading to significant mortality among specific tree species. These outbreaks have been predominantly driven by pathogenic fungi and oomycetes; however, bacterial pathogens have also caused severe and economically significant forest diseases. One notable example is *Xylella fastidiosa*, a xylem-limited bacterium that infects a wide range of economically important plants, including grapevine, olive, almond, plum, peach, and lemon trees (Sicard *et al.*, 2025).

Fungal pathogens are among the most significant threats to forest health, as they infect trees through spores that spread via wind, water, or human activity. They often cause foliar

diseases, cankers, root rots, and vascular wilts. Fungi are responsible for the near extinction of American chestnut (*Castanea dentata*) in North America due to chestnut blight. The causal agent, *Cryphonectria parasitica,* was introduced in the late 19th century from Asia, causing American chestnut population frequency to decline from 36% in 1934 to just 0.5% in 1993 (Loo, 2009). As a result, the species was largely replaced by oak, maple, and hemlock in affected forests (Elliott and Swank, 2008). The first report of this invasive pathogen in Europe was in 1938, it has caused widespread decline of European chestnut (*Castanea sativa*) (Biraghi, 1946). Two fungal pathogens (*Ophiostoma ulmi* and *Ophiostoma novo-ulmi*) were responsible for two major pandemics of Dutch elm disease (DED). *O. ulmi* first emerged in northwestern Europe around 1910, spreading across Europe, central Asia, and North America until the 1940s, since most of the trees had already died. The disease reemerged in the 1950s, this time caused by *O. novo-ulmi*, which led to widespread mortality of *Ulmus* spp. in Europe, North America, and western Asia (Brasier, 1979). By the early twentieth century, *O. novo-ulmi* had killed approximately 30 million mature elm trees (Brasier and Webber, 2019). In conifers, *Dothistroma pini* and *Dothistroma septosporum* have caused one of the most important foliar diseases of *Pinus* spp. in the world, red band needle blight. Although this disease was primarily a problem in the southern hemisphere, its geographic range and intensity have increased dramatically since the late 1990s (Watt *et al.*, 2009). The disease causes premature defoliation and reduced growth rates, resulting in economic and visual damage, and in some cases, mortality. In certain areas, the mortality rate has been reported to reach approximately 90% in trees aged 50 years or older due to these pathogens (Sturrock *et al.*, 2011). Pine species are also affected by pine pitch canker (PPC) disease, caused by *Fusarium circinatum* (Wingfield *et al.*, 2008). This fungus is an air-borne and seed-borne pathogenic, which was first reported in California in 1986 (Gordon *et al.*, 2001) and subsequently recorded in Europe. The disease is now present throughout the world, causing severe ecological losses in both forest ecosystems and nurseries (Zamora-Ballesteros *et al.*, 2022). *F. circinatum* is on the European and Mediterranean Plant Protection Organization (EPPO) A2 quarantine list (EPPO, 2025a).

Among oomycetes, we also find pathogens that pose a significant threat to forest ecosystems worldwide, causing devastating diseases that impact forests. Although historically classified as fungi due to their phenotypic similarity to filamentous fungi, oomycetes are phylogenetically close to diatoms and brown algae (Thines, 2014). They possess distinct biological characteristics, such as cellulose-based cell walls and unique reproductive structures. The spread of these pathogens is often facilitated by human activities, such as the trade of infected plant material, and exacerbated by climate change (Sturrock *et al.*, 2011). Many

species within the genera *Phytophthora* are among the most destructive oomycete pathogens affecting forests. *Phytophthora ramorum* is considered the most destructive pathogen of oaks worldwide, causing sudden oak death, sudden larch death and ramorum blight. *P. ramorum* is a highly adaptable and invasive pathogen with a broad host range. Its ability to withstand hot, dry summers and persist through the production of resilient chlamydospores has contributed to its rapid spread in North America and Europe (Garbelotto and Hayden, 2012). As a result, *P. ramorum* has caused the mortality of tens of millions of trees, posing a significant threat to the landscape and ecosystem services provided by the affected forests (Ghelardini *et al.*, 2022). Also affecting oaks, *Phytophthora cinnamomi* is the main factor associated with cork and holm oak decline in Mediterranean basin (de Sampaio e Paiva Camilo-Alves *et al.*, 2013). However, this oomycete has a broad host range and has also been responsible for Jarrah (*Eucaliptus marinata*) dieback in Western Australia, devastating an area of 282,000 hectares (Boyd *et al.*, 2013), and it is associated with ink disease in chestnut (Vettraino *et al.*, 2005). *P. cinnamomi* causes root rot and has the potential to destroy natural plant communities worldwide, leading to significant ecological and economic impacts on forestry, horticulture, and the nursery industry (Kamoun *et al.*, 2015). *Phytophthora lateralis* has triggered severe epidemics of cedar root disease in western North America, reappearing multiple times over the past century. It has now spread to European landscape plantations, where it is believed to disperse through airborne sporangia (Robin *et al.*, 2011). Several *Phytophthora* species have emerged in recent years, causing severe damage to various tree species, such as *Phytophthora austrocedrae*, which was responsible for a lethal disease of increasing concern in native Cupressaceae in South America and has recently emerged in Scotland, where it is killing native junipers (Greslebin *et al.*, 2007). *Phytophthora alni* has become a major forest pathogen, devastating alder populations and spreading into forest stands beyond riparian areas (Jung and Blaschke, 2004). Conifer species are also vulnerable to *Phytophthora* infections. *Phytophthora pinifolia* has caused one of the most rapid emergences of a forest pathogen ever recorded, affecting approximately 60,000 hectares of *Pinus radiata* in Chile within just two years between 2004 and 2006 (Durán *et al.*, 2008).The most recent outbreak involves *Phytophthora pluvialis*, which has been linked to a new defoliating disease affecting *P. radiata* and Douglas-fir in New Zealand (Scott, 2014). Interestingly, this pathogen had previously been detected in western Oregon forests without causing any noticeable disease (Reeser, 2013). Another pathogenic oomycete that poses a threat to forests is the genus *Pythium*, which affects species such as *Prunus serotina*, *Fagus sylvatica*, and *Acacia* spp. Some species within this genus are important plant pathogens with worldwide distribution, causing root rot, collar rot, fruit rot, and damping-off in seedlings (Li *et al.*, 2021).

Invasive fungal and oomycete pathogens pose a serious threat to forest ecosystems, driving large-scale changes in forest structure and tree species composition. Their impact extends beyond biodiversity loss, often resulting in severe ecological disruption and significant economic damage. In some cases, these pathogens have led to the complete eradication of host species. Due to their aggressive nature and broad host range, they present a major challenge for forest health, requiring vigilant monitoring and the development of effective, sustainable management strategies.

2. Current disease management strategies and their limitations

The management of forest pests and diseases involves a range of strategies, each with varying degrees of effectiveness and environmental impact, including silvicultural practices, chemical control through pesticides, biological control and genetic resistance. While these methods remain essential, they often come with limitations, such as ecological concerns, regulatory restrictions, or limited long-term effectiveness. To enhance forest resilience, integrated management has become a key strategy, combining multiple control methods and early detection of forestry diseases in a sustainable and holistic manner. However, in the context of climate change and increasing global trade, even this comprehensive strategy faces limitations and may not be sufficient to fully mitigate the growing threats to forest health. These challenges have intensified the search for innovative and environmentally sustainable alternatives.

2.1. Silvicultural management

Evidence of successful use of silviculture to minimize damage from invasive species remains limited. Silvicultural practices can prevent the impacts of forest diseases. However, their effectiveness is highly dependent on the timing of infection, as eradication becomes nearly impossible once a pathogen is well established.

In the early stages of disease emergence, silviculture focuses on more intensive or localized measures that attempt to significantly limit the outbreak (Waring and O'Hara, 2005). Sanitation is a common silvicultural approach to reduce pathogen abundance, which involves removing trees that have been infected or colonized in order to reduce inoculum in the stand. However, sources of inoculum are neither easy to identify nor easy to predict due to the cryptic nature of many pathogens, which are often not detected until tree mortality has occurred (Muzika, 2017). Other common silvicultural approaches include thinning, pruning, prescribed fire, and the removal of alternative hosts. While these methods can be effective, they also pose

potential risks that must be carefully evaluated based on site conditions and species-specific responses. For example, efforts to control white pine blister rust by eliminating its alternate host faced significant challenges, as removing a native plant species proved difficult (Zeglen *et al.*, 2010). Additionally, fire and thinning have both been shown to increase the abundance of alternate hosts, potentially exacerbating disease pressure. Pruning lower branches was implemented to reduce inoculum since they are more susceptible to infection. However, thinning may promote the development of lower branches, increasing vulnerability to disease (Muzika, 2017).

Once a pathogen is established and begins to spread, silvicultural management focuses on limiting its progression by modifying stand structures, adjusting tree species composition, and enhancing tree vigor. When resistant phenotypes are identified in natural forests, silvicultural practices can be implemented to promote resistant trees while reducing the abundance of susceptible individuals. However, the success of this strategy relies on accurately identifying resistant trees, which can be challenging (Koch, 2010). Additionally, silvicultural practices intended to improve vigor may undermine systemic induced resistance, potentially increasing vulnerability to infection (Bonello, 2010).

Silvicultural approaches to managing invasive pathogens are largely preventive and primarily effective during the early stages of disease establishment. However, these methods have significant limitations when it comes to controlling fast-spreading and unpredictable outbreaks. Given the accelerating impacts of climate change and globalization, silvicultural management is insufficient to address the unpredictable outbreaks of forest pathogens (Ramsfield *et al.*, 2016).

2.2. Use of chemical treatments: fungicides and their environmental impact

The use of chemical pesticides and fungicides has played a crucial role in protecting plants and crops, significantly reducing losses caused by pests and diseases. Fungicides can play a preventive role by blocking pathogen infection before symptoms appear, or a curative function by acting after infection has occurred. Both approaches help reduce disease progression (Kasanen *et al.*, 2022). These synthetic compounds act by inhibiting critical biological processes in pathogens, thereby preventing spore germination, disrupting fungal cell membranes, or inhibiting key metabolic pathways (Lucas *et al.*, 2015).

Certain chemical fungicides have been employed to mitigate tree diseases in plantations and mainly in nurseries. For instance, Carbendazim and Propiconazole have been used to treat

stem canker in oak trees, leading to improvements in disease symptoms, canker depth and number, and callus thickness in Iranian forest ecosystems (Karami *et al.*, 2018). Phosphonates, the most effective chemical group against oomycetes, have been applied to combat *P. cinnamomi* in Jarrah Forest bioregion species in Australia (Shearer and Crane, 2009), *P. ramorum* in oaks and tanoaks in California (Garbelotto *et al.*, 2007), and *P. pluvialis* in *P. radiata* plantations in New Zealand (Rolando *et al.*, 2014). Triazoles have been widely used in forest plantations and nurseries to control oak powdery mildew, pine needle cast disease, and needle blight in larch (Okorski *et al.*, 2015), as well as to manage oak wilt in mature forest stands in the USA (Eggers *et al.*, 2005). However, concerns have been raised regarding their potential negative impacts on non-target vegetation and alterations to the fungal community in tree stumps, highlighting the need for careful assessment of their ecological consequences (Vasiliauskas *et al.*, 2005; Westlund and Nohrstedt, 2000). Similarly, morpholine preparations used in forest nursery containers against powdery mildew may result in less efficient use of mycorrhizal vaccines (Okorski *et al.*, 2015).

Despite the effectiveness of certain treatments, chemical control of forest diseases poses significant limitations and several ecological and environmental concerns that must be carefully considered. The availability of fungicides for managing major forest pathogens remains limited, and their efficacy is influenced by various factors, including host condition, pathogen biology, the mode of action of active compounds, and their persistence in the environment (Kasanen *et al.*, 2022). Chemical control of forest diseases may gradually lose its effectiveness due to the emergence of fungicide-resistant pathogen strains. Many fungal and oomycete pathogens have developed resistance mechanisms, such as mutations in target genes, allowing them to survive fungicidal treatments. To mitigate the risk of resistance development, several strategies have been proposed, including the use of an efficient fungicide dosage, alternating or mixing different fungicide types, adjusting application intervals, and applying early in disease development (Okorski *et al.*, 2015). Multitarget fungicides are less likely to cause resistance development in pathogens as multiple mutations are required for fungicide resistance in the pathogen genome. However, nonspecific action of fungicide means that they can directly affect non-target organisms, posing a threat to beneficial microorganisms (Yang *et al.*, 2011). As the potential chances of fungicide resistance may increase in the future, this underscores the need for alternative, sustainable disease management strategies. However, the risk of fungicide resistance has been insufficiently explored in the context of forest pathogens (Okorski *et al.*, 2015). Moreover, concerns regarding the widespread use of chemical fungicides extend beyond efficacy, as they pose potential threats to human health, microbial communities and plant

biodiversity, and ultimately for ecosystems. In Europe, the use of chemicals in forestry is extremely limited due to strict legislation and specific conditions for the use of crop protection products. The European Union Directive 2009/128/EC promotes the reduction of chemical pesticide use, encouraging the adoption of environmentally friendly management strategies, particularly in forest ecosystems (Zamora-Ballesteros *et al.*, 2022). As a result, the number of available fungicides for forestry remains very limited. Therefore, while chemical control remains an important tool in forest disease management, its limitations and environmental concerns highlight the need for more sustainable and integrated approaches.

2.3. Biological control

Biological control relies on the use of living organisms to suppress plant pathogens and mitigate disease severity. This strategy is based on natural interactions such as competition for resources, antibiosis, parasitism, and induced resistance, which contribute to preventing infection, reducing host colonization, and limiting pathogen survival (Kasanen *et al.*, 2022). As a sustainable alternative to chemical treatments, biocontrol agents (BCAs) represent an alternative to synthetic fungicides with reduced environmental impact. One key advantage of biological control is that most BCAs exhibit a narrow host range, making them unlikely to negatively impact non-target species within the ecosystem. Additionally, since many BCAs are present in the host's environment, their use poses minimal risk for the ecosystem (Rabiey *et al.*, 2019). Unlike chemical fungicides, the ultimate goal of biological control is not to completely eradicate a pathogen, but rather to reduce its population below a threshold that minimizes ecological and economic impact. BCAs can be derived from a wide range of biological sources, including viruses, bacteriophages, bacteria, fungi, and even higher organisms such as nematodes, mites, and insects. This strategy can suppress plant pathogens through several natural mechanisms. These include antagonism, where they compete with pathogens for space and nutrients; antibiosis, which involves the production of inhibitory or toxic secondary metabolites; and hyperparasitism, where the biocontrol organism directly attacks and degrades the pathogen’s structures (Galli *et al.*, 2024).

Several successful study cases of biological control in forestry have demonstrated its potential as an effective alternative to synthetic fungicides with a lower environmental impact. For example, numerous BCAs have been tested for the management of DED, with many showing promising results *in vitro* but providing only short-term protection in field studies, such as nonpathogenic fungi *Trichoderma viride* and *Verticillium dahlia* and certain strains of *Pseudomonas (*Kasanen *et al., 2022)*. Additionally, efforts to combat the disease have also

focused on controlling its insect vectors, which facilitate its spread. In this regard, biocontrol strategies using fungal species such as *Trichoderma harzianum, T. polysporum*, and *Scytalidium lignicola* have been explored (Jassim *et al.*, 1990). Research has also sought to determine whether endophytic microorganisms could contribute to elm tolerance against DED. However, the antagonistic activity of the various fungi tested varies on different or comparable substrates and conditions (Awan and Asiegbu, 2021). Furthermore, efforts to combat the disease have also focused on controlling its insect vectors, which facilitate its spread. In this regard, biocontrol strategies using fungal species such as *Trichoderma harzianum, T. polysporum*, and *Scytalidium lignicola* have been explored (Jassim *et al.*, 1990). One of the most promising was *Verticillium albo-atrum* WCS850, which demonstrated strong biocontrol potential and was used as a preventive commercial treatment (Postma and Goossen-van de Geijn, 2016). However, since its application required annual injections and lacked curative properties, its use was limited in large-scale forestry.

To control root and stem rot in coniferous tree species caused by the *Heterobasidion annosum*, several fungal species have been investigated for their potential as competitors and antagonists. Among these, *Phlebiopsis gigantea* has demonstrated strong efficacy and has been widely used as a biocontrol agent against this *Heterobasidion* in Europe (Pratt *et al.*, 2000). However, the potential impact of these treatments on non-target organisms within forest ecosystems remains insufficiently studied. Additionally, recent research has raised concerns regarding the efficacy of biocontrol with *P. gigantea*, highlighting possible limitations in its antagonistic capacity under natural conditions (Żółciak *et al.*, 2020). In response to these challenges, the search for alternative biocontrol strategies has led to the exploration of other microbial species, including bacteria such as *Bacillus subtilis* and *Pseudomonas fluorescens*, as well as endophytic fungi and actinobacteria from the genus *Streptomyces* (Kasanen *et al.*, 2022). These microorganisms have demonstrated antagonistic activity against *Heterobasidion* in controlled *in vitro* assays; however, extensive field trials are still needed to assess their efficacy under natural forest conditions.

Another form of biological control involves the use of mycoviruses to induce hypovirulence in fungal pathogens. One notable example is the use of hypovirulent isolates of *C. parasitica* to control chestnut blight. In this pathogenic fungus, a hypovirulent strain was discovered to harbor a mycovirus known as Cryphonectria hypovirus 1 (CHV-1), which reduces the virulence of the fungus in chestnut trees (Shapira *et al.*, 1991). While uninfected (virulent) strains aggressively penetrate and destroy the bark and cambium, leading to wilting and tree mortality, CHV-1-infected (hypovirulent) strains typically form superficial cankers that heal over

time without endangering host survival (Choi and Nuss, 1992). The ability of CHV-1 to be transmitted between strains of *C. parasitica* was exploited to develop a biological control strategy, where co-inoculation of virulent isolates with hypovirulent ones significantly reduced canker severity in *C. sativa* (Zamora *et al.*, 2014). As a result, this BCA has proven effective in controlling chestnut blight across Europe and in certain regions of the US.

The selection of appropriate biocontrol agents should not only prioritize their effectiveness against the target pathogen but also consider their broader ecological impact, particularly on soil biodiversity and overall forest ecosystem stability. While numerous microbial species have shown promise as potential biocontrol agents, many of these approaches have yet to be widely adopted or commercialized. Major challenges in developing BCAs are the identification, characterization, formulation and application of the agents. Furthermore, BCAs are generally not curative, and their use often needs to be complemented with other management strategies, such as chemical or silvicultural control, to achieve effective and long-term disease suppression.

2.4. Genetic resistance

Another approach to disease control focuses on developing new adapted forests with acceptable resistance against biotic stresses. This can be achieved through traditional breeding methods such as the introduction of new varieties, crossing and hybridization, selection in successive generations, provenance tests, as well as modern approaches including genetic engineering and gene editing. The molecular basis of pathogen-hosts interactions remains largely unknown. Advancing this knowledge is essential for understanding the genetic variability within the host and for enhancing resistance to disease.

Advances in molecular biology and genomics, particularly through next-generation sequencing (NGS), have enabled high-throughput genotyping and the assessment of genetic diversity in forest trees species (Younessi-Hamzekhanlu and Gailing, 2022). These technologies have facilitated the discovery of numerous single nucleotide polymorphism (SNP) markers, which are widely used in both quantitative trait loci (QTL) mapping and genome-wide association studies (GWAS) to identify genomic regions linked to disease resistance. These two methods can identify markers associated with the desired trait to use in marker-assisted selection (MAS) of superior genotypes (Younessi-Hamzekhanlu and Gailing, 2022). Comparative transcriptomic further enhances these approaches by revealing patterns of gene expression associated with different levels of susceptibility, providing valuable insights into the molecular mechanisms underlying disease resistance (Hernandez-Escribano *et al.*, 2020; Zamora-Ballesteros *et al.*,

2021). More recently, genomic selection (GS) has emerged as a promising strategy to predict resistant phenotypes early in the breeding cycle, accelerating the development of disease-resistant genotypes in trees (Ahmar *et al.*, 2021). Together, these advances help clarify the molecular mechanisms underlying responses to forest diseases and accelerate breeding programs aimed at selecting resistant genotypes.

These molecular approaches are now being integrated into breeding programs for various forest species, where improving resistance to major pathogens is a key priority. In the case of chestnut, breeding efforts in both Europe and North America have been primarily directed toward developing resistance to the two major diseases affecting this species, *C. parasitica* and *P. cinnamomi*. This has involved the strategic use of Asian chestnut species, which have co-evolved with these pathogens, to introduce resistance genes into more susceptible species, and the selection of naturally resistant genotypes (Fernandes *et al.*, 2022).

Similarly, for the restoration of elm populations, which have been severely impacted by DED, several tolerant clones have been developed through traditional hybridization between native species and Asian elms (Martín *et al.*, 2019). This constitutes one of the most extensive and long-standing forest tree breeding programs worldwide. The first initiatives began in the Netherlands in the early 20th century and laid the foundation for coordinated breeding efforts across Europe, including Italy and Spain (Mittempergher and Santini, 2004). In Spain, the breeding program has successfully produced and evaluated several native *Ulmus minor* clones with high levels of tolerance to *O. novo-ulmi*, the causal agent of DED (Martín *et al.*, 2014).

Likewise, in response to the severity of the decline and mortality processes affecting holm oak and cork oak, which threaten the sustainability of their forests in the Iberian Peninsula, the Spanish Ministry for the Ecological Transition (MITECO) established in 2019 a working group for the selection of genotypes of *Quercus ilex* and *Quercus suber* that are tolerant to water stress and root rot caused by *P. cinnamomi* (RedPAC, 2020).

Despite advances in genomics, several factors continue to limit genetic resistance application in forest trees. Financial constraints are significant, especially for ecologically important yet economically less valuable forest species. Although several genetic studies have been conducted for model crops and trees, available data for most forest species remain limited and insufficient. Biologically, defining and validating durable resistance phenotypes in long-lived trees is time-consuming, often requiring a decade or more of field observation. Furthermore, resistant genotypes must be carefully evaluated to ensure they retain desirable growth traits and ecological functions without introducing unintended trade-offs. Genetic diversity must also be

maintained across breeding populations to ensure long-term adaptability, making selection strategies more complex than in crops. Additionally, many forest pathogens exhibit high evolutionary potential, leading to the emergence of new, more virulent strains that may overcome existing genetic resistance, which requires continuous breeding efforts. Finally, resistance to many diseases in forest trees is controlled by several genes rather than just one, which makes it harder to improve through breeding (Sniezko *et al.*, 2023).

2.5. Integrated Management

Given the complexity of forest disease dynamics, a single management approach is unlikely to provide complete protection against emerging pathogens. Integrated disease management combines multiple management strategies, such as chemical and biological control, genetic resistance, and silvicultural practices, to enhance forest resilience. Moreover, integrated disease management is not limited to control methods alone; it also includes essential support tools such as monitoring, early detection, and risk assessment. Early detection is a key preventive strategy that helps determine when and how to apply appropriate control measures or treatments. An effective way to prevent large-scale outbreaks is to detect and remove infected trees at the early stages of infection. However, early-stage infections often do not produce visible changes in tree morphology or color, which makes detection challenging through conventional methods (Yu *et al.*, 2021). To overcome this limitation, advanced technologies have been developed, including hyperspectral imaging (HSI) using unmanned aerial vehicles (UAVs), light detection and ranging (LiDAR), and other remote sensing (RS) techniques. These tools could identify physiological changes at the individual tree level before visible symptoms appear (Yu *et al.*, 2022). As a result, forest diseases have been managed using all available resources, with decision-making strategies that prioritize economic viability, and environmental safety to ensure optimal and effective control. Historically, many forest pathogens have been addressed through this comprehensive and strategic approach to integrated disease management (Karami *et al.*, 2018; Kasanen *et al.*, 2022; Zamora-Ballesteros *et al.*, 2022).

Despite the implementation of integrated disease management strategies, the limitations of chemical treatments and the insufficient efficacy of other control methods highlight the urgent need for new pathogen control approaches. The lack of effective solutions can interfere with the protection of vital resources such as food and timber, so it is essential to continue to investigate environmentally sustainable alternatives that are effective against tree diseases.

3. Pathogens of study: *Fusarium circinatum* and *Phytophthora cinnamomi*

Given the significant impact of forest pathogens and the current lack of effective control strategies, this thesis focuses on two forest pathogens for which no efficient management methods are currently available. Emerging technologies based on RNA interference (RNAi), such as Spray-Induced Gene Silencing (SIGS), offer promising new approaches to overcome these challenges. To explore the potential of SIGS as a disease control strategy in forestry, we selected two pathogens with contrasting lifestyles and infection strategies: the vascular fungus *F. circinatum* and the soil-borne oomycete *P. cinnamomi*. These organisms are major threats to forest ecosystems worldwide, as described in Introduction Section 1.2. While most SIGS studies have been limited to foliar pathogens, our objective was to broaden its applicability by evaluating its performance against both vascular and root-infecting pathogens. Through this approach, we aimed to assess the versatility and potential of SIGS as a novel tool for forest disease management. In this section, we provide a more detailed overview of the pathogens selected for this study and the diseases they cause

3.1. *Fusarium circinatum,* the causal agent of Pine Pitch Canker in conifers

Fusarium circinatum Nirenberg & O'Donnell (teleomorph *Gibberella circinata*), is an ascomycete fungus that causes pine pitch canker (PPC), a destructive disease of conifers, particularly pines, which is widespread worldwide. *F. circinatum* is considered a vascular and canker pathogen and causes significant issues not only in plantations and natural forests but also in forest nurseries (Wingfield *et al.*, 2008). In the latter, *F. circinatum* is primarily introduced through seeds and can be either symptomatic or asymptomatic. This can have severe consequences as asymptomatic plants may later be transplanted to the field, spreading the disease to areas where it was not previously present. Symptoms caused by *F. circinatum* in nursery plants include root and collar rot, shoot and tip dieback, and eventually seedling mortality (Wingfield *et al.*, 2008). In addition, controlling *F. circinatum* spread in greenhouses is challenging because it can persist in the soil for extended periods (Serrano *et al.*, 2017). This means that used containers could potentially serve as a source of inoculum. In adult trees, PPC is characterized by the development of resin-soaked cankers that cause deformations in the trunk and major branches and severe infections can girdle trees, leading to foliage discoloration, shoot dieback, and extensive canopy decline (Zamora-Ballesteros *et al.*, 2022).

The causal agent of pine pitch canker is distributed worldwide (Figure 1), with particular prevalence in Mediterranean, subtropical and some temperate regions (Drenkhan *et al.*, 2020). The first report of PPC occurred in 1946 in North Carolina (USA) on *Pinus virginiana* (Hepting and

Roth, 1946), and in California it was identified in 1986 and rapidly disseminated due to the temperate climate, the vulnerability of the host *P. radiata*, and the abundance of insects that functioned as disease vectors (Gordon *et al.*, 2001). *F. circinatum* has since spread throughout the US, as well as to several countries in South America (including Chile, Uruguay, Colombia and Brazil), Asia (Japan and South Korea), Africa (where it is present only in South Africa) and Europe (in Spain, Portugal, France and Italy, although it has been successfully eradicated in the latter two) (Zamora-Ballesteros *et al.*, 2022). Spain is the most affected country, with *F. circinatum* stablished in five regions, mainly in the Atlantic-coast and Cantabrian areas where climate conditions are favorable to the pathogen.

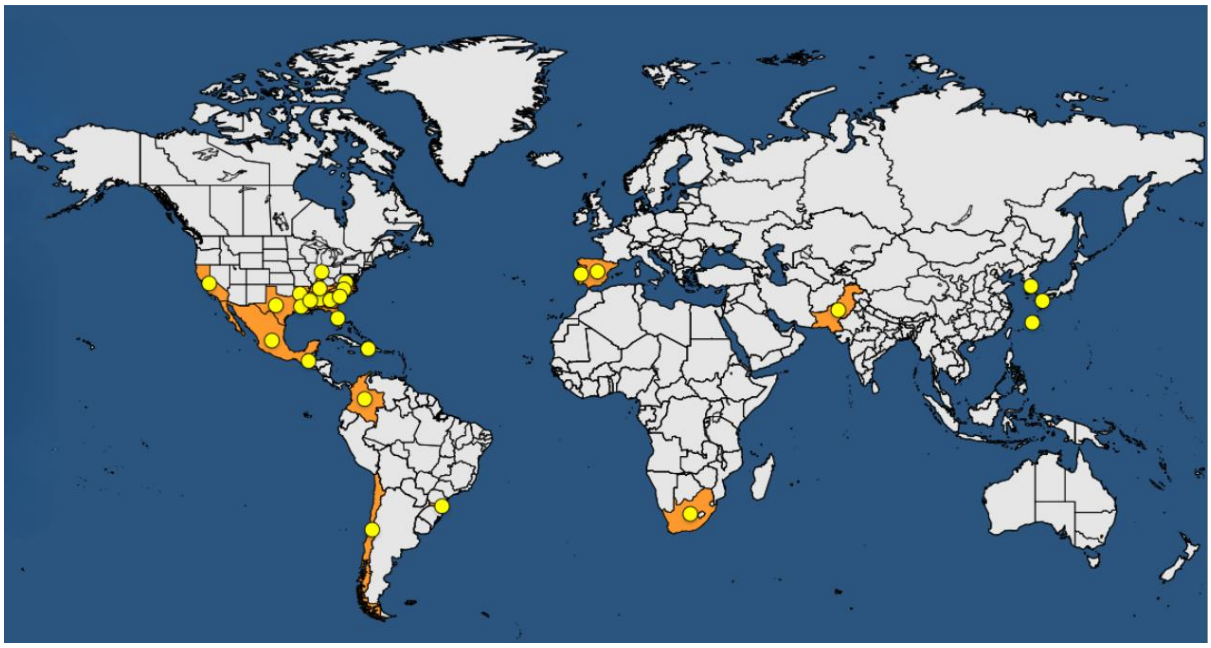

Figure 1. *F. circinatum* distribution map. EPPO Global Database, last updated: 2025-03-31.

PPC affects at least 67 *Pinus* species, 18 *Pinus* hybrids, and 6 non-pine tree species (Woodward *et al.*, 2025). *P. radiata* is the most susceptible pine species to this disease and is heavily affected due to its widespread use in large-scale forestry in southern hemisphere countries (Zamora-Ballesteros *et al.*, 2022). It is highly valued for its timber in many parts of the world due to its moderately fast growth and versatile wood (Sánchez *et al.*, 2003), and is one of the most widely planted tree species globally and is still cultivated in various countries, including New Zealand, Australia, Chile, South Africa, and southwestern Europe. In northern Spain, for example, there are large *P. radiata* plantations covering about 287,000 hectares, which is approximately 25% of the country's coniferous timber resources (EPPO, 2025b). Indeed, PPC appeared for the first time in Spain in *P. radiata* nurseries in Galicia (Collar, 1995) and subsequently spread to forest plantations.

In terms of economic and ecological impact, severe losses have occurred in forest ecosystems and nurseries due to *F. circinatum*. Outbreaks in Florida in the 1970s led to an estimated loss of 0.4–0.9 million m^3 of pine timber per year between 1974 and 1979, and in California the costs of removing and replacing dead trees have been projected to reach several million USD (EPPO, 2025b). Also in US, *F. circinatum* also affected the Christmas tree industry, increasing operating costs and losses of planting stock. In South Africa, costly sanitation measures and seedling losses affects all nurseries in the country (EPPO, 2025b). Further countries have documented significant losses: in Chile approximately 4.3 million pine seedlings (about 0.65% of production) had to be destroyed in 2006–2012 due to *F. circinatum*, resulting in 332,000€ of direct losses (Zamora-Ballesteros *et al.*, 2019). In Spain, the disease has caused severe yield losses in plantations and nurseries. For example, in 2017, a nursery in Galicia culled more than 25,000 *P. radiata* seedlings to contain an outbreak (EPPO, 2019). As a result, the species is disappearing in the country and being replaced by eucalyptus due to its profitability and lack of alternative species for planting. This change has had serious consequences for avian and herbaceous species (Goded *et al.*, 2019) and an indirect economic impact due to shorter rotation cycles and market differentials. In addition, diseases such as PPC could significantly reduce forestry activities and associated employment contributing to the depopulation and population ageing in rural areas of Europe. Moreover, projections show that if PPC invades currently disease-free regions, such as Australia or New Zealand, the economic damage could be enormous (Zamora-Ballesteros *et al.*, 2019).

F. circinatum is transmitted primarily asexually, via the production of microconidia and macroconidia. Airborne conidia naturally infect fresh wounds on trees, and, under favorable environmental conditions, the conidia germinate. The pathogen then colonizes the host tissues, initially growing into the stem pitch before spreading through the phloem and xylem. As the fungus progresses, it forms conidiophores within the pith cavities, a process which may facilitate the spread of conidia to various parts of the plant (Martín-Rodrigues *et al.*, 2013).

The primary route for long-distance dispersal is the movement of infected seeds, which can carry the pathogen either externally or internally (Wingfield *et al.*, 2008; Zamora-Ballesteros *et al.*, 2019). Other potential pathways include the trade of contaminated wood, bark, or low-quality packaging materials (Zamora-Ballesteros *et al.*, 2022). In the field, *F. circinatum* disperses naturally through wind and rain, while environmental factors like humidity and coastal climates favor disease development (Drenkhan *et al.*, 2020). Fresh wounds caused by meteorological events may create entry points for the pathogen (Sakamoto and Gordon, 2006). Insects also play a crucial role: many bark beetles, pine weevils, shoot feeders, and sucking

insects act as vectors, carriers, or wounding agents, facilitating the spread of *F. circinatum* across trees and forests (Zamora-Ballesteros *et al.*, 2022). Altogether, both human-mediated and natural dispersal pathways have contributed to the global expansion of PPC, highlighting the complexity of managing this serious forest health threat.

There is currently no cure or eradication method for PPC in established forests. In practice, management focuses on prevention and sanitation aiming to reduce the probability of the pathogen entering new areas (Zamora-Ballesteros *et al.*, 2019). Fungicidal or biological treatments have shown limited success, leaving the destruction of infected plants and the implementation of quarantine measures as the primary control strategies (EPPO, 2025b). The selection and development of tree germplasm resistant to pathogens is considered the most robust approach to reducing diseases losses, but also a challenge, as breeding pines for resistance is slow and the host range for *F. circinatum* is unusually broad, thereby complicating genetic resistance (Woodward *et al.*, 2025). As previously discussed in the introduction, the case of *F. circinatum* clearly highlights the lack of effective control strategies and underscores the urgent need to develop new, more efficient and sustainable approaches, such as SIGS.

3.2. *Phytophthora cinnamomi,* a serious threat to Mediterranean forests

Phytophthora cinnamomi Rands (1922) is an oomycete regarded as the most important pathogen causing root rot in woody species. It is particularly associated with diseases affecting important *Fagaceae* species, such as oaks and chestnuts, but also eucalypts, pines, or members of the *Ericaceae* family (Robin *et al.*, 2012). It has a worldwide distribution (Figure 2), causing the most severe damage in tropical and subtropical regions, as well as in temperate climates and Mediterranean areas, where it is responsible for high mortality rates in oak woodlands and pasturelands, leading to the disease known as holm oak decline (Burgess *et al.*, 2017). Although several other pathogens and pests have been associated with cork (*Q. suber*) and holm oak (*Q. ilex*) decline, varying in their aggressiveness to the trees, only *P. cinnamomi* was associated with the overall mortality outbreaks occurring in South Europe since the 1980s. Consequently, the potential impact of this pathogen in Mediterranean *Fagaceae* ecosystems is a major concern in countries such as Spain, Portugal, France, Italy, and Turkey (Mora-Sala *et al.*, 2019).

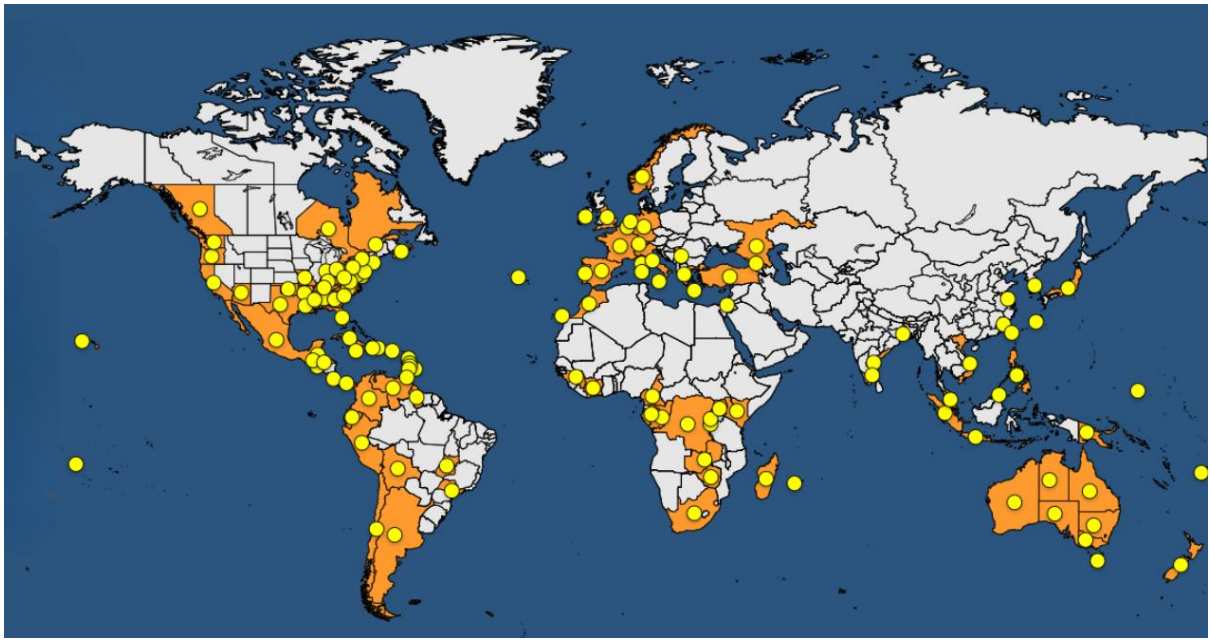

Figure 2. *P. cinnamomi* distribution map. EPPO Global Database, last updated: 2025-06-10.

P. cinnamomi has a broad host range, infecting more than 5.000 vascular plants, including both annual herbaceous and perennial species. Climate change is expected to significantly influence the distribution and impact of *P. cinnamomi* in the coming decades. Predictive models suggest that rising temperatures will drive the potential range expansion of *P. cinnamomi* along the western coast of Europe, with its spread moving one to several hundred kilometers eastward from the Atlantic coast within the next century (Sturrock *et al.*, 2011). These projections underscore the growing threat posed by *P. cinnamomi* to forest ecosystems in temperate climates under future global warming scenarios.

The infection process of this soilborne oomycete involves the colonization of fine root tissues by motile zoospores, initially penetrating the rhizodermis and subsequently advancing into the cortex and vascular tissues. In infected plant tissues, *P. cinnamomi* produces sporangia within the affected roots, as well as resting structures such as chlamydospores, stromata-like hyphal aggregations and selfing oospores (Redondo *et al.*, 2015). Resting structures allow the pathogen to survive in the soil under unfavorable environmental conditions like hot and dry Mediterranean summers, making *P. cinnamomi* a highly resilient organism well adapted to a range of climates. *P. cinnamomi* leads to the massive death of fine roots, significantly reducing the tree's ability to absorb water and nutrients from the soil. Infected trees often exhibit extensive reduced fine root biomass, stomatal conductance, and leaf water potential. As a result, infected trees are more susceptible to drought stress, due to combined effects of reduced root mass and degraded vascular tissue (Sena *et al.*, 2018). Symptoms in evergreen oaks can be acute, with rapid death of the entire crown in one growing season, or chronic, with slow thinning of the crown,

leaf chlorosis, defoliation, branch death, and proliferation of epicormic shoots for several years before the tree dies (Morales-Rodríguez *et al.*, 2025).

Environmental factors such as climate, soil properties and water availability significantly influence disease severity and the susceptibility of hosts to *P. cinnamomi*. Disease development is particularly favored by warmer environments. The occurrence of heavy rainfall events appears to favor *P. cinnamomi* sporulation and disease development while in times of drought it is able to survive in resistance structures and wait for suitable conditions to sporulate and infer new hosts (Morales-Rodríguez *et al.*, 2025). Fine-textured soils with high moisture content can facilitate pathogen survival and infection, while drought conditions can exacerbate disease impact by stressing the host trees (Corcobado *et al.*, 2013). The incidence of *P. cinnamomi* is also influenced by the susceptibility of the plant community and its capacity to induce pathogen sporulation. The pathogen can persist in the roots of both symptomatic and asymptomatic annual and herbaceous perennial plant species (Crone *et al.*, 2013b). Furthermore, human activities and wildlife play a key role in the spread of *P. cinnamomi,* Spores can be passively transported via contaminated soil adhering to vehicles, forestry equipment, and animals such as wild boar and ungulates, which are abundant in Mediterranean forests (Vannini *et al.*, 2021). In addition, the presence of roadways and drainage systems facilitate downhill and waterborne inoculum spread (Vannini *et al.*, 2021). The combined effects of biotic and abiotic stresses underscore the complexity of managing oak decline and highlight the need for integrated approaches that consider both pathogen control and environmental conditions (Ruiz Gómez *et al.*, 2018).

Significant ecological impact has been attributed to *P. cinnamomi* in Mediterranean forests, mainly through its involvement in Ink Disease of chestnuts and La Seca of oaks, which have led to long-term tree decline and habitat degradation. Ink disease is widespread throughout the chestnut distribution range, but its causal agents vary regionally. While *P. cambivora* predominates in Greece, and Italy, *P. cinnamomi* is the main agent in the Iberian Peninsula (Vettraino *et al.*, 2005). In Portugal, studies reported chestnut tree mortality due to ink disease at 31% between 1995 and 2002, and 27% between 2002 and 2004, across more than 12,000 hectares (Martins *et al.*, 2007). Oak decline due to *P. cinnamomi* root rot, known as *La Seca*, affects mainly in Spain and Portugal in *dehesa* and *montado* systems. In Spain, *La Seca* has led to the loss of approximately 500,000 trees and over €1 million annually since 2001, resulting in the decline of around 150,000 hectares of oak *dehesas* over the past two decades (Cortes Generales, Senado, 2010). In Andalusia, *P. cinnamomi* is estimated to affect 22% of holm and cork oak stands, rising to 44% in the case of *Q. ilex* (Sánchez-Cuesta *et al.*, 2021). Additionally,

nursery surveys in Spain have reported the presence of *P. cinnamomi* in nurseries from four Spanish regions (Mora-Sala *et al.*, 2022).

Regarding the management of *P. cinnamomi*, chemical control using trunk injections of fosetyl-aluminum and potassium phosphonate was used in the past, although current regulations require specific approval for fungicide application in each target crop. Biological control strategies have also been investigated to improve soil health. Nevertheless, the most effective approach remains integrated management, which combines different treatments with regular monitoring, risk assessment, sanitation practices and the certification of propagation material (Morales-Rodríguez *et al.*, 2025).

4. RNAi-based technologies: emerging sustainable tools for plant disease control

Given the increasing limitations of available disease management strategies, there is an urgent need to explore novel, sustainable alternatives for forest disease control. Recent advances in molecular biology, biotechnology, and plant pathology have opened new avenues for environmentally friendly approaches. Among these, RNAi-based control technologies are gaining popularity as innovative and effective tools for pathogen management, offering high specificity and reduced environmental impact (Bocos-Asenjo *et al.*, 2022). These strategies are based on a natural biological process conserved in most eukaryotes, RNA interference, through which essential genes of pathogens can be selectively silenced. To harness this mechanism for disease control, several RNAi-based approaches have emerged. Among them, Host-Induced Gene Silencing (HIGS) and Spray-Induced Gene Silencing (SIGS) stand out as the most suitable for forestry applications. These strategies differ primarily in the method by which the RNA molecules are applied or delivered to the pathogen.

4.1. Introduction to RNAi

RNAi is a natural biological process in which double-stranded RNA (dsRNA) molecules trigger the degradation of specific messenger RNA (mRNA) sequences, thereby silencing the gene and preventing the synthesis of corresponding proteins.

It was first described by Fire *et al.* (1998) in the nematode *Caenorhabditis elegans*, revolutionizing the field of molecular genetics, leading to the awarding of Andrew Z. Fire and Craig C. Mello with the Nobel Prize in Physiology or Medicine in 2006 (Fire and Mello, 2006). Their research aimed to silence specific genes in *C. elegans* to study their functions. Initially, they attempted gene silencing by injecting complementary RNA to the target mRNA, but unexpectedly, the most effective silencing was achieved by introducing a mixture of sense and

antisense RNA strands, which hybridized to form dsRNA. Remarkably, injecting only a few dsRNA molecules per cell was sufficient to completely silence the expression of the target gene (Fire *et al.*, 1998). Although RNAi was formally identified through Fire *et al.* (1998) work, similar mechanisms had already been reported under different names, including post-transcriptional gene silencing (PTGS) in tobacco and petunia plants (Napoli *et al.*, 1990; Rothstein *et al.*, 1987), and quelling in the fungus *Neurospora crassa* (Romano and Macino, 1992). Since then, RNAi mechanisms has also been identified in a wide range of organisms, including plants and fungi but also insects (Hammond *et al.*, 2000) and mammals (Elbashir *et al.*, 2001). This gene silencing mechanism is broadly conserved across eukaryotes, with only a limited number of species, such as the yeast *Saccharomyces cerevisiae* and the fungus *Ustilago maydis*, lacking RNAi activity due to the loss of some essential components of the RNAi machinery (Wytinck *et al.*, 2020).

Functionally, RNAi is thought to have evolved primarily as a defense mechanism against viruses and transposable elements that pose a threat to the integrity of the host genome. The presence of foreign genetic material, frequently in the form of dsRNA, activates the RNAi pathway, leading to the targeted silencing of these invaders (Obbard *et al.*, 2009). In addition to its protective role, RNAi is crucial for the regulation of endogenous gene expression and protein levels (Bramlett *et al.*, 2020).

The discovery of RNAi and subsequent research on RNAi have greatly expanded our understanding of gene regulation. Beyond its role as a powerful tool for studying gene function (Mello and Conte, 2004), RNAi has opened up possibilities for its use in gene therapy and disease control in fields such as medicine, agriculture and forestry.

4.2. Understanding the mechanism and core elements of RNAi

RNAi is a highly conserved gene-silencing mechanism in eukaryotic cells, that involves several fundamental processes: (a) the Dicer-mediated processing of dsRNA into small RNAs (sRNAs), (b) the formation and activity of the RNA-induced silencing complex (RISC), (c) the sequence-specific degradation of target mRNAs, and (d) the silencing signal amplification via RNA-dependent RNA polymerases (RdRps) (Figure 3).

RNAi mechanism is initiated when dsRNA molecules are recognized and processed by Dicer or Dicer-like (DCL)[1] proteins, generating either microRNAs (miRNAs) from endogenous hairpin precursors, or small interfering RNAs (siRNAs) from long exogenous dsRNAs. These

[1] Dicer refers to the enzyme in animals and humans; Dicer-like is its counterpart in plants and fungi.

sRNAs typically range in length 19-25 nucleotides (nt), of which 21-25 nt are the most frequently reported in fungi (Chang *et al.*, 2012; Chen *et al.*, 2015). The resulting sRNA duplexes are subsequently incorporated into a multiprotein complex known as the pre-RNA-induced silencing complex (pre-RISC), which includes an Argonaute (AGO) protein. Within this complex, the sRNA duplex is unwound into two single strands: the passenger strand and the guide strand. The passenger strand is typically ejected, while the guide strand remains bound to AGO, forming mature RISC (Iwakawa and Tomari, 2022). The guide strand then directs the RISC to complementary sequences on target mRNAs by homologous base-pairing. Upon recognition, the AGO protein cleaves the target mRNA, leading to the sequence-specific degradation of the mRNA and the subsequent downregulation of gene expression (Timmons *et al.*, 2001; Wilson and Doudna, 2013). In certain organisms, the RNAi is further amplified by RdRps, which utilize the target mRNA as a template to generate new dsRNAS (Wilson and Doudna, 2013). These dsRNAs will then serve as substrate for dicer to produce siRNAs known as secondary siRNA. Secondary siRNAs are subsequently loaded into RISC, enabling the sustained degradation of homologous mRNAs and thereby reinforcing and prolonging the silencing effect.

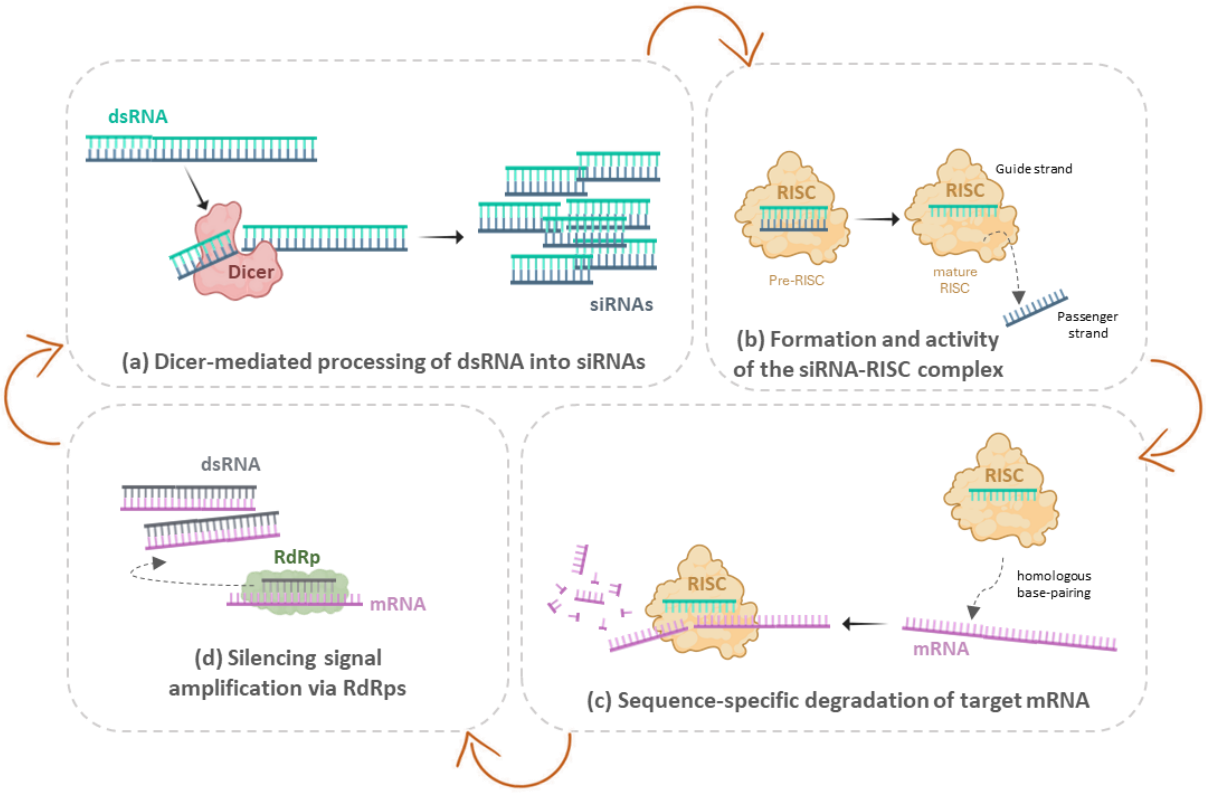

Figure 3. Schematic Representation of the RNAi Mechanism triggered by exogenous dsRNA. (a) The process is initiated by the Dicer-mediated cleavage of dsRNA into siRNAs. (b) siRNAs are incorporated into RISC, where the duplex is unwound and the guide strand is retained. (c) Guide strand directs RISC to complementary sequences on target mRNAs, leading to their cleavage and degradation. (d) Silencing signal is amplified by RdRps, which generate dsRNAs from mRNA templates to serve again as substrates for Dicer enzyme.

Because RNAi-mediated silencing relies on the recognition of complementary sequences, only mRNAs containing stretches of homology with the siRNAs are affected, being a highly specific process. However, perfect homology between the siRNA and the entire target mRNA is not essential. Effective silencing typically requires only a short region of complementarity of about 8 base pairs (bp), known as seed sequence (Bartoszewski and Sikorski, 2019).

The key components of the RNAi pathway are the Dicer/DCL proteins, RISC complex and AGO proteins, and RdRps.

4.2.1. Dicer or DCL proteins

Dicer/DCL proteins are highly conserved enzymes with ribonuclease activity which generates sRNA from long dsRNAs. These multiple-domain proteins usually possess RNase III domains, a Piwi-Argonaute-Zwille (PAZ) domain, a domain of unknown function 283 (DUF283) and dsRNA-binding (dsRBD) domains. PAZ is responsible for the recognition of the end of dsRNA, then RNase III cleavage domains are responsible for processing dsRNAs into siRNAs, and dsRNA-binding (dsRBD) domains determines substrate specificity and the length of the resulting siRNA products (Mosquera *et al.*, 2025). After cleavage, Dicer generates 2-nt overhang at the 3' region in each strand (Zhang *et al.*, 2004).

4.2.2. RISC complex and AGO proteins

RISC is a multiprotein complex that facilitates the degradation of target mRNAs through sequence-homology, guided by siRNAs. Thus, siRNA plays a vital role in RISC, enabling its transition from a pre-RISC to a mature RISC complex, and guiding it to specifically bind and degrade the target mRNA (Iwakawa and Tomari, 2022). Among the components of the RISC complex, the main one is the argonaute (AGO) protein. AGO comprises three components: the N-terminal PAZ domain, while the P-element induced wimpy (PIWI) domain is in the mid and C-terminal. These proteins possess RNase activity to cleave target mRNAs with the PAZ domain facilitating RNA binding and protein–protein interactions, while the PIWI domain is essential for the endonucleolytic cleavage of the targeted mRNA (Parker, 2010). AGO catalytic activity is essential for the proper functioning of the siRNA pathway (Iwakawa and Tomari, 2022). Most organisms encode multiple AGO proteins, often with distinct roles, reflecting the need for specificity in the interaction between AGOs and different classes of small RNAs. However, not all AGO proteins exhibit endonucleolytic (cleavage) activity; for example, in mammals, only

AGO2 has been shown to possess slicer activity, while AGO1, AGO3, and AGO4 bind small RNAs but lack catalytic function (Liu *et al.*, 2004).

4.2.3. RdRps

RdRps are enzymes that play a crucial role in amplifying RNAi response by synthesizing new dsRNA from single-stranded RNA (ssRNA) (Wilson and Doudna, 2013). The interaction between mature RISC and the target mRNA is required for the recruitment of RdRps. RdRps then catalyze the synthesis of long dsRNAs using the target mRNA as template. These dsRNA will then serve as substrates for Dicer enzyme, leading to the production of abundant secondary siRNAs (Zhang and Ruvkun, 2012). These enzymes are present in many fungi, plants, and certain animals; however, not all eukaryotic organisms possess them. Although RdRp activity is not strictly required for RNAi-mediated gene silencing, it plays a key role in enhancing the effectiveness and durability of silencing effect through the production of abundant secondary siRNAs (Song *et al.*, 2018b).

4.3. Applications of RNAi in plant protection

In recent years, RNAi-based technologies have emerged as promising, sustainable alternatives for plant disease control, enabling the specific targeting of pathogen genes without harming the environment (Bocos-Asenjo *et al.*, 2022). Two major RNA-based plant protection strategies have emerged as promising and viable alternatives for effective disease management in agricultural and forest ecosystems: Host-Induced Gene Silencing (HIGS), which is based on the phenomenon of cross-kingdom RNAi, where small RNAs produced by the host plant are transferred to invading pathogens to silence their genes; and Spray-Induced Gene Silencing (SIGS), which exploits environmental RNAi, using exogenously applied dsRNA on plant surfaces to induce gene silencing directly in the pathogen without the need for genetic modification of the host.

4.3.1. HIGS: silencing from within the plant

RNA molecules can move across cellular barriers between hosts and pathogens to induce gene silencing via RNAi. This communication between interacting organisms is bidirectional and is known as cross-kingdom RNAi (Weiberg *et al.*, 2013). It has been observed that a wide range of hosts exchange sRNAs with their pathogens. In plant-pathogen interactions, hosts send endogenous sRNAs to knockdown crucial virulence genes in their pathogen counterparts to reduce its pathogenicity (Cai *et al.*, 2018a; Zhang *et al.*, 2016), and conversely, pathogens deliver sRNAs targeting plant genes to silence the host immune responses (Dunker *et*

al., 2020; Ji *et al.*, 2021; Wang *et al.*, 2017; Weiberg *et al.*, 2013). Thus, sRNA communication between host and pathogen plays an important role in pathogen virulence and host resistance through RNAi (Mann *et al.*, 2023). Recent studies have illuminated the mechanisms of this bidirectional RNA exchange, highlighting a key role for extracellular vesicles (EVs) in sRNA trafficking (Cai *et al.*, 2018b; He *et al.*, 2021; Hou *et al.*, 2019) and revealing that many sRNAs also travel outside of EVs in protein–RNA complexes (Zand Karimi *et al.*, 2022). Furthermore, new evidence shows that even host messenger RNAs (mRNAs) can also travel inside EVs and are biologically active when translated into the fungal pathogen cells (Wang *et al.*, 2024).

HIGS consists of an RNAi-based plant protection strategy that exploits the phenomenon of RNAi cross-kingdom (Nowara *et al.*, 2010). HIGS involves the genetic modification of plants to express RNAs designed to target and silence specific genes in pathogens, thereby enhancing the plant's resistance to disease (Figure 4) (Koch and Wassenegger, 2021). HIGS was initially demonstrated to be highly effective against viral plant pathogens, conferring a mean of 90% resistance against the targeted viruses in 75 studies that were reviewed by Koch and Wassenegger (2021). Since then, HIGS was shown to be effective against a variety of different pathogens and pests: insects (Baum *et al.*, 2007; Mao *et al.*, 2007), fungi (Nowara *et al.*, 2010), oomycetes (Eschen-Lippold *et al.*, 2012) and nematodes (Huang *et al.*, 2006).

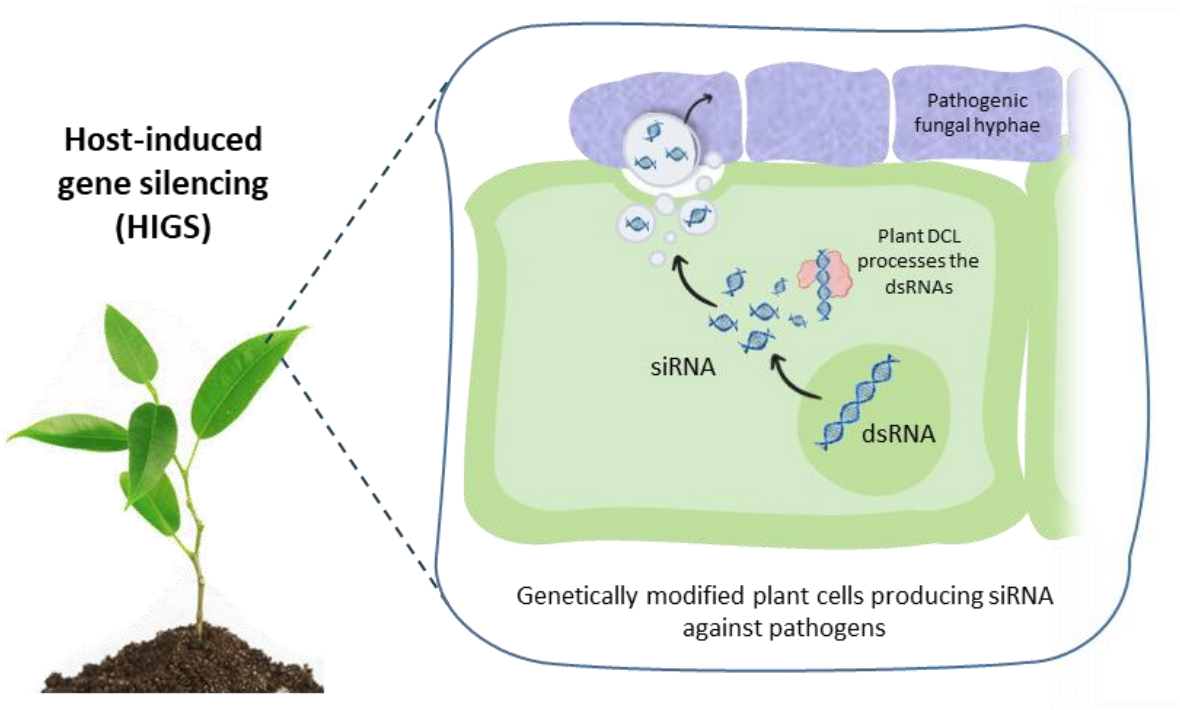

Figure 4. Schematic representation of HIGS in plants. The host plant is genetically modified to produce dsRNA molecules that target essential genes in the invading pathogen. Once the pathogen infects the plant, these miRNAs reach the pathogen, where they trigger RNAi-mediated gene silencing. This results in the downregulation of the target genes in the pathogen, thereby conferring resistance to the host plant.

To date, more than 170 studies have been published exploring the potential of HIGS for plant protection and it has demonstrated significant promise as a tool for controlling a broad spectrum of plant pathogens and pests (Koch and Wassenegger, 2021). However, HIGS practical application faces considerable limitations. The main drawback of HIGS lies in the need to genetically transform the host plants. This process is often complex, time-consuming, and costly, and in many crop and forest species, efficient transformation protocols are either lacking or not yet well established. Additionally, strict regulatory frameworks in regions such as the European Union severely limit or prohibit the deployment of genetically modified organism (GMO) and can take up to 10 years to reach commercial release (Bocos-Asenjo *et al.*, 2022). Public concerns about HIGS and political barriers further hinder HIGS acceptance and commercialization. Moreover, HIGS-based strategies are not considered very effective in postharvest products. These factors collectively limit the widespread implementation of HIGS in current agricultural and forestry practices, emphasizing the need for alternative RNAi-based strategies that do not require plant transformation, such as SIGS.

4.3.2. SIGS: an innovative, non-transgenic approach.

RNAi can also be triggered by externally encountered dsRNA, a process known as environmental RNAi (eRNAi) (Tabara *et al.*, 1998; Timmons and Fire, 1998; Whangbo and Hunter, 2008). By designing dsRNAs that specifically target essential genes in pathogens, eRNAi offers a promising strategy for disease control in plants (Forster and Shuai, 2020; Höfle *et al.*, 2020; Nerva *et al.*, 2020; Werner *et al.*, 2020). This is the basis of SIGS, a technology that involves the exogenous application of dsRNA molecules onto plant surfaces to confer protection against pathogenic organisms (Figure 5) (Wang and Jin, 2017).

Although eRNAi was first observed in the nematode *Caenorhabditis elegans*, where gene silencing was successfully triggered either by soaking the organism in a dsRNA solution (Tabara *et al.*, 1998) or by feeding it bacteria engineered to produce dsRNAs (Timmons *et al.*, 2001; Timmons and Fire, 1998), it was not until 2016 that this mechanism was effectively translated to plant protection, when Wang *et al.* (2016) and Koch *et al.* (2016) showed that topical application of dsRNAs conferred resistance to *Botrytis cinerea* and *Fusarium graminearum*, respectively.

Since then, SIGS has emerged as a promising tool against pests and pathogens, and the number of studies exploring its applications has grown exponentially, reflecting a rising trend in published research focused on SIGS-based strategies for plant protection (Mosquera *et al.*, 2025). Several studies have reported notable success through the external application of dsRNAs targeting essential or disease-associated genes in pathogenic fungi, such as *B. cinerea* (Wang *et*

al., 2016), *F. graminearum* (Koch *et al.*, 2016), *Fusarium asiaticum* (Song *et al.*, 2018a), *Sclerotinia sclerotiorum* (Mcloughlin *et al.*, 2018), *Rhizoctonia solani* and *Aspergillus niger* (Qiao *et al.*, 2021), *Phakopsora pachyrhizi* (Hu *et al.*, 2020), *Austropuccinia psidii* (Degnan *et al.*, 2022), *Aspergillus flavus* (Niño-Sánchez *et al.*, 2021) or even oomycetes, such as *Phytophthora infestans* (Kalyandurg *et al.*, 2021) and *Phytophthora capsici* (Cheng *et al.*, 2022).

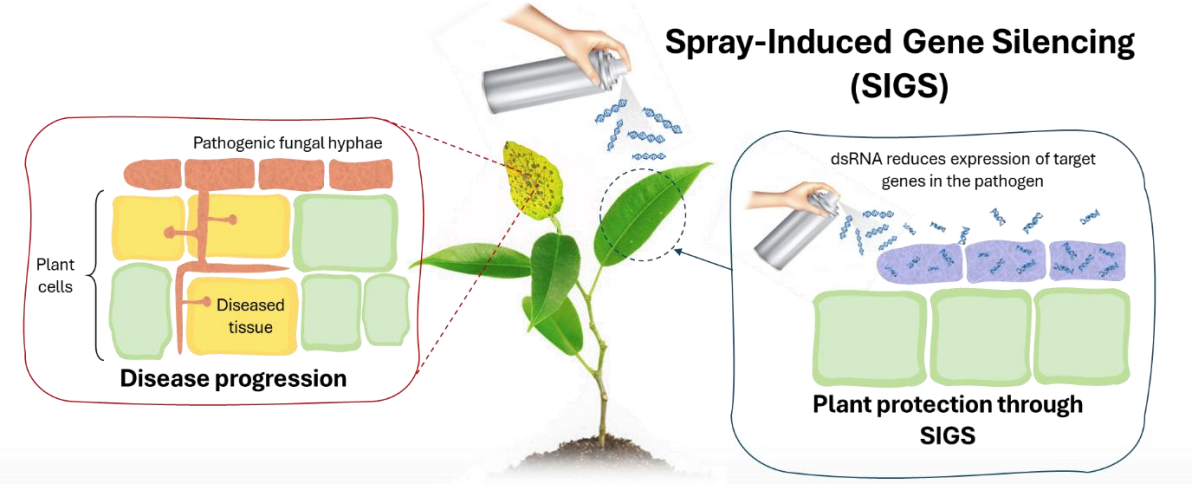

Figure 5. Schematic representation of SIGS. Left: In the absence of SIGS, the pathogen infects the plant, colonizing host tissues and causing disease symptoms. **Right**: When dsRNA is applied to the plant surface via SIGS, the RNA molecules are taken up by the pathogen (or the plant and transferred to the pathogen), leading to gene silencing of essential pathogen genes. This results in impaired infection, thereby enhancing plant protection.

SIGS represents a highly versatile and adaptable strategy for plant disease management. One of its greatest advantages lies in its flexibility: numerous dsRNA molecules can be designed to target a single gene or silence multiple genes simultaneously within a single pathogen, or even to act against multiple pathogens at once. This allows rapid response to emerging threats, rendering a versatile solution for a broad spectrum of pathogens across multiple crops (Taning *et al.*, 2020). Importantly, to date, there is no evidence that pathogens can develop resistance to SIGS. Unlike conventional pesticides, point mutations in the target sequence would not necessarily impair dsRNA efficacy, as new molecules can be easily redesigned to restore silencing. In fact, the only plausible resistance mechanism would require the pathogen to suppress its own RNAi machinery, an adaptation that could significantly compromise its fitness and pathogenicity. This makes SIGS not only effective, but also more robust against long-term resistance development. In addition, dsRNAs applied topically can be taken up by plant tissues and translocated to untreated areas, ensuring broader protection silencing (He *et al.*, 2023; Wang and Dean, 2020). SIGS has also proven effective against fungal pathogens during post-harvest stages, where HIGS has limited application (Nerva *et al.*, 2020; Wang *et al.*, 2016). From an environmental perspective, dsRNA is considered low-risk: it degrades naturally, is already present in food, and lacks toxicity, posing minimal risk of accumulation in the ecosystems

(Bachman *et al.*, 2020). Still, careful design is needed to avoid unintended silencing of non-target organisms. Finally, unlike HIGS, SIGS does not require the genetic transformation of host plants, which simplifies its application and improves its regulatory and social acceptance. Altogether, these features position SIGS as a practical, innovative, and sustainable alternative to conventional pesticides and transgenic approaches.

Nevertheless, this strategy also faces some key challenges, including the short protection window due to RNA instability under field conditions (light, oxygen, and temperature): 5–10 days, usually one week, with the efficacy of dsRNA decreasing over time (Koch *et al.*, 2016; Qiao *et al.*, 2021; Wang *et al.*, 2016). Additionally, nucleases present on plant surfaces can degrade dsRNA before it reaches the pathogen (Quilez-Molina *et al.*, 2024). Advances like inorganic nanoparticle (e.g., BioClay™, carbon dots, gold nanoparticles…), organic carriers (e.g., liposomes, and EVs), or even engineered bacteria producing dsRNA, are being developed to enhance stability and uptake (Figure 6) (Bocos-Asenjo *et al.*, 2022; Mosquera *et al.*, 2025; Niño-Sánchez, personal communication, 2024). All these formulations not only protect RNA molecules from degradation but also facilitate their uptake by pathogens (Wang *et al.*, 2023a). To ensure efficient delivery, the properties of these carriers such as particle size, shape, dsRNA dosage, the ratio of carrier to dsRNA, and duration of treatment are being optimized. This area represents a major focus of current research, with ongoing efforts to enhance delivery systems for better stability, uptake efficiency, and practical application in the field.

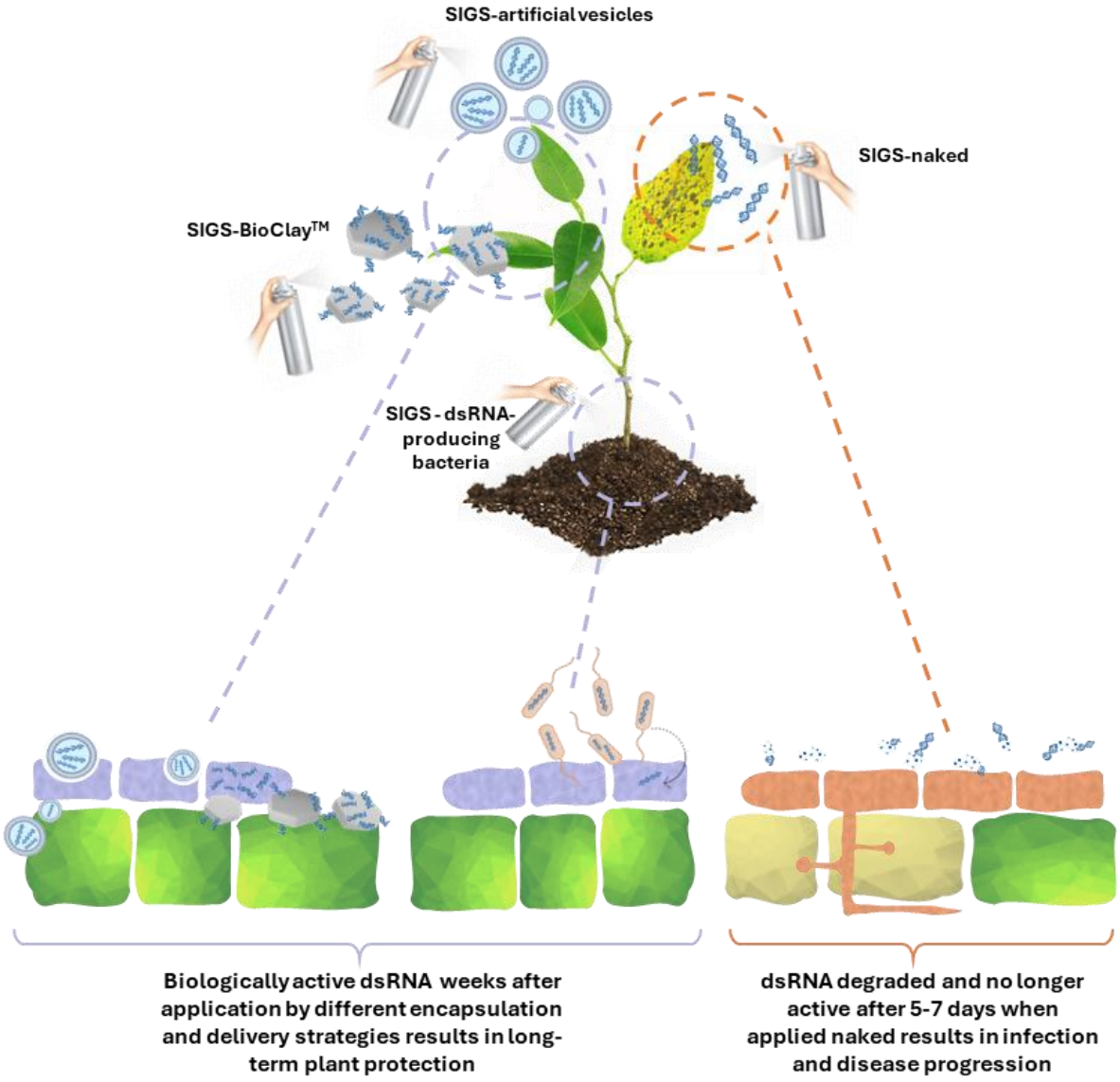

Figure 6. Schematic representation of the effect of dsRNA formulation on the effectiveness of SIGS. Left: Encapsulation of dsRNA or its delivery through engineered bacteria enhances its stability and prolongs biological activity, allowing for more effective uptake by pathogens and extended protection of the plant over time. **Right:** When naked dsRNA is applied, it is rapidly degraded by environmental factors such as UV light, temperature, and nucleases, resulting in a short protection window (typically 5–7 days).

Another limitation is the efficient uptake of dsRNA by the pathogen. SIGS strategies are highly dependent on dsRNA molecules managing to enter the pathogen cells (Qiao *et al.*, 2021). dsRNA molecules can either remain on the plant surface and be taken up by the fungus directly or be taken up by the plant (direct uptake) or being internalized and possibly processed into siRNAs by the plant host and then transferred to fungal cells (indirect uptake) (Cai *et al.*, 2018b; Koch *et al.*, 2016; Song *et al.*, 2018b; Wang *et al.*, 2016) (Figure 7). Interestingly, by indirect uptake, siRNA molecules can travel systematically through the plant (Koch *et al.*, 2016). This systemic movement enhances the efficiency of SIGS by providing broader protection beyond the initial treatment area. Before entering plant or fungal cells, dsRNAs have to cross some physical

barriers, such as the pathogen´s cell wall and plasma membrane and, in the case of indirect uptake, the plant cuticle as well (Garcia-Rubio *et al.*, 2020; Qiao *et al.*, 2021). These structural barriers can significantly limit the internalization of RNAi-inducing molecules into both fungal and plant cells (Bennett *et al.*, 2020; Šečić and Kogel, 2021).

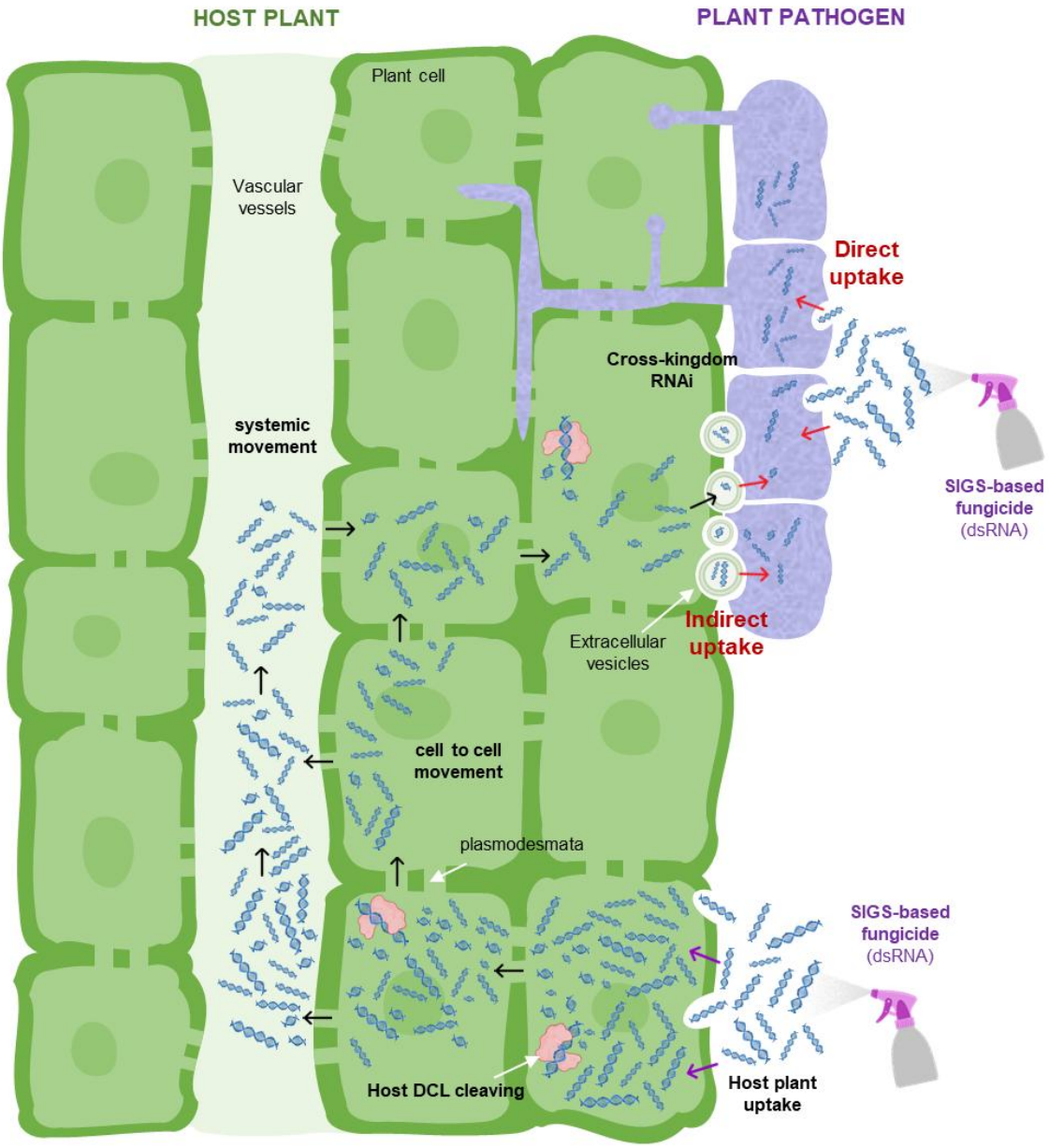

Figure 7. Schematic representation of direct and indirect uptake pathways of dsRNAs by plant pathogens (modified from Mosquera *et al.*, 2025). Via direct uptake dsRNAs are sprayed and absorbed directly by the pathogen at the site of infection. Via indirect uptake dsRNA is first absorbed by the plant cells, where it may be processed into siRNAs or remain as dsRNA. These silencing molecules can then move throughout the plant via the vascular system, reaching tissues distant from the application site. Pathogens colonizing plant tissues can subsequently take up the sRNA molecules, leading to the silencing of the target genes.

dsRNA uptake efficiency by target pathogens varies widely. Certain fungi, such as *S. sclerotiorum, Rhizoctonia solani, Aspergillus niger*, and *Verticillium dahliae*, have shown a strong ability to directly internalize dsRNA, enabling effective gene silencing (Qiao *et al.*, 2021). In

contrast, others like *Colletotrichum gloeosporioides* or some *Phytophthora* spp. exhibit poor direct uptake, which reduces the success of SIGS-based strategies (Qiao *et al.*, 2021; Wang *et al.*, 2023b). Additionally, factors such as the developmental stage of the pathogen and the physical condition of the plant surface can influence uptake efficiency (Bocos-Asenjo *et al.*, 2022; Degnan *et al.*, 2022; Höfle *et al.*, 2020; Mosquera *et al.*, 2025; Werner *et al.*, 2020). Ultimately, the effectiveness of SIGS is highly dependent on the specific characteristics of each pathogen.

Economically, while the cost of dsRNA production has dropped significantly (from 12,500 USD/g in 2008 to 60 USD/g in 2018 and less than 0.5 USD/g nowadays), large-scale use still demands affordable synthesis methods. Innovations like microbial fermentation and cell-free systems offer scalable, low-cost solutions. Several biotech companies and multinationals are now investing in these technologies, signaling a shift toward commercial viability (Bocos-Asenjo *et al.*, 2022).

In conclusion, SIGS presents a promising and eco-friendly plant protection strategy with significant potential for application against forest pathogens, where the effectiveness of conventional control methods is often limited and chemical treatments are highly restricted. Furthermore, SIGS enables the silencing of key pathogen genes without the need to generate transgenic plants, an important advantage given that genetic transformation protocols are lacking for most forest species and that the use of GMOs faces strong regulatory and social barriers. The topical application of dsRNAs in SIGS approach offers considerable opportunities for the treatment of forest diseases, and its adaptability to target emerging pathogens makes it particularly suitable for responding to new disease outbreaks in forest ecosystems. However, for SIGS to become a practical tool for forest disease management, it is essential to overcome several technical challenges. Careful design of dsRNA molecules and optimization of delivery strategies are crucial to enhance dsRNA uptake and stability, thereby ensuring prolonged biological activity and effective silencing of target genes within the pathogen.

4.4. Key considerations for effective SIGS strategy

After a comprehensive understanding of SIGS strategy and evaluating its potential for controlling plant pathogens, with a particular focus on those impacting forest ecosystems, there are several key factors that determine its efficacy that were comprehensively reviewed by Mosquera *et al.* (2025).

Firstly, it is essential to confirm that the target pathogen possesses a functional RNAi pathway, in order to develop RNAi-based fungicides. The core components of the RNAi pathway and their functionality have been characterized in several plant pathogenic fungi (Mosquera *et al.*, 2025). Interestingly, the number of genes encoding these components can vary considerably among species. Some fungi, such as *Schizosaccharomyces pombe*, possess only a single copy of DCL, AGO, and RdRp (Sigova *et al.*, 2004). In contrast, many other fungal species contain multiple copies of these genes (Qiao *et al.*, 2021; Wang *et al.*, 2016), which may exhibit functional redundancy, have lost functionality, or may not be required for RNAi activity under certain conditions.

When selecting target genes for SIGS, researchers often focus on essential genes crucial for pathogen growth (Christiaens *et al.*, 2020) or on pathogenicity genes involved in host colonization and virulence (Idnurm and Howlett, 2001). While essential genes enable broad inhibition of pathogen development across its life cycle, pathogenicity genes offer greater specificity but are often more difficult to identify and target, as they tend to be expressed only at certain stages and are frequently absent or poorly annotated in genomic data (Mosquera *et al.*, 2025). dsRNAs can be designed to target either a single gene or multiple genes. While single-gene targeting simplifies design, multi-gene targeting is especially advantageous when dealing with paralogous genes, tightly regulated pathways, or genes prone to resistance, as it helps prevent functional compensation (Koch *et al.*, 2019; Qiao *et al.*, 2021; Wang *et al.*, 2016).

Careful design of dsRNA molecules is essential for achieving efficient target gene silencing. Targeting accessible regions within the target gene, with low secondary structure and within exonic sequences, particularly toward the 3'-end of mRNA, tends to enhance silencing outcomes (Bohula *et al.*, 2003; Vickers *et al.*, 2003; Westerhout and Berkhout, 2007). Regarding molecule size, the optimal dsRNA length for effective gene silencing varies among fungal species. While some studies have reported higher efficacy with shorter molecules (Degnan *et al.*, 2022; Höfle *et al.*, 2020), others have observed enhanced silencing with longer dsRNAs (Werner *et al.*, 2020). To minimize off-target effects in SIGS strategies, target sequence specificity must be maximized by selecting regions unique to the pathogen for the design and avoiding sequences that share significant homology with plant genes, beneficial microbes, or non-target organisms (Wang *et al.*, 2023c). Some Bioinformatic tools are available to predict potential off-target interactions by screening candidate dsRNAs against host and environmental transcriptomes (Bocos-Asenjo *et al.*, 2022; Mosquera *et al.*, 2025).

Finally, to enhance SIGS efficiency and overcome barriers like poor dsRNA uptake and instability, strategies such as surfactants which facilitate dsRNA penetration through plant stomata (Degnan *et al.*, 2022), endocytosis stimulants which improve dsRNA internalization in plants (Bennett *et al.*, 2020), and nanocarriers (Jain *et al.*, 2022) have been developed. Nanocarriers have emerged as powerful tools, not only protecting dsRNA molecules from environmental degradation and enhancing cellular uptake but also promoting their systemic movement within the plant, resulting in more prolonged protection (Niño-Sánchez *et al.*, 2022). SIGS nanocarriers under study include organic nanocarriers like lipid vesicles and protein- or polymer-based nanoparticles, inorganic carriers such as layered double hydroxide (LDH) clays and silica nanoparticles, and carbon-based materials like carbon dots and nanotubes. Among these, LDH is probably the most explored option for the delivery of dsRNAs into plant and fungal cells, as it releases dsRNA molecules in a controlled manner as the clay degrades (Jain *et al.*, 2022).

As forest health continues to decline under the combined pressures of global change, invasive pathogens, and ineffective management strategies, it becomes increasingly urgent to explore new solutions. Forest diseases continue to pose a serious threat to ecologically and economically important tree species worldwide. Pathogens such as *F. circinatum* and *P. cinnamomi*, along with others described earlier, have contributed to the decline of both native forests and commercial plantations, with severe consequences for biodiversity, ecosystem services, and timber production. Despite efforts to control these pathogens, current strategies often prove insufficient due to several limitations. These challenges highlight the urgent need for innovative, sustainable, and targeted approaches to disease control. In this context, RNAi has emerged as a powerful and versatile tool. Its sequence specificity, low environmental impact, and adaptability make it especially suitable for the management of forest pathogens. Among RNAi-based methods, SIGS offers a promising alternative that does not require host transformation and may represent a realistic solution for controlling diseases in trees. Therefore, we aimed to explore the use of SIGS against *F. circinatum* and *P. cinnamomi* as model systems to evaluate its potential for the control of diverse forest diseases.

Hypotheses and objectives

The previous chapter focused on outlining the challenges in the treatment of forest diseases, as well as the important impacts they have on society, economy and ecology. Despite the limitations of current treatment options for forest diseases, new environmentally friendly technologies are emerging that offer potential solutions. One such technology is SIGS (Spray-induced gene silencing) strategy, which has the potential to be a valuable tool in forest management due to its ease of application, safety, and specificity. However, it has not yet been used against forest pathogens. This chapter shows the hypotheses that have been proposed throughout this research, along with the main objective of the research and the specific objectives that have been set out to achieve it.

1. Hypotheses

RNA-based technologies have opened new possibilities in the fight against pathogenic organisms. Based on the mechanism of RNA interference, there are two distinct methodologies: HIGS, which is based on the production of silencing molecules by the plant, which are then delivered to the pathogen, thereby triggering the silencing of target genes in the pathogen; and SIGS, which is based on the ability of some organisms to uptake RNAs from the environment (Cai *et al.*, 2018a; Niu *et al.*, 2021). For its application against plant pathogens, SIGS offers an important advantage since it does not require the generation of genetically modified plants. As a result, this methodology is potentially easy to apply and rapidly scalable, as well as sustainable and environmentally friendly (Wang and Jin, 2017). This has prompted extensive investigation in recent years into the efficacy of this approach in managing pathogens and crop pests, particularly fungal pathogens of importance in agriculture such as *Botrytis cinerea*, *F. graminearum*, and *S. sclerotiorum* (Kim *et al.*, 2023; McRae *et al.*, 2023; Pant and Kaur, 2023; Qiao *et al.*, 2023; Werner *et al.*, 2020).

However, this technology is largely unexplored in the field of forest pathology. SIGS could be an effective method for controlling many of the pathogens that threaten tree species;

however, it is necessary to investigate whether these pathogens are susceptible to this technology. This can be achieved by conducting tests to determine if they possess the essential RNAi machinery components, if they are capable of taking up dsRNA, and identifying suitable target genes for their control. Moreover, it has been demonstrated that the design of silencing molecules and the selection of target genes are crucial considerations for the development of more effective treatments and the avoidance of adverse effects in other organisms (Šečić and Kogel, 2021). Based on this knowledge, we propose that the use of SIGS could provide a potential avenue for the control of pathogens in forests, where most diseases currently lack effective treatments and the use of chemical fungicides is highly restricted. In light of the above, this study proposes that SIGS technology is an effective approach to controlling pathogens that cause forest diseases. To test this technology, we have selected two very different pathogens: an airborne fungus affecting conifers (*F. circinatum*) and a soil-borne pathogenic oomycete infecting among other species *Quercus* spp. (*P. cinnamomi*). The potential of SIGS will be assessed in these pathogens, which present a greater challenge due to their vascular nature, as opposed to foliar pathogens, which are easier to apply and already widely studied.

The following hypotheses were proposed at the beginning of this dissertation:

- The effectiveness of dsRNA silencing can be enhanced through the optimization of molecule design.
- *F. circinatum* and *P. cinnamomi*, like other species of their genus, possess RNAi machinery and are susceptible to control by SIGS.
- *F. circinatum* and *P. cinnamomi* are able to take up dsRNA molecules from the environment, either directly or indirectly.
- It is possible to control the infection of *F. circinatum* and *P. cinnamomi* using SIGS technology.

2. Objectives

The primary objective of this doctoral dissertation is to investigate the potential applications of SIGS technology in the management of tree pathogens. To this end, two distinct systems will be tested to ascertain the scope for the use of SIGS in the control of forest diseases: a pathogenic fungus, *F. circinatum,* and a pathogenic oomycete, *P. cinnamomi*.

Specific objectives:

I. To enhance the efficiency of SIGS silencing through the optimization of dsRNA design and production. To achieve this objective, the following aspects were proposed:

A. To select target genes in *F. circinatum* and *P. cinnamomi* based on their relevance in pathogen development and survival.
B. To design the dsRNA molecules taking into account important aspects that have an impact on the efficiency of the technique.
C. To obtain the designed dsRNA molecules in a cost-effective manner, in sufficient quantity and with sufficient quality for testing.

II. To apply SIGS technology to a relevant forest pathogenic fungus and evaluate the efficiency of the technique and the designed molecules in controlling the disease.

III. To use SIGS technology against a significant forest pathogenic oomycete and assess the efficiency and limitations of the technique in the control of the disease.

Methods

1. Organisms

1.1. Bacteria

The bacterial strains used in this study were two *Escherichia coli* strains (Table 1):

- TOP10 Chemically Competent *Escherichia coli*: this strain is widely used for cloning purposes due to its high transformation efficiency and lack of endonuclease (endA1) and recombinase (recA) activity, which allows for the efficient generation of a high number of transformants from a ligation reaction, particularly when working with low-efficiency ligations (Liu *et al.,* 2018). However, strain TOP10 has a functional RNase III that degrades dsRNA so it is unable to produce dsRNA (Delgado-Martín and Velasco, 2021). This strain was utilized for low-efficiency ligation transformations.
- RNaseIII-null mutant *Escherichia coli* HT115(DE3): this is a derivative of *E. coli* K12 specifically engineered for RNA interference (RNAi) applications. It has a T7 RNA polymerase gene under lacUV5 control and lacks RNase III activity, enabling efficient production of double-stranded RNA (dsRNA). This non-pathogenic *E. coli* strain is an RNaseIII-null mutant that allows dsRNA production and accumulation without fitness cost, being one of the most widely expressed systems for dsRNA production (Dasgupta *et al.,* 1998; Tenllado *et al.*, 2003; Timmons *et al.*, 2001). This strain was utilized for producing dsRNA.

Table 1. *E. coli* strains used for cloning

Strain	Genotype	Use
TOP10 Chemically Competent *E. coli*	F- mcrA Δ(mrr-hsdRMS-mcrBC) Φ80lacZΔM15 Δ lacX74 recA1 araD139 Δ(araleu)7697 galU galK rpsL (StrR) endA1 nupG	Cloning
RNaseIII-null mutant *E. coli* HT115(DE3)	F-, mcrA, mcrB, IN(rrnD-rrnE)1, rnc14::Tn10(DE3 lysogen: lacUV5 promoter-T7 polymerase	dsRNA production

1.2. Fungi

Fusarium circinatum isolate used in this work, Fc072V, belongs to mating type 2 (MAT-2). It was obtained from diseased *P. radiata* trees in Cantabria, northern Spain, during a previous study in the Forest Entomology and Pathology Laboratory (University of Valladolid) (Zamora-Ballesteros *et al.*, 2021).

1.3. Oomycetes

Phytophthora cinnamomi strain PH2003 used in this study was kindly provided by the Centro de Sanidad Forestal de Calabazanos (Palencia, Spain). This strain was originally isolated from a *Castanea sativa* specimen.

1.4. Plants

a. Spinacia oleracea

For the dsRNA rapid efficacy test against *F. circinatum*, young spinach detached leaves were obtained fresh from the local market. These leaves were free of fungicides and other chemical treatments that could potentially interfere with the growth of *F. circinatum*.

b. Pinus radiata

P. radiata, the most susceptible host of *F. circinatum* was used to assess dsRNA efficacy against the pathogenic fungi in forest seedlings. *P. radiata* seeds (Provenance: Galicia, Spain) were provided by the Serranillo National Nursery (Guadalajara, Spain).

c. Lupinus angustifolius

L. angustifolius seedlings were employed in preliminary assays for assessing dsRNA efficacy against the pathogenic oomycete *P. cinnamomi*. *L. angustifolius* var. 'Primadonna' seeds used in this study were generously provided by the Nordic Seed Company (Galten, Denmark).

d. Nicotiana benthamiana

N. benthamiana is the most widely used experimental plant. We employed *N. benthamiana* wild type (WT) seedlings to perform preliminary assays against *P. cinnamomi*.

e. Quercus ilex

Q. ilex acorns were kindly provided by the Central Forest Nursery of the Junta de Castilla y León (Valladolid, Spain). The provenance of the acorns was RP.2 Cuenca Central del Duero (Spain).

2. Cloning vectors

2.1. T777T

Enhanced RNAi vector for *C. elegans*. T777T plasmid (Addgene plasmid # 113082; http://n2t.net/addgene:113082; RRID: Addgene_113082) is an improved variant of the L4440 plasmid (Addgene plasmid # 1654 ; http://n2t.net/addgene:1654 ; RRID:Addgene_1654). The T777T plasmid backbone is a vector designed for efficient production of double-stranded RNA (dsRNA) in *E. coli* HT115(DE3) cells (Sturm *et al.*, 2018). Key features of the T777T vector include two T7 promoter sites in opposite directions adjacent to two T7 polymerase termination sequences, and a *lacZ* coding region and its regulator sequences (promoter and terminator) between the two T7 promoters (Figure 8). *lacZ* gene serves as a selectable marker for confirming successful cloning or insertion of dsRNA template sequences. The promoters are recognized by the T7 RNA polymerase-inducible β-D-1-thiogalactopyranoside isopropyl (IPTG), which means that transcription of the gene of interest can be induced by adding this compound. The expression of this plasmid in bacteria leads to the production of an RNA strand corresponding to the fragment between the promoter and terminator. Thus, this plasmid enables the production of RNA strands of the fragment in both senses, forming double-stranded RNA of the inserted sequence. The plasmid also contains selective antibiotic resistance markers to ensure stable maintenance and selection of the plasmid in *E. coli* strains during cloning and dsRNA production.

T777T map

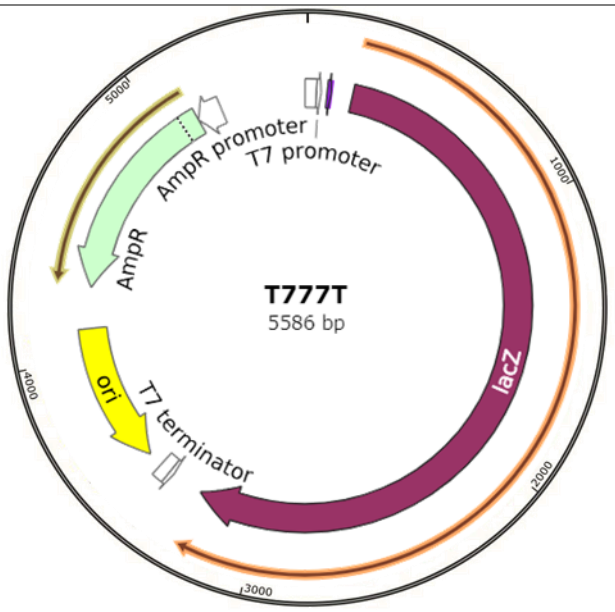

Feature	Location (bp)	Size	Direction	Type
T7 terminator	2 - 49	48	—	Terminator
T7 promoter	50 - 68	19	→	Promoter
lacZ	199 – 3,246	3,048	→	CDS

T7 promoter	3,379 – 3,397	19	←·	Promoter
T7 terminator	3,398 – 3,445	48	—	Terminator
ori	3,507 – 4,095	589	←·	Rep_origin
AmpR	4,266 – 5,126	861	←·	CDS
AmpR promoter	5,127 – 5,231	105	←·	Promoter

Figure 8. Circular map of the T777T illustrating key features. Including locations, sizes and senses of the essential functional elements: T7 promoters, T7 terminator, lacZ gene for blue-white screening and ampicillin resistance cassette.

3. Culture media and conditions

3.1. Bacteria

- Liquid Cultures: Cultures were grown in Luria-Bertani (LB) broth medium [containing 10 g Tryptone (Scharlab S.L., Barcelona, Spain), 10 g NaCl (Panreac Química S.L.U., Barcelona, Spain), 5 g Yeast Extract (Scharlab S.L., Barcelona, Spain) per L] in sterile Erlenmeyer flasks or tubes. Cultures were incubated in a shaking incubator at 37°C with constant agitation at 250–300 rpm to ensure aeration. When required, ampicillin (Sigma Aldrich, MO, USA) was added to a final concentration of 100 µg/mL. For dsRNA induction, HT115(DE3) transformants were grown in 500 mL flasks containing 100 mL of LB liquid medium with Amp100 at 37°C at 250 rpm. When the optical density at 600 nm (OD_{600}) was 0.8, cultures were supplemented with IPTG (NZYTECH, Lisbon, Portugal) at a final concentration of 1.0 mM and incubated under the same temperature and agitation conditions until reaching the stationary phase (between 4 and 8 h).
- Solid Cultures: Bacteria were seeded onto LB agar plates [containing 10 g Tryptone (Scharlab S.L., Barcelona, Spain), 10 g NaCl (Panreac Química S.L.U., Barcelona, Spain), 5 g Yeast Extract (Scharlab S.L., Barcelona, Spain), 15 g agar per L] and incubated in a static incubator at 37°C for 16–18 h until colonies were visible. Plates were stored at 4°C for up to two weeks. When required, ampicillin (Sigma Aldrich, MO, USA) was added to a final concentration of 100 µg/mL after autoclaving the media.
- Long-term storage: glycerol stocks of the bacterial strains were prepared from liquid cultures grown to the logarithmic phase (OD_{600}≈ 0.6–0.8). Glycerol was added to a final concentration of 30% (v/v), and the stocks were stored at -80°C.

3.2. Fungi

- Solid Culture: *F. circinatum* mycelium was cultured on Potato Dextrose Agar (PDA) (Scharlab S.L., Barcelona, Spain) plates at 25ºC for three days.
- Long-term storage: *F. circinatum* mycelium was preserved in glycerol (15%) at -80ºC.
- Induction of spore production: *F. circinatum* was cultured in a 250 mL flask with 100 mL of GOX liquid medium at 180 rpm and 25ºC for 48-72 h. GOX is a sporulation medium containing 60 g of sucrose (Sigma Aldrich, MO, USA), 7 g of NaNO3 (Sigma Aldrich, MO, USA), 3 g of peptone (Condalab, Madrid, Spain), 1 g of KH_2PO_4 (Panreac Química S.L.U., Barcelona, Spain), 0.5 g of $MgSO_4 \cdot 7H_2O$ (Panreac Química S.L.U., Barcelona, Spain), and 0.5 g of KCl (Panreac Química S.L.U., Barcelona, Spain) per L at a pH of 7. The cultures were filtered twice through sterile cheesecloths to remove hyphae. The spores were then collected by centrifugation at 4,400 x g for 10 min. The spores were suspended in sterile distilled water and counted using a Neubauer chamber or hemocytometer. The spore solution was adjusted to the optimal concentration using sterile distilled water.
- Spore germination: spore suspension was seeded in 5 ml of Potato Dextrose Broth (PDB) (Scharlab S.L., Barcelona, Spain) at a final concentration of 5×10^5 spores/ml. The suspension was then incubated for 8 h at 80 rpm and 23ºC. Germinated *F. circinatum* spores were used to assess dsRNA uptake ability.

3.3. Oomycetes

- Solid Culture: *P. cinnamomi* PH2003 was grown for 5 days at 25ºC on V8 medium (10%) [containing 10% V8® juice clarified with 10 g/L $CaCO_3$ (Panreac Química S.L.U., Barcelona, Spain) and 16 g agar (Panreac Química S.L.U., Barcelona, Spain) per L.
- Long-term storage: *P. cinnamomi* mycelium was stored in sterile cryotubes with sterile distilled water at room temperature.
- Zoospore production: mycelial plugs of 1 cm diameter were excised from an actively growing *P. cinnamomi* culture and transferred to a Petri dish containing pond water. Subsequently, the plates were placed at approximately 30 cm from an overhead light source and incubated at room temperature. Sporangia formation was typically observed after a period of three days. At this stage, the pond water was replaced with cold distilled water, and the plates were maintained in darkness for approximately 30 min to stimulate zoospore release. Multiple cold-water treatments were applied to enhance zoospore release.

3.4. Plants

a. *Pinus radiata*

Pine seeds were initially immersed in water for 24 h, replacing the water every 12 h. They were then maintained in hydrogen peroxide 3% (H_2O_2) for 15 min, washed three times with sterile distilled water and finally immersed in sterile distilled water for 30 min to remove the remaining hydrogen peroxide. Subsequently, sterilized *P. radiata* seeds were individually sown in germination trays containing a twice-autoclaved (105 kPa, 120 °C, 30 min) mixture of peat and vermiculite (1:1, v/v). The pines were cultivated for four months in a growth chamber at 21.5ºC, under a 16/8 h light/dark photoperiod, and were irrigated weekly.

b. *Lupinus angustifolius*

L. angustifolius seeds were surface-sterilized by immersion in a 1% (v/v) sodium hypochlorite (NaClO) (Panreac Química S.L.U., Barcelona, Spain) solution for 5 min under continuous agitation. Seeds were then thoroughly rinsed with sterile ultrapure water at least four times to remove any residual bleach. To promote uniform water absorption, seeds were subsequently soaked in sterile ultrapure water for 10 min before sowing. For germination, a vermiculite mixture was prepared by combining vermiculite and ultrapure MilliQ® water in a 2:1 ratio within a sterile ziploc bag. The sterilized seeds were sown in the moistened vermiculite and incubated at room temperature for three days to facilitate germination. After this period, the germinated seedlings were transferred to a hydroponic system and maintained in a growth chamber under a photoperiod of 16/8 h (day/night), with a temperature regime of 25ºC (day)/20ºC (night) and a daylight intensity of ~6000 lux (60–100 µmol m^{-2} s^{-1}).

c. *Nicotiana benthamiana*

N. benthamiana seeds were surface-sterilized by immersion in 70% ethanol (EtOH) (Panreac Química S.L.U., Barcelona, Spain) for 2 min, followed by two washes with MilliQ® water. Subsequently, a second sterilization step was performed using a 1% sodium hypochlorite (NaClO) (Panreac Química S.L.U., Barcelona, Spain) solution for 5 -10 min, after which the seeds were thoroughly rinsed with MilliQ® water to remove any residual bleach. The sterilized seeds were sown in Petri dishes containing Murashige & Skoog (MS) medium, prepared with 4.33 g/L MS salts (Sigma Aldrich, MO, USA), 8 g/L sucrose (Sigma Aldrich, MO, USA), and 3.2 g/L Phytagel (Sigma Aldrich, MO, USA), adjusted to a pH of 5.7–5.8. The plated seeds were stratified at 4ºC for 24 h to enhance germination before being transferred to a controlled growth chamber. Germination and seedling development occurred under a photoperiod of 16/8 h (day/night), with a temperature regime of 25ºC (day)/20ºC (night) and a daylight intensity of ~6000 lux (60–100

µmol m^{-2} s^{-1}). After 15 days, seedlings were carefully removed from the culture medium and transferred to a hydroponic system with Hoagland solution (Sigma Aldrich, MO, USA) within the same controlled environment. Plants remained in hydroponic culture for approximately two weeks until they developed sufficient root length for subsequent experimental trials.

d. *Quercus ilex*

Q. ilex acorns were surface sterilized by first rinsing them under running tap water for 2–3 min to remove dirt and debris. They were then immersed in 70% EtOH for 30 s to 1 min to ensure complete surface sterilization. After ethanol treatment, acorns were rinsed three to four times with sterile MilliQ® water to remove any remaining ethanol residues. Sterilized acorns were then placed on sterile filter paper and allowed to air dry under sterile conditions before sowing. Once dried, acorns were individually sown in germination trays (96 mL per cell) containing a twice-autoclaved (105 kPa, 120 °C, 30 min) mixture of peat, vermiculite, and perlite in a 2:1:1 ratio. The trays were maintained in a greenhouse under controlled conditions (20–25°C during the day, 15–18°C at night, under a 16/8 h light/dark photoperiod, and irrigated weekly) for five months to allow for germination and seedling development. For hydroponic plant trials, the acorns were also planted in vermiculite, which was kept at room temperature permanently moistened. After 15 days, when the acorn has germinated and developed roots, the seedlings were transferred to hydroponic culture in test tubes with sterile distilled water and maintained in a growth chamber (21.5°C, and a 16/8 h light/dark photoperiod) for another 15 days.

4. Cloning

Plasmid cloning is the process by which a specific DNA sequence (the insert or fragment of interest) is inserted into a plasmid. In this study, the dsRNA templates generated by Overlap Extension Polymerase Chain Reaction (OE-PCR) were cloned into the plasmid T777T, which was designed for dsRNA production (Sturm *et al.*, 2018), obtaining the plasmids T777T-FcPTP-dsRNA, T777T-FcVDS-dsRNA, T777T-FcCHS-dsRNA, T777T-PcPTP-dsRNA, T777T-PcDDS-dsRNA, T777T-PcDCL-dsRNA and T777T-YFP-dsRNA. The following methodology was used:

4.1. Restriction enzyme reaction

To ensure successful insertion of the dsRNA templates into the vector, a digestion with specific restriction enzymes was conducted. We selected restriction enzymes with a single cutting point to cut plasmid and fragments and leave sticky ends to facilitate insertion (Table 2). Between 0.5 µg and 5 µg of DNA were used per reaction in a 50 µL volume, following the temperature and incubation specifications provided by the manufacturer. Plasmid digestion was

verified through 1% agarose gel electrophoresis. The 2.3 kb band was then excised and purified using NucleoSpin® Gel and PCR Clean-up (Macherey-Nagel, Düren, Germany).

Table 2. Restriction Enzymes (RE) used in this study. These RE exhibit a single point of cleavage in both the vector and insert, situated in the region between the T7 promoters and terminators.

RE	Cut site	Ends	Manufacturer	Digestion
KpnI	GGTAC/C	sticky	New England Biolabs, Ipswich, MA, USA	T777T-YFP-dsRNA; T777T-FcCHS-dsRNA; T777T-FcPTP-dsRNA; T777T-FcVDS-dsRNA; T777T-PcDCL-dsRNA; T777T-PcPTP-dsRNA, T777T-PcEDS-dsRNA
BglII	A/GATCT	sticky	New England Biolabs, Ipswich, MA, USA	T777T-YFP-dsRNA; T777T-FcCHS-dsRNA; T777T-FcVDS-dsRNA; T777T-PcDCL-dsRNA; T777T-PcPTP-dsRNA; T777T-PcEDS-dsRNA
SacII	CCGC/GG	sticky	New England Biolabs, Ipswich, MA, USA	T777T-FcPTP-dsRNA

Point of cleavage indicated by a "/"

4.2. DNA ligation reaction

The digested fragments and plasmid were joined through a ligation reaction. Ligation was performed in 20 µL reactions using T4 DNA ligase (Thermo Fisher, Waltham, MA, USA). The ligation was optimized using an insert:vector ratio of 3:1. The ligation was performed according to the enzyme specifications and subsequently inactivated by incubation at 65 °C for 10 min.

The resulting recombinant plasmids were initially transformed into *E. coli* TOP10 cells, a strain commonly used for low-efficiency ligation transformations, as described in Methods Section 5. Subsequently, the purified plasmids were transformed into the dsRNA-producing *E. coli* strain HT1115 (DE3).

5. Bacterial transformation

The plasmids T777T-FcPTP-dsRNA, T777T-FcVDS-dsRNA, T777T-FcCHS-dsRNA, T777T-PcPTP-dsRNA, T777T-PcDDS-dsRNA, T777T-PcDCL-dsRNA and T777T-YFP-dsRNA were initially transformed into TOP10 Chemically Competent *E. coli* cells by heat shock method. The plasmids extracted from TOP10 transformants were subsequently employed for the transformation of RNaseIII-null mutant *E. coli* strain HT115(DE3) by heat shock method, which is capable of producing dsRNA. Transformations were conducted using the heat shock method.

5.1. *Escherichia coli* competent cells preparations

Competent cells of two strains of *E. coli* TOP10 and *E. coli* HT115 (DE3) were prepared for cloning the plasmids following the standard protocol with calcium chloride (Sambrook and Russell, 2006). Preinoculum of the corresponding bacterial strains was prepared in 3 ml of LB liquid medium and incubated overnight at 37ºC and 250 revolutions per minute (rpm). 1 ml of this

preinoculum was added to 200 ml of fresh LB medium in a 1/2 L flask and incubated in a shaker at 37ºC and 250 rpm until the OD_{600} reached 0.3-0.4 (measured in a spectrophotometer). From this point forward, all procedures were carried out at 4 °C to maintain cell viability. The culture was centrifuged at 4000 rpm for 10 min to obtain a pellet which was resuspended in a solution containing 2 ml 0.1M $CaCl_2$ and 800 µL 50% glycerol and stored at -80ºC.

5.2. *Escherichia coli* transformation by heat shock method

Heat shock method was used for plasmid propagation. Plasmids were pooled with a 50 µl volume of the previously prepared competent cells and incubated for 30 min on ice. This was followed by a heat shock at 42 ºC for 50 s -1 min, immediately transferred to ice for 2 min. After that, 450 µl of LB liquid medium were added to the mixture, which was then incubated for 1 h and 15 min at 37ºC and 250 rpm. Transformants were screened in LB Amp_{100} solid medium plates incubated overnight at 37ºC. The bacterial colonies that integrated the plasmid were capable of growth on an antibiotic-supplemented medium, due to the presence of an ampicillin resistance cassette within the plasmid. Transformants were further verified by colony PCR (see Methods Section 10.2). In this reaction, where the region between the T7 promoters was amplified, bands of the size of the inserts were observed, indicating that the cloning was successful. To verify the accuracy of the inserts, a miniprep was conducted using the NucleoSpin® Plasmid Kit (Macherey-Nagel, Düren, Germany) for the isolation and purification of recombinant plasmid from the bacterial cultures. The plasmids were used for the amplification of the region between the T7 promoters by PCR. PCR products were sequenced by Sanger sequencing through the company Stab Vida, and the sequences were analyzed using Geneious software to confirm the correct insert sequences.

6. Primer design

PCR primers were designed with the sequence of the beginning of the fragment (forward - F) and with the reverse complement sequence of the end of the fragment (reverse - R) of the fragment to be amplified (Table 3). Primers parameters were studied using Oligo Calc tool (http://biotools.nubic.northwestern.edu/OligoCalc.html), adjusting the sequence to have a GC-content around 40-60% and melting temperature (T_m) of ~60ºC. We designed the primers to end in C/G to minimize wobble during primer extension.

Primers for OE-PCR have been designed in accordance with the following specifications:

- Outer primers include the sequence of the corresponding restriction site: KpnI recognition sequence was added at the 5' end of the first forward and BglII or SacII (only

for the FcPTP-dsRNA fragment because this sequence already contained a BglII recognition site) in reverse orientation at the 5' end of the first reverse. In addition, at the 5' end of all outer primers, there was added a sitting sequence, which is necessary for efficient RE cleavage and is usually arbitrary.

– The rest of the primers included at the 5' end a sequence of 20 nt of the gene immediately upstream in the dsRNA design in the case of the forward primer or 20 nt in reverse orientation of the gene immediately downstream in the dsRNA molecule in the case of the reverse primer.

Table 3. Primers specifically designed for PCR performed in this research.

Name	Sequence	T_m (ºC)	Use
KpnI_yfp_F*	ctgaacggtaccCGGCCTGCAGTGCTTCGCC	60	OE-PCR
BglII_yfp_R*	ggtcatagatctCTCGTCCATGCCGAGAGTGATCC	60	OE-PCR
KpnI_Fc-chs1_F*	ctgaacggtaccCGTCACATTCTCCTGGTTCTCACTC	60	OE-PCR
Fc-chs1_R	gagggtcgtagtgttcttcgTGTTTCCGAGAGCGAGGACGAATTG	60	OE-PCR
Fc-chs2_F	cgtcctcgctctcggaaacaCGAAGAACACTACGACCCTCATACG	60	OE-PCR
Fc-chs2_R	gatcggaggaagtcgaggaaACATGGTGATGCTCACAGGTGAAATTGAC	60	OE-PCR
Fc-chs3b_F	acctgtgagcatcaccatgtTTCCTCGACTTCCTCCGATCCG	60	OE-PCR
Fc-chs3b_R	gtactgatcatcttggtagtGTAAATACGACACCTAGAATTTCTCCTGTCC	60	OE-PCR
Fc-gls1_F	attctaggtgtcgtatttacACTACCAAGATGATCAGTACTACGATCAAGG	60	OE-PCR
BglII_Fc-gls1_R*	ggtcatagatctGCCATTGTCGTAGTATCCATCTTGGTATTG	60	OE-PCR
KpnI_Fc-pp2a_F*	ctgaacggtaccACCCTCAACGAATCACAATCCTCCG	60	OE-PCR
Fc-pp2a_R	aaagttaaaaagtcgaacatGCTTGGGGAGAGGCCGCC	60	OE-PCR
Fc-ppg1_F	atggcggcctctccccaagcATGTTCGACTTTTTAACTTTGAGCGTTGTGATC	60	OE-PCR
Fc-ppg1_R	ggcggcctctccccaagcCGAGGTGAAAGGGAGAATTCGTCG	60	OE-PCR
Fc-sit4_F	gaattctccctttcacctcgCCAACAGAGATCACAAACCCCAAGTTG	60	OE-PCR
Fc-sit4_R	cgcagaagagtagagggataTCTCCCAGGAAAATGTATCGAGTATCGG	60	OE-PCR
Fc-tap42_F	cgatacattttcctgggagaTATCCCTCTACTCTTCTGCGCGCG	60	OE-PCR
SacII_Fc-tap42_R*	ggtcatccgcggGTCTCGCGCCGCCTACGAG	60	OE-PCR
KpnI_Fc-vps51_F*	ctgaacggtaccTCTTTCAAAGAGCTTGAAGATCAAATCCAGATTC	60	OE-PCR
Fc-vps51_R	ttcttttcaagaagagattgTGAAGGAACAGCCTTCAGGCCAAAGC	60	OE-PCR
Fc-dctn1_F	gcctgaaggctgttccttcaCAATCTCTTCTTGAAAAGAAGAACAGTCGCG	60	OE-PCR
Fc-dctn1_R	gcgaatgagctctggcagacCTTGAGGTTCTCGACTGGTCGGTTC	60	OE-PCR
Fc-sac1_F	gaccagtcgagaacctcaagGTCTGCCAGAGCTCATTCGCAAAGC	60	OE-PCR
BglII_Fc-sac1_R*	ggtcatagatctCTTCATCGCTGCTGTCGATGCGTAC	60	OE-PCR
KpnI_Pc-dcl1_F*	ctgaacggtaccCAACGTGAATAACAGGAGGAAGCAGAAG	60	OE-PCR
Pc-dcl1_R	cgtgcccaataaattcgtcaCCTTGTACTCTCGTCTATCTCGATACC	60	OE-PCR
Pc-dcl2.1_F	agatagacgagagtacaaggTGACGAATTTATTGGGCACGATCCAAGTTAC	60	OE-PCR
Pc-dcl2.1_R	atgctcttcccgccgtagcgGTCCTCCACGTACAAATTGCCATTCTTC	60	OE-PCR
Pc-dcl2.2_F	gcaatttgtacgtggaggacCGCTACGGCGGGAAGAGCATG	60	OE-PCR
BglII_Pc-dcl1_R*	ggtcatagatctACGTGTGCAGGCGGTTCAGGAAG	60	OE-PCR
KpnI_Pc-pp2a_F*	ctgaacggtaccGCGCGGCAACCACGAGAGC	60	OE-PCR

Pc-pp2a_R	atgcggatctggtcgagcgtGCGCGTGGTCCAGCGTGTC	60	OE-PCR
Pc-ppg1_F	cgacacgctggaccacgcgcACGCTCGACCAGATCCGCATCATC	60	OE-PCR
Pc-ppg1_R	agaccgtcacggggctgctcTGATGCGCTCTGCAGATTAGCTGAATG	60	OE-PCR
Pc-sit4_F	ctaatctgcagagcgcatcaGAGCAGCCCCGTGACGGTC	60	OE-PCR
Pc-sit4_R	ctgcgtgttgtgcagctcgaGCAGCAGCGTGATGCGGTCC	60	OE-PCR
Pc-tap42_F	ggaccgcatcacgctgctgcTCGAGCTGCACAACACGCAGCTG	60	OE-PCR
SacII_Pc-tap42_R*	ggtcatagatctGTCCAAGAACTCGGTGAGGAAGAC	60	OE-PCR
KpnI_Pc-dhcr7_F*	ctgaacggtaccATGCCCGAGATCATCTCGGCGC	60	OE-PCR
Pc-dchcr7_R	cttgcaacggacttggatttCCGCAGCGGCAGTTGGTG	60	OE-PCR
Pc-dctn1_F	ttcaccaactgccgctgcggAAATCCAAGTCCGTTGCAAGCCCAC	60	OE-PCR
Pc-dctn1_R	ttcgtcgtcctgtgcgcgtgGACGCCATGCTCATCGTTTGCG	60	OE-PCR
Pc-sac1a_F	caaacgatgagcatggcgtcCACGCGCACAGGACGACGAAC	60	OE-PCR
Pc-sac1a_R	cggcgtgagcgtgggcaggtCTAGCATCATGTTCACGAGGCTGTG	60	OE-PCR
Pc-sac1b_F	cctcgtgaacatgatgctagACCTGCCCACGCTCACGCC	60	OE-PCR
BglII_Pc-sac1b_R*	ggtcatagatctCGATTTGTTCCAGAAGAAGCGGTCG	60	OE-PCR
T777T_seqF	GCACTAAATCGGAACCCTAAAGGGAG	60	Colony PCR Sanger sequencing
T777T_seqR	CGCGGCCTTTTTACGGTTCCTGG	60	Colony PCR Sanger sequencing
Fc-rpb2_qF	ACCCGTCTTCACAGTTCACC	60	qPCR biomass
Fc-rpb2-qR	TGTCTTCAATCGCTTGTTGC	60	qPCR biomass
So-actin_qF	TGTTGCCCCAGAAGAGCACCCT	60	qPCR biomass
So-actin_qR	AGAACGGCCTGAATGGCAACATACA	60	qPCR biomass
Pc-ef1a_qF	GAGATCAAGAACGAGGTGTCCACG	60	qPCR biomass
Pc-ef1a_qR	GCATGTTGCCCGACTTCTCGATCAT	60	qPCR biomass
Qi-gadph_qF	GGGCCGTGGAGCTGCACAAAACATCA	60	qPCR biomass
Qi-gadph_qR	TGGGACACGGAAGGCCATTCCAGTA	60	qPCR biomass

* Outer primers for OE-PCR
F – Forward primer; R – Reverse Primer
seq – primer for sanger sequencing; -q- primer for qPCR
Letters in grey correspond to the sitting sequence and letters in red correspond to restriction sites for OE-PCR
Lower cases correspond to complementary overhangs and capital letters to the specific gene sequence for OE-PCR
These primers were synthesized in Integrated DNA Technologies (IDT, Coralville, IA, USA).

7. dsRNA production

7.1. dsRNA *in vitro* synthesis

dsRNA molecules were synthesized *in vitro* using the MEGAscript™ RNAi Kit (Thermo Fisher, MA, USA), which allows the *in vitro* synthesis of dsRNA molecules from a DNA template. The transcription reactions were assembled in a final volume of 20 µl as indicated in Table 4. Briefly, gene-specific DNA templates containing opposing T7 promoter sequences were used to

drive simultaneously *in vitro* transcription of sense and antisense RNA strands. The transcription reaction was incubated at 37 °C for 2 - 4 h. Then, the complementary RNA strands were annealed by heating at 75 °C for 5 minutes, followed by slow cooling to room temperature.

Table 4. Transcription reaction for the synthesis of labeled dsRNA

Amount	Component
to 20 µL	double-distilled water (ddH_2O)
1–2 µg	T777T-YFP-dsRNA
2 µL	2 µL 10X T7 Reaction Buffer
2 µL	ATP solution (75 Mm)
2 µL	CTP solution (75 Mm)
2 µL	GTP solution (75 Mm)
2 µL	UTP solution (75 Mm)
2 µL	T7 Enzyme Mix

To synthesize fluorescein-labeled dsRNA we followed the commercial protocol modified by Hamby *et al.* (2020), using fluorescein-labeled nucleotides instead of those provided in the kit. T777T-YFP-dsRNA plasmid was used as a template in the reaction. The transcription reactions were assembled as previously described; however, instead of the recommended 2 µL of each nucleotide, 2 µL of Fluorescein Labeling Mix (Roche, Basel, Switzerland) were used. This mix contains a nucleotide formulation specifically designed for RNA labeling with fluorescein-12-uridine triphosphate (UTP).

The size and integrity of synthesized dsRNA were assessed by agarose gel electrophoresis (see Methods Section 9). dsRNA samples were then stored at -80°C until use.

8. Nucleic acids isolation

8.1. Sample homogenization

Fungal, oomycete and plant samples were immediately homogenized in liquid nitrogen upon collection. The samples were grinded using a mortar and a pestle without allowing them to thaw to avoid nucleic acid degradation. This process was completed until a uniform powder-like consistency was achieved. Following this, approximately 250 mg from each sample was transferred into Eppendorf tubes. These samples were then stored at -80°C until utilized for DNA or RNA extraction.

8.2. DNA extraction

The DNA from the fungal, oomycete and plant tissues homogenized samples was extracted using the cetyl trimethyl ammonium bromide (CTAB) method protocol (Chen and Ronald, 1999). This method is suitable for extracting and purifying DNA from plants and fungi,

and it is particularly effective for removing polysaccharides and polyphenolic compounds. A total of 700 µL of pre-warmed (65°C) extraction buffer [2% w/v CTAB, 1.42 M NaCl, 20 mM EDTA, 100 mM Tris-HCl, pH 8.0, 2% w/v polyvinylpyrrolidone (PVP-40), 5.0 mM ascorbic acid, 4.0 mM diethyldithiocarbamic acid] were added to the frozen, previously grinded samples. 7 µl RNase A (20 mg/ml) were added to the mixture and then stirred and incubated at 65°C for approximately 5 min. Subsequently, 570 µl of a chloroform:isoamyl alcohol mixture (24:1) were added, and the mixture was shaken manually and subjected to centrifugation at 13,000 rpm for 10 min at room temperature. The upper phase, which contained the DNA, was transferred to a new Eppendorf tube. The DNA was precipitated by adding 0.7 volumes of isopropanol, mixing the solution, and immediately spinning it at 13,000 rpm for 5 min. The DNA pellet was washed with 70% ethanol, air-dried, and suspended in 50 µl of nuclease-free water. Subsequent to extraction, the DNA was utilized for fungal biomass analysis in accordance with the protocol detailed in Methods Section 10.4.

8.3. RNA extraction

a. Plant RNA extraction with commercial kit

Total RNA was extracted from homogenized plant tissue, specifically *Q. ilex* leaves, using the commercial Total RNA Purification Kit (Norgen Biotek, Ontario, Canada) following manufacturer specifications. Briefly, samples were lysed using the provided lysis solution, followed by ethanol addition to adjust binding conditions. The lysate was passed through the purification column by centrifugation, allowing RNA to bind to the silica membrane. The column was then washed with the provided Wash Solutions to remove contaminants. Finally, RNA was eluted in RNase-free water and stored at -80°C until further use. Subsequent to extraction, the RNA was used for *P. cinnamomi* biomass analysis in accordance with the protocol in Methods Section 10.3 and 10.4.

b. Total RNA extraction by TRIzol® method

TRIzol® (Thermo Fisher, MA, USA) RNA extraction is suitable for total RNA extraction from a wide range of biological sources, including plants and bacteria, in this study it was mainly used to extract RNA from bacteria for subsequent dsRNA production after IPTG induction. RNA was extracted following the instructions specified by the manufacturer. Briefly, the bacterial cells were concentrated by centrifugation at 4,400 x g for 5 min and 1 ml of TRIzol® was added for every 100 mg of pellet, homogenized in a vortex and centrifuged for 10 min at 12,000 x g. The supernatant was transferred to a new tube and 200 µL of chloroform (Sigma Aldrich, MO, USA) were added for each mL of TRIzol® used previously. The sample was manually shaken for 15

seconds and then incubated at room temperature for 3 min. Afterward, it was centrifuged for 15 min at 12,000 x g. The supernatant was then carefully transferred to a new Eppendorf tube containing cooled isopropanol (Sigma Aldrich, MO, USA) (1:1). The mixture was incubated for 10 min at RT and centrifuged at 12,000 x g for 10 min. The resulting RNA pellet was washed twice with 1 mL of 75% EtOH (v/v) (Panreac Química S.L.U., Barcelona, Spain). After washing, the mixture was centrifuged at 7,500 x g for 5 min. Finally, 50 µL ddH_2O was added and incubated at 60°C for 10 min to resuspend the precipitate. The entire extraction process, including centrifugation, was performed at 4°C to avoid RNA degradation.

Some protocol modifications were implemented in the washing steps, where different concentrations of isopropanol were tested to identify the optimal conditions for selecting the largest dsRNAs and enhancing the extraction process. Finally, better results were obtained by performing two washes with 65% EtOH (v/v) (Panreac Química S.L.U., Barcelona, Spain), which enriched the dsRNAs.

c. dsRNA purification

After RNA isolation, an additional dsRNA purification step was required to obtain high-purity dsRNA for subsequent. The various dsRNA purification methods employed included:

- RNA Clean & Concentrator

RNA Clean & Concentrator (Zymo Research, CA, USA) commercial kit was used to purify RNA. According to the manufacturer's instructions, 2 volumes of RNA Binding Buffer were added to RNA sample and mixed thoroughly. Subsequently, an equal volume of ethanol absolute (Panreac Química S.L.U., Barcelona, Spain) was added and mixed to facilitate binding. The mixture was then transferred to a column provided by the kit, and centrifuged, discarding the flow-through afterward. Following this, 400 µl of RNA Prep Buffer was added to the column and centrifuged, discarding the flow-through. The column was washed with 700 µl of RNA Wash Buffer and centrifuged, followed by a second wash step with 400 µl of RNA Wash Buffer. The column was then carefully transferred to a RNase-free tube, and 15 µl of DNase/RNase-Free Water was added directly to the column matrix and centrifuged to elute the purified RNA.

- Purification with MEGAscript™ RNAi kit

Total RNA was purified using the commercially available MEGAscript™ RNAi kit (Thermo Fisher, MA, USA). Although this kit is designed for the synthesis of dsRNA *in vitro*, it was used here to purify dsRNA produced by bacteria, following only a part of the protocol originally provided with the kit. The extracted RNA was purified in accordance with step E of the commercial protocol of the kit. Then, a dsRNA binding mix was prepared by adding 10X Binding Buffer, nuclease-free

water, and ethanol to the dsRNA solution. This mix was then applied to a filter cartridge and centrifuged to bind the dsRNA, followed by two washes with 500 µL Wash Solution. Finally, dsRNA was eluted by applying 50 µL of preheated ddH_2O (95°C) onto the filter and centrifuging at maximum speed.

- NucleoSpin RNA Virus (Macherey-Nagel, Düren, Germany)

A commercial RNA extraction kit, originally designed for the isolation of RNA from RNA viruses, was adapted for the purification of dsRNA produced in bacteria. Following initial extraction with TRIzol®, the dsRNA was further purified using this commercial kit, starting from step 2 of the manufacturer's protocol. The binding conditions were adjusted by adding 600 µL of absolute ethanol to the samples. The mixture was then applied to the provided purification columns and centrifugated at 8,000 × g for 1 min, followed by three consecutive washes using the buffers supplied in the kit. Finally, purified dsRNA was eluted in 50 µL of RNase-free water and stored at -80°C until further use.

- Enzymatic treatment

– DNase I

After extracting total RNA from bacteria, 10 µL (total 10–20 µg) was treated with DNase I (Thermo Fisher, MA, USA), to remove residual DNA. The reaction mixture consisted of 3 µL DNase I, 5 µL DNase buffer, 10 µL total RNA, and 32 µL nuclease-free water, making a final volume of 50 µL. The mixture was incubated at 37°C for 15 min. Following the treatment, dsRNA was purified and concentrated using the Zymo RNA Clean & Concentrator kit, following the protocol described in 8.3.b Methods Section.

– DNase I + RNase A

Following TRIzol® extraction of total RNA from bacterial cultures, a volume of 10 µL (equivalent to 10–20 µg of total RNA) was subjected to DNase I and RNase A treatments to eliminate residual DNA and single-stranded RNA, respectively. The reaction mixture was prepared in a 50 µl volume as follows: 3 µl of DNase I Ambion™ (2 U/µl) (Thermo Fisher, MA, USA), 5 µl of DNase buffer, 1 µl of RNase A (Thermo Fisher, MA, USA), 10 µl of NaCl 3.5 M, 10 µl of total RNA, and 21 µl ddH_2O. The reaction was incubated at 37°C for 45 min to ensure complete digestion of DNA and single-stranded RNA contaminants. Following enzymatic treatment, dsRNA was purified and concentrated using the Zymo RNA Clean & Concentrator Kit, (Zymo Research, CA, USA).

– DNase I + RNase T1

Total RNA extracted from bacteria using TRIzol® was treated with DNase and RNase enzymes to remove DNA and ssRNA, respectively. This process digests the DNA template and any unannealed ssRNA, while leaving double-stranded RNA (dsRNA). The reaction was carried out in a 50 µl volume, using 2 µl of DNase I Ambion™ (2 U/µl) (Thermo Fisher, MA, USA) and 1 µl of RNase T1 (1000 195 U/µl) (Thermo Fisher, Waltham, MA, USA) in x1 DNase buffer (Thermo Fisher, MA, USA) per 10 µg of total RNA, and incubated for 45 min at 37ºC. Afterward, enzymes were removed using the RNA Clean & Concentrator Kit (Zymo Research, CA, USA) following the protocol described in Methods Section 8.3.c.

Following all the extractions and purification steps, size and integrity of dsRNA or rRNA were analyzed by agarose gel electrophoresis, as described in Methods Section 9. RNA concentration of each sample was quantified by spectrophotometry, as outlined in Methods Section 8.4.

8.4. Nucleid acid quantification

Nucleid acids concentration and purity were determined by measuring the absorbance at 260 nm (A_{260}), 280 nm (A_{280}) and 230 nm (A_{230}) in the NanoPhotometer® N60 UV-Vis spectrophotometer (Implen GmbH, Munich, Germany). Two µl of DNA or RNA samples were used for the measurements. The calculations of DNA and RNA concentration are based on a variant of the Beer's law equation, utilizing the adjusted A_{260} value of nucleic acids. The A_{260}/A_{280} and A_{260}/A_{230} ratio were employed to determine the purity of the nucleic acid and the presence of contaminants, with an optimal range of 1.8 to 2.

9. Electrophoresis

Agarose gel electrophoresis was used to analyze the size and integrity of nucleic acids. Gels were prepared by dissolving 1% (w/v) agarose (Thermo Fisher Scientific, Waltham, MA, USA) in 1X TAE buffer (40 mM Tris-acetate, 1 mM EDTA, pH 8.0) and heating until fully dissolved. Once cooled to approximately 50°C, GelRed nucleic acid stain (Biotium, Fremont, CA, USA) was added to the gel at a final concentration of 1:10,000, following the manufacturer's instructions, to allow visualization of nucleic acids under UV light. Electrophoresis was performed in a horizontal gel electrophoresis system with 1X TAE buffer as the running buffer. The 1X TAE buffer was prepared by diluting a 50X stock solution consisting of 2 M Tris base, 1 M acetic acid, and 50 mM EDTA (pH ~8.3). The samples were mixed with 6X loading dye (containing glycerol and bromophenol blue) before loading onto the gel. A DNA ladder (GeneRuler 1 kb DNA Ladder, Thermo Fisher Scientific)

was used as a molecular weight marker. Gels were run at 80–120 V until adequate separation of the bands was achieved, approximately 30–40 min in our assays. DNA or RNA bands were visualized with a UV transilluminator at 365 nm.

10. Polymerase chain reaction

10.1. Overlap Extension PCR

To produce dsRNAs we first generated DNA template sequences based on the previous *in silico* dsRNA design. DNA templates were obtained by Overlap Extension Polymerase Chain Reaction (OE-PCR), using complementary DNA (cDNA) from *F. circinatum* and *P. cinnamomi* as the starting material. The cDNA was synthesized (see Methods Section 10.3) from RNA extracted from each pathogen (see Methods Section 8.3). The cDNA was employed instead of DNA to avoid the amplification of intronic regions, given that the dsRNAs were designed on coding regions. OE-PCR consists of three main steps (Figure 9). First, each gene fragment was amplified separately by conventional PCR and flanked with the required complementary overhangs by using special primers (construction of the fragments). A second PCR reaction was carried out by combining previously obtained PCR products, in which complementary overhangs bind pairwise, and the polymerase extends the DNA strands (overlap extension). A final PCR reaction was performed to amplify the assembled sequences using outer primers targeting the external overhangs (amplification).

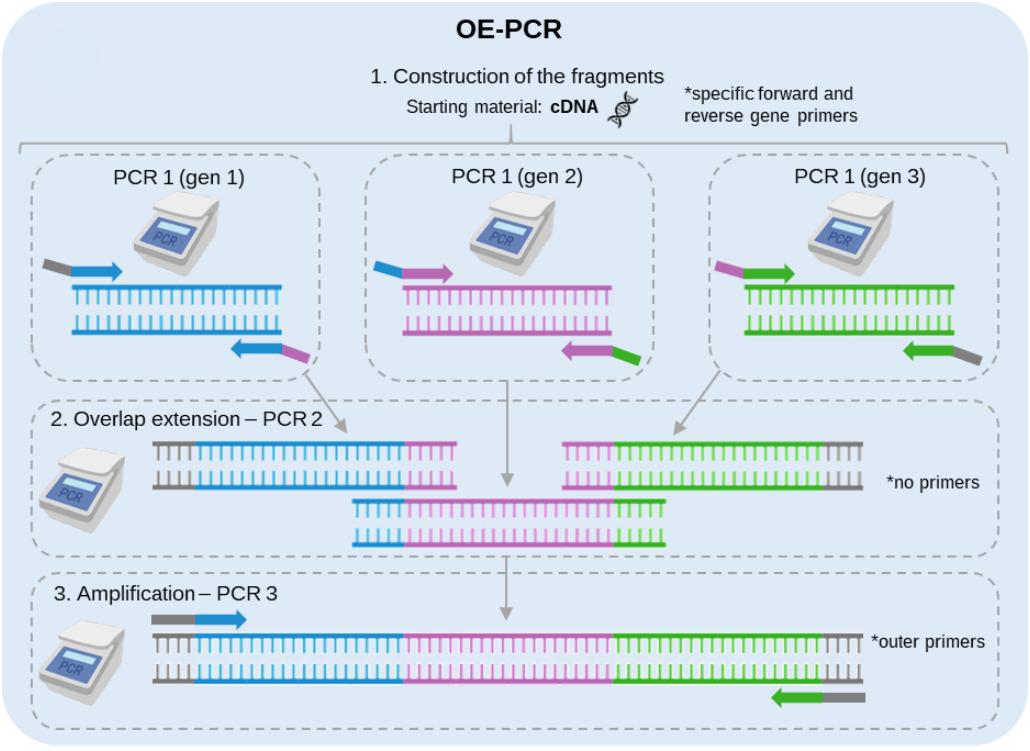

Figure 9. Overlap Extension PCR schematic diagram and steps. OE-PCR methodology was used to obtain DNA custom templates for dsRNA production.

The enzyme used for the polymerase chain reactions was FastGene Taq DNA Polymerase (Nippon Genetics, Tokyo, Japan). All amplifications were performed using the thermocycler Veriti™ 96-Well Fast Thermal Cycler (Applied Biosystems™, Thermo Fisher Scientific, Waltham, MA, USA) in a final volume of 50 µL and following the enzyme protocol, which consisted of: an initial denaturation step at 95ºC for 3 min; variable number of cycles (15 – 35 depending on reaction) consisting of 95ºC for 30 s, specific annealing temperature (T_a) for 30 s, and 72ºC for 1 min 30 s; and a final extension at 72ºc for 10 min. OE-PCR entailed 3 PCR reactions with the following characteristics:

- PCR 1: Construction of fragments

  cDNA was used as starting material. Each gene was amplified individually with its corresponding pair of forward and reverse primers. Specifications: T_a = 57ºC; cycles: 35.

- PCR 2: Overlap extension

  This reaction was performed using the amplified and purified fragments from PCR1 without the addition of primers. Specifications: T_a = 60ºC; cycles: 15.

- PCR 3: Amplification

  In the last reaction, the PCR products from PCR2 are amplified by adding solely 1U of polymerase enzyme and the outer primers of each custom sequence, without adding any other PCR components. Specifications: T_a = 64ºC; cycles: 20. The amplified fragments were checked for size by agarose gel electrophoresis and purified using the NucleoSpin® Gel and PCR Clean-up kit (Macherey-Nagel, Düren, Germany) according to the instructions of the manufacturer.

Differences in T_a across the three PCR steps reflect the distinct requirements of each stage in the OE-PCR process. In the first step, a lower Ta is used to facilitate robust primer binding and efficient amplification of the individual gene fragments. In the second step, the temperature is raised slightly to enhance the specific hybridization of the overlapping complementary regions between fragments, in the absence of primers. The third step involves the utilization of the highest T_a to ensure high specificity during the amplification using the external primers.

OE-PCR enables the amplification of fragments of different genes, and their subsequent assembly to obtain custom dsRNA template sequences. The resulting PCR products were analyzed by electrophoresis (see Methods Section 9). The sizes of the molecules observed on an agarose gel corresponded to the sizes of the molecules designed *in silico* (Figure 10).

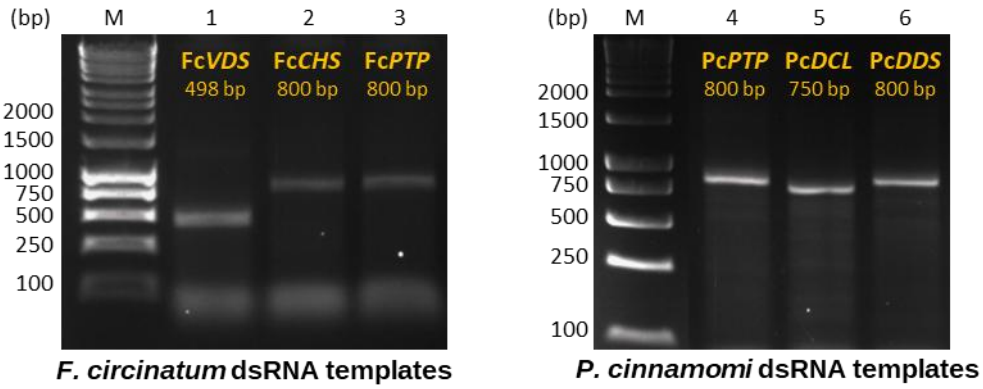

Figure 10. Verification of dsRNA template synthesis by OE-PCR. dsRNA templates generated by OE-PCR were visualized in agarose gels (1%) and compared to the molecular weight marker (M). Bands corresponding to the expected sizes were observed: 498 bp (FcVDS), 800 bp (FcCHS, FcPTP, PcPTP, PcDDS), and 750 bp (PcDCL); confirming the successful amplification and assembly of the target sequences for dsRNA production.

10.2. Colony PCR

To preliminary and quickly confirm that the bacteria have successfully incorporated the plasmid with the insert of interest (and not the recirculated plasmid with no insert), a PCR was performed on the single colonies grown on solid LB Amp_{100} plates after transformation. Primers used in this PCR were designed to amplify the insert flanked by the T7 promoters (Table 3). The reaction was performed in a 25 µL volume using FastGene Taq DNA Polymerase and consisting of: an initial denaturation step at 95ºC for 3 min; 35 cycles of 95ºC for 30 s, 60ºC for 30 s, and 72ºC for 1 min 30 s; and a final extension at 72ºc for 10 min. PCR products were visualized on a 1% agarose gel, confirming the amplification of fragments of the correct size (corresponding insert size + ~160 base pairs). Amplifications were purified with NucleoSpin® Gel and PCR Clean-up kit (Macherey-Nagel, Düren, Germany) and sent for further analysis by Sanger sequencing to the company Stabvida (Caparica, Portugal).

10.3. cDNA synthesis

cDNA was synthesized from total RNA by RT-PCR using SuperScript™ IV reverse transcriptase enzyme (Thermo Fisher, Waltham, MA, USA) according to the manufacturer´s instructions. The RT-PCR included two sequential steps conducted in the thermocycler Veriti™ 96-Well Fast Thermal Cycler (Applied Biosystems™, Thermo Fisher Scientific, Waltham, MA, USA). For each 20 µL reaction, 1 µg of total RNA was combined with 2.5 µM Oligo(dT) and 10 mM dNTP mix in a final volume of 13 µL. The mixture was heated in the thermocycler at 65 °C for 5 minutes and immediately placed on ice for at least 1 minute. This step enables primers to bind with the template RNA. Then, 4 µL of 5X SuperScript™ IV Buffer, 1 µL of 100 mM DTT, 1 µL of RNaseOUT™ Recombinant Ribonuclease Inhibitor (40 U/µL), and 1 µL of the enzyme

SuperScript™ IV Reverse Transcriptase (200 U/µL) were added to each reaction for cDNA synthesis. The final mix was incubated at 50 °C for 10 minutes, followed by enzyme inactivation at 80 °C for 10 minutes. The resulting cDNA was stored at –20 °C until further use.

10.4. Quantitative polymerase chain reaction (qPCR)

F. circinatum and *P. cinnamomi* biomass was estimated by qPCR to assess pathogen growth. For the quantification of *F. circinatum* biomass in spinach leaves, RNA polymerase II subunit B (Fc*RPB2*) was used as the fungal reference gene, while spinach actin gene (So*Actin*) served as the plant housekeeping gene for normalization. These genes have been previously validated in related studies (Liu *et al.*, 2019; Xie *et al.*, 2021). For *P. cinnamomi* biomass quantification in *Q. ilex* leaves, elongation factor 1-alpha (Pc*EF1α*) was selected as the pathogen reference gene, and glyceraldehyde 3-phosphate dehydrogenase (Qi*GAPDH*) was used for host normalization (Romero-Rodríguez *et al.*, 2018).

1 µl of the cDNA or DNA was used in 20 µl reactions with Phusion™ High-Fidelity DNA Polymerase (Thermo Fisher, Waltham, MA, USA), containing 0.4 µL of 1:1000 SYBR™ Green I Nucleic Acid Gel Stain (Thermo Fisher, Waltham, MA, USA), and housekeeping gene-specific primers (Table 4) at a final concentration of 1 µM. The qPCR reactions were performed using the QuantStudio 6 Flex Real-Time PCR System (Applied Biosystems) and a protocol consisting of an initial activation step at 94°C for 2 min 30 s, followed by 40 cycles of 94°C for 15 s, 60°C for 20 s, and 72°C for 30 s. The QuantStudio Real-Time PCR v1.7.1 software was used to determine the cycle threshold (Ct) value. To determine the relative amount of pathogen growth, we used the 2-ΔΔCt method (Livak and Schmittgen, 2001) to correlate the amplification levels of the Fc*RPB2* or Pc*EF1α* genes with those of the So*Actin* or Qi*GAPDH* gene. We normalized the amount of target transcript to the amount of *S. oleracea* or *Q. ilex* transcripts in each case, following the gene relative quantification method (Livak and Schmittgen, 2001). For relative quantification, Ct values from mock control samples in spinach assays and from PH2003 control samples in *Q. ilex* assays served as references (Wang *et al.*, 2016).

11. Microscopy

11.1. Confocal laser scanning microscopy (CLSM) for uptake evaluation

a. *F. circinatum* uptake assessment

5 µL of *F. circinatum* germinated spores (5 ×10^5 spores/ml) (see Methods Section 3.2) were placed on the surface of microscopy slides containing 3 ml of Potato Dextrose Agar (PDA) (Scharlab S.L., Barcelona, Spain) and treated with 10 µl of fluorescein-labelled dsRNA at a

concentration of 100 ng/µL. The slide cultures were kept in the dark for 3 h in an opaque box on moistened filter paper to maintain humidity. Next, the slides were treated with 20 U of micrococcal nuclease (MNase) enzyme (Thermo Fisher, Waltham, MA, USA) for 30 min at 37°C to remove external fluorescein-labelled double-stranded RNAs (Qiao *et al.*, 2021). Finally, the samples were analyzed using CLSM with a Leica SP8 system. Fluorescence was detected using an excitation wavelength of 491 nm and an emission detection range of 500–550 nm. The presence of fluorescent signals within the germinated spores was interpreted as evidence of dsRNA internalization.

b. *Phytophthora cinnamomi* uptake assessment

The assessment of the direct uptake ability of *P. cinnamomi* was conducted at the University of Queensland (Brisbane, Australia) during a research stay. Zoospores, sporangia and *P. cinnamomi* mycelium were collected following the protocol described in Methods Section 3.3, then incubated overnight or for 24 h at room temperature in the dark with 5 µL of dsRNA labeled with Cyanine 3-UTP (Cy3) at a concentration of 250 ng/µL, diluted in Milli-Q water. Following incubation, samples were washed and treated with 75 U of micrococcal nuclease (New England BioLabs, Ipswich, MA, USA) for 30 min at 37 °C to remove excess external Cy-labeled dsRNA. Samples were then examined using a Zeiss LSM700 confocal microscope, with Cy3 fluorescence detected at an excitation wavelength of 555 nm and emission range of 559–640 nm. Internalization of dsRNA was assessed based on the presence of Cy3 fluorescence within the oomycete structures, which would indicate uptake of the labeled molecules.

12. Infection assays and symptoms quantification

12.1. Preliminary screening of infection systems

Initial efforts to assess dsRNA efficacy against *F. circinatum* involved exploratory infection assays using a variety of plant tissues, including rose petals, tomato fruits, cucumber, lamb lettuce leaves and young spinach leaves. These preliminary tests were carried out prior to establishing the detached spinach leaf assay as the standardized model system (see Methods Section 12.2). These assays aimed to identify a suitable system for observing *F. circinatum* infection and symptom development under controlled conditions. Inoculations were performed using spore suspensions of *F. circinatum* prepared at concentrations of 10^4, 10^5, 10^6, and 10^7 spores/mL. Spores were suspended in either sterile distilled water, diluted PDB, or diluted GOX. For tomato fruits, the surface was punctured at the inoculation site to facilitate fungal entry. All

inoculated tissues were placed in moist chambers at room temperature to maintain high humidity and promote infection development.

12.2. Detached spinach leaves assay

This method was intended as a preliminary evaluation to assess the designed dsRNA molecules prior to their analysis in the primary host of *F. circinatum*. 10 µL drops of the treatments (100 ng/µl) were applied to the abaxial side of detached spinach leaves. Mock control was applied to the left of the midrib, and treatments were applied to the right of the midrib. The leaves were then inoculated with 10 µl of a suspension containing 10^5 spores/ml of *F. circinatum* at the same point where the dsRNA treatments were applied. Leaves were placed on moist paper in a sealed container at room temperature (25ºC) to maintain high humidity, which promotes spore germination and ensures more uniform infection development across samples. To evaluate lesion size, two necrotic lesion diameters per leaf were measured 4 days after inoculation using a digital caliper. Lesion size was calculated as circle area ($A=\pi ab$), where a and b represent the semi-major and semi-minor axes, respectively. For fungal biomass assessment, material was collected at 4 dpi, from which DNA was extracted and subsequently analyzed by qPCR, following the protocol described in Methods Section 10.4.

12.3. *Pinus radiata* assays

a. *Fusarium circinatum* inoculation in pine seedlings

Inoculations were performed using the stem inoculation technique (Zamora-Ballesteros *et al.*, 2021). Briefly, a wound was made with a sterile scalpel approximately 1–2 cm above the collar of each plant, after carefully removing the needles from the area. Each seedling was inoculated in the wound with 10 µL of *F. circinatum* spore suspension at a concentration of 10^5 spores ml^{-1}. This concentration was selected as it consistently resulted in successful infection while still allowing for the observation of differences in disease progression between treatment groups. Non-inoculated seedlings were subjected to the same procedure but received 10 µL of sterilized distilled water. Treatments were administered by different approaches:

- Drop application: applying 5 µl of the corresponding dsRNA treatment (300 ng/µL) directly to the inoculation site.
- Spray application: aerial parts of each seedling were sprayed with 1 mL of the respective dsRNA treatment (300 ng/µL).
- Drop + spray: a combination of both methods described above.

Seedlings were maintained in a phytotron under controlled conditions (21.5°C; 16/8 h light/dark photoperiod) for 35 days.

b. Evaluation of SIGS treatments in pines

PPC symptoms in nurseries include chlorosis, shoot and tip dieback, desiccation, collar rot, and wilting (Wingfield *et al.*, 2008). To assess disease progression in *P. radiata* seedlings treated with SIGS, the severity scale originally described by Correll *et al.* (1991) was adapted to better capture the symptom dynamics observed under our experimental conditions (Figure 11). The original scale ranged from 0 to 4, with values reflecting increasing levels of necrosis, wilting, and plant death. In this study, we modified the scale to include a broader range (0–5) and added intermediate symptom categories to enhance the precision and accuracy of disease scoring. The revised scale is as follows: 0 - healthy plant with no symptoms; 1 - presence of resin or necrosis at the point of inoculation and healthy foliage; 2 - presence of resin or necrosis at the point of inoculation, green foliage and slight damping-off; 3 - noticeable damping-off symptoms, slight wilting and yellowing in the tip; 4 - severe wilting and yellowing and noticeable dieback; and 5 - dead plant.

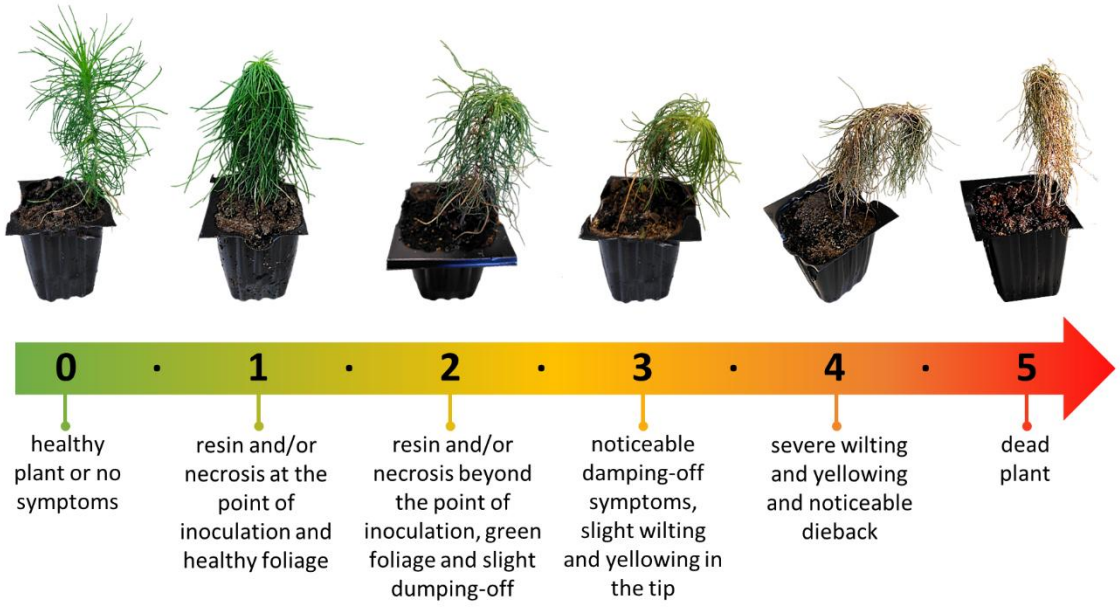

Figure 11. Disease score scale developed to assess SIGS strategy against *F. circinatum* in *P. radiata* seedlings (modified from Bocos-Asenjo *et al.*, 2024). This scale was modified from the empirical scale of Correl *et al.* (1991), with the objective of increasing its suitability for the experiments. The seedlings in this study were visually scored according to this scale, with scores ranging from 0 to 5. Intermediate points were also included to provide more extensive information and enhance the accuracy of the measurements.

12.4. *Lupinus angustifolius* assays

Three-day-old *L. angustifolius* seedlings were utilized for trials under hydroponic conditions. The experiments were conducted in containers with six lupin seedlings submerged into sterile distilled water. Lupin seedlings exhibiting similar morphological characteristics, were carefully selected to avoid potential phenotypic effects. Each seedling was treated as a replicate, and the entire experiment was repeated twice.

Four distinct approaches for dsRNA application were used in the assays: (A) root soaking in dsRNA solution prior to pathogen inoculation, (B) direct application to the pathogen, (C) foliar spraying onto the aerial parts of the plants, and (D) dilution into the hydroponic growth medium.

A. Root soaking: seedling root were submerged into dsRNA solutions (300 ng/µL) for 24 h in darkness at room temperature. Thereafter, the seedlings were transferred to a container with sterile distilled water and inoculated with the pathogen.
B. Direct application to the pathogen: mycelial plugs of 1 cm diameter from 5-days-old *P. cinnamomi* culture were soaked in dsRNA (300 ng/µL) and incubated at room temperature in darkness for 24 h. Thereafter, 3 plugs of the pretreated mycelium were inoculated into each experiment container onto the hydroponic medium.
C. Foliar application: dsRNA solution (300 ng/µL) with 0.01% Tween-20 (Sigma Aldrich, MO, USA) to enhance adherence was sprayed evenly on the leaves of *L. angustifolius* seedlings. Seedlings were maintained in a growth chamber for 24 h before pathogen inoculation.
D. Dilution into the hydroponic growth medium: dsRNA was added to the hydroponic solution at a final concentration of 300 ng/µL. The seedlings were maintained in this dsRNA-containing hydroponic medium for 24 h in a growth chamber prior to pathogen inoculation.

Inoculation with *P. cinnamomi* was carried out by introducing three mycelial plugs into each test container. The plugs, 1 cm in diameter, were excised from the actively growing outer edge of 5-day-old cultures, a region selected for its high biological activity. After inoculation, the trials were maintained in a growth chamber under controlled environmental conditions: a 16/8 h light/dark photoperiod, and a temperature regime of 25 °C during the day and 20 °C at night.

Disease severity was evaluated at 7 dpi by calculating the percentage of necrotic root tissue. Total root length and the length of necrotic lesions (in cm) were measured with a digital

caliper, and the percentage of root necrosis was calculated accordingly. Percentage of visible lesion length was calculated using the formula:

$$\frac{\text{Length of visible root lesion}}{\text{Total root lengt}} \times 100$$

This value was used as the primary indicator of infection severity across treatments.

12.5. *Nicotiana benthamiana* assays

One-month-old *N. benthamiana* seedlings that exhibited similar morphological characteristics, were carefully selected to avoid potential phenotypic effects. The experiments were conducted in containers with four seedlings submerged into a hydroponic medium. Each seedling was treated as a replicate, and the entire experiment was repeated twice. The roots of the seedlings were immersed in 300 ng/µL dsRNA solutions in Eppendorf tubes for 24 h at room temperature in darkness. After the incubation period, the seedlings were transferred back to the experimental containers containing Hoagland's solution. The pathogen was inoculated by adding 3 mycelial plugs of 1 cm diameter of *P. cinnamomi* excised from the actively growing outer edge of 5-day-old cultures directly to the hydroponic medium. Pieces of uninoculated culture medium were used for non-inoculated control plants. The trial was maintained for 7 days in a culture chamber, after which time the seedlings had developed symptoms. Plants were photographed and canopy area (cm^2) was measured using the Image J software (Schneider *et al.*, 2012).

12.6. *Quercus ilex* assays

a. Seedlings assays

Two types of *Q. ilex* plant material were used: five-month-old plants grown in a peat-based substrate under greenhouse conditions, and one-month-old seedlings cultivated hydroponically.

In the five-month-old plants, four different inoculation strategies were for *P. cinnamomi* in SIGS assays:

A. Direct mycelial plug inoculation: *P. cinnamomi* mycelium plugs were thoroughly mixed with the substrate, and *Q. ilex* plants were replanted with this substrate and properly irrigated.
B. Mycelial suspension irrigation: a mycelial suspension was prepared by incubating several plugs of *P. cinnamomi* in a flask with PDB (Scharlab S.L., Barcelona,

Spain) for 5 days under agitation at 125 rpm and 25°C The resulting culture was homogenized and filtered through sterile cloth to remove large mycelial fragments. The filtrate was applied to plants via irrigation. A sample of the suspension was plated onto V8 media to confirm the viability of the mycelium after homogenization.

C. Root saturation with inoculated water: *Q. ilex* plants were temporarily submerged in water containing active *P. cinnamomi* mycelium to promote root infection.
D. Stem inoculation: a 1 cm diameter mycelial plug from *P. cinnamomi* was placed onto a wound made in the stem using a sterile scalpel. The inoculation site was sealed with Parafilm® to prevent desiccation and contamination. Control plants were equally wounded.

In the case of one-month-old seedlings grown hydroponically, inoculation was performed by introducing 1 cm diameter *P. cinnamomi* mycelial plugs directly into the hydroponic solution.

Following inoculation, both control and inoculated plants were kept in separate growth chambers under controlled conditions at a temperature of 21.5°C, and a 16/8 h light/dark photoperiod. Plants were monitored for symptom development over a period of one month. Disease evaluation was conducted through visual inspection, focusing on external symptoms such as wilting, chlorosis, and overall plant vigor. For root-based inoculation methods, plants were carefully uprooted and washed with sterile distilled water to allow for the observation of root lesions and necrosis. The percentage of necrotic root tissue was calculated based on measurements of total root length and lesion length, using a digital caliper. In stem-inoculated plants, lesion length around the inoculation point was measured.

b. *Quercus ilex* detached leaves assay

The youngest fully developed leaves of *Q. ilex* seedlings, grown in greenhouse under controlled conditions, were selected for this assay. Leaves of uniform size were placed underside up in glass Petri dishes, with moistened filter paper to maintain high humidity. dsRNA solutions (300 ng/µL) or sterile water, as appropriate for each treatment, were applied by spraying the abaxial side of the leaves. After application, the plates were sealed with Parafilm to preserve humidity and ensure prolonged exposure of the leaf tissue to the treatments. Treated leaves were kept in darkness at room temperature until inoculation. 24 h post-treatment, *P. cinnamomi* was inoculated onto the leaves. For inoculation, 2 mm^2 mycelial plugs were excised from an actively growing 5-day-old culture. A small incision was made with a pipette tip on the abaxial surface of each leaf, near the midrib, and a mycelial plug was carefully placed over the

wound. Pieces of uninoculated culture medium were used for non-inoculated control plants. Plates were then sealed with Parafilm® to maintain humidity and promote favorable conditions for infection. Plates were maintained on the laboratory bench at room temperature.

Lesion development was assessed through photographic documentation at 2, 3, and 4 dpi. Disease progression was monitored by measuring necrotic lesion area and calculating the percentage of necrosis relative to total leaf area. This quantification was performed using the image segmentation, spatial transformations and image analysis modules from the pliman package (Olivoto, 2022), under R programming environment (R Core Team, 2024). For pathogen biomass analysis, the plant material was collected at 2 dpi, from which RNA was extracted and subsequently analyzed by qPCR, following the protocol described in Methods Section 10.4.

13. Software and databases

13.1. Target gene search

Target genes for dsRNA design were selected through a literature search for genes that are essential for plant pathogens and genes that have been shown to be effective in controlling pathogens when silenced by RNAi transformants. Orthologous genes in the pathogens of the study were identified using the protein sequences of selected genes from the National Center for Biotechnology Information (NCBI), using the online NCBI BLASTp tool used to compare a protein query to the protein database. The reference genomes ASM2404739v1 and ASM1869171v1 (NCBI database) were used to search for genes encoding the selected proteins in *F. circinatum* and *P. cinnamomi*, respectively.

13.2. Identification of *Fusarium circinatum* and *Phytophthora cinnamomi* silencing components

The search for the RNAi machinery in *F. circinatum* and *P. cinnamomi* was conducted through comparative analysis, using NCBI GenBank database. For this search, the protein sequence of RNAi components of other well-described pathogens (*F. graminearum* and *P. infestans*, respectively) were employed as queries, whose sequences were obtained from literature. The BLASTp tool (https://blast.ncbi.nlm.nih.gov/Blast.cgi?PAGE=Proteins) was employed to search within protein databases using a protein query, thereby narrowing the search to the study pathogen (taxid 48490 in the case of *F. circinatum* and taxid 4785 in the case of *P. cinnamomi*). The most significant hits, as indicated by the highest e-values, were selected for further analysis.

13.3. Sequence analysis

Geneious Prime 2023.0.4 bioinformatics software was employed for sequence data analysis, *in silico* design of dsRNA sequences and plasmids, search for RE cleavage points and primer design. Additionally, the software was employed for sequence visualization and the generation of figures such as those presented in this study.

13.4. Target accessibility

The mRNA sequences of the selected genes were evaluated using the RNAxs webserver (http://rna.tbi.univie.ac.at/cgi-bin/RNAxs/RNAxs.cgi). This web tool is based on the RNAplfold v2.6.4 program (Bernhart *et al.*, 2011; Lorenz *et al.*, 2016), which calculates locally stable secondary structure - pair probabilities to assess the mRNA target site accessibility. RNAxs provided us with information on the accessibility in 8 and 16 nt stretches within our sequences. The output was fed into a custom-made R script in R Statistical Software (v4.4.0; R Core Team 2024) to obtain plots of site accessibility throughout the complete mRNA target sequence and search for the most accessible regions between 165-250 nt, depending on the number of targets included in the designed dsRNA molecule. The site accessibility was scored by a penalty according to a pre-determined accessibility threshold (0.011 for 8-nt and 0.001 for 16-nt). Regions with the highest scores were then selected through a visual inspection of the plots and considered for the *in silico* design of the dsRNA.

13.5. Conserved domains

The sequence motif search tool MOTIF (https://www.genome.jp/) was used to identify functional domains of the proteins against Pfam (Mistry *et al.*, 2021), Prosite (https://prosite.expasy.org/) and NCBI-CDD (https://www.ncbi.nlm.nih.gov/cdd/) databases. Pfam provides high-quality, curated domain alignments optimized for detecting conserved protein families across broad evolutionary distances. Prosite is effective for identifying functional motifs and biologically relevant patterns. NCBI-CDD offers broad coverage through the integration of multiple domain models and structural annotations. Using multiple databases increases reliability and allows for more comprehensive functional annotation.

13.6. Off-target identification

To ensure that the designed molecules do not have unintended effects on the plant host or other beneficial organisms, the shortlisted target regions were compared with the host plant CDS sequences using BLASTn (https://blast.ncbi.nlm.nih.gov/Blast.cgi). The siRNA-Finder (si-Fi) software (siFi21_1.2.3-008) (Lück *et al.*, 2019) was also employed to further identify any

unintended effects in other organisms with the following settings: 21 nt siRNA size (default) and 19 nt siRNA size, mismatches=0 (default) and mismatches=1. The transcriptomes of *P. radiata* (PRJNA822053) and *Q. ilex* (PRJEB27528) were employed as databases in the search for off-targets.

13.7. 3D protein structure analysis

The 3D structures of the study proteins were modelled using the SWISS-MODEL structure homology-modelling server (https://swissmodel.expasy.org/), accessible via the Expasy web server (Waterhouse *et al.*, 2018). The tool generates multiple models based on the input sequence and a database of templates. The model with the highest Global Model Quality Estimate (GMQE) value was selected for its analysis. GMQE score, unique to SWISS-MODEL, assesses the overall quality of the model based on its homology with available templates, template coverage, and sequence identity. The selected model structures were viasually compared using the Structure Comparison tool provided by the SWISS-MODEL server. Protein structures comparison was quantitative analyzed using the PyMOL Molecular Graphics System, Version 3. 1 (Schrödinger, LLC), using MatchAlign value and Root Mean Square Deviation (RMSD). MatchAlign value reflects the quality of the sequence alignment, with higher scores generally indicating a superior alignment, which may be correlated with structural similarity. which may correlate with structural similarity. RMSD is used to quantify structural differences, indicating the average distance between the atoms of the superimposed protein structures.

14. Statistics

All analyses were performed using R Statistical Software (v4.4.0; R Core Team 2024):

- Spinach detached leaves assay: each treatment was independently evaluated in three separate experiments, using at least 30 spinach leaves per treatment. Each leaf was considered a biological replicate. Differences in lesion size and fungal biomass growth between dsRNA-treated and mock-treated part of the leaves were analyzed using the Wilcoxon rank test. Statistical significance was determined for *p*-values less than 0.05.
- *P. radiata* assays:
  - dsRNA application method: trials were conducted using at least five plants per treatment and application method. Differences between treatments were assessed using the Wilcoxon non-parametric rank test. *P*-values of multiple

comparisons were adjusted using Holm-Sydak posthoc correction. A threshold of p-value < 0.05 was used to determine statistical significance.

  - dsRNA efficacy evaluation: at least 35 seedlings per treatment were evaluated in this assay. Ordered logistic regression (OLR) was used to analyze differences in disease scores. The variables considered in this study were treatment type, and assessment days post-inoculation (25 dpi, or 35 dpi). The Brant test was used to check the assumption of proportional odds (not significant, p-value ≥ 0.05 for all variables).

- *L. angustifolius* assays:
  - dsRNA application method assay: trials were conducted using at least five plants per treatment. An unpaired t-test was used to compare the treated group to the PH2005 control. Assumptions of normality and equal variances were considered acceptable. Non-inoculated control was included to confirm plant health but was not considered in the statistical analysis.
  - dsRNA efficacy assays: two independent trials were performed with at least six plants per treatment. Kruskal-Wallis test was performed to detect overall differences in the percentage of necrotic root among treatments. Upon detecting a significant global effect, pairwise Wilcoxon rank-sum tests were conducted to compare each dsRNA treatment to the *Mock control*. The resulting p-values were adjusted using Holm's method to control for multiple comparisons.
- *N. benthamiana* assays: four independent experiments were conducted using at least 4 plants per treatment. Kruskal-Wallis test was used to assess overall differences among treatment groups. Upon identifying a significant global effect, pairwise Wilcoxon rank-sum tests were performed to compare each dsRNA treatment against the Mock control. Holm's method was applied to adjust the resulting p-values for multiple comparisons.
- *Q. ilex* leaves assay:
  - Necrosis assessment in *Q. ilex* leaves: this experiment was repeated three times independently, using at least eight leaves per treatment in each assay, resulting in a total of 24 biological replicates per treatment. The dataset was combined, and treatments and time points (2, 3 and 4 dpi) were treated as categorical factors. Visual inspection of data distributions was conducted using boxplots and QQ plots to assess normality. Since the assumptions of

normality were not met, non-parametric tests were employed: Kruskal-Wallis test was used to detect general differences between treatments, followed by Wilcoxon rank test adjusted with Holm's method for specific comparisons between the control and treatments. Differences in necrotic areas between dsRNA treatments and control condition were assessed by means of Welch t-test, with Holm correction for multiple comparisons, for each time point. Statistical significance was determined for *p*-values less than 0.05.

- *P. cinnamomi* biomass assessment: for qPCR analysis, at least 3 biological replicates were used per treatment. For each biological replicate, 3 technical replicates were performed for each target gene during the qPCR assay. Expression levels are presented as relative quantification (RQ) values, calculated using the $2^{-\Delta\Delta Ct}$ method. Error bars represent the exponentially transformed standard error, computed as $RQ \cdot 2^{\pm SE}$, where SE is the standard error of the $\Delta\Delta Ct$ values. This transformation reflects the log-normal distribution of qPCR data and provides biologically meaningful intervals in the linear scale. To assess whether the relative expression levels (RQ) of each treatment significantly differed from that of PH2003 (used as a reference with RQ = 1), a one-sample t-test was performed for each treatment. The test statistic was calculated as the difference between the sample mean and the reference value, divided by the exponentially transformed standard error. Differences were considered statistically significant at p-value < 0.05. Significance levels are indicated as: p-value < 0.05 (*), p-value < 0.01 (**).

Results and discussion

Chapter 1

New advances in design and production of dsRNA for SIGS disease control in forestry

This chapter focuses on enhancing the efficiency of SIGS technology by optimizing the design and production of dsRNA molecules. To achieve this, the following actions were proposed:

- To select appropriate target genes based on their importance in pathogen development and survival.
- To carefully design dsRNA with improved silencing efficiency.
- To develop a cost-effective dsRNA production protocol using genetically modified bacteria, ensuring sufficient quantity and quality for experimental application.

The results of optimizing the design and production process of dsRNA molecules to increase the efficiency of the SIGS technique are described in this results section. This optimization has not previously been documented in the existing literature, where the studies on SIGS are based on a trial-and-error approach. To the best of our knowledge, this is the first attempt to adjust the parameters of this process. All this learning has been consolidated and published as a step-by-step methodological guide to facilitate the use of SIGS-based approaches in plant protection (Mosquera *et al.*, 2025).

1. Selection of target genes to improve SIGS efficacy

The selection of effective target genes was crucial for the success of SIGS strategy to control diseases. Depending on the function and significance of target genes to the pathogen, and the efficiency of their silencing, disease inhibition will either be achieved or not.

In a literature review phase, special emphasis was placed on identifying genes involved in essential metabolic pathways that could serve as effective targets for SIGS. The selection process prioritized genes previously shown to be critical for pathogen survival or virulence, especially those participating in fundamental processes such as cell wall biosynthesis, or signal transduction. Preference was given to gene targets that had already been successfully silenced in plant pathogens through RNA interference approaches. Additionally, particular attention was paid to studies involving pathogens belonging to the same genus as those under investigation in this study, as this increased the likelihood of cross-species functional conservation and silencing efficacy. Based on these criteria, in this dissertation, we selected several genes involved in three essential metabolic pathways. Thus, a total of three dsRNA molecules were designed for each pathogen in the study, intended for use in future SIGS-based assays.

1.1. Design criteria for dsRNA constructs: single-gene vs. multi-gene targeting

The dsRNA molecules developed in this study were specifically designed to target 3 to 4 genes. This multi-target approach aimed to enhance disease reduction and was based on two key reasons: (1) if the target gene has paralogs, all of them must be silenced to prevent the gene from performing its function; and (2) by silencing several genes within the same metabolic pathway, the likelihood of disrupting the pathway is higher compared to targeting a single gene.

Although both approaches, using a single gene as a target or multiple simultaneously, have been demonstrated to be effective in pathogen control by SIGS, some studies have indicated that simultaneous silencing of multiple genes may result in greater efficacy of the RNAi silencing mechanism (Koch *et al.*, 2019; Mumbanza *et al.*, 2013; Qiao *et al.*, 2021). Targeting a single gene may therefore have less effect on the pathogen, either because this gene has paralogs that compensate for its loss of function or due to the complexity of some metabolic pathways. This has been demonstrated in *F. graminearum*, where spraying barley leaves with a dsRNA construct targeting three paralogous genes (FgCYP51A, FgCYP51B, and FgCYP51C) of the pathogen resulted in a greater reduction in symptoms than applying single (CYP-A, CYP-B, CYP-C) or double (CYP-AC, CYP-BC, CYP-AB) dsRNA constructs (Koch *et al.*, 2019). Likewise, studies silencing DCL (a potential RNAi target that presents paralogs) often aim to target all *dcl* genes present in the pathogen (Haile *et al.*, 2021; Qiao *et al.*, 2021; Wang *et al.*, 2016). Other studies achieved a significantly greater reduction in disease severity by applying three dsRNA molecules simultaneously, thus targeting three distinct genes involved in cell wall synthesis and regulation, rather than targeting two or a single gene (Yang *et al.*, 2021a). Similarly, effective pathogen reduction was achieved with the application of a single dsRNA targeting several genes at different

points within the same pathway, thereby blocking the pathway (Qiao *et al.*, 2021). This approach was adopted in our study in order to disrupt very complex pathways that are subject to tight regulation. Silencing several genes at different points in the pathway may help to overcome such regulation and increase the chances of silencing.

This multi-target approach was key for optimizing the design of the dsRNAs in this study. Beyond enhancing the efficacy of the technique, it may also contribute to reducing the incidence of resistance development in the pathogen, which is more prevalent with a single target. This is because a mutation in that particular gene would be sufficient for the pathogen not to respond to SIGS treatment (Zimmermann *et al.*, 2007). Accordingly, each dsRNA molecule generated in the course of the study was designed to simultaneously target between 3 and 4 genes within a metabolic pathway. This strategy was intended to maximize the impact of RNA interference on pathogen fitness and virulence.

1.2. Criteria for functional target selection in dsRNA design

Given the suitability of genes involved in fungal growth, development, and pathogenicity as RNAi targets, several genes with established functions in *F. circinatum* and *P. cinnamomi* pathobiology were identified from published literature. The following genes were identified as suitable candidates for RNAi: ***chs1, chs2, chs3b*** and ***gls1***, which are involved in the cell wall biogenesis pathway; ***pp2a, ppg1, sit4*** and ***tap42***, which are involved in the signal transduction pathway*;* ***vps51, dctn1, sac1*** and ***dhcr7***, which are involved in the vesicle trafficking pathway; and ***dcl1*** and ***dcl2***, which are involved in the synthesis of components of the RNAi machinery.

We hypothesized that silencing essential genes could reduce pathogen growth throughout the entire disease cycle, from its arrival in the host to an advanced stage of the disease. This would make SIGS a preventive treatment for disease, but it could also be curative, controlling the disease once the pathogen is established. Essential genes have been extensively studied and described in model organisms, including *Candida albicans, Aspergillus fumigatus*, *Cryptococcus neoformans,* and *Saccharomyces cerevisiae* (Firon and D'Enfert, 2002; Seringhaus *et al.*, 2006). These genes are conserved among fungi and play fundamental roles in biological functions such as lipid biosynthesis, cell wall formation, amino acid metabolism, and protein synthesis among others. Due to their substantial evolutionary conservation, essential genes exhibit a high degree of sequence similarity across different fungal species, facilitating their identification and highlighting their potential as targets for antifungal drug development (Fu *et al.*, 2021; Liang *et al.*, 2024). Many works have utilized essential genes as targets for RNAi-based strategies, highlighting *dcl* (Wang *et al.*, 2016) or *cyp51* (Koch *et al.*, 2016), which are the

targets of many fungicides, such as the azoles. Considering all the above, and following an exhaustive review of the relevant literature, the essential genes targeted in this study were identified in the following metabolic pathways (Table 5):

Table 5. Overview of pathways and genes chosen for each pathogen

Metabolic Pathway	*F. circinatum*	*P. cinnamomi*
Signal transduction	*pp2a, ppg1, sit4, tap42*	*pp2a, ppg1, sit4, tap42*
Vesicle trafficking	*vps51, dctn1, sac1*	*dhcr7, dctn1, sac1*
Cell wall biogenesis	*chs1, chs2, chs3b, gls1*	
RNAi machinery		*dcl1, dcl2*

- Signal transduction

A total of four genes in the TOR (target of rapamycin) signaling pathway in both *F. circinatum* and *P. cinnamomi* were selected for the design of dsRNA molecules, named **FcPTP-dsRNA** and **PcPTP-dsRNA**, respectively. TOR is a conserved serine/threonine kinase that plays a central role in nutrient signal transduction, regulating cell growth and proliferation in response to environmental signals in eukaryotes (Yu *et al.*, 2014). We specifically targeted a signal transduction pathway due to the crucial role of this process in fungi and oomycetes, which is responsible for translating extracellular signals into specific cellular responses (Vangalis *et al.*, 2023; Zhang *et al.*, 2021). This is essential for the control of a wide range of cellular processes (such as development, cellular differentiation, DNA damage response, cell cycle progression, pathogenic and symbiotic interactions, asexual and sexual reproduction, primary and secondary metabolism, stress adaptation, autophagy, and apoptosis), which are vital for the survival of these organisms (Kück, 2022). Despite the significance of TOR signaling pathway for pathogenic organisms, as far as we know it had never been disrupted by RNAi before. In this study, we developed dsRNA molecules for both pathogens, *F. circinatum* and *P. cinnamomi,* targeting the following genes:

- ***pp2A***, ***ppg1***, and ***sit4***, encode for three 2A phosphatases. These phosphatases interact with the phosphatase 2A-associating protein (tap42) in the TOR signaling pathway. In *F. graminearum*, *pp2A* is essential for pathogen survival, and *sit4* and *ppg1* are important for cell integrity (Yu *et al.*, 2014).
- ***tap42*** encodes for a phosphatase 2A-associating protein and seems to be crucial for the fungus since no deletion mutants of this gene could be obtained (Yu *et al.*, 2014). Rapamycin acts in the TOR signaling pathway preventing the association between the TAP42 complex and the TOR complex. Several *Fusarium* species have been described

as strongly inhibited by rapamycin treatment (López-Berges *et al.*, 2010; Teichert *et al.*, 2006; Yu *et al.*, 2014).

- Vesicle trafficking

The generation of the **FcVDS-dsRNA** and **PcDDS-dsRNA** molecules was based on the studies of Cai *et al.* (2018b) and Qiao *et al.* (2021b), which identified potential targets for SIGS in the vesicle trafficking pathway. Based on the occurrence of bidirectional sRNA trafficking and cross-kingdom RNAi in *Arabidopsis–Botrytis cinerea* pathosystem, Cai *et al.* (2018b) conducted a study to identify sRNAs transferred from the plant to the pathogen during infection to inhibit pathogen virulence. Their findings revealed that *Arabidopsis*-transferred sRNAs targeted genes in *B. cinerea* with a bias toward vesicle trafficking pathways. They performed a functional analysis on some of the sRNAs that showed selective accumulation in the plant vesicles, revealing three target genes in vesicle trafficking pathway: protein sorting 51 (*vps51*), dynactin (*dctn1*), and suppressor of actin (*sac1*) genes. The relevance of these genes was confirmed by generating mutants, which exhibited reduced virulence on *Arabidopsis* plants. This study highlights the crucial role of vesicle trafficking in supporting numerous physiological functions in eukaryotic cells. This pathway facilitates communication among components of the endomembrane system within a cell, between cells, and between a cell and its external environment (Abubakar *et al.*, 2023). Vesicle trafficking is required for the transcellular secretion of large molecules through the cell wall, such as proteins, lipids, polysaccharides and pigments (Rodrigues *et al.*, 2015). In pathogenic fungi, several of these vesicular components are associated with fungal virulence. Besides, vesicle trafficking plays a crucial role in oomycetes as well, especially during infection when they secrete numerous effector proteins to suppress the plant immune response and reprogram plant metabolism (King *et al.*, 2024). Oomycetes also use this pathway to achieve exocytosis of a mucilage-like covering that protects the cysts from desiccation, and proteins that enable cysts to adhere to surfaces during zoospore encystment (Hardham, 2006). Building on the findings of Cai *et al.* (2018b), Qiao *et al.* (2021) evaluated whether SIGS targeting vesicle trafficking genes could be employed to control gray mold disease. They generated a dsRNA targeting *vps51, dctn1*, and *sac1* genes of *B. cinerea*, which was then sprayed on different plant materials that were subsequently infected with *B. cinerea*. Their results indicated that all plant materials treated with dsRNA showed a reduction in symptoms. Additionally, they found that the mRNA expression levels of each of the target genes were also reduced in *B. cinerea* treated with dsRNA. Furthermore, this gene combination has been successfully utilized against *Sclerotinia sclerotiorum, Rhizoctonia solani, Aspergillus niger,* and

Verticillium dahliae (Qiao *et al.*, 2021). These genes have also been successfully employed by Qiao *et al.* (2023) and Niño-Sánchez *et al.* (2022), who, in addition, were able to extend the protection window by several weeks through the use of artificial vesicles (AVs) and Bioclay™, respectively. Based on this evidence, dsRNA molecules were developed to disrupt vesicle trafficking pathway in both *F. circinatum* and *P. cinnamomi*. The following genes were selected for dsRNA construction:

- ***vps51*** encodes a subunit of the Golgi-associated retrograde protein (GARP) complex. This multisubunit complex is essential for the tethering of endosome-derived transport vesicles to the late Golgi, thus functioning primarily in retrograde transport. Luo *et al.* (2011) observed in *C. elegans* that deletion mutants of the GARP complex subunits exhibited altered lysosomal morphology. Furthermore, *vps51* has been demonstrated to contribute to the basic functioning of the GARP complex in *C. elegans*. This has also been observed in yeast (Conibear *et al.*, 2003; Reggiori *et al.*, 2003), and mammalian cells (Pérez-Victoria *et al.*, 2010), in which small interfering RNA-mediated knockdown of *VPS51* resulted in the missorting of lysosomal enzymes, as well as impairment of protein retrieval to the trans-Golgi network and autophagy. The loss of GARP function has been demonstrated to compromise the growth, fertility, and/or viability of defective organisms (Bonifacino and Hierro, 2011), making it an attractive target for SIGS technology.
- ***dctn1*** encodes the largest polypeptide of the dynactin complex and is essential for its function. The dynactin complex collaborates in bidirectional transport, as it is required for the cytoplasmic dynein-driven movement of organelles along microtubules (Deacon *et al.*, 2003). As previously stated, the Δ*dctn1* deletion mutant strain of *B. cinerea* exhibited a reduction in virulence on *Arabidopsis* (Cai *et al.*, 2018b). Furthermore, in this study, they generated transgenic Arabidopsis plants that overexpressed and knocked out the sRNAs that target *dctn1* in the pathogen. The results demonstrated that overexpression of the sRNAs resulted in reduced susceptibility of the plant to *B. cinerea*, while knockout caused the opposite, increased susceptibility in *Arabidopsis*. This indicates that the silencing of *dctn1* by the delivery of sRNAs to the pathogen contributed to the development of host immunity, thereby reinforcing the significance of this gene for the pathogen. Furthermore, it has been demonstrated that this gene plays a pivotal role in animal cells, and its silencing can result in significant cellular damage (Borg *et al.*, 2023).

Variants that are deleterious to the *dctn1* gene in mammalian cells have been linked to the development of amyotrophic lateral sclerosis disease (Borg *et al.*, 2021).

- ***sac1*** is a lipid phosphatase that regulates several cellular processes, including cytoskeleton organization, membrane trafficking and cell signaling (Del Bel and Brill, 2018). In filamentous fungi, the actin cytoskeleton plays a role in vesicle transport to polarized growth zones, in the formation of septa and endocytosis. This gene is therefore relevant to vesicle trafficking. (Zhang *et al.*, 2015) observed that in a *sac1*-disrupted mutant of the fungus *Candida albicans*, hyphal development and biofilm formation was attenuated. Furthermore, the gene deletion significantly affected the cell wall integrity of the fungus, making it more sensitive to stress and reducing its virulence.
- ***dhcr7*** encodes for a 7-dehydrocholesterol reductase. Given that *vps51* was not identified in *P. cinnamomi*, the dsRNA for vesicle trafficking was designed to instead target this gene involved in esterol metabolism. Sterols play several important roles in living cells: in membrane structure and function, in cell growth and development, in signaling and regulation, and, in the case of pathogenic organisms, in pathogenicity and host interactions. Fungal organisms can produce their own sterol called ergosterol, which is a crucial lipid component of plasma membrane involved in its integrity and organization, providing membrane fluidity. Ergosterol is therefore a key component of vesicles (Rodrigues, 2018). Fungal ergosterol is thought to act as a pathogen-associated molecular pattern (PAMP) that triggers plant immunity during infection. However, oomycetes are unable to synthesize sterols; they are sterol auxotrophs. Therefore, sterol auxotrophy of oomycetes could be considered an advantage due to the loss of such a warning signal and the emergence of strategies to acquire these essential compounds (Der *et al.*, 2024). Nevertheless, despite the inability of oomycetes to synthesize sterols, remnants of this synthesis pathway are still present in their genomes, including the preservation of the homologue of *dhcr7* (Wang *et al.*, 2021). In *P. capsici*, *dhcr7* has been shown to be necessary to transform the sterol recruited from the medium for better use in brassicasterol (a plant-synthesized sterol), which appears to be essential for mycelium development and the pathogenicity of zoospores (Wang *et al.*, 2022). In Wang *et al.* (2022) study, knockouts of *P. capsici* generated by CRISPR/Cas-9 were employed to demonstrate that *dhcr7* is essential for germ tube development and growth during an early stage of the infection process. This makes it a promising candidate for SIGS-targeting in

Phytophthora species. In addition, certain genes of the mevalonate pathway (also involved in sterol synthesis) have been identified in oomycetes. (Yang *et al.*, 2021b) found that deletion of a gene in this pathway in *Phytophthora sojae* affected the growth, spore production, and virulence of the pathogen, thereby reinforcing the importance of these pathways in *Phytophthora* genus.

- Cell wall biogenesis

A total of four genes were obtained for inclusion in the **Fc*CHS*-dsRNA** molecule designed to target cell wall biogenesis pathway in *F. circinatum*: *chs1, chs2, chs3b* and *gls1*. This pathway was selected because the fungal cell wall plays a crucial role in survival, virulence, and communication of fungal organisms with their external environment. This structure is essential for maintaining cell viability and morphology, as well as for mediating host-pathogen interactions (Geoghegan *et al.*, 2017). Inhibition of this fungal structure could lead to cell death, which makes this structure an attractive target for the control of pathogenic fungi by, among other methods, SIGS technology. The cell wall of fungi is primarily composed of chitin and glucans, along with other components, and its composition can vary among different fungal species. Chitin is a critical structural element, and disruption of its synthesis leads to malformed and osmotically unstable fungal cells (Bowman and Free, 2006). In addition, during the early stages of infection, chitin is essential for the formation of infection structures (Fernandes *et al.*, 2016). This pathway was only interrupted in *F. circinatum* because oomycetes, unlike fungi, have a cell wall that lacks chitin. The cell wall of oomycetes is composed of cellulose; a highly abundant macromolecule found in nearly all plant groups. To mitigate potential off-target effects in plant species, we decided to develop the third dsRNA molecule against *P. cinnamomi* to disrupt a different metabolic pathway. After a comprehensive review of pertinent literature, the following genes of *F. circinatum* were selected in this pathway for the design of Fc*CHS*-dsRNA:

- ***chs1*, chs2** and ***chs3b*** genes encode for three chitin synthases, which are suitable candidates for disrupting the cell wall biogenesis pathway. Previous studies have demonstrated that silencing *chs1* and *chs2* in other *Fusarium* species affects mycelial growth and virulence (Cheng *et al.*, 2015; Xu *et al.*, 2010). As with the deletion of *chs3b* in *F. graminearum*, which appears to be lethal, and its silencing by HIGS resulted in reduced mycelial growth (Cheng *et al.*, 2015; Liu *et al.*, 2016).
- ***gls1*** gene encodes for the β-1,3-glucan synthase. Glucan is another essential component of fungal organisms as the central core of the cell wall is comprised of a branched β-1,3-glucan cross-linked to chitin (Latgé, 2007). β-Glucans are produced

by the β-1,3-glucan synthase, which is the pharmacological target of numerous antifungal drugs. *gls1* was found to be lethal in *Colletotrichum graminicola*, and its silencing by RNAi in transgenic fungal strains produced developmental abnormalities and non-pathogenicity (Oliveira-Garcia and Deising, 2013). (Chen *et al.*, 2016) produced transgenic plants that targeted *gls1* of *Fusarium culmorum* and achieved similar results in fungal morphology and disease reduction.

- RNAi machinery

The third dsRNA molecule developed against *P. cinnamomi* in this study targets its RNAi machinery. This is a common strategy for disease control by SIGS in fungal pathogens (Qiao *et al.*, 2021; Wang *et al.*, 2016; Werner *et al.*, 2020). However, the silencing of RNAi machinery components has only been observed in oomycetes in *Plasmopara viticola* (Haile *et al.*, 2021), with no evidence of such silencing in *Phytophthora* spp. Given the efficacy of *dcl* gene silencing in the management of pathogenic fungi, we decided to apply this strategy to *P. cinnamomi*. A dsRNA molecule named **PcDCL-dsRNA** was designed to silence *dcl1* and *dcl2* genes in *P. cinnamomi*. Several RNAi studies have targeted key components of the silencing machinery of both fungal and oomycete pathogens. The interference of the fungal pathogen *Botrytis cinerea*'s Dicer-like genes *(dcl1* and *dcl2)* by sRNAs through in-plant expression by HIGS and external application by SIGS resulted in a significant reduction in gray mold disease on fruits, vegetables and flowers (Wang *et al.*, 2016). Qiao *et al.* (2021) similarly silenced the *dcl1* and *dcl2* genes in *B. cinerea, S. sclerotiorum* and *V. dahliae* by external application of dsRNAs, thereby inhibiting the infection. In *F. graminerarum*, SIGS application of dsRNA constructs targeting key components of the RNAi machinery (DCL and AGO) was also confirmed to protect barley leaves (Werner *et al.*, 2020). Furthermore, (Mukherjee *et al.*, 2024) recently demonstrated the successful control of white mold infection caused by *S. sclerotiorum* by silencing a crucial component of the fungal small RNA pathway, AGO2. This approach has also been successfully used in pathogenic oomycetes, as evidenced by the case of *Plasmopara viticola,* in which silencing *dcl1* and *dcl2* severely affected the virulence of the pathogen and even showed a curative role for the disease caused by the oomycete in grapevine leaves (Haile *et al.*, 2021). This evidence supports the crucial role of these genes for pathogenic organisms. The genes selected in this pathway for control of *P. cinnamomi* were:

- ***dcl1*** and ***dcl2*** are two *dcl* paralogous genes which encode DCL proteins. As part of the RNAi machinery, DCL proteins process dsRNA into miRNAs, which will then be further processed, triggering gene silencing. This process is essential for the self-regulation of

gene expression in organisms and therefore its disruption can severely affect pathogen development. The number of *dcl* genes varies across species. In some of the most extensively studied species of the genus *Phytophthora*, including *P. infestans*, *P. sojae*, and *P. ramorum*, two *dcl* genes have been reported (Fahlgren *et al.*, 2013). Our analysis of the genome of *P. cinnamomi* revealed the presence of two paralogous *dcl* genes, which are orthologous genes to *Phytophthora* spp. *dcl1* and *dcl2*, as evidenced by the homology of their proteins. These genes were selected for the design of the PcDCL-dsRNA molecule used in this project.

In conclusion, as a result of the comprehensive process of selecting genes according to their relevance to the pathogenic organism and the previous studies on their silencing these genes were shortlisted for initial experiments (Table 6).

Table 6. Results of the selection of metabolic pathways and essential genes as RNAi targets against *F. circinatum* and *P. cinnamomi*

Pathogen	Pathway	Gene	Encoded protein	Protein ID	Reference
F. circinatum	Signal transduction	*pp2a*	Serine threonine phosphatase PP2A catalytic subunit	KAF5688398.1	(Yu *et al.*, 2014)
		ppg1	Serine/threonine-protein phosphatase PP2A catalytic subunit	KAF5683879.1	(Yu *et al.*, 2014)
		sit4	Serine/threonine-protein Phosphatase PP1-1	KAF5690545.1	(Yu *et al.*, 2014)
		tap42	TAP42 component of the Tor signaling pathway	KAF5688382.1	(Yu *et al.*, 2014)
	Vesicle trafficking	*vps51*	Hypothetical protein FCIRC_4363	KAF5683607.1	(Cai *et al.*, 2018b)
		dctn1	Tip elongation 1	KAF5656821.1	(Cai *et al.*, 2018b)
		sac1	Phosphatidylinositide phosphatase SAC2	KAF5666971.1	(Cai *et al.*, 2018b)
	Cell wall biogenesis	*chs1*	Chitin synthase 1	KAF5654678.1	(Cheng *et al.*, 2015)
		chs2	Chitin synthase 2	KAF5678417.1	(Cheng *et al.*, 2015)
		chs3	Chitin synthase 3	KAF5658513.1	(Cheng *et al.*, 2015)
		gls1	1,3-beta-D-glucan synthase subunit	KAF5676366.1	(Chen *et al.*, 2016)
P. cinnamomi	Signal transduction	*pp2a*	Serine/threonine-protein phosphatase PP2A	KAG6614488.1	(Yu *et al.*, 2014)
		ppg1	Serine/threonine-protein phosphatase PP-X isozyme 2	KAG6609755.1	(Yu *et al.*, 2014)

		sit4	Phytochrome-associated serine/threonine protein phosphatase	KAG6586554.1	(Yu *et al.*, 2014)
		tap42	TOR signaling pathway regulator	KAG6619275.1	(Yu *et al.*, 2014)
	Vesicle trafficking	*dhcr7*	7-dehydrocholesterol reductase	KAG6587262.1	(Wang *et al.*, 2022)
		dctn1	Dynactin subunit 1	KAG6622924.1	(Cai *et al.*, 2018b)
		*sac1*a	Phosphatidylinositide phosphatase SAC1	KAG6619881.1	(Cai *et al.*, 2018b)
		*sac1*b	Phosphatidylinositide phosphatase SAC1	KAG6623134.1	(Cai *et al.*, 2018b)
	RNAi machinery	*dcl1*	Dicer-like 1	KAJ8558851.1	(Fahlgren *et al.*, 2013)
		dcl2.1	Dicer-like 2	KAG6594204.1	(Fahlgren *et al.*, 2013)
		dcl2.2	Putative dicer-like	KAG6610731.1	(Fahlgren *et al.*, 2013)

The target genes were selected based on their essential functions for pathogen development. This selection allowed the design of the following dsRNA molecules:

Against *F. circinatum*:

- **FcCHS-dsRNA** – targeting chs1, chs2, chs3b and gls1 in cell wall biogenesis pathway.
- **FcPTP-dsRNA** – targeting pp2a, ppg1, sit4, tap42 in the signal transduction pathway.
- **FcVDS-dsRNA** – targeting *vps51*, *dctn1* and *sac1* in vesicle trafficking pathway.

Against *P. cinnamomi*:

- **PcDCL-dsRNA** – targeting Dicer-like (*dcl1* and *dcl2*) genes involved in the synthesis of components of the RNAi machinery.
- **PcPTP-dsRNA** – targeting pp2a, ppg1, sit4, tap42 in the signal transduction pathway.
- **PcDDS-dsRNA** – targeting *dhcr7*, *dctn1* and *sac1* in vesicle trafficking pathway.

2. Optimization of the dsRNA design for enhanced efficacy of the technique

To date, most SIGS approaches rely on the random selection of sequences within the target genes, without a systematic rationale behind dsRNA design. In contrast, we developed a systematic approach aimed at maximizing gene silencing efficiency through a more methodical design process.

Current evidence shows that selecting an appropriate target gene alone is not sufficient; the design must also consider features such as the length of the molecule, the accessibility of the sequence, and the target region within the gene (Mosquera *et al.*, 2025). Studies have

demonstrated that the optimal dsRNA length appears to depend on the uptake ability of the pathogen and the activity of its DCL enzymes, with effective molecules ranging from 150 to over 1,500 nt, depending on the species. In addition, it is known that different regions of the same gene can result in different silencing efficiencies, and highly structured or inaccessible RNA regions are less susceptible to degradation by the RNAi machinery. Finally, selecting the appropriate target region is important not only for ensuring silencing efficiency but also for minimizing off-target effects, among other considerations. Each of these factors was effectively integrated into the final dsRNA designs, resulting in optimized dsRNA constructs.

2.1. Determination of suitable dsRNA length for enhanced SIGS efficiency

The dsRNA molecules produced in this study exhibited lengths between 498 bp and 800 bp, depending on the number of genes targeted. Each molecule was successfully assembled with sequential fragments of 165 to 250 bp from each selected gene. The rationale behind this decision was to generate a larger variety of efficient siRNAs that would induce the desired silencing effect. This is consistent with that observed by Werner *et al*. (2020), who found that longer dsRNAs (658 bp-912 bp) were more effective against *F. graminearum* than shorter dsRNAs (173 bp-193 bp). However, the length of dsRNA molecules has been the subject of contradictory findings, with Degnan *et al*. (2022) and Höfle *et al*. (2020) observing decreased silencing efficiency with increasing dsRNA length. The maximum length of the molecules of the study was set at 800 base pairs (bp) in order to align with the findings of Höfle *et al*. (2020), which indicated a decline in efficiency for molecules exceeding 800 bp in length. In addition, Höfle *et al*. (2020) observed that dsRNAs larger than 1.5 kb applied by SIGS dsRNA could not be taken up by the pathogen *in vitro*, as no gene silencing was observed. *In planta*, spraying these long molecules produced the lowest symptom reduction efficacy, underlining the different uptake in SIGS between *in vitro* and in planta application. In contrast, HIGS is not limited by the size of the dsRNA precursor used to transform plants. This suggests that dsRNA molecules too large to be absorbed will be less effective. In SIGS, the efficacy of dsRNA depends on the pathogen's ability to uptake these molecules (Qiao *et al.,* 2021; Cheng *et al.,* 2022; Wang *et al.,* 2023) and the properties of the DCL protein in each organism. However, to date, there is insufficient evidence to determine which length of dsRNA is the most effective for spray-induced gene silencing, and this is likely to depend on the individual pathosystem.

Therefore, a maximum dsRNA length of 800 bp was selected in this study based on three main considerations: (1) to allow the inclusion of multiple gene fragments within a single molecule, maximizing the potential for simultaneous silencing; (2) to promote the generation of

a diverse pool of effective siRNAs; and (3) to avoid the reduced efficacy and limited uptake observed with longer dsRNAs (>800 bp). This length provided a suitable balance between silencing efficiency and uptake ability.

2.2. Assessment of mRNA accessibility to enhance silencing efficiency

Another important consideration in dsRNA design is the location of the target region within the coding sequence. There is currently no conclusive evidence on whether targeting the 5' or 3' end of the mRNA yields better silencing results. Targeting a region close to the 5' end may offer the advantage of rapid mRNA degradation before protein translation can occur, potentially leading to a strong and immediate silencing effect through primary siRNAs. In contrast, selecting a region closer to the 3' end might enhance the production of secondary siRNAs, potentially leading to a more prolonged silencing effect. This is because, if RdRps initiate the amplification of the silencing signal from the 3´end, they can use a longer stretch of intact mRNA as a template, which may lead to the generation of a larger pool of secondary siRNAs and contribute to a more robust and sustained silencing response. Given this uncertainty, both theoretical mechanisms were taken into account during the design process, acknowledging that the optimal target position may vary depending on the gene, the organism, and the RNAi machinery involved.

Moreover, mRNA accessibility is a critical factor to consider in order to ensure the optimal design of dsRNA molecules. Therefore, we developed a custom tool based on RNAxs outputs processed with a custom R script, which allows the identification and visualization of the most accessible region within target mRNAs. This approach generates visual profiles of cumulative accessibility scores, calculated for 8-nt or 16-nt subregions and summed across a user-defined sliding window within a target mRNA (ranging from 165 to 250 nt in this study). This tool guided the selection of optimal target sites for dsRNA design (Figure 12).

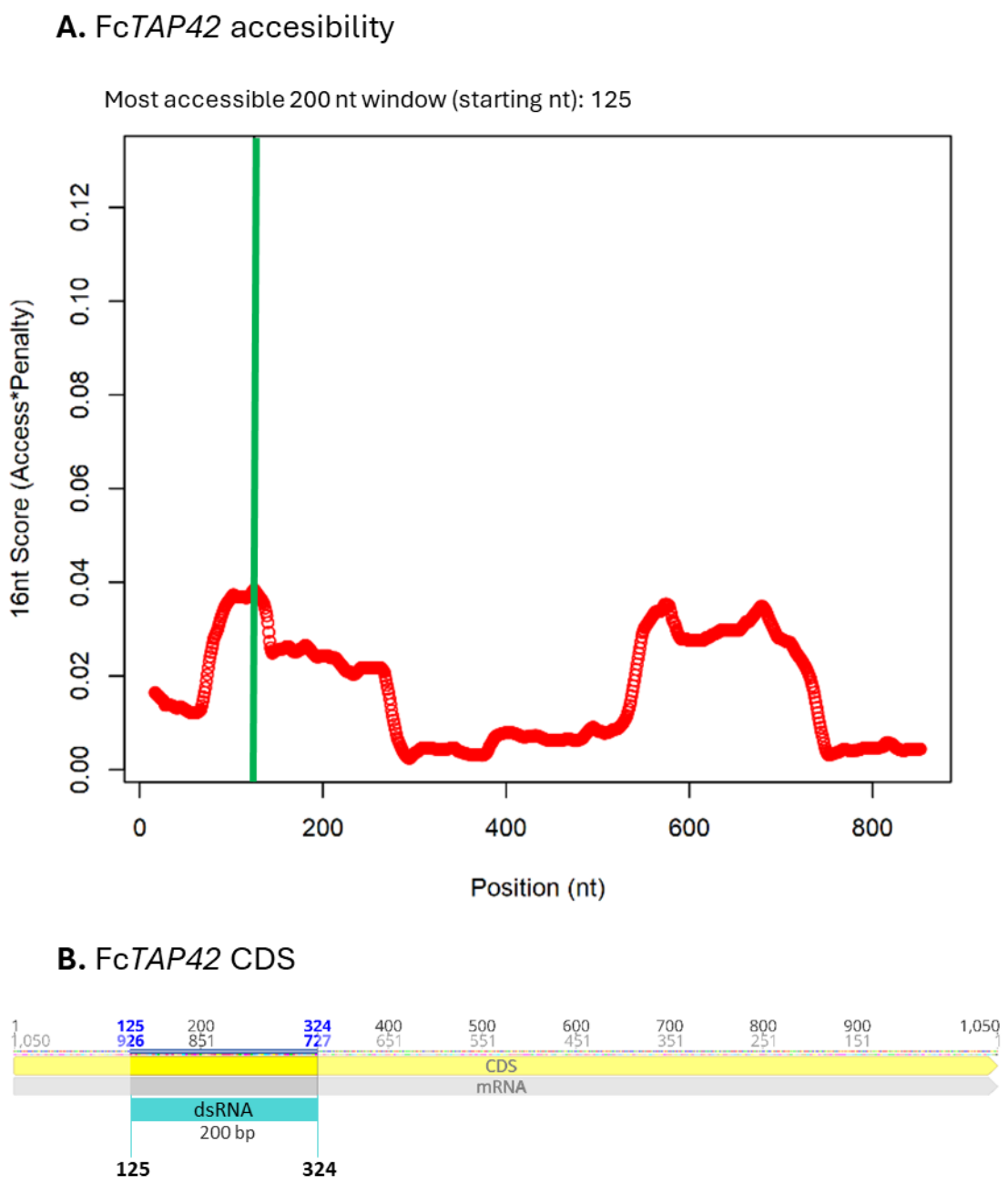

Figure 12. Influence of target mRNA accessibility analysis on decision making for dsRNA design. A. Accessibility profile of one of the study mRNA sequences (Fc*TAP42*) generated in R from RNAxs output. Each red point represents the total accessibility score for a 200-nt window starting at the corresponding nt position in the mRNA. The green vertical line indicates the starting nt (125) of the most accessible 200-nt window. **B.** Graphical representation of the selected target region (highlighted in blue) within the Fc*TAP42* mRNA, generated using Geneious. used for dsRNA design. This region, starting at position 125, was chosen based was selected for dsRNA design based on the accessibility profile shown in panel A.

This approach allowed the identification of the most accessible target regions; however, their potential off-target effects needed to be further evaluated, as described in the following section (2.3). For this reason, some dsRNAs were not designed in the regions identified by the accessibility analysis (indicated by an asterisk in Table 7). Furthermore, disruption of the protein at the end can result in the generation of incomplete but functional protein, which would render

the dsRNAs highly inefficient. In these instances, we proceeded to identify a more suitable area within the CDS with optimal accessibility, a decision based on the accessibility plots generated as part of our analysis.

The most accessible regions identified in the target mRNAs using this approach, and the corresponding starting positions selected for dsRNA design are summarized in Table 7.

Table 7. Selected target regions of genes for dsRNA design based on sequence accessibility

Target pathogen	Gene	CDS length	Starting nt of most accessible stretch	Chosen starting nt	Fragment length
F. circinatum	*PP2A*	975	377	377	200
	PPG1	949	445	445	200
	SIT4	1206	322	322	200
	TAP42	1050	125	125	200
	VPS51	2442	2054*	1606	168
	DCTN1	2433	17*	1828	165
	SAC1	2841	2414*	1714	165
	CHS1	2937	1929	1929	200
	CHS2	3555	111	111	200
	CHS3b	2712	1681	1681	200
	GLS1	5838	104	104	200
P. cinnamomi	*PP2A*	960	762*	342	200
	PPG1	927	683*	520	200
	SIT4	963	692*	177	200
	TAP42	1161	963*	218	200
	DHCR7	1308	412	412	200
	DCTN1	1917	1219	1219	200
	SAC1a	2226	1803	1803	200
	SAC1b	1839	332	332	200
	DCL1	4989	930	930	250
	DCL2.1	2820	2103	2103	250
	DCL2.2	2151	1903	1900	250

*Mismatch between most accessible stretch and fragment selected for dsRNA design

Previous studies have shown that secondary structure in the target transcript has a major effect on RNAi efficacy and therefore, dsRNA molecules with more accessible target sites are more susceptible to silencing (Bohula *et al.*, 2003; Kretschmer-Kazemi Far and Sczakiel, 2003; Westerhout and Berkhout, 2007). During RNAi, the RISC complex interacts with a region of the mRNA strand that is complementary to the siRNA guide strand and its cleavage generally requires base pairing in the seed and central region of small RNAs (Iwakawa and Tomari, 2022). Consequently, the target region of the mRNA should be accessible to facilitate the formation of the siRNA/rRNA duplex.

2.3. Evaluation of gene target sites to minimize off-target effects

The most accessible target region within each gene, as identified in Section 2.2 of this chapter, was thoroughly evaluated to reduce the risk of off-target effects and to maximize the efficiency of RNAi-mediated silencing. The target region within a gene is of utmost importance, as different silencing efficiencies have been observed in targeting different regions within *cyp51* of *Golovinomyces orontii*, leading to variable results in terms of reductions in fungal development (McRae *et al.*, 2023). This highlights the significance of the specific target region in determining the efficacy of the RNA interference approach. Additional considerations were taken into account based on current knowledge: targeting introns has proven ineffective for inducing silencing (Vickers *et al.*, 2003; Westerhout and Berkhout, 2007), and conserved regions tend to be shared across species, thereby increasing the risk of off-target effects. Accordingly, target regions were selected exclusively within exonic sequences and, following a detailed analysis of conserved domains, these regions were avoided during dsRNA design (Figure 13A). In some cases, it was not feasible to avoid targeting conserved domains due to their extensive coverage across the protein sequence, as observed in Fc*TAP42* (Figure 13B). In such cases, accessibility was prioritized, and an in-depth off-target analysis was conducted to ensure sequence specificity and reduce unintended silencing. All target regions were verified to be free of off-target potential using the nBLAST tool and si-Fi software, confirming that none of the resulting siRNAs shared 21- or 19-nt perfect matches with the transcriptomes of *P. radiata* or *Q. ilex*. Thus, the selected regions for dsRNA were both accessible and highly specific, with no predicted off-target effects in the host species.

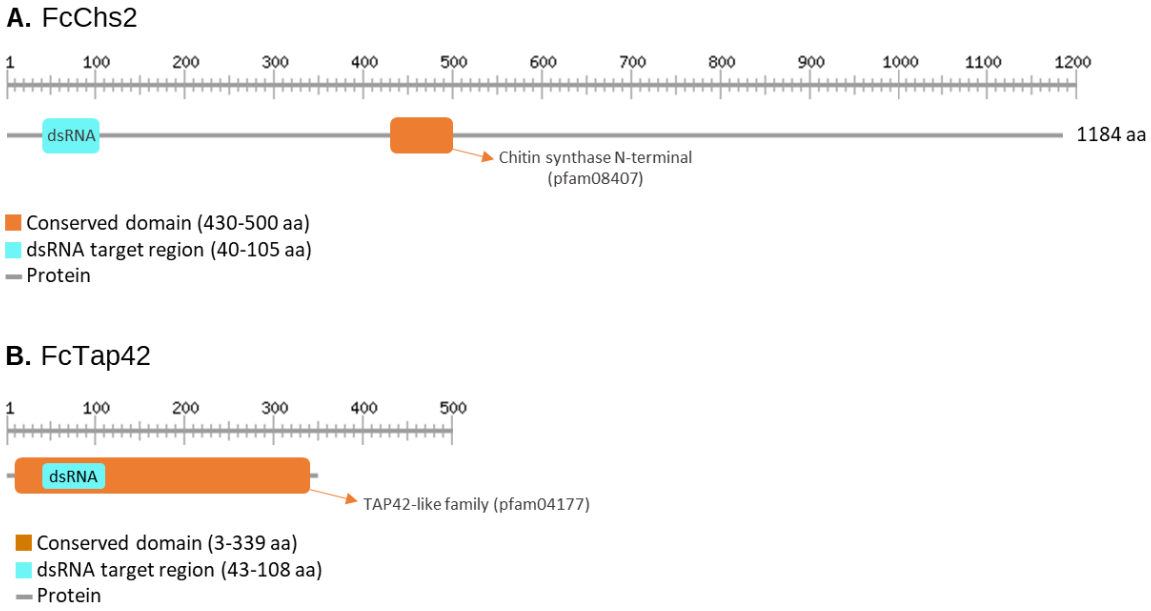

Figure 13. Exploration of conserved domains to avoid off-target effects in dsRNA design. Here we illustrate the use of protein domain databases to scan the conserved domains of the proteins and make decisions in dsRNA design.

A. In this example, the *F. circinatum* Chs2 protein of 1184 amino acids (aa) was analyzed, and a conserved N-terminal chitin synthase region was identified (in orange). The predesigned dsRNA (in blue) did not overlap with the highly conserved area. **B.** *F. circinatum* Tap42 protein of 349 aa possesses a TAP42-like family domain (in orange) that cannot be avoided in dsRNA design (in blue).

The final outcome of this comprehensive selection process was the *in silico* design of the dsRNA molecules utilized in the study (Table 8). Sequences were designed based on selected gene fragments identified in prior accessibility and specificity analyses. Fragment lengths range from 498 to 800 nt, depending on the number of gene regions included per molecule. As a mock control, YFP-dsRNA was designed to target the yellow fluorescent protein (*YFP*) gene, which is not present in any of the pathogens tested, in order to determine if the effect of the dsRNA treatments is related to the sequence specificity of the designed molecules.

Table 8. Mock control and pathogen-specific dsRNAs sequences developed in this study.

Function	dsRNA	Sequence
Mock control	YFP-dsRNA (517 nt)	CGGCCTGCAGTGCTTCGCCCGCTACCCCGACCACATGAAGCAGCACGACTTCTTCAAGTCCGC CATGCCCGAAGGCTACGTCCAGGAGCGCACCATCTTCTTCAAGGACGACGGCAACTACAAGACC CGCGCCGAGGTGAAGTTCGAGGGCGACACCCTGGTGAACCGCATCGAGCTGAAGGGCATCGAC TTCAAGGAGGACGGCAACATCCTGGGGCACAAGCTGGAGTACAACTACAACAGCCACAACGTCT ATATCATGGCCGACAAGCAGAAGAACGGCATCAAGGTGAACTTCAAGATCCGCCACAACATCGA GGACGGCAGCGTGCAGCTCGCCGACCACTACCAGCAGAACACCCCCATCGGCGACGGCCCC GTGCTGCTGCCCGACAACCACTACCTGAGCTACCAGTCCGCCCTGAGCAAAGACCCCAACGAG AAGCGCGATCACATGGTCCTGCTGGAGTTCGTGACCGCCGCCGGGATCACTCTCGGCATGGAC GAGCTGTACAAG
dsRNA sequences against *F. circinatum*	FcPTP-dsRNA (800 nt)	ACCCTCAACGAATCACAATCCTCCGAGGAAACCACGAGTCCCGTCAGATCACTCAGGTCTACGG TTTCTACGACGAATGCCTCCGTAAATATGGAAACGCTAATGTCTGGAAGTATTTTACCGACCTCTTTG ACTACCTCCCCCTCACTGCCCTGATCGACAACCAAATCTTCTGTCTTCATGGCGGCCTCTCCCCA AGCATGTTCGACTTTTTAACTTTGAGCGTTGTGATCAACGACCAAATATTTTGCGTCCATGGAGGCCT TTCCCCTTCTATCCATTCTATCGACCAGATCAAAATTATAGATCGTTTCCGCGAGATCCCCCATGAA GGTCCCATGGCCGATCTCGTCTGGTCTGATCCTGACCCTGAGCGCGACGAATTCTCCCTTTCACC TCGCCAACAGAGATCACAAACCCCAAGTTGAGGAAGAAGATAAAGTCTTCGGGCGAGAATGCAAC ATCCAGCGGCGTGGAGGAGACCGAGGCAGTCGAGGCAGAGGAAGATCCTGATTCCACAATGGC AGACCAGACCGAATCTGGCGTCACAGTCAACAAGTCAAGTCAAAGTGCCGATACTCGATACATTTT CCTGGGAGATATCCCTCTACTCTTCTGCGCGCGACCAAGTCTCAGCTCTTGCGCTCTTTTCCTCCA ACGAAGGACTTGAGGACGTTTCTACATCAGATCTACCTTATCTGCTTCTCGACGCCCACGTTGCGG AGCTCGTACAAAAGACCCCCAATCAAAGCCCTGACCAACGCCTAGAGGTCCTCTCCAAGTCTCG CGCCGCCTACGAG
	FcVDS-dsRNA (498 nt)	TCTTTCAAAGAGCTTGAAGATCAAATCCAGATTCTCTGGGATGAACGGGCTGAGTCATCGCACAAC GGTAAAGTGGCCATGTACTTCCTCCGTGTTTTACGAGATATCCGACATCAGTTACCAGAGCGCCCT TCCATCAAGAGCTTTGGCCTGAAGGCTGTTCCTTCACAATCTCTTCTTGAAAAGAAGAACAGTCGC GAGGACGAGCTCGAGAAGGAGCTTGAAACAATCCGTCAGAACGGTACAGCGGCCAACAGGTCTT CTTTCAGAGACTCCCGAGACACCGTCGTAATGGCCCAGGCAATGGAGAACCGACCAGTCGAGAA CCTCAAGGTCTGCCAGAGCTCATTCGCAAAGCATATGCTGGAAGTTCAACTCAAGGAGGAAGGCT TTGACATGAGTGCGCAGTCTGACCAAGTGACTGCTTGGTTCAACACCCTCTGGGCGGACAATGGC GACGCTGTGTCAAAACAGTACGCATCGACAGCAGCGATGAAG
	FcCHS-dsRNA (800 nt)	CGTCACATTCTCCTGGTTCTCACTCGCGTCTTTCTACCTCACCACCACCATCATCATGAAGCTTGTC GGAACGCCCCAGGTTCTCTCCGGATACCATGGTTGGCCATTTGGCGATACAGCCACGCCGATTG TTAATGTCCTGATCAAATATATATACATCGCCTTCCTCGTCCTCCAATTCGTCCTCGCTCTCGGAAA CACGAAGAACACTACGACCCTCATACGTATGTACCACCCTCATCACCCAGCCAGATTCAGACACA GACACCTCCTGCACGCCCTCCCTCCTCTCCTTCTGTTTCCCCTTCTACCTCATGTTCAAAGACAAC

		ACCCTCCCCTCTCAAACCGCCAGTAGCGTTTCCTCCTCCATTGTCAATTTCACCTGTGAGCATCAC CATGTTTCCTCGACTTCCTCCGATCCGATCACACTTTCTTGCGAAAGTTTGCCTTCTTCATCGAATTC ATCTTCAACACTATCAACATGATCTTCGCTTGGTTTGCTATTGGTAACTTCTTCCTCGTTTTCAAGATT CTCACAACAAGTTTGGGAGACGATTCGTTACTGGGGCGGACAGGAGAAATTCTAGGTGTCGTATTT ACACTACCAAGATGATCAGTACTACGATCAAGGCTACGACAACCGTGGCCCAAATCACAATAACA ACAATAACAACAATAACCATGATGGCTACTACGATGAATCTGGTTACTACAACGCCGACCCAAATA ACCCCTACCAGCAGGATGGAGGCTATTACGACGGCCACGATCAATACCAAGATGGATACTACGA CAATGGC
dsRNA sequences against *P. cinnamomi*	PcPTP-dsRNA (800 nt)	GCGCGGCAACCACGAGAGCCGCCAGATCACGCAGGTCTACGGCTTCTACGACGAGTGCCTGC GCAAGTACGGCAACGCCAACGTGTGGAAGTACTTCACGGACCTGTTCGACCACCTGCCCATGAC GGCGCTCATCGAGAACCGCGTCTTCTGCATGCACGGCGGTCTGTCCCCGTCCATCGACACGCT GGACCACGCGCACGCTCGACCAGATCCGCATCATCGACCGCAAGCAGGAGGTCCCGCACGAC GGCGCTATGTGCGACTTGATGTGGTCCGACCCTGAGGACATTGATGGCTGGGGCCTCAGTCCTC GTGGTGCGGGATACCTTTTCGGCGGAGACGTCGTGGAGAAGTTCAACCAAACGAACGACATTCAG CTAATCTGCAGAGCGCATCAGAGCAGCCCCGTGACGGTCTGCGGCGACATCCACGGCCAGTTC TTCGACCTGCTGGAGCTCTTCCGCTGCGGTGGAGACATCCAGGACACCAACTACATCTTCATGGG CGACTTCGTGGACCGCGGACACAACAGCGTGGAGACCTTCGAGCTGCTGCTGTGCCTCAAGGC GCGCTACCCGGACCGCATCACGCTGCTGCTCGAGCTGCACAACACGCAGCTGTACGCCTTCTG CCTCGAGTACTACCTAGGTATGCTCACGCCCAAGCAGAGCTTCTTCCAACAGCAGCCCAAGGAC GAGCGAGGGCAGCGCCAGGGCCCCTCGGACCACACGCGCAACGTCGTGTTCCGCATCAAGTT CCTGCGCGAGGCCGACGTCTTCCTCACCGAGTTCTTGGAC
	PcDDS-dsRNA (800 nt)	ATGCCCGAGATCATCTCGGCGCTCAACGTCTTCAGCTTCATCTTCTGCCTCTTCCTGTACGTCAAG GGCGCGTTCCTGTGGCAGTCGTCGAGCGACGCCGGCACGTCGGGCAACCCCGTGTTCGACTTC TACTGGGGCACGGAGCTGTACCCGCGCGTGCTGGGCTGGGACGTCAAGCTCTTCACCAACTGC CGCTGCGGAAATCCAAGTCCGTTGCAAGCCCACCGCGTGCCCCGAAGCCGACCGCCGCGTCTT TCGGGCTACGTCCTGGTGGCGATCAGGAACAACTGATGGACAAGCAGCTCTGGGACTTGTACTAC TTCGGCATTTCGGACGAAGCGCCTGAGGTCGGCAAATTCAGAGATTCGGATGGATTTACGCAAAC GATGAGCATGGCGTCCACGCGCACAGGACGACGAACGATTGCAGGCGCCCTGCAAGACGGCG TGAATTCAGTCACCCGCTATTATCTCAACAACTTTTCTGACGGTATCCGCCAAGACTCTTTCGACTT GCTCGTTGGAAACTTCACACCGGATAAGCGAGACGAGTCACCGTTCACCTTCCAGCAGCAGCAC AGCCTCGTGAACATGATGCTAGACCTGCCCACGCTCACGCCGCAGCAGGAGCAGGACGAGCAG AGCTACATCGACATGATCACCACGGACATCGAGAAGCAGAAGCTGCACTTCGCCAAGGACTTCG ACCTCACGCACTCGCTGCAGCGAATCGCGGCTTTTGACGGCAAGAAGGGCAGCATCGCGGAGC GCGCGGACGACCGCTTCTTCTGGAACAAATCG
	PcDCL-dsRNA (750 nt)	CAACGTGAATAACAGGAGGAAGCAGAAGCAGCAGGGCAGCGGGGAACTAGCGGACGACCTGAT GAATGGAGAGGAGATTGAGAGCGACGCTGGAAATGAACCGGAGGATGGAGAAGTGGACGAAAAT GAAGACGAAGTCGAAATGATGGATGTCACCAGCCACGAGCACGAAAATTCAAAGACTGCGAAAAC AGATCGCTTGATTGCAAGATTTATAGGGCCTGGTATCGAGATAGACGAGAGTACAAGGTGACGAAT TTATTGGGCACGATCCAAGTTACGAACGCATCGAATTCCTTGGTGATGCTGTGCTGCAACTCTTGTC GTCTGAGTTCCTTGTGGATGCTTTTCCGTACCACCAGGAACACCTTCTTACCCAAGTGCGGTCGTC ACTAGTGAAAAACAAGAAGCTGGCGATCGTTGCGCGCAATGCTGGCTATGAGGAGTTCATTCGATT GGGGAATGAGGTCAAGAAGAATGGCAATTTGTACGTGGAGGACCGCTACGGCGGGAAGAGCATG TTCACAGCGGAGCTCAATCTACCGATTGAGCTGGAACTGGAAACTTTTCGGAGCGATCCCATGCC GTCCAAGGCTGGTGCCAGAGCTGCTGCAGCCTTCAGTGCATGTCAGAAGCTTTTGGATCAGCAAC TTCTTGATGAATCGTTGAATTCGATCTACCGCACCACCAAGGTGAAGTCTTCGTCCAACACGCGGG ACTTGACCTTCTTCCTGAACCGCCTGCACACGT

Sequences underlined in different colors represent fragments of different genes.

3. Optimization of a bacteria-based dsRNA production system

As a result of our research, we successfully developed an optimized dsRNA production methodology based on genetically engineered *Escherichia coli* HT115(DE3), which enabled rapid, flexible, and cost-effective production of high-purity dsRNA for use in various experimental

assays. This system proved highly efficient and adaptable, meeting the evolving demands of the study while maintaining consistent yield and quality.

The requirement for substantial amounts of dsRNA for *in vivo* assays described in Chapter 2 and 3 prompted the development of this solution. There are several options to produce dsRNA. These include synthesis by *in vitro* transcription, cell-free and microbial-based dsRNA production (Bocos-Asenjo *et al.*, 2022). *In vitro* transcription methods, such as those offered by the commercial MEGAscript™ RNAi Kit, deliver excellent quality and purity, and were therefore used in specific experiments like uptake assays. However, their high cost made them unsuitable for large-scale applications such as *in planta* spraying assays. An alternative option is provided by a commercial company like Genolution, which offers affordable prices (e.g., 1 µg of dsRNA for 0.1€) but with extended delivery times of up to three months. However, due to the nature of our study, dsRNA needed to be produced progressively, allowing for flexibility in response to changing experimental factors without relying on lengthy production timelines.

To overcome these constraints, we optimized a bacteria-based dsRNA production system for the rapid production of dsRNA, ensuring a high degree of purity while producing sufficient quantities for emerging assays. This approach was both cost-effective and adaptable, allowing us to maintain a steady supply of dsRNA as experimental demands evolved. The specific results of this optimization process are presented here, detailing improvements in production efficiency, induction conditions, extraction methods and enhancement of dsRNA yield and purity.

3.1. Plasmid selection for enhanced dsRNA production

The choice of plasmid is particularly important when working with inducible expression systems. For the efficient production dsRNA in *Escherichia coli* HT115(DE3), we selected the T777T plasmid, which includes two T7 promoters in opposite orientations flanking the insert site, along with two T7 transcriptional terminators. This configuration enables the simultaneous transcription of both sense and antisense RNA strands from the insert, resulting in the formation of dsRNA. T777T is an improved variant of the L4440 (Addgene plasmid # 1654 ; http://n2t.net/addgene:1654 ; RRID:Addgene_1654), which features a dsRNA production cassette with inducible control of insert expression in both directions. The L4440 plasmid has been used to produce long, non-specific RNA fragments from the vector backbone, which reduces the efficiency of RNAi (Sturm *et al.*, 2018), whereas the T777T vector enhances the efficiency of the dsRNA produced by incorporating two T7 terminators that prevent transcription beyond the insert and reduce the production of non-specific RNA. These features, including tight

transcriptional control, improved terminator design, and compatibility with the HT115(DE3) system, make T777T a highly suitable vector for reliable, cost-effective, and scalable dsRNA production. It was therefore selected for all constructions in this study.

The T777T vector, previously reported as a reliable tool for dsRNA production (Sturm *et al.*, 2018), was successfully employed in this study to generate dsRNA constructs targeting the forest pathogens *F. circinatum* and *P. cinnamomi*. As a result, gene-specific dsRNA templates were successfully cloned into the T777T plasmid to enable bacterial production of dsRNA, as shown *in silico* in Figure 14. These included: T777T-FcCHS-dsRNA (3105 bp), T777T-FcPTP-dsRNA (3137 bp), T777T-FcVDS-dsRNA (2803 bp), T777T-PcDCL-dsRNA (3055 bp), T777T-PcPTP-dsRNA (3105 bp), T777T-PcDDS-dsRNA (3105 bp) and T777T-YFP-dsRNA (2822 bp).

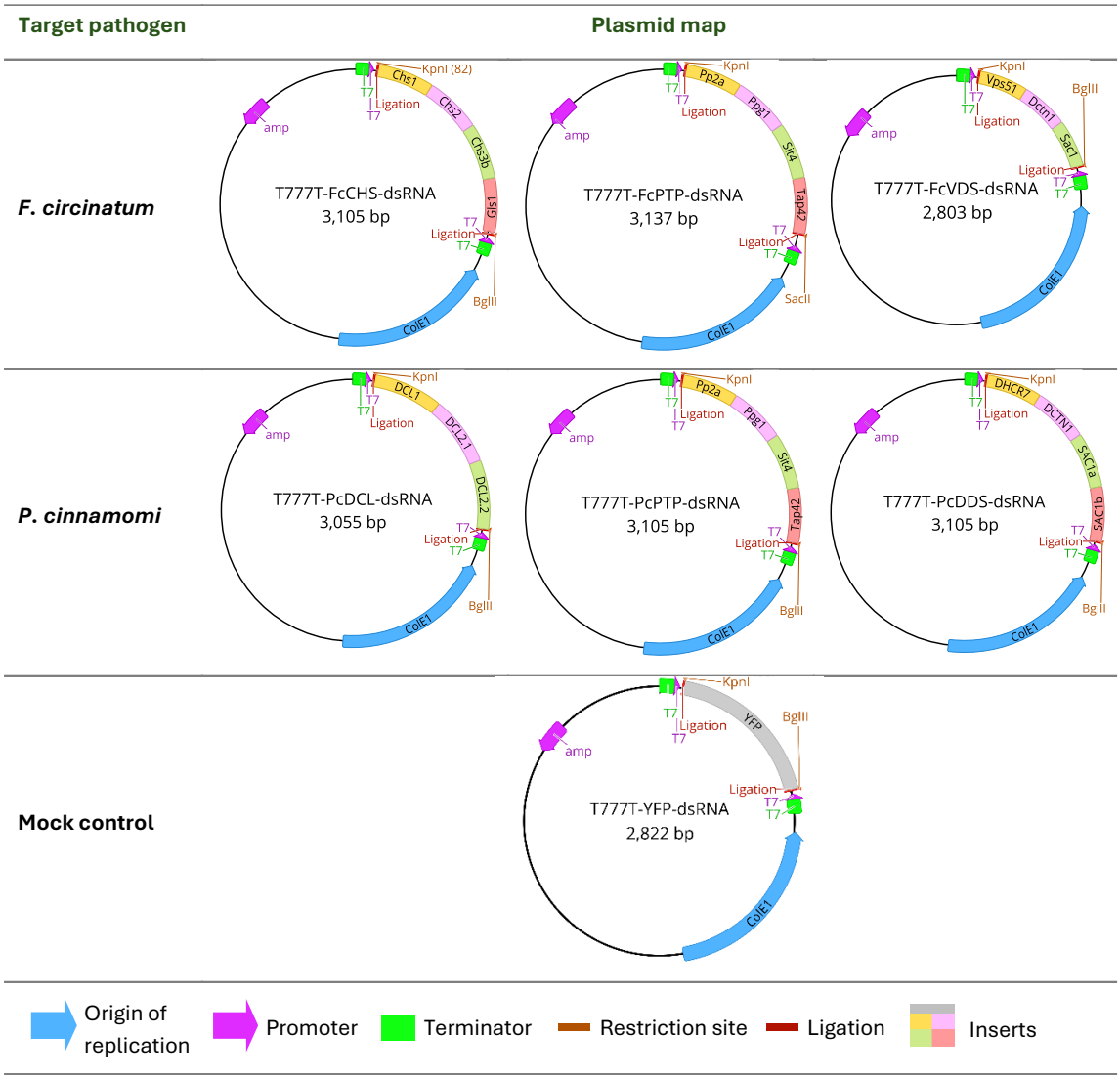

Figure 14. *In silico* construction of dsRNA-expressing plasmids using the T777T vector. Plasmid maps display key plasmid features, including the inserted gene fragments, T7 promoters and terminators, restriction sites, and antibiotic resistance markers.

3.2. Improving the protocol for induction and extraction of dsRNA

To optimize dsRNA production in *E. coli* HT115(DE3), we evaluated a range of induction conditions by varying both the concentration and timing of IPTG application, as well as the incubation period post-induction. Specifically, we tested IPTG concentrations of 0.5, 1.0, and 1.5 mM, applied either once or in two separate doses (double induction). In single induction treatments, IPTG was added when cultures reached optical densities (OD_{600}) of 0.5, 0.8, or 1.0. In double induction treatments, a second dose of IPTG was added 4 h after the first. Additionally, incubation times following induction were tested at 1, 4, 8, 15, 20, and 24 h to evaluate the effect on dsRNA yield. The optimal results were achieved by adding 1.0 mM IPTG once, when the optical density (OD_{600}) of the bacterial culture was 0.8 and after incubation for 4 - 8 h. These conditions consistently yielded the highest dsRNA quantities.

3.3. Purification strategy for dsRNA integrity and yield

dsRNA extraction using TRIzol® method yielded total RNA, including both double-stranded RNA and single-stranded RNA from the bacteria. Consequently, a final purification of the dsRNA was conducted to obtain high-quality dsRNA suitable for downstream applications. To achieve this, several strategies were evaluated to efficiently eliminate residual nucleic acids while minimizing the loss of dsRNA (Figure 8A).

First, we evaluated different enzymatic digestion protocols. DNase I was used to eliminate residual DNA, while two ribonucleases, RNase A and RNase T1, were tested to degrade ssRNA. We then tested various commercial purification and clean-up kits. These included the RNA Clean and Concentrator kit from Zymo Research, the purification step included in the MEGAscript RNAi kit from Thermo Fisher, and the NucleoSpin RNA Virus kit from Macherey-Nagel.

In the enzymatic treatments (Figure 15A, left), DNase I digestion alone and the treatment with RNase A combined with DNase I, partially reduced contamination. However, the best result was obtained with a combination of DNase I and RNase T1, which effectively removed DNA and ssRNA without compromising dsRNA integrity, as evidenced by a clear and sharp band in electrophoresis gel. Commercial cleaning kits demonstrated varying levels of efficiency in recovering dsRNA (Figure 15A, right). The RNA Clean and Concentrator kit from Zymo Research produced a visible band, while the MEGAscript™ purification step and the NucleoSpin RNA Virus kit resulted in significant degradation of the nucleic acids, suggesting poor recovery or loss of integrity during the process. The unpurified sample showed the presence of significant

contaminants. The evaluation of dsRNA integrity by agarose gel electrophoresis was complemented by spectrophotometric quantification, including absorbance ratio measurements to assess its purity.

Finally, the most effective purification procedure for dsRNA involved enzymatic treatment with DNase I and RNase T1 enzymes to remove any residual DNA and ssRNA, respectively, followed by a clean-up process using RNA Clean and Concentrator kit from Zymo Research to remove the enzymes used for purification (Figure 15B). This optimized protocol yielded between 2 and 3 µg of high-purity (A_{260}/A_{280} and A_{260}/A_{230} ratio range = 1.8 to 2) dsRNA per 50 ml of induced bacterial culture. This procedure resulted in the production of sufficient quantities and high quality of FcCHS-dsRNA, FcPTP-dsRNA, FcVDS-dsRNA, PcDCL-dsRNA, PcPTP-dsRNA, PcDDS-dsRNA and YFP-dsRNA, which were used in the experimental assays described in the following chapters.

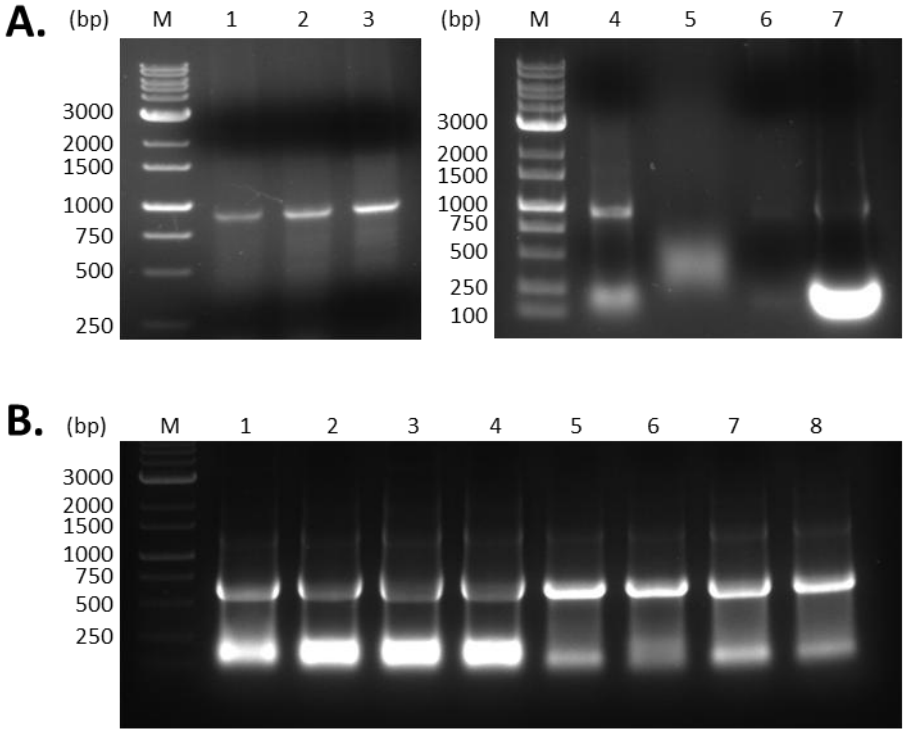

Figure 15. Assessment of dsRNA purification protocols. A. Different purification and clean-up protocols were tested to achieve quality dsRNA. On the left different enzymatic assays were tested: lane 1 corresponds to digestion with DNase I, lane 2 corresponds to digestion with DNase I and RNase A, and lane 3 corresponds to digestion with DNase I and RNase T1 (all enzymes were from Thermo Fisher, Waltham, MA, USA). On the right several commercial purification and cleaning kits were tested: lane 4 corresponds to RNA Clean & Concentrator (Zymo Research, Irvine, 197 CA, USA), lane 5 corresponds to purification step of the MEGAscript™ RNAi kit (Thermo Fisher, Waltham, MA, USA), lane 6 corresponds to NucleoSpin RNA Virus (Macherey-Nagel, Düren, Germany), and lane 7 corresponds to total RNA extracted with TRIzol. On the right different enzymatic assays were tested: lane 5 corresponds to digestion with DNase I, lane 6 corresponds to digestion with DNase I and RNase A, and lane 7 corresponds to digestion with DNase I and RNase T1 (all enzymes were from Thermo Fisher, Waltham, MA, USA). dsRNA analyzed in the gels corresponded to FcCHS-dsRNA (800 bp). **B.** Established protocol consisted in an enzymatic treatment using DNase I and RNase T1, to remove any excess DNA and ssRNA respectively, and a clean-up step using a commercial kit, which improved the visualization of the dsRNA band on agarose gel. Lanes 1-4 show the dsRNA band before purification step and lanes 5-8 show the purified dsRNA band. dsRNA analyzed in this gel corresponded to YFP-dsRNA (517 bp).

The T777T plasmid was originally designed to produce dsRNA in bacteria that were to be ingested by *C. elegans* nematodes, and thus, the isolation and purification of the dsRNA was not a necessary step. To conclude, a key outcome of this work has been the successful development and optimization of a reliable method for synthesizing and purifying high-quality dsRNA in the laboratory. This work has optimized the isolation and purification steps to obtain dsRNA that meets the relevant requirements for use in assays against pathogenic fungi and oomycetes in plants. Moreover, the optimization process has facilitated subsequent experiments and may prove useful in future studies with other fungal pathogens. The results of this section demonstrated the successful development of an efficient method to produce custom-designed dsRNA using microorganism-based production systems, resulting in the generation of sufficient quantities of high-quality dsRNA. Importantly, we are currently working to further improve, reduce the cost of, and scale up this dsRNA production process in collaboration with Professor Li-Hung Chen from the National Taiwan University.

Chapter 2

Spray Induced gene silencing (SIGS) for the control of Pine Pitch Canker caused by *Fusarium circinatum*

This section aims to demonstrate the efficacy of the molecules produced in the previous section (Chapter 1) using SIGS methodology in the control of a relevant forest pathogenic fungus, *F. circinatum,* which causes a devastating disease in pine species worldwide. To this end, the following actions were proposed:

- To assess SIGS requirements for optimal functioning by conducting an *in silico* study of the RNAi machinery and evaluating the ability of the pathogen to uptake dsRNA molecules from the environment.
- To find a rapid method to evaluate molecules against *F. circinatum* by testing different plant materials and optimizing infection and treatment application conditions.
- To evaluate the efficacy of SIGS technique on pine trees under nursery conditions by applying dsRNA treatments to seedlings and assessing their effect on disease progression and fungal development.

1. Assessment of SIGS requirements for effective disease control

The efficacy of SIGS technology in controlling pathogens depends on the presence of the central core elements of the RNAi machinery (Shabalina and Koonin, 2008). Additionally, the successful uptake of the dsRNA molecules by the pathogen is a crucial prerequisite for the success of SIGS. The initial step in our work with *F. circinatum* was to ascertain these requirements.

1.1. RNAi machinery is conserved in *Fusarium circinatum*

The essential components for the functioning of the RNAi silencing mechanism in fungi are DCL, AGO, and RdRps. As a brief reminder, DCL are responsible for recognizing and cleaving long dsRNA molecules into siRNAs, which are the effectors of gene silencing. These siRNAs are then loaded onto AGO, which play a central role in guiding the silencing complex to complementary mRNA targets, leading to their cleavage, preventing the production of specific proteins. RdRps amplify the silencing signal by synthesizing secondary siRNAs from target mRNAs, enhancing the robustness and durability of the RNAi response.

To identify the RNAi machinery of *F. circinatum*, we used the well-known pathogen *F. graminearum*, one of the most studied in the *Fusarium* genus. This allowed us to leverage the existing knowledge about the RNAi machinery of *F. graminearum*, which has been identified and well characterized search (Chen *et al.*, 2015; Son *et al.*, 2017). Given the close evolutionary relationship between these pathogens, the *F. graminearum* RNAi-related proteins were employed as a reference for the identification of orthologous proteins within the *F. circinatum* proteome. The *in silico* analysis of RNAi core components in *F. circinatum* revealed the presence of two DCL, three AGO, and four RdRp (Table 9).

Table 9. Identification of RNAi-related proteins in *F. circinatum* using homology-based analysis with *F. graminearum* amino acid sequences

F. graminearum RNAi proteins (GenBank)	aa identity (%)	Orthologous proteins in *F. circinatum* (GenBank)	Description	Protein length (aa)	Gene length (bp)	Domains
FgDCL1 (XP_011328775.1)	62.28%	FcDCL1 (KAF5660727.1)	Putative DCL	1500	4632	Dicer dimer, Helicase ATP Binding, Helicase C-terminal, PAZ, RNase IIIa, RNase IIIb
FgDCL2 (XP_011321198.1)	56.82%	FcDVL2 (KAF5684693.1)	Putative DCL	1603	5111	Dicer dimer, dsRBD, Helicase ATP Binding, Helicase C-terminal, RNase IIIa, RNase IIIb
FgAGO1 (XP_011319975.1)	58.98%	FcAGO1 (KAF5672919.1)	Putative DGO	1051	3302	ArgoN, L1, L2, MID, PAZ, Piwi.
FgAGO2 (XP_011316005.1)	80.28%	FcAGO2 (KAF5667017.1)	Putative AGO	988	3020	ArgoN, L1, L2, MID, PAZ, Piwi.
FgAGO1	30.81%	FcAGO3 (KAF5663384.1)	Putative AGO	1481	6429	ArgoN, Fungal_trans, L1, L2, MID, PAZ, Piwi.
FgAGO2	29.08%					
FgRdRp1 (XP_011326113.1)	71.36%	FcRdRp1 (KAF5661793.1)	Putative RdRp	1392	4232	RNA dependent RNA polymerase
FgRdRp2 (XP_011320016.1)	62.53%	FcRdRp2 (KAF5659760.1)	Putative RdRp	1374	4178	RNA dependent RNA polymerase

FgRdRp3 (XP_011317398.1)	73.17%	FcRdRp3 (KAF5658320.1)	Putative RdRp	1269	3983	RNA dependent RNA polymerase
FgRdRp4 (XP_011320958.1)	32.17%	FcRdRp1 (KAF5661793.1)	Putative RdRp	1392	4232	RNA dependent RNA polymerase
FgRdRp5 (XP_011328717.1)	75.54%	FcRdRp4 (KAF5685686.1)	Putative RdRp	1732	5390	RNA dependent RNA polymerase

Note - Domain abbreviations refer to functional regions typically involved in RNAi mechanisms: ArgoN – Argonaute N-terminal domain; Dicer dimer – Dicer dimerization domain; dsRBD – Double-stranded RNA-binding domain; Fungal_trans – Fungal transcription factor domain; Helicase ATP Binding – ATP-binding region of helicase; Helicase C-terminal – C-terminal region of helicase; L1 – Linker 1 domain; L2 – Linker 2 domain; MID – Middle domain of Argonaute; PAZ – Piwi/Argonaute/Zwille domain; Piwi – P-element Induced Wimpy testis domain; RNA-dependent RNA polymerase – Catalytic domain for RNA synthesis; RNase IIIa / RNase IIIb – Ribonuclease III domains.

The comparative analysis of protein sequences identified two DCL proteins in *F. circinatum* (FcDCL1 and FcDCL2). We conducted a detailed examination of protein domain architecture. Both DCL identified in *F. circinatum* exhibited domain architectures similar to *F. graminearum* proteins (Figure 16). Six domains were identified in FcDCL1 in the Pfam database. Two of these domains (Helicase ATP Binding domain, Helicase C-terminal domain) possess helicase activity, which catalyzes the cleavage of double-stranded nucleic acids in an energy-dependent manner (Caruthers and McKay, 2002). The protein contains a Dicer dimerization domain (Dicer dimer), which is found in members of the dcl family of proteins and is essential for dcl activity (Ye *et al.*, 2007) .It also contains a PAZ domain, which are found in AGO and DCL protein families and functions as a nucleic acid binding domain exhibiting a strong preference for single-stranded nucleic acids (RNA or DNA) or for RNA duplexes with single-stranded 3' overhangs (Ma *et al.*, 2004). Additionally, it possesses two neighboring Ribonuclease III domains (RNase IIIa and RNase IIIb), which are double-stranded RNA-specific endonucleases that, in eukaryotes, are involved in RNA interference and gene silencing by miRNA (Lau *et al.*, 2012). FcDCL2 also contains six domains that align with the aforementioned, except for the PAZ domain, which is absent, and a dsRDB domain (double-stranded RNA-binding domain) which is present at the end of the sequence, whose main function is to bind dsRNA. The proteins identified in *F. circinatum* as dcl exhibit elements of a typical dcl protein architecture, although they lack some of the typical domains, since the domain composition of dcl varies within and among species (Ciechanowska *et al.*, 2021). The functional core of dcl, comprising the PAZ domain and the two RNases III, is present in FcDCL1, whereas FcDCL2 lacks the PAZ domain. This domain is also absent in the FgDCL2 sequence analyzed from *F. graminearum*. However, FcDCL2 and FgDCL2 possess a dsRDB domain at the end of the sequence that has been shown to be necessary for substrate binding when the dcl lacks the PAZ domain (Ma *et al.*, 2012). There are some examples in literature of dcl proteins that lack PAZ domain, such as the green alga *Chlamydomonas reinhardtii* dcl3 (Valli *et al.*, 2016). *F. circinatum*, like *F. graminearum* (Chen *et al.*, 2015) and other fungi, such as the model species of RNAi mechanism in fungi *N. crassa*

(Catalanotto *et al.*, 2004), has two DCL. It should be noted, however, that the number of DCL homologs may vary among species. For instance, the fungus *Schizosaccharomyces pombe* has a single DCL copy (Sigova *et al.*, 2004), while plants often have several DCL, with *Arabidopsis thaliana* having four (Liu *et al.*, 2009).

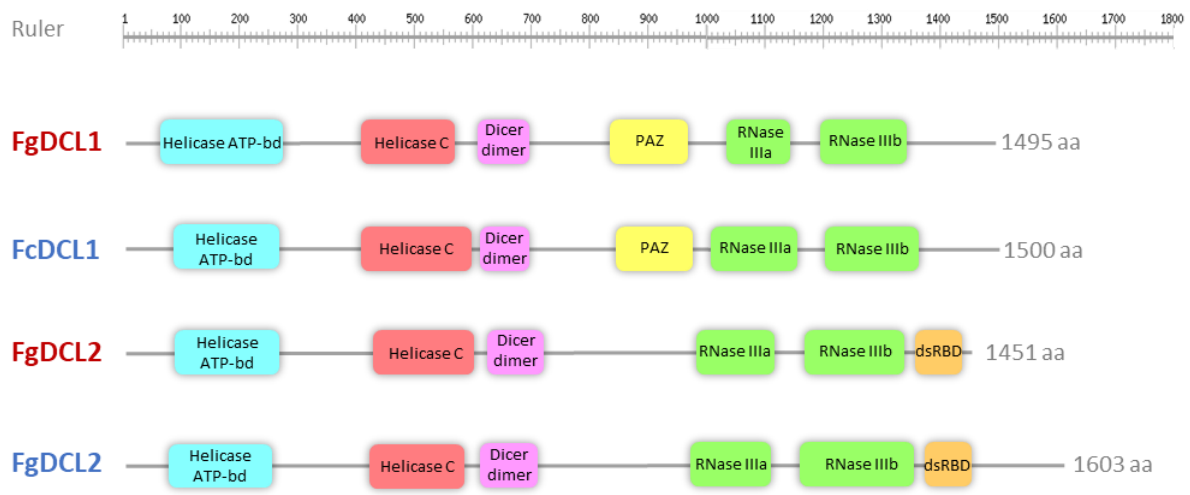

Figure 16. Two proteins identified in *F. circinatum* were found to be homologous to DCL1 and DCL2 of *F. graminearum*, suggesting a conserved role in RNA interference machinery. DCL domains are present in the proteins. Domains were predicted against Pfam database using MOTIF tool. Lines represent the full length of the protein. Boxes represent the identified domains and are labeled with different colors: Helicase ATP-bd (blue), Helicase C (red), Dicer dimer (pink), PAZ (yellow), RNase IIIa and RNaseIIIb (green), and dsRBD (orange).

The *in silico* search yielded three hypothetical AGO in *F. circinatum*, whereas the reference pathogen, *F. graminearum*, exhibited only two. (Chen *et al.*, 2015). The proteins designated as FcAGO1 and FcAGO2 exhibited 58.98% and 80.28% homology with FgAGO1 and FgAGO2, respectively. A third protein was identified in *F. circinatum* (FcAGO3) that exhibits a lower degree of similarity to FgAGO1 and FgAGO2. Specifically, FcAGO3 displays 30.81% and 28.08% homology with FgAGO1 and FgAGO2, respectively. A BLASTp search confirmed that FcAGO3 was not a duplicate of FcAGO1 or FcAGO2. The results demonstrated that they were only 35.15% and 29.41% similar, respectively. Given that FcAGO3 was approximately 500 aa longer than the other AGO proteins, we considered the possibility that this was a misannotation. To re-annotate, we identified an upstream methionine in close proximity to the initial functional domain, commencing at amino acid residue 573. A methionine located at position 407 in the protein was selected as the start of FcAGO3, and the sequence homology analyses were repeated. It was observed that FcAGO3 still showed low homology against the AGO proteins of *F. graminearum* (30.56 and 29.08% respectively) and *F. circinatum* (35.15 and 29.41% respectively). Furthermore, a multiple sequence alignment (Clustal Omega 1.2.2) of the three FcAGO proteins revealed significant differences between the three proteins (Figure 17.A). This suggests that *F. circinatum* may possess a third AGO protein, and that FcAGO3 is not a

misannotated copy of FcAGO1 or FcAGO2. Interestingly, the presence of three AGO proteins has also been reported in *Fusarium fujikuroi* (Pardo-Medina *et al.*, 2024). The AGO proteins are highly conserved between species, yet their number varies considerably between organisms. For instance, the yeast *Schizosaccharomyces pombe* has a single copy, *Arabidopsis thaliana* plant has ten, and *Caenorhabditis elegans* possess twenty-seven (Höck and Meister, 2008). The number of AGO proteins has also been found to be variable in the fungal kingdom. The RNAi model fungus, *N. crassa*, has two AGO (Cogoni and Macino, 1999; Cogoni and Macino, 2000), as does *F. graminearum*. However, the rice pathogen *Magnaporthe oryzae* has three (Nakayashiki *et al.*, 2006), and the forest pathogen affecting chestnut trees, *C. parasitica*, has four AGO (Sun *et al.*, 2009).

FcAGO1, FcAGO2 and FcAGO3 proteins contain six domains (ArgoN, L1, PAZ, L2, MID, and Piwi) which have been identified in other AGO orthologs (Figure 17.B). AGO proteins are characterized by the presence of PAZ and Piwi domains, and structurally they present two lobes called PAZ lobe and Piwi lobe. ArgoN domain is the N-terminal domain of ago proteins in eukaryotes. It has been demonstrated to be essential for small RNA duplex unwinding in the RISC complex, although it is not required for initial RISC loading or subsequent target binding and cleavage (Kwak and Tomari, 2012). ArgoN is linked via L1 (Linker 1 domain) to the PAZ domain, which is present in DCL and AGO proteins. It may function here by recognizing the characteristic 3' overhangs of siRNAs (processed from dsRNA by the dcl enzyme) within RISC complexes (Lingel *et al.*, 2003). The next domain found in the FcAGO proteins identified in *F. circinatum* is L2 (Linker 2 domain), which links the two lobes of this protein. The MID domain serves to anchor small RNAs onto the ago protein, binding the sRNA 5´end, and lastly the Piwi domain represents the catalytic site for ssRNA (for example, mRNA) slicing guided by double-stranded siRNA (Wei *et al.*, 2012). Therefore, the proteins FcAGO1, FcAGO2 and FcAGO3 identified in *F. circinatum* exhibit the necessary domains to function as AGO, including the functional domains PAZ, MID, and Piwi. Furthermore, the evidence presented here provides further support for the hypothesis that FcAGO3 represents a third AGO present in *F. circinatum*.

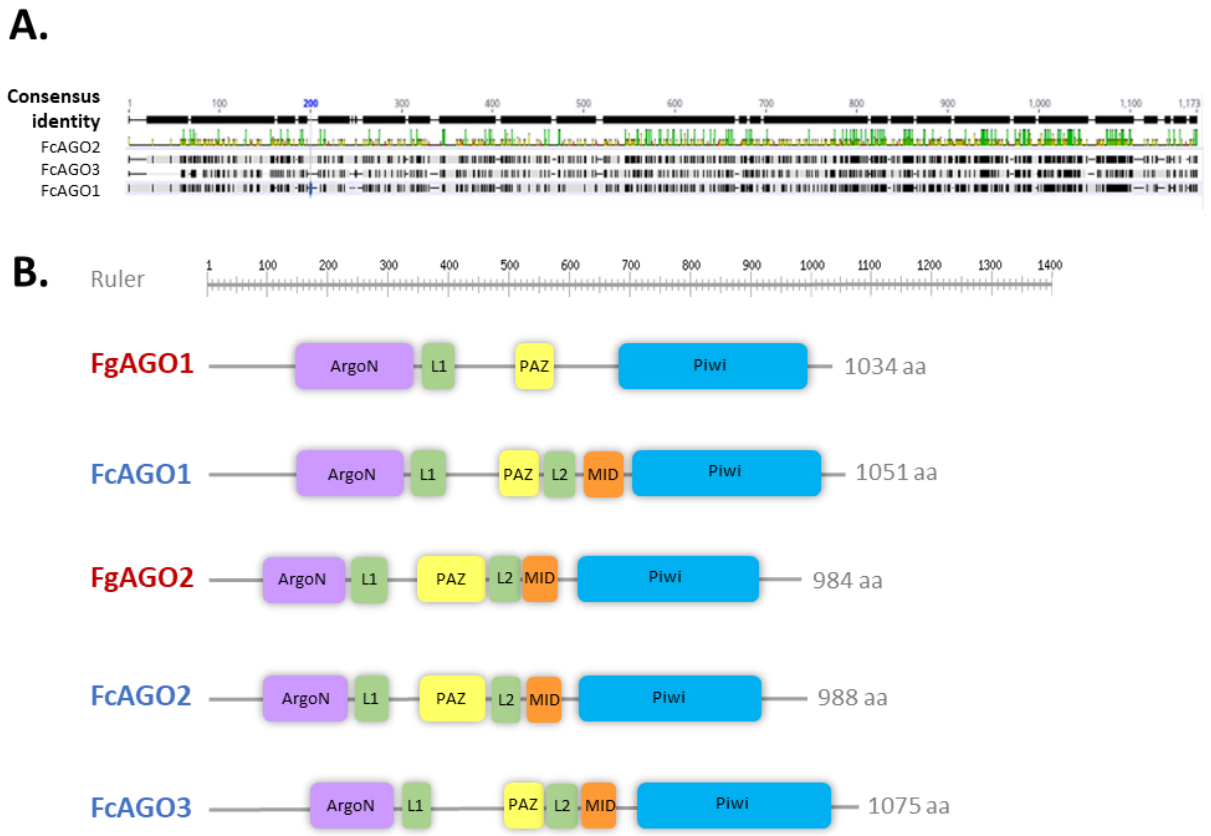

Figure 17. *F. circinatum* has 3 putative AGO proteins with functional AGO domains. A. Multiple alignment of amino acid sequences FcAGO1, FcAGO2 and FcAGO3 by Clustal omega 1.2.2. program using seeded guide trees and hidden Markov models (HMM) profile-profile techniques. The resulting alignment was then visualized with Geneious to analyze similarity between proteins. **B.** Conserved domains of AGO proteins from *F. graminearum* and *F. circinatum*. Domains were predicted against Pfam database using MOTIF tool. Lines represent the full length of the protein. Boxes represent the identified domains and are labeled with different colors: ArgoN in purple, L1 and L2 in green, PAZ in yellow, MID in orange and Piwi in blue.

The study of the RNAi machinery components concluded with an analysis of the RNA-dependent RNA polymerases (RdRps). RdRps are involved in the amplification of silencing signals through the generation of secondary siRNAs complementary to the target mRNA. Many eukaryotic organisms encode more than one RNA-dependent RNA polymerase (RdRp) that probably arose as a result of gene duplication. Four RdRps have been identified in *F. circinatum* from the FgRdRps proteins described in *F. graminearum* (Chen *et al.*, 2015). *F. graminearum* possessess five RdRPs; however, our analysis of the *F. circinatum* genome revealed only four orthologs, as no sequences with sufficient similarity to FgRdRP4 were identified in *F. circinatum*. However, the related fungus *F. fujikuroi* (cause of bakanae disease) also encodes five RdRP homologs (Pardo-Medina *et al.*, 2024). In general, most *Fusarium* genomes examined contain around four to five *RdRp* genes, reflecting a conserved gene-silencing apparatus across the genus. Notably, a recent comparative transcriptomic study did not identify an ortholog of Fg*RdRP4* gene in *F. circinatum* when BLASTing known *F. graminearum* RNAi components

(Zamora-Ballesteros *et al.*, 2020). These findings suggest that *F. circinatum* likely possesses only four RdRps.

The identified proteins were designated as FcRdRP1-4. The conserved domains analysis of both *F. graminearum* and *F. circinatum* proteins revealed that they all possess an RdRp domain, which is characteristic of RNA-dependent RNA polymerases and a highly conserved domain in fungi (Figure 18).

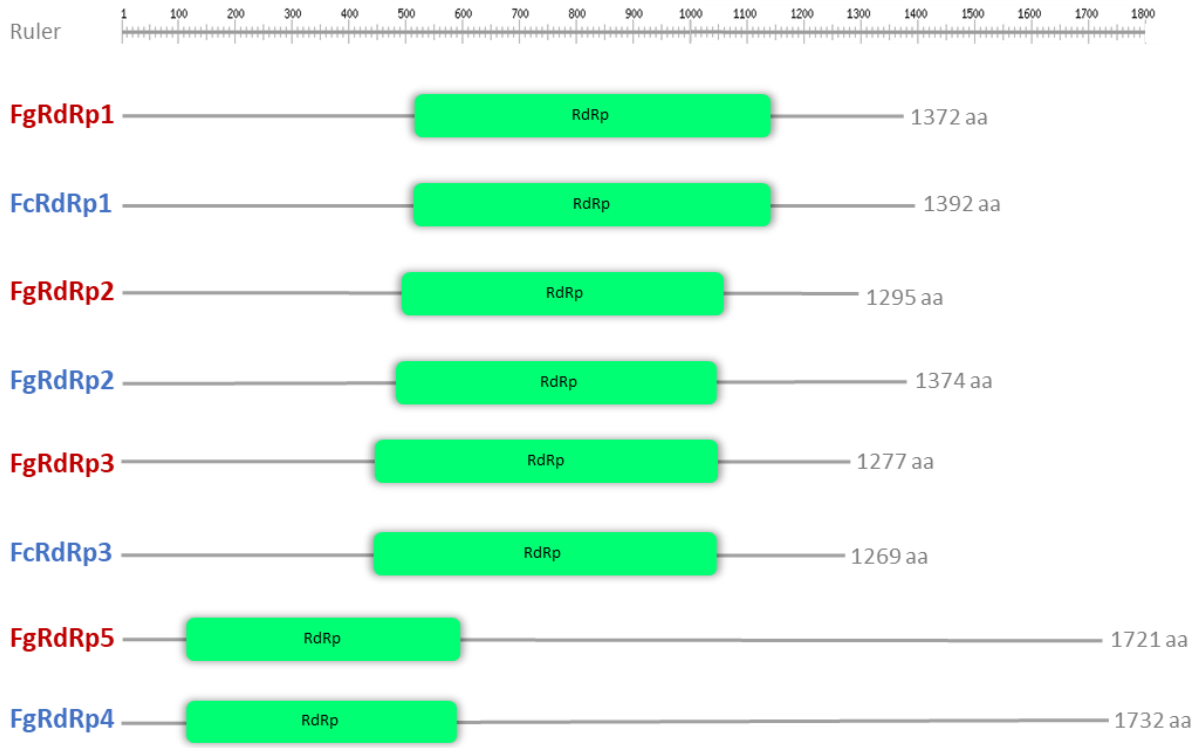

Figure 18. *F. circinatum* has four putative RdRps, which are fundamental components of its RNAi machinery. Domains were predicted against Pfam database using MOTIF tool. Lines represent the full length of the protein. Boxes in green represent the RdRP domains.

To complement the sequence-based homology analyses, we conducted a comparative analysis of the three-dimensional (3D) structures of the putative RNAi-related proteins identified in *F. circinatum*. While sequence alignments provide valuable insights into evolutionary relationships, they do not always predict functional equivalence, as distinct amino acid sequences can fold into structurally similar and functionally equivalent conformations, as seen in the case of isoenzymes. Given that protein function is fundamentally determined by its three-dimensional structure, analyzing structural conservation offers a more direct assessment of functional conservation. Thus, structural modeling was carried out to assess the degree of similarity between *F. circinatum* proteins and their orthologs in *F. graminearum*, thereby supporting the functional annotation beyond conventional sequence alignments (Figure 19). The 3D structure analysis of the putative DCL identified in *F. circinatum* indicates that FcDCL1 and

FcDCL2 are homologous to FgDCL1 and FgDCL2 in *F. graminearum*, respectively. The superposition of the 3D protein structures demonstrated a high proportion of green regions (agreement between structures), indicating a high degree of conservation of the backbone and overall protein conformation. Most conserved regions correspond to the active site, as visualized by the green-colored regions, while divergence was observed in the N-terminal region (red areas). This finding was also visually corroborated for AGO and RdRps. FcAGO1 and FcAGO2, which exhibited structural similarities with FgAGO1 and FgAGO2, respectively. The RdRps of *F. circinatum* exhibited conserved structural organization relative to those of *F. graminearum*. The quantitative data for these alignments were obtained using PyMOL, yielding high MatchAlign values, which indicate that the alignments between the protein structures are of good quality. The root-mean-square deviation (RMSD) values obtained in the comparative analyses were found to be relatively low, with each value below 0 (Table S1), indicating that the structures under comparison are either identical or exhibit a high degree of similarity. These results indicate a strong structural alignment and high similarity between protein models, thus suggesting that the function of RNAi proteins may be conserved between *F. graminearum* and *F. circinatum*.

It has been demonstrated through functional studies of genes encoding the *F. graminearum* silencing machinery that, although both *dcl* and *ago* exhibit partial functional overlap, there are notable differences in their functionality. Chen *et al.* (2015) demonstrated that the RNAi components DCL2 and FgAGO1 are essential for silencing. The study observed, through phylogenetic analyses, that FgDCL2 and FgAGO1 may play a role in the RNAi pathway, while the combination of FgAGO2 and FgDCL1 may be required for the meiotic silencing by unpaired DNA (MSUD) pathway in *F. graminearum*. The authors additionally characterized the physiological and cellular functions of RNAi components in *F. graminearum* by constructing deletion mutants. Their findings revealed that FgDCL2 and FgAGO1 play a significant role in hairpin RNA (hpRNA)-induced gene silencing and that FgDCL2 is involved in miRNA-like small RNA (milRNA) generation in *F. graminearum* (Chen *et al.*, 2015). Gaffar *et al.* (2017) showed that FgDCL1 and FgDCL2 are essential proteins for environmental RNAi, as evidenced by the compromised SIGS phenotypes observed in Δ*dcl1* and Δ*dcl2*, and the complete insensitivity to dsRNA exhibited by the *dcl1/dcl2* double mutant. Werner *et al.* (2020) observed that the expression of *ago1* remained unchanged when dsRNA treatments were applied for its silencing. Based on these findings, they postulate that FgAGO1 is required for the binding of SIGS-associated siRNAs in *F. graminearum*. However, the researchers also noted that Δ*ago1* mutants exhibited only slight deficiencies in SIGS and were less responsive to dsRNA treatments. This suggests that FgAGO1 and FgAGO2 may have overlapping functions in binding SIGS-derived siRNAs (Gaffar *et al.*, 2019). The findings

underscore the necessity for further studies to elucidate the mechanistic role of *F. graminearum* RNAi components in SIGS. Additionally, functional studies have indicated that sexual ascosporogenesis is primarily regulated by FgDCL1 and FgAGO2, whereas FgDCL2 and FgAGO1 play a role in the development and germination of asexual conidia (Gaffar *et al.*, 2019; Son *et al.*, 2017). These studies corroborate the involvement of RNAi pathways in conidiation, ascosporogenesis, and pathogenicity of *F. graminearum*. Many RdRps play a role in maintaining and amplifying gene silencing signals, synthesizing RNA. However, the precise modes of their action may differ considerably. The physiological and biological functions of *RdRp* genes in *F. graminearum* remain largely unclear. Studies have encountered difficulties in characterizing these proteins, as the five existing RdRps in the *F. graminearum* genome may function redundantly (Chen *et al.*, 2015). Phylogenetic analyses of the five FgRdRps revealed that they could be clustered into four distinct groups. Notably, FgRdRp1 and FgRdRp4 demonstrated a close relationship with the Quelling Defective 1 (QDE1) of *N. crassa*, a RdRp that can initiate de novo gene silencing in this model fungus (Chen *et al.*, 2015; Qian *et al.*, 2016). Considering their findings, Chen *et al.* (2015) proposed a RNAi pathway in *F. graminearum*, in which small RNA precursors, such as dsRNA or hpRNA, were processed primarily by FgDCL2. Subsequently, the siRNAs/ex-siRNAs are loaded onto FgAGO1, which then targets the cognate mRNA for gene silencing. The amplification of the sRNA pool may be associated with RdRp proteins. They postulated that FgDCL1 and FgAGO2 play a minor or no role in the milRNA- and hpRNA-induced gene silencing pathway of *F. graminearum*.

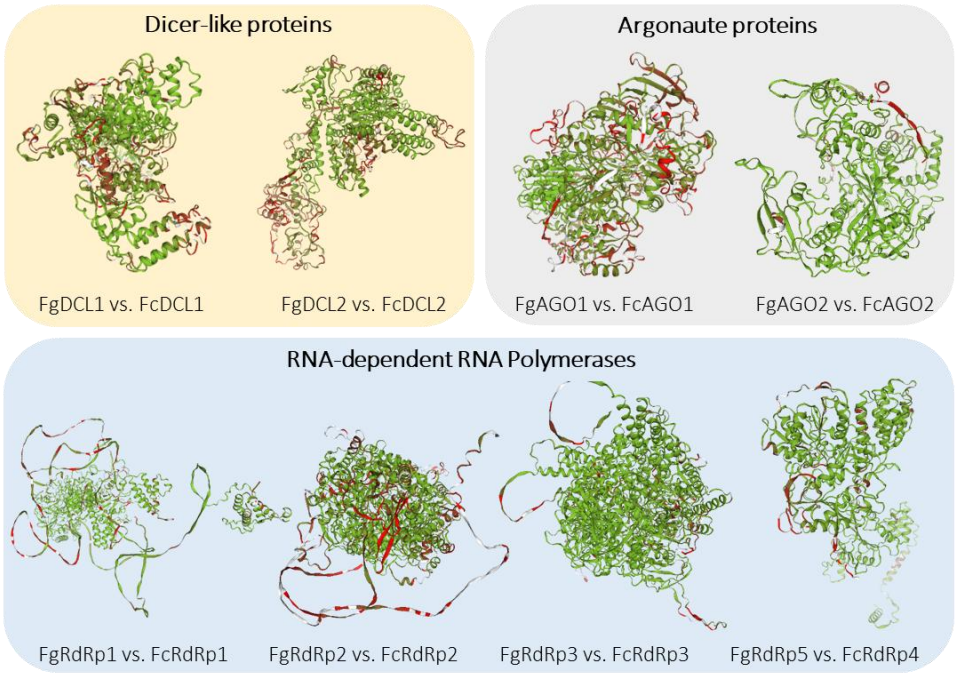

Figure 19. Comparative analysis of the 3D structures of the proteins of *F. graminearum* and *F. circinatum*: DCL, AGO and RdRp. The 3D structures of the *F. circinatum* RNAi proteins were found to be highly similar to their orthologues in *F. graminearum*. Individual structures were predicted using SWISS-MODEL and compared using the

structure comparison tool. Regions in green indicate good structural alignment between the proteins and red regions signify areas of poor alignment or significant structural differences between the proteins.

The 3D structural analysis of the putative FcAGO3 protein revealed that it exhibited no similarity to either FgAGO1 and FgAGO2, or FcAGO1 and FcAGO2. The high proportion of regions colored red (Figure 20) and high RMSD values (Table S1), indicated a significant structural difference between the proteins. This suggests that FcAGO3 represents a third AGO protein with unique characteristics in *F. circinatum*. Therefore, the function of the putative third AGO in *F. circinatum* cannot be elucidated based on *F. graminearum* studies. To determine *in silico* the function of this protein, it would be beneficial first to carry out phylogenetic analyses with other AGO3 from fungal pathogens, and then to conduct functional analyses utilizing deletion mutants or knockouts.

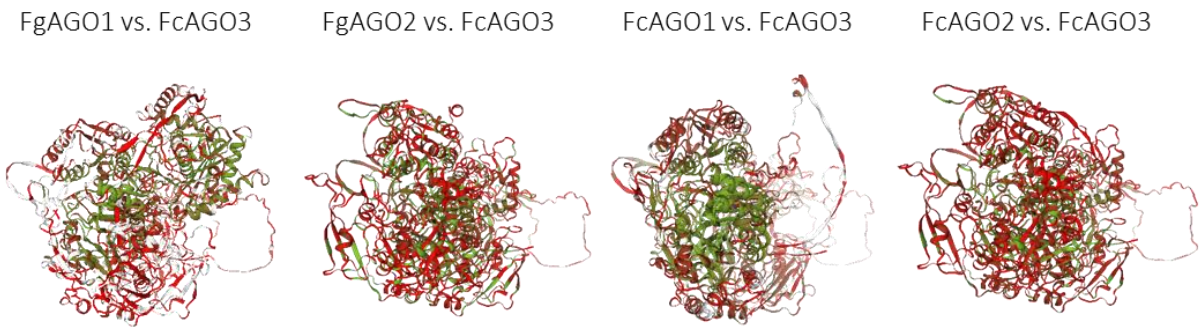

Figure 20. Structural comparative analysis of the FcAGO3 against other ago proteins in *F. graminearum* and *F. circinatum*. The 3D structure of the FcAGO3 was found to diverge significantly from other AGO in *F. graminearum* and *F. circinatum*. Individual structures were predicted using SWISS-MODEL and compared using the structure comparison tool. Regions in green indicate good structural alignment between the proteins and red regions signify areas of poor alignment or significant structural differences between the proteins.

The findings of *in silico* analyses collectively indicate that *F. circinatum* hold the necessary functional RNAi silencing machinery. Specifically, two dcl, three ago, and four RdRp proteins have been identified in comparison to the RNAi components described in *F. graminearum*. Although further research is required to clarify the specific roles of *F. circinatum* RNAi machinery, the structural homology between RNAi proteins of *F. graminearum* and *F. circinatum* strongly suggests that *F. circinatum* possesses a functional RNAi machinery for SIGS control strategy. This is mostly supported by the presence of FcDCL2, FcAGO1 and FcRdRps, which are critical for gene silencing and the amplification of silencing signals. These findings lend support to the hypothesis that the pathogen *F. circinatum* may represent a viable target for a SIGS-based biocontrol strategy. Notably, a preliminary experiment demonstrated that exogenous application of dsRNA targeting green fluorescent protein (*GFP*) in *F. circinatum* mutants resulted in a measurable decrease in *GFP* expression, providing evidence that the RNAi machinery in this species is not only present but also functionally active in mediating gene silencing (Rammuki, 2024). However, further research should be conducted to characterize the

precise function of RNAi proteins in *F. circinatum*. This should include an expression analysis of the genes encoding the RNAi machinery, a proteomic analysis of the proteins identified *in silico*, and a co-immunoprecipitation study to identify interactions among RNAi components. To determine the function of these proteins, it is essential to develop knockout or deletion mutants and assess their impact on fungal growth, pathogenicity, and gene silencing efficiency. Additionally, further complementation studies and transcriptome and sRNA sequencing are necessary to evaluate the influence of specific RNAi components. This would improve our understanding of RNAi mechanisms in *F. circinatum* and their prospective applications in fungal pathogen control strategies.

1.2. *Fusarium circinatum* is able to uptake and internalize externally applied dsRNA molecules

The uptake of the dsRNA by the pathogen is a necessary prerequisite for the activation of the RNAi machinery and ultimately for the function and success of SIGS. The ability of pathogens to directly take up dsRNA can be evaluated by exposing the fungus to fluorescently labeled dsRNAs (Hamby *et al.*, 2020). Many studies have shown that numerous pathogens are able to uptake dsRNA from the environment (Degnan *et al.*, 2022; McRae *et al.*, 2023; Qiao *et al.*, 2021). Qiao *et al.* (2021) observed that pathogenic organisms that had demonstrated a higher uptake ability of environmental dsRNAs significantly inhibited plant disease symptoms. It should be noted that not all pathogens have the same ability to directly incorporate dsRNA *in vitro*. For instance, *Trichoderma virens* and *Colletotrichum gloeosporioides* demonstrated limited to no uptake (Qiao *et al.*, 2021). However, dsRNAs may also be taken up indirectly by the fungus internally within a plant (Biedenkopf *et al.*, 2020). Our results show that three hours after dsRNA treatment, we observed fluorescent signals inside the germinating fungal spores using CLSM. Notably, these signals persisted even after treating the sample with an endonuclease that degrades both single- and double-stranded DNA and RNA (Figure 21). This observation suggests that the labeled dsRNAs were incorporated into the fungal structures rather than merely adhering to the surface.

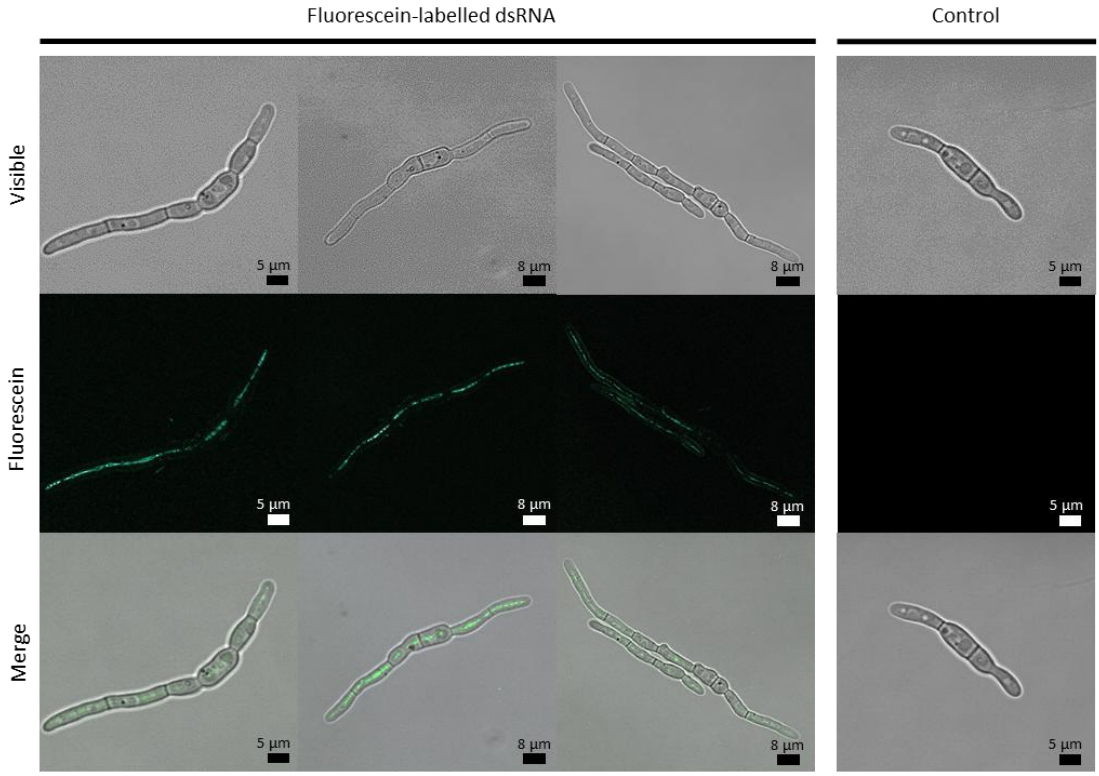

Figure 21. *F. circinatum* can uptake externally applied (modified from Bocos-Asenjo *et al.*, 2024). Fluorescein-labelled dsRNA was applied to *F. circinatum* germinating spores 3 h before visualization using CLSM. MNase used to degrade external labelled dsRNA and ensure the absence of dsRNA adhesion to the fungal cell wall. Fluorescence was observed inside the treated germlings, indicating that the pathogen was able to uptake the labeled molecules. The absence of fluorescent signal was observed in untreated *F. circinatum* germlings (images on the right). The upper panels (visible) show the bright field, showing fungal structures. The immediately following panels (fluorescein) present images of the fluorescein signal. The lower panels (merge) illustrate the superimposition of the bright field and fluorescein images, showing the merge of the mycelial structures and fluorescein signals.

Furthermore, fluorescence was observed across multiple Z-stacks, indicating that dsRNA was located inside of the mycelium in different focal planes within germinating spores (Figure 22). This suggests that the dsRNA was internalized soon after spore germination, highlighting the rapid uptake of dsRNA by *F. circinatum*. Our results demonstrated that *F. circinatum* can efficiently uptake externally applied dsRNAs. These results are consistent with findings in other species of *Fusarium* genus, such as *F. graminearum* (Koch *et al.*, 2016) and *F. oxysporum* f. sp. *lycopersici* (Ouyang *et al.*, 2023). The direct uptake of dsRNA by *F. circinatum* is a crucial finding that supports the potential of RNA-based approaches for the control of fungal pathogens. This finding, along with the presence of RNAi machinery in the pathogen, suggests that SIGS might be effective in controlling the disease caused by *F. circinatum* in pine trees. This approach could lead to the development of effective and environmentally friendly methods for managing fungal diseases in forestry.

Figure 22. Fluorescent signals were found internally in the structures of *F. circinatum* (modified from Bocos-Asenjo *et al.*, 2024). Z stack confocal images of a germinated spore of *F. circinatum* treated with fluorescein labeled dsRNA showed the presence of fluorescence inside the germling, demonstrating that the pathogen is able to uptake external dsRNA molecules. The complete Z stack consisted of 5 images across a depth of 8.64 µm. Images were taken on a Leica Microsystems SP8 system; scale bars correspond to 8 µm.

2. Validation of *Fusarium circinatum* target genes for its use in SIGS

Prior to conducting trials on the primary host of the pathogen (pine trees), a methodology was established to quickly evaluate the efficiency of dsRNA molecules produced against *F. circinatum*. This was necessary because trials on pine seedlings were time-consuming, requiring four months for plant growth and an additional month for symptom evaluation. Given the absence of previous studies using SIGS against tree diseases, this study is the first to develop a rapid preliminary methodology for evaluating newly designed molecules against forest pathogens.

To explore the potential of the molecules developed in Chapter 1, a series of preliminary assays were conducted in different plant material. The treatments applied across these experiments are summarized in Table 10.

Table 10. Summary of treatments used in SIGS evaluation assays against *F. circinatum*

Treatment name	*F. circinatum* inoculation (+/-)	dsRNA application (300 ng/µl)
Water	-	(-) ddH_2O
FC072V	+	(-) ddH_2O
Mock control	+	YFP-dsRNA (non-specific dsRNA)
FcCHS-dsRNA	+	FcCHS-dsRNA
FcPTP-dsRNA	+	FcPTP-dsRNA
FcVDS-dsRNA	+	FcVDS-dsRNA
Fcmix-dsRNA	+	FcCHS-dsRNA + FcPTP-dsRNA + FcVDS-dsRNA

2.1. Detached spinach leaves showed consistent infection with *Fusarium circinatum* spores, providing a rapid method for evaluating dsRNA molecules

To develop a rapid dsRNA evaluation test, we conducted infection assays on various plant materials that were readily available in the local market, including rose petals, tomato fruits, cucumber slices, lamb lettuce leaves, and young spinach leaves, using different concentrations of *F. circinatum* spores (10^4, 10^5, 10^6 and 10^7 spores/ml) (Figure 23A). The

symptoms were monitored daily, and at 4 dpi, a consistent infection and necrotic lesions on the abaxial side of young spinach leaves were identified. The lesions were readily quantifiable using a digital caliper, rendering this plant material an optimal approach for evaluating dsRNA molecules in subsequent assays. Consistent infections in rose petals and tomato fruits were also observed, though the former deteriorated easily due to senescence, making it difficult to evaluate necrosis due to *F. circinatum*. The latter did not show necrosis but mycelium, which made them less suitable for the development of this methodology. The remaining plant material used in the experiment did not exhibit any consistent infection (Figure 23B). The infection rate was found to be more consistent when the abaxial leaf surface was infected. This surface is generally more susceptible to infection by several fungal pathogens, which is probably due to the ease of entry of the pathogen into the apoplastic duct through the stomata (Caseys *et al.*, 2024). Additionally, we observed that 10^5 spores ml^{-1} was the minimum concentration at which consistent infections were achieved in all spinach samples. The screening allowed us to reduce the number of spores used while maintaining the reliability of the assays, which better reflects conditions in nature and allows for more accurate observation of the effect of the dsRNA molecules in subsequent experiments. This is the first time that *F. circinatum* assays have been conducted on a non-forest plant for virulence and treatment evaluation. *F. circinatum* has been demonstrated to be capable of colonizing maize (Swett and Gordon, 2009) and other grass species (Hernandez-Escribano *et al.*, 2018; Swett *et al.*, 2014; Swett and Gordon, 2012) without inducing symptoms. Indeed, *F. circinatum* has been documented to maintain an endophytic association with a grass species (Swett and Gordon, 2015). Nevertheless, it has never been described as being able to infect and cause negative effects on plants other than conifers. Other studies have also employed diverse plant material to assess the efficacy of SIGS or even to evaluate dsRNA encapsulation strategies. For instance, (Qiao *et al.*, 2021; Qiao *et al.*, 2023) infected grape fruits (host plant) with *B. cinerea*, as well as other agriculturally relevant plant materials, such as rose petals for their expected color change in the infected area, tomato fruits, and lettuce leaves. Although some of these materials were not optimal for *F. circinatum* assays, the use of young spinach leaves was highly suitable and served to establish the methodology for the rapid assessment test of dsRNA molecules.

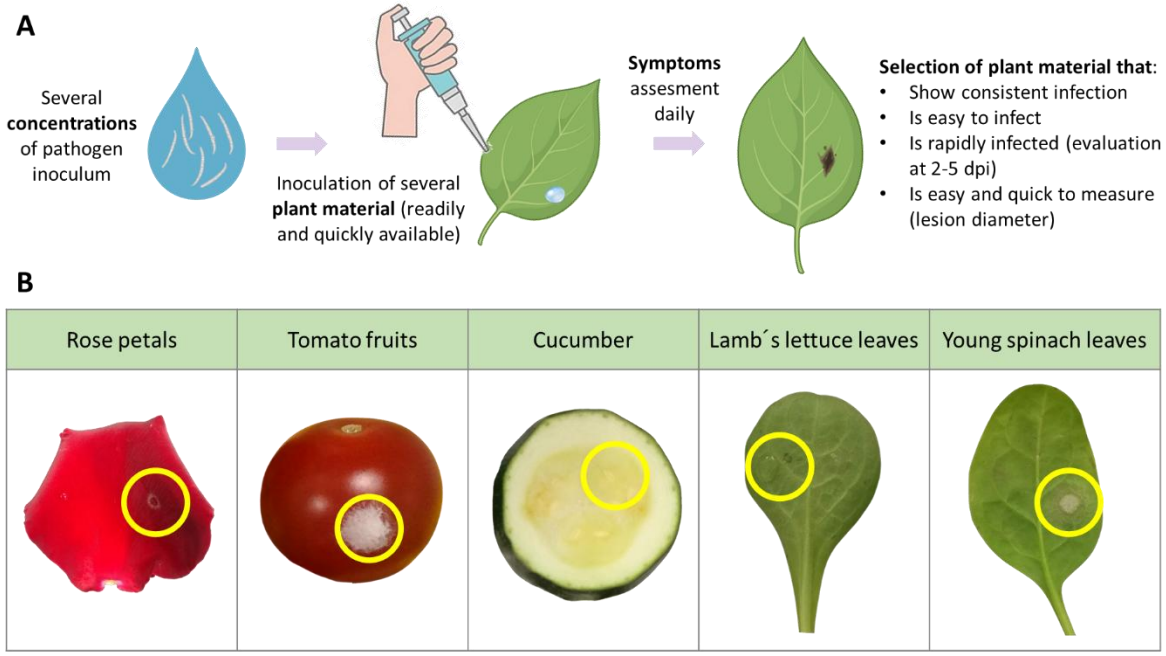

Figure 23. Workflow for setting up a preliminary rapid test for evaluating dsRNAs. A. *F. circinatum* infection assays were conducted applying spore dilutions of several concentrations on various plant materials. Symptoms were subsequently evaluated for consistent infection and easy to measure necrotic lesions. This allowed us to establish a quick and easy methodology for evaluating dsRNA treatments. **B.** The plant tissues subjected to testing exhibited a range of symptoms in response to infection by *F. circinatum*. Rose petals and spinach leaves exhibited defined necrotic lesions, while tomato fruits demonstrated mycelial growth at the point of inoculation. In contrast, cucumber and lamb lettuce leaves did not exhibit clear and measurable lesions. The yellow circle indicates the infection points in each representative sample.

2.2. Bioassays conducted on spinach leaves enabled the rapid confirmation of the molecules' efficacy for subsequent, more complex assays in host plants

The experiment involved applying the dsRNA treatments (FcCHS-dsRNA, FcPTP-dsRNA, FcVDS-dsRNA) and mock control (YFP-dsRNA) to the abaxial surface of the leaf, followed by inoculating *F. circinatum* spores in the treated area. The treatments were applied dropwise at a concentration of 100 ng/µl (as used in Qiao *et al.* (2021) to simulate a commercial application). Despite the consistency of infections observed on spinach, the lesions exhibited considerable variability between individual leaves. Consequently, we applied mock control to one side of the leaf and the dsRNA treatment to the other, enabling us to conduct a pairwise comparison. The development of symptoms was evaluated at 4 dpi by measuring the diameter of lesions and calculating the necrotic area using the area of a circle formula. The area data were utilized to conduct a pairwise comparison between each treatment and the control. The results demonstrated that all three treatments exhibited a protective effect against *F. circinatum*. All three treatments were found to have a protective effect against *F. circinatum* (Figure 24). Compared to mock control, all dsRNA treatments resulted in a reduction of necrotic lesions development (Figure 24A). Disease severity (based on the mean lesion size) decreased

significantly in all treatment groups compared to the control group (mock control). Specifically, disease severity decreased by 35% (*p*-value < 0.01) in the FcCHS-dsRNA treatment group, 33% (*p*-value < 0.01) in the FcPTP-dsRNA treatment group, and 43% (p-value < 0.01) in the FcVDS-dsRNA treatment group (Figure 24B, Table S2). Pairwise comparison with the mock control indicated that the observed reduction in the treatments FcCHS-dsRNA, FcPTP-dsRNA and FcVDS-dsRNA was likely due to the silencing of the specific target genes of each molecule, rather than an effect of the dsRNA molecule itself. In addition to assessing the disease progression, we analyzed the biomass of *F. circinatum* in each part of the leaf (treated and mock) by qPCR to verify whether the treatments had resulted in a reduction in fungal biomass. Consequently, following the measurement of the lesions, each leaf part (mock control and dsRNA treatment) was excised, and DNA was extracted. qPCR analysis of fungal biomass using the RNA polymerase II second largest subunit (*RPB2*) gene and the actin gene as housekeeping genes for *F. circinatum* and spinach, respectively, confirmed a reduction in fungal growth with dsRNA treatments. The relative amount of fungal growth was reduced by 36% (*p*-value < 0.01) in FcCHS-dsRNA, 40% (p-value < 0.01) in FcPTP-dsRNA, and 46% (p-value = 0.06) in FcVDS-dsRNA compared to the mock control (Figure 24C, Table S3). Therefore, FcCHS-dsRNA, FcPTP-dsRNA and FcVDS-dsRNA reduced fungal growth and symptoms incidence on detached spinach leaves.

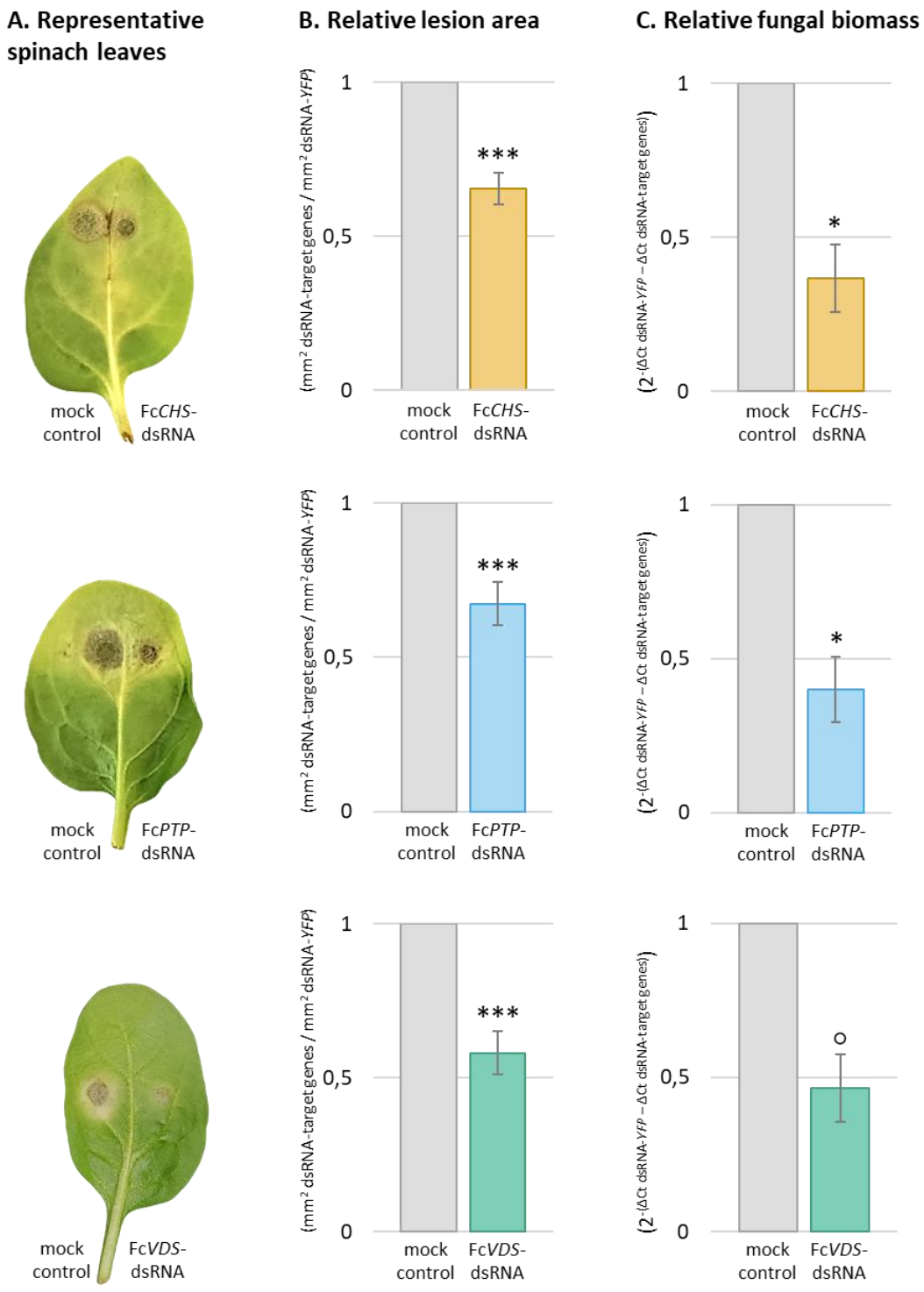

Figure 24. Application of designed dsRNAs against essential genes reduces the virulence of *F. circinatum* in detached spinach leaves (modified from Bocos-Asenjo *et al.*, 2024). **A.** Representative detached spinach leaves show smaller necrotic lesion size in the assessed treatments (FcCHS-dsRNA, FcPTP-dsRNA, FcVDS-dsRNA) as compared to the mock control at 4 dpi. **B.** Relative lesion size depicts the reduction of disease severity in the applied treatments (FcCHS-dsRNA, FcPTP-dsRNA, FcVDS-dsRNA) as compared to the mock control at 4 dpi, which were measured with the help of an electronic caliper, assigning a value of 1.0 to the lesion size area in the control treatment. **C.** Quantification of fungal biomass by means qPCR (2^-ΔCt method) shows a reduction of *F. circinatum* in dsRNAs treatments (FcCHS-dsRNA, FcPTP-dsRNA, FcVDS-dsRNA) as compared to the mock control treatment. Level of statistical significances is determined by non-parametric Wilcoxon rank test (°: *p*-value < 0.10, *: *p*-value < 0.05, **: *p*-value < 0.01, ***: *p*-value < 0.001). Bars and error bars represent mean relative values ± SEs between biological replicates.

The dsRNA molecules employed in the study demonstrated a reduction in pathogen virulence by 33 to 43% in spinach detached leaves, as evidenced by the average lesion size caused by *F. circinatum*. This reduction was corroborated by a 36 to 46% decrease in fungal biomass in leaves treated with dsRNA. This collectively indicates that targeting cell wall biogenesis, signal transduction, and vesicle trafficking genes by SIGS is an effective approach for reducing *F. circinatum* virulence. The reduction of fungal biomass is slightly greater than the reduction of spot disease, a finding that is consistent with the results reported by (Niño-Sánchez *et al.*, 2022) in tomato fruits infected with *B. cinerea*. The impact of SIGS on fungal biomass is more pronounced than on lesion size. This discrepancy may be attributed to the fact that although the pathogen is affected by the treatments and its biomass grows less, the symptoms on the plant develop rapidly at the beginning of the infection. Consequently, although *F. circinatum* was less virulent with the treatments, visually the necrosis was not reduced to the same extent as fungal biomass. Furthermore, when measuring the necrotic area, we only consider two dimensions of pathogen growth. However, the pathogen also grows through plant cell layers in three dimensions, which makes the biomass measurement more sensitive and the differences more pronounced with this method.

In summary, screening dsRNAs on detached spinach leaves proved to be a rapid and easy method that allowed us to evaluate the efficacy of the molecules against *F. circinatum* within 4 days. This test may spare the testing of a large number of molecules in long-lasting assays on pine seedlings. Therefore, this methodology was intended as a reliable preliminary evaluation to assess the dsRNA molecules prior to their analysis in the *F. circinatum* primary host (*P. radiata*). In conclusion, there is readily inoculable and measurable plant material susceptible to forest diseases. Consequently, in studies investigating the efficacy of treatments, particularly in the context of tree diseases, it would be advantageous to search for such material in order to facilitate rapid and time-efficient evaluations in the initial stages of the experiments.

3. SIGS mediated control of *Fusarium circinatum* in pine seedlings

The above results demonstrated that: (1) *F. circinatum* possesses the essential RNAi machinery components; (2) *F. circinatum* is able to uptake dsRNAs from the environment; and (3) the dsRNA molecules generated in this study have an effect on the pathogen in preliminary assays. Here we evaluated the effectiveness of SIGS strategy in controlling *F. circinatum* in 4-month-old pine seedlings, addressing the issue of Pine Pitch Canker in nurseries. This study was conducted on the host tree *P. radiata*, which is considered the most susceptible species to PPC (Zamora-Ballesteros *et al.*, 2021).

3.1. Standardization of infection conditions and disease evaluation for RNAi-based assays in *Pinus radiata*

Prior to conducting *in vivo* assays in pines to assess SIGS technology, the optimal inoculum and dsRNA concentration for infecting pine seedlings and applying treatments were determined. Following an evaluation of the inoculum concentration, 10^5 spores ml^{-1} was identified as the optimal amount for use in our trials as it was the minimum inoculum concentration that resulted in observable symptoms. This approach enabled a more comprehensive assessment of the SIGS treatments effects. dsRNA was used at a concentration of 300 ng/µl, according to our preliminary trials in pine seedlings with different concentrations of dsRNA. Typically, the application concentrations of dsRNA by SIGS range from 20 to 300 ng. Previous studies have indicated that 20 or 100 ng/µl is effective in detached material (Hu *et al.*, 2020; Qiao *et al.*, 2021; Ruiz-Jiménez *et al.*, 2021), while 300 ng is optimal on live plants (Niño-Sánchez *et al.*, 2022). The use of higher concentrations of dsRNA was dismissed, as several studies have demonstrated that once the optimal effect is reached, further increases in concentration do not elicit a stronger silencing response (Mcloughlin *et al.*, 2018; Ruiz-Jiménez *et al.*, 2021). In addition, an excess of dsRNA may result in nonspecific effects due to saturation of the RNAi pathway and activation of defense or immune pathways (Haller *et al.*, 2019).

Disease assessment for SIGS assays in pine seedlings is complicated as PPC symptoms are not easily quantifiable. It was therefore essential to develop a scale to measure the progression of the disease, enabling us to observe the effect of the treatments. In order to obtain an optimal methodology for testing dsRNA in pine trees, we developed our own scale based on the scale of Correll *et al.* (1991) to measure the disease score (Figure11). To develop the scale, a large set of infection assays were performed on 4-month-old *P. radiata* seedlings and disease symptoms were monitored and documented photographically over time. The resulting scale allowed for the categorization of symptom severity in a reproducible manner, enabling the evaluation of dsRNA treatment effects under standardized conditions.

3.2. dsRNA application method was optimized for a more accurate evaluation of SIGS assays

In order to determine the most appropriate dsRNA application methodology for the following assays, we tested several approaches: (a) drop application at the inoculation point; (b) spray application on the aerial part of the plant; and (c) a combination of both (drop + spray). Using these approaches, dsRNA treatments and non-inoculated, PH2003 and mock controls were evaluated at 2-, 3-, 4- and 5-weeks post inoculation according to the modified disease

scale. After statistical analysis of the data collected, we did not obtain significance of the treatments versus control with the drop and spray application methods (*p*-value > 0.05). However, the drop + spray method showed significant differences between the three treatments and mock control at week 2 (mock control W2 mean = 2.40 ± 0.55; FcCHS-dsRNA W2 mean = 0.60 ± 0.55; FcPTP-dsRNA W2 mean = 1.60 ± 0.55; FcVDS-dsRNA W2 mean = 1.20 ± 0.45; p-value < 0.05). Application of FcCHS-dsRNA, FcPTP-dsRNA and FcVDS-dsRNA using this combined method reduced disease in pine seedlings in the second week after inoculation with *F. circinatum*. In the case of FcCHS-dsRNA treatment, this reduction in symptoms was maintained until week 4 (mock control W3 mean = 2.50 ± 0.35; FcCHS-dsRNA W3 mean = 1.80 ± 0.27; mock control W4 mean = 2.30 ± 0.27; FcCHS-dsRNA W4 mean = 1.40 ± 0.42; *p*-value < 0.05). As a result, the combined method of drop and spray application proved to be the most effective, and a slight delay of the disease could be observed in FcCHS-dsRNA, FcPTP-dsRNA and FcVDS-dsRNA treatments, apparently more pronounced in the case of dsRNA targeting cell wall biogenesis (Figure 25, Table S4, Table S5). This is probably because dsRNA reaches the pathogen in two ways, through direct and indirect uptake. The dsRNA applied by droplets at the point of inoculation would result in the direct uptake by the pathogens cells, thus triggering the RNAi response. While dsRNA sprayed on the plant surface would be taken up by the pathogen indirectly (through the plant). It has been demonstrated that plants are capable of absorbing dsRNAs, potentially processing them into siRNAs and transferring them to fungal cells (Koch *et al.*, 2016; Wang *et al.*, 2016). Interestingly, some studies have demonstrated an effective spray-induced control of pest and pathogens in local (sprayed) and distal (non-sprayed) plant tissue, the latter involving a systemic spreading of dsRNA through the plant vascular system (Biedenkopf *et al.*, 2020; Delgado-Martín *et al.*, 2022; Koch *et al.*, 2016). All this suggests that dsRNA can be absorbed by both the pathogen and the plant, and can also move systemically, providing protection against *F. circinatum* through two pathways, including distal parts of the plants. This could explain the more favorable results observed with this combined methodology of dsRNA application in pine seedlings. Consequently, the drop + spray application approach was selected as the methodology for dsRNA application in the subsequent trials.

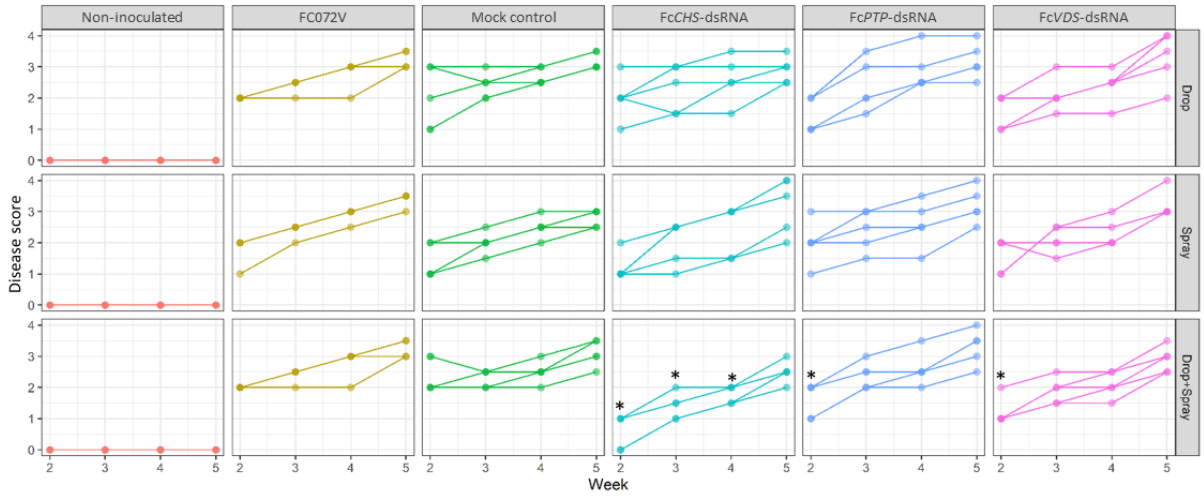

Figure 25. Drop + spray approach proved to be more effective for dsRNA application and seedling protection. We assessed the effect of different approaches of dsRNA treatment application on *P. radiata* seedlings infected with *F. circinatum*: drop treatment, spray treatment, and drop+spray treatment. All treatments applied by drop + spray have been demonstrated to delay the symptoms of *F. circinatum* infection by week 2 post inoculation. Symptoms were visually assessed for 5 weeks using the disease score scale. Each point represents a biological replicate (n=5), and each color corresponds to a different treatment. Y-axis corresponds to disease score and X-axis to the evaluation week. The asterisks (*) indicate statistically significant differences, as determined by the Wilcoxon non-parametric rank test against the mock control ($p < 0.05$).

3.3. All treatments achieved a significant reduction in PPC disease in *Pinus radiata* seedlings

To evaluate the effect of dsRNA treatments on *F. circinatum* infection in pines, four-month-old *P. radiata* seedlings were treated with dsRNAs designed in the study (FcCHS-dsRNA, FcPTP-dsRNA, FcVDS-dsRNA), individually and in combination (Fcmix-dsRNA). Non-inoculated, FC072V and mock controls were included to assess the specificity and baseline of symptom development. dsRNA was applied dropwise in the point of inoculation, and additionally, 1 ml of dsRNA was sprayed onto the aerial part per plant (drop + spray approach). The plants were kept in a controlled environment with regulated water and light conditions and were assessed at 25 and 35 dpi using the disease score scale.

Trial results indicated that non-inoculated seedlings remained healthy throughout the trial, with a disease score of 0 ± 0 (mean ± SD). In contrast, FC072V had a mean disease score of 2.38 ± 0.48 at 25 dpi and 3.74 ± 0.66 at 35 dpi. The mean disease score of the mock control was 2.54 ± 0.57 at 25 dpi and 3.77 ± 0.61 at 35 dpi. Therefore, no significant differences were observed between these two treatments, FC072V and mock control (p-value 25 dpi = 0.83; p-value 35 dpi = 0.99). This result was expected because mock control is not pathogen sequence specific and should have no virulence-reducing effect. Thus, statistical calculations were then performed using mock control treatment as a reference control. At 25 dpi, the pathogen virulence in seedlings treated with FcCHS-dsRNA, FcPTP-dsRNA, FcVDS-dsRNA, and Fcmix-dsRNA was

reduced compared to the mock control. At this time point, the FcCHS-dsRNA treatment showed the greatest reduction (mean = 1.49 ± 0.77), decreasing virulence by 41.57% compared to the mock control (p-value < 0.01 according to OLR test). The FcPTP-dsRNA (mean = 1.67 ± 0.8) and Fcmix-dsRNA (mean = 1.8 ± 0.80) treatments reduced pathogen virulence by 34.27% and 29.21%, respectively (*p*-value < 0.01 according to ORL test). FcVDS-dsRNA (mean = 2.01 ± 0.84) had the least pronounced effect on reducing symptoms, decreasing them by 20.77% (*p*-value < 0.05 according to ORL test) (Figure 26; Table S6). At 35 dpi, all treatments exhibited statistically significant differences compared to the mock control (YFP-dsRNA mean = 3.77 ± 0.61) with symptom reductions ranging from 14.02% to 23.11% (*p*-value < 0.01 according to OLR test), depending on the treatment. The FcCHS-dsRNA treatment (mean = 2.9 ± 0.56) was the most effective in controlling the disease also at 35 dpi.

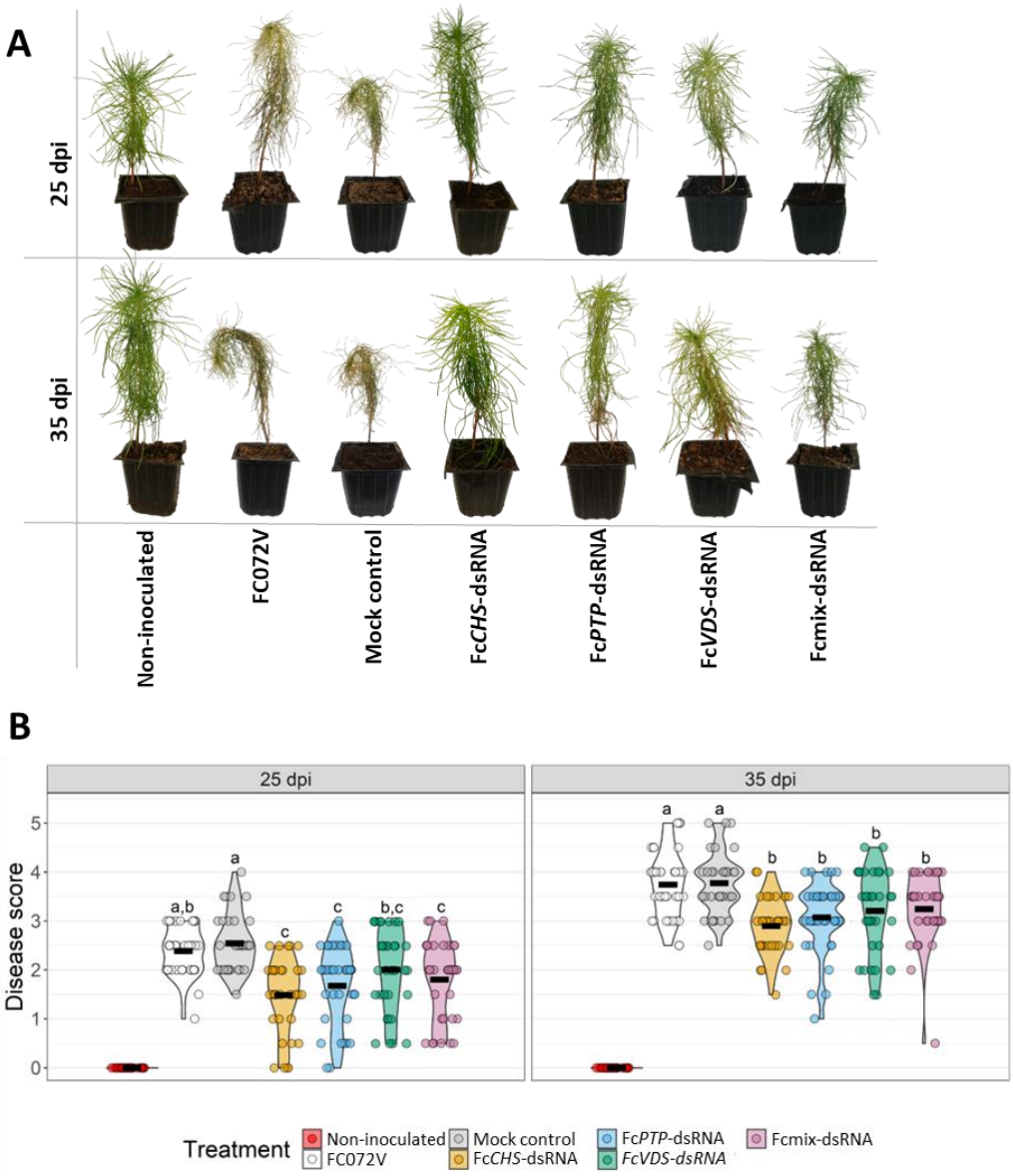

Figure 26. dsRNAs treatments inhibited *F. circinatum* virulence in *P. radiata* young plants (modified from Bocos-Asenjo *et al.*, 2024). **A.** Representative images of trial treatments taken at two time points (25 dpi and 35 dpi). **B.** Violin

plot showing the distribution of disease scores for each treatment applied according to the scale at two time points (25 dpi and 35 dpi). Black horizontal bars depict the mean disease score, and each point represents a biological replicate (n=35). Statistically significant differences are indicated by different letters determined by OLR test (*p*-value < 0.05).

Although there was no statistical difference between the FcCHS-dsRNA, FcPTP-dsRNA, FcVDS-dsRNA, and Fcmix-dsRNA treatments, FcCHS-dsRNA provided the greatest protection for pine trees. FcCHS-dsRNA targets the enzymes responsible for the synthesis of chitin and glucan. Chitin is essential in the formation of infection structures during the initial stages of infection (Fernandes *et al.*, 2016). Therefore, we suggest that the application of FcCHS-dsRNA may prevent spore germination at an early stage, reducing the effectiveness of the primary inoculum, while the other FcPTP-dsRNA and FcVDS-dsRNA applications may slow fungal growth. This was precisely observed by (Saito *et al.*, 2022), who demonstrated that SIGS treatments targeting chitin synthase genes against *Phakopsora pachyrhizi* resulted in a greater reduction in lesions on leaves when dsRNAs were co-treated together with *P. pachyrhizi* spores than when applied at 0 h or 24 h before inoculation. The team proposed that the dsRNAs were directly taken up by fungal cells, resulting in more effective gene silencing when it was co-applied with the pathogen (Saito *et al.*, 2022). This may have been the case in the present study, in which dsRNAs were co-applied with *F. circinatum* spores to pine seedlings, resulting in a notable reduction in disease severity, particularly in the case of Fc*CHS*. Similarly, Yang *et al.* (2021a) targeted genes involved in cell wall biogenesis, achieving a significant reduction in *F. graminearum* growth *in vitro*, as well as in detached leaves and spikelets of wheat plants, and a decrease in toxin production. In conclusion, targeting genes involved in cell wall biogenesis appears to be a promising strategy for controlling plant pathogenic fungi. Furthermore, since the plant cell wall is not composed of chitin, genes responsible for chitin synthesis represent a valuable target to mitigate off-target effects on host plants.

The simultaneous application of the three molecules silencing different metabolic pathways (Fcmix-dsRNA) did not demonstrate increased efficacy compared to the individual application of each dsRNA treatment (FcCHS-dsRNA, FcPTP-dsRNA, FcVDS-dsRNA). This might be because the final concentration of each molecule was only one-third of that used when applied individually. Tripling the concentration was not considered because it would have prevented an equimolecular comparison with the other treatments in the trial. Indeed, further studies have demonstrated that a combination of dsRNA molecules does not result in a more significant impact than the individual application of the molecules (Niño-Sánchez *et al.*, 2021). Furthermore, it has been observed that applying a high concentration of dsRNA can saturate the RNAi machinery (Haller *et al.*, 2019; Zhang *et al.*, 2020), potentially decreasing the efficacy of

SIGS treatments. Yang *et al.* (2021a) also observed no improvement when spraying mixtures of two or three dsRNA constructs on wheat leaves compared to the protection provided by each construct individually.

In summary, our findings indicated that the application of SIGS is an effective method for reducing the virulence of *F. circinatum* on pine seedlings. Reduction was more pronounced at 25 dpi than at 35 dpi across all treatments. Specifically, FcCHS-dsRNA reduced disease severity by nearly 42% compared to the mock control at 25 dpi; however, this effect decreased to 23% ten days later. Furthermore, at 25 dpi, plants treated with dsRNAs exhibiting a disease severity rating of less than or equal to 1.5 constituted 42%, whereas the untreated and mock control groups constituted 2%. These results suggest that the disease progressed over time, indicating that a single application of dsRNA was effective in delaying the development of symptoms, but not in halting disease progression entirely. In other studies, a delay in disease development has also been observed, as demonstrated for several pathogens (Niu *et al.*, 2021) and other *Fusarium* species (Koch *et al.*, 2016; Ouyang *et al.*, 2023; Tretiakova *et al.*, 2022). Regular re-application of dsRNAs may be a feasible solution to overcome the issue of loss of efficacy over time due to RNA degradation. Interestingly, recent studies have shown that a dsRNA spray can effectively prevent and cure infection by *Austropuccinia psidii* (Degnan *et al.*, 2023). The established infection of this pathogen in *Syzygium jambos* was cured by spraying dsRNA at key points in the fungal life cycle. Accordingly, the sequential application of dsRNA treatments yields improved disease control outcomes. However, such strategy is more costly, requiring increased amounts of dsRNA and more frequent applications across extensive geographical areas. Consequently, this strategy is not likely to be economically viable outside of laboratory settings. To address these limitations, recent advancements have focused on developing dsRNA delivery systems using nanocarriers. These include artificial vesicles (Qiao *et al.*, 2023), clay nanoparticles (BioClay™) (Mitter *et al.*, 2017; Niño-Sánchez *et al.*, 2022) and carbon-based (Wang *et al.*, 2023b), among others. Nanocarriers not only protect dsRNA from degradation but also improve cellular uptake by the pathogen, potentially allowing a single application to achieve effective and sustained protection. Studies utilizing nanocarriers have shown promising results. In addition to delaying symptom onset, a higher proportion of plants (approximately 20%, depending on the specific pathosystem and carrier used) exhibited effective disease control.

Nevertheless, the findings of this study suggest that SIGS has the potential to be an effective tool for the management of *F. circinatum* and lay the scientific foundation for improving and addressing the challenges of this technology in forest pathogens.

Chapter 3

SIGS as a tool against the pathogenic oomycete *Phytophthora cinnamomi* affecting holm oak trees

Here we demonstrate the potential of SIGS technology against a particularly destructive plant pathogenic oomycete. The dsRNA molecules produced in Chapter 1 were successfully employed to reduce the virulence of *P. cinnamomi*. In order to achieve this objective, the following actions were proposed:

- To verify that *P. cinnamomi* meets the requirements to be controlled by SIGS technology by confirming the presence and expression of core RNAi machinery genes and evaluating the uptake ability of exogenous dsRNA molecules.
- To preliminary assess the effect of dsRNA molecules against *P. cinnamomi* in model plants by conducting hydroponic root assays using *L. angustifolius* and *N. benthamiana*, and monitoring pathogen development following treatment with specific dsRNAs.
- To evaluate the effect of SIGS against *P. cinnamomi* in the host by conducting *in vitro* and *in planta* assays in *Q. ilex*, and monitoring pathogen development following treatment with specific dsRNAs.

1. Evaluation of SIGS requirements for effective disease control

Similar to the approach followed with *F. circinatum*, it was essential to confirm that *P. cinnamom*i possesses the main components of the RNAi machinery and to assess its ability to uptake externally applied dsRNA molecules.

1.1. RNAi machinery is conserved in the pathogenic oomycete *Phytophthora cinnamomi*

The essential components necessary for the functionality of RNAi mechanism and, consequently, for the effective functioning of SIGS technology, were identified in *P. cinnamomi* through an in *silico* comparative protein analysis. The RNAi machinery *of P. cinnamomi* was identified through examination of the RNAi machinery of *P. infestans*, a significant plant pathogen responsible for the destructive late blight disease in numerous crops, particularly potatoes and tomatoes (Nowicki *et al.*, 2012). It has therefore been subject to several investigations in an effort to control it with SIGS. As a result, the RNAi machinery has been extensively identified and characterized (Fahlgren *et al.*, 2013; Vetukuri *et al.*, 2011), allowing us to use this knowledge to identify the homologous machinery in *P. cinnamomi*. In view of the close evolutionary relationship between these oomycetes, RNAi-related proteins from *P. infestans* were used as reference for the identification of orthologous proteins within the *P. cinnamomi* proteome. The *in silico* analysis revealed the presence of two DCL, four AGO, and one single RdRp in *P. cinnamomi* (Table 11). These findings are further supported by previous experimental studies in which RNAi has been successfully used in *P. cinnamomi* (Ferreira *et al.*, 2023; Pascoal-Ferreira *et al.*, 2023). Such studies provide clear evidence that the RNAi machinery in this oomycete is not only present but also fully functional and capable of mediating effective gene silencing.

Table 11. Identification of RNAi-related proteins in *P. cinnamomi* using *P. infestans* proteins as query sequences, by establishing homology between the amino acid sequences.

***P. infestans* RNAi proteins (GenBank)**	**aa identity (%)**	**Orthologous proteins in *P. cinnamomi***	**Description**	**Protein length (aa)**	**Gene length (bp)**	**Domains**
PiDCL1 (EEY55353.1)	82.59%	**PcDCL1** (KAJ8558851.1)	Putative DCL	2236	6836	Dicer dimer, RNase IIIa, RNase IIIb
PiDCL2 (KAF4042611.1)	77.94%	**PcDCL2** (KAG6594204.1)	Putative DCL	939	2973	RNase IIIa, RNase IIIb, dsRBD
PiAGO1 (EEY67432.1)	82.68%	**PcAGO1** (KAG6611995.1)	Putative AGO	926	2781	ArgoN, L1, PAZ, L2, MID, Piwi
PiAGO2* (EEY67433.1)	82.56%	**PcAGO1** (KAG6611995.1)	Putative AGO	926	2781	ArgoN, L1, PAZ, L2, MID, Piwi
PiAGO3 (EEY61151.1)	91.84%	**PcAGO3** (KAG6614512.1)	Putative AGO	1288	3867	ArgoN, L1, PAZ, L2, MID, Piwi
PiAGO4 (EEY61191.1)	77.92%	**PcAGO4** (KAG6614629.1)	Putative AGO	1243	3831	ArgoN, L1, PAZ, L2, MID, Piwi
PiAGO5 (EEY61192.1)	89.88%	**PcAGO5** (KAG6614827.1)	Putative AGO	1281	3846	ArgoN, L1, PAZ, L2, MID, Piwi
PiRdRp1 (EEY56917.1)	74.58%	**PcRdRp1** (KAJ8569256.1)	Putative RdRp	2159	6760	RNA dependent RNA polymerase

*PiAGO1and PiAGO2 are co-orthologues with PcAGO1, therefore, the name AGO2 was not assigned to any protein in *P. cinnamomi*.

The comparative analysis of protein sequences identified two DCL proteins in *P. cinnamomi* (named as PcDCL1 and PcDCL2). In *P. infestans*, a single DCL protein was initially identified (Vetukuri *et al.*, 2011). However, subsequent research revealed the presence of a second DCL (Fahlgren *et al.*, 2013), a finding that aligns with the identification of DCL2 in several *Phytophthora* spp. and other oomycetes, such as *Pythium* spp. (Fahlgren *et al.*, 2013; Piombo *et al.*, 2023). Using PiDCL1 and PiDCL2 as queries, our search yielded two DCL proteins present in the proteome of *P. cinnamomi*, a result that is consistent with the aforementioned findings. The amino acid sequences of PiDCL1 and PcDCL1 exhibited a high degree of similarity, with 82.59% sequence identity. However, PcDCL1 displayed an unusually large size, with the first functional domain (Dicer dimer) beginning at residue 1242. This observation prompted a comparative analysis of DCL1 protein lengths in other *Phytophthora* species using the NCBI database. Although some variation in size was observed among species, DCL1 proteins with a domain architecture comparable to that of PiDCL1 and PcDCL1 generally ranged from 1,300 to 1,700 aa, with most around 1600. This pattern was found in species such as *Phytophthora pseudosyringae*, *Phytophthora sojae*, *Phytophthora oleae*, and *Phytophthora cactorum*, while *Phytophthora nicotianae* exhibited a slightly shorter DCL1 of approximately 1,300 aa. Despite this variability, PiDCL1 remained the longest DCL1 protein identified in the BLAST analysis. This led us to consider the possibility that the protein might be misannotated. We examined the sequence identifying a methionine or start codon (ATG) present in the coding sequence (CDS) of the protein upstream of the Dicer dimer domain and preceded by a TATA box. The TATA box is a promoter indicator sequence observed in eukaryotic systems, suggesting the potential for read-through transcription (Burley, 1996). The newly annotated protein, designated as PcDCL1b, comprised 1,143 aa. We also observed that the expected ATG at the expected position was mutated. This observation, combined with the structural similarity of shorter dcl1 proteins in closely related species, supports the decision to consider a reannotated, shorter version of PcDCL1 for comparative analysis.

A comparative analysis of the conserved domains of dcl proteins revealed that PiDCL1 and PcDCL1 exhibited high similarity, as did PiDCL2 and PcDCL2. However, a notable divergence was observed in both pathogens between DCL1 and DCL2. DCL1 possesses a single Dicer dimerization domain (Dicer dimer) and two ribonuclease III domains (RNase IIIa and RNase IIIb). In contrast, DCL2 possesses two RNase III domains but lacks a Dicer dimer domain (Figure 27). We also identified a double-stranded RNA-binding domain (dsRDB) in DCL2, though its presence is reported to be highly variable. This variability aligns with the well-documented diversity among dcl proteins. Furthermore, dcl sequences of *Phytophthora* species have demonstrated greater

similarity to dcl proteins of yeast and fungal representatives, such as *Sacharomyces pombe* and *N. crassa*, than to those of plants and other higher eukaryotes (Vetukuri *et al.*, 2011). The domain architecture of DCL2 in *Phytophthora* spp. is more similar to the Drosha proteins. Indeed, phylogenetic analyses of DCL2 have determined that DCL2 homologs of oomycetes form a cluster with Drosha homologs (Bollmann *et al.*, 2016). Thus, these results demonstrated that the proteins identified in *P. cinamomi* as PcDCL1b and PcDCL2 possess domains that are characteristic of DCL proteins and that are involved in RNA interference activity.

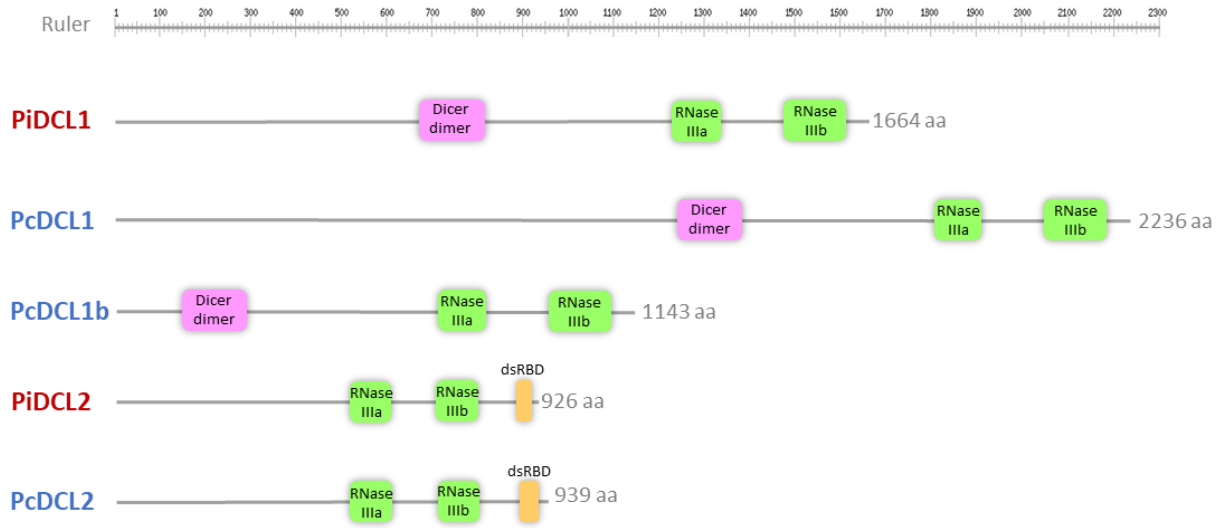

Figure 27. Domain architecture of DCL proteins identified in *P. cinnamomi* genome based on *in silico* predictions. Two distinct DCL proteins were identified in *P. cinnamomi*, one of them (PcDCL1b) was reannotated due to its unusual length. Protein domain organization was predicted using Pfam database and MOTIF tool. Horizontal lines represent the full amino acid sequence of each protein, and colored boxes indicate conserved domains: Dicer dimer (pink), RNase IIIa and RNaseIIIb (green), and dsRBD (orange).

The paralogous PiAGO1 and PiAGO2 proteins from *P. infestans* (Vetukuri *et al.*, 2011) yielded a match in *P. cinnamomi*, an AGO protein that we designated as PcAGO1. Comparative analysis further identified three additional AGO proteins in *P. cinnamomi* (designated as PcAGO3, PcAGO4 and PcAGO5), which are orthologous to PiAGO3, PiAGO4 and PiAGO5, respectively. This *in silico* study therefore revealed that *P. cinnamomi* putatively harbors four AGO proteins, while *P. infestans* possesses five. Analyses of other *Phytophthora* spp. and oomycetes have yielded varying numbers of AGO proteins. For instance, *P. plurivora* has six, *P. colocasiae* has five, and *P. cactorum* possesses four AGO (Piombo *et al.*, 2023). Piombo *et al.* (2023) also indicated that the oomycete species in their study had only one AGO belonging to clade 1, while the number of AGO proteins in clade 2 is variable, which aligns with our findings. As previously described (see Chapter 2. Section 1.1), AGO contains several conserved domains that are critical for their function in RNA silencing. The analysis of the conserved domains in PcAGO proteins confirmed the presence of all characteristics AGO domains: ArgoN, L1, PAZ, L2, MID, and Piwi (Figure 28). Briefly, these include domains involved in siRNA unwinding and RISC

complex assembly (ArgoN), anchoring of the 3' and 5' ends of the guide RNA (PAZ and MID), and catalytic cleavage of the target mRNA (Piwi), all of which are crucial for effective gene silencing (Bollmann *et al.*, 2018). The presence of these key domains provides compelling evidence that the identified proteins will function as AGO, enabling the RNAi pathway to operate in *P. cinnamomi* with the involvement of other essential components. In addition, we examined the coding sequences of PcAGO4 and PcAGO5 for upstream methionine codons and promoter elements such as TATA boxes, in order to identify potential annotation errors that could explain their extended lengths. This analysis did not provide sufficient evidence to support alternative annotations, suggesting that the current predictions likely reflect genuine structural features.

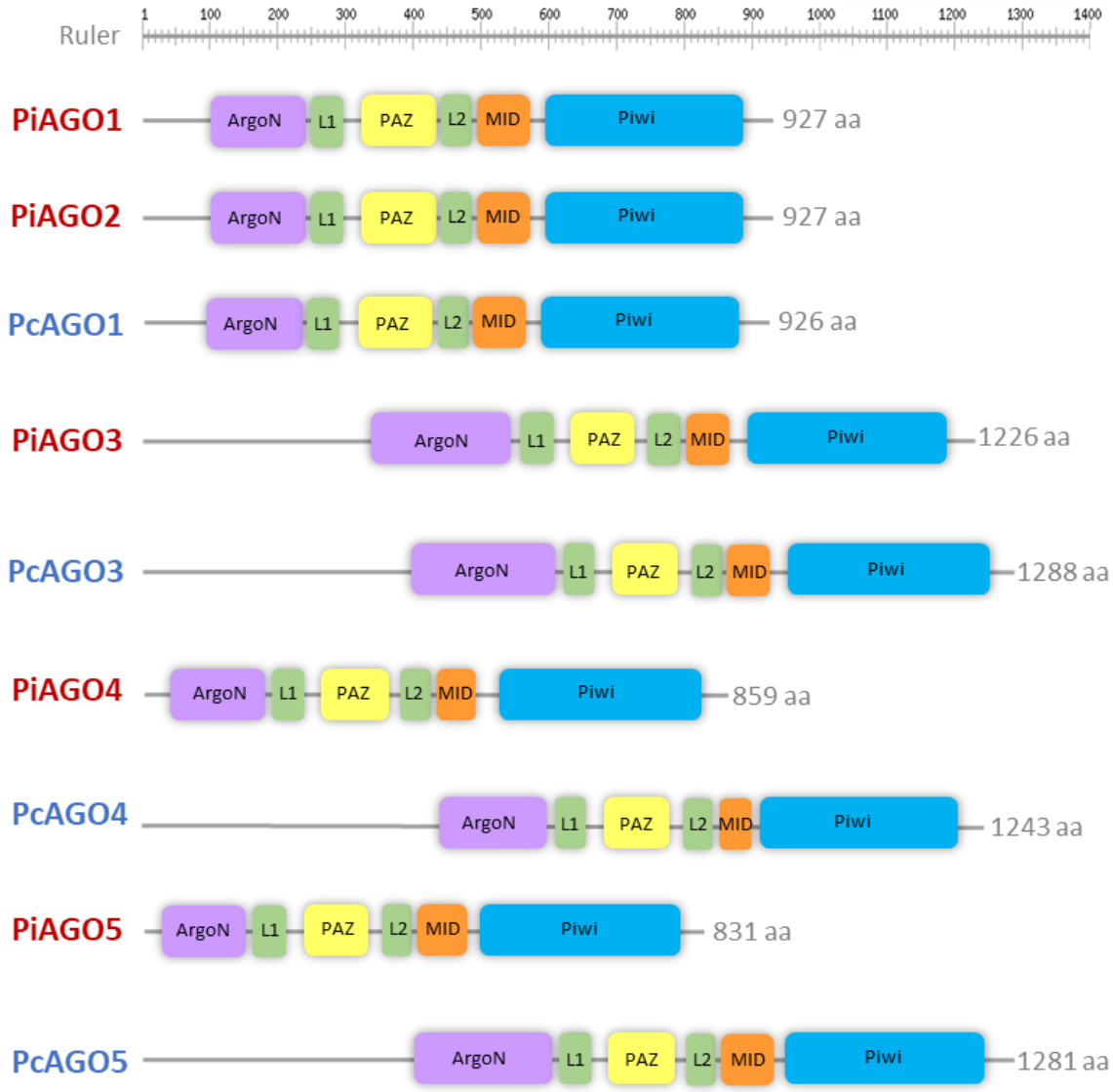

Figure 28. Domain architecture of AGO proteins in *P. infestans* and *P. cinnamomi* predicted *in silico*. Four AGO were identified *in silico* in *P. cinnamomi* all of which display the canonical functional domains characteristic of AGO. The figure compares the domain organization of AGO proteins from *P. infestans* (PiAGO1–PiAGO5) and *P. cinnamomi* (PcAGO1–PcAGO5). Protein domain organization was predicted using Pfam database and MOTIF tool. Lines represent the full amino acid length of each protein, and colored boxes indicate conserved domains: ArgoN (purple), Linker 1 and 2 (L1 and L2, green), PAZ (yellow), MID (orange), and Piwi (blue).

An RNA-dependent RNA polymerase (RdRp) was identified by BLASTp analysis in *P. cinnamomi*, designated PcRdRp1 (Figure 29). A single RdRp has also been identified in other *Phytophthora* species (Piombo *et al.*, 2023). While the number of these proteins is highly variable in other species, as evidenced by the case of *F. circinatum*, which had four RdRps. Some oomycetes, such as *Phytium periplocum*, have more than one RdRp (Piombo *et al.*, 2023). The discrepancy in the number of RdRps among different organisms may be reflected in the sRNA populations (Piombo *et al.*, 2023), although this requires further experimental confirmation. The identified protein exhibited the characteristic domain of RdRp.

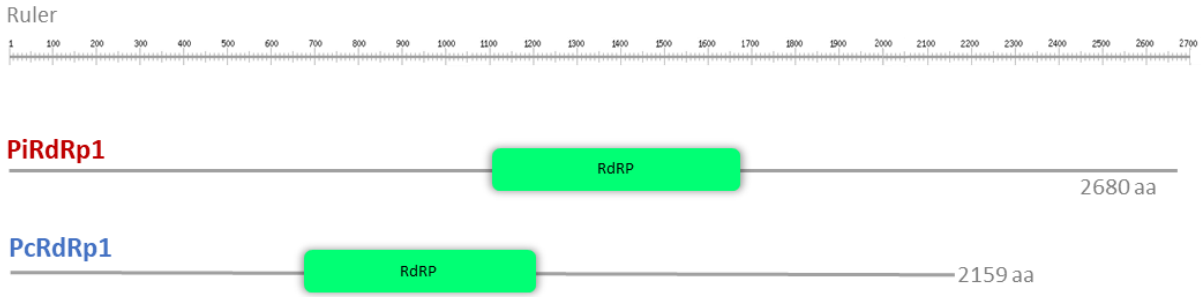

Figure 29. Comparative domain structure of RdRps in *P. infestans* and *P. cinnamomi*. Both species harbor a single RdRp with a conserved catalytic domain. Domains were predicted using the Pfam database via the MOTIF tool. Horizontal lines indicate the full-length proteins, and green boxes represent the predicted RdRp domain.

The final stage of the comparative analysis involved a comparison of the structures of *P. infestans* and *P. cinnamomi* RNAi proteins. It was observed that the RNAi components of both pathogens are structurally similar, thereby reaffirming the previous analyses of domain architecture and sequence homology. Visualization of the structural alignments revealed a higher proportion of green regions, which indicated good alignments of the structures, while red regions (in lower proportion in our alignments) signified low similarity or divergence (Figure 30). Most conserved regions correspond to the active site, as visualized by the green-colored regions, while divergence was observed in the N-terminal region (red areas). The quantitative data for these alignments were obtained using PyMOL, yielding high MatchAlign values, which indicate that the alignments between the protein structures are of good quality. The root-mean-square deviation (RMSD) values obtained in the comparative analyses were found to be relatively low (Table S7), indicating that the structures under comparison are either identical or exhibit a high degree of similarity. This analysis showed that RNAi components structure is well-conserved and have a high degree of similarity, suggesting that the function of the RNAi proteins may be conserved between *P. infestans* and *P. cinnamomi*.

In *P. infestans*, PiDCL1 is involved in generating predominantly 21-nt sRNAs, as sRNAs of this size were absent in *dcl1*-silenced lines (Vetukuri *et al.*, 2012). Furthermore, an accumulation

of longer sRNAs (24–25 nt) occurred in these transformants, suggesting that PiDCL2 may be involved in their generation. However, this hypothesis requires further experimental verification, for example through the generation of transformants with silenced *dcl2*. The results of Vetukuri *et al*. (2012) also suggested that PiAGO4 and PiAGO5 are involved in the accumulation of 32 nt sRNAs, while PiAGO1 negatively impacts on 32 nt sRNA accumulation. The specific function of PiAGO3 and PiRdRp1 in the generation of sRNAs remained unclear, as the study was unable to obtain knockdowns of the genes encoding these RNAi components. A study conducted by (Fahlgren *et al.*, 2013) on several *Phytophthora* spp., including *P. infestans*, revealed that endogenous small RNA populations exhibited a bimodal distribution, with a peak on 21 and 25 nt sRNAs. This finding supported the hypothesis previously proposed by Vetukuri *et al*. (2012) that each dcl produces sRNAs of one of the two size groups. This is analogous to the manner in which plants differentiate sRNA pathways with the involvement of specific dcl proteins (Axtell, 2013). Moreover, *Phytophthora* AGO proteins may be subdivided into two or more functional groups that could stabilize 21- or 25-nt sRNAs (Fahlgren *et al.*, 2013). The distinct sRNA size classes may be associated with specific roles in RNA silencing. Fahlgreen *et al*. (2013) and Vetukuri *et al*. (2012) proposed that 21-nt sRNAs are involved in posttranscriptional silencing, whereas longer sRNAs are associated with transcriptional silencing. This has been previously reported in *A. thaliana* (Wang *et al.*, 2011). However, further analysis of RNA silencing-deficient lines is required to confirm these hypotheses and to identify any functional differences between the two small RNA size classes.

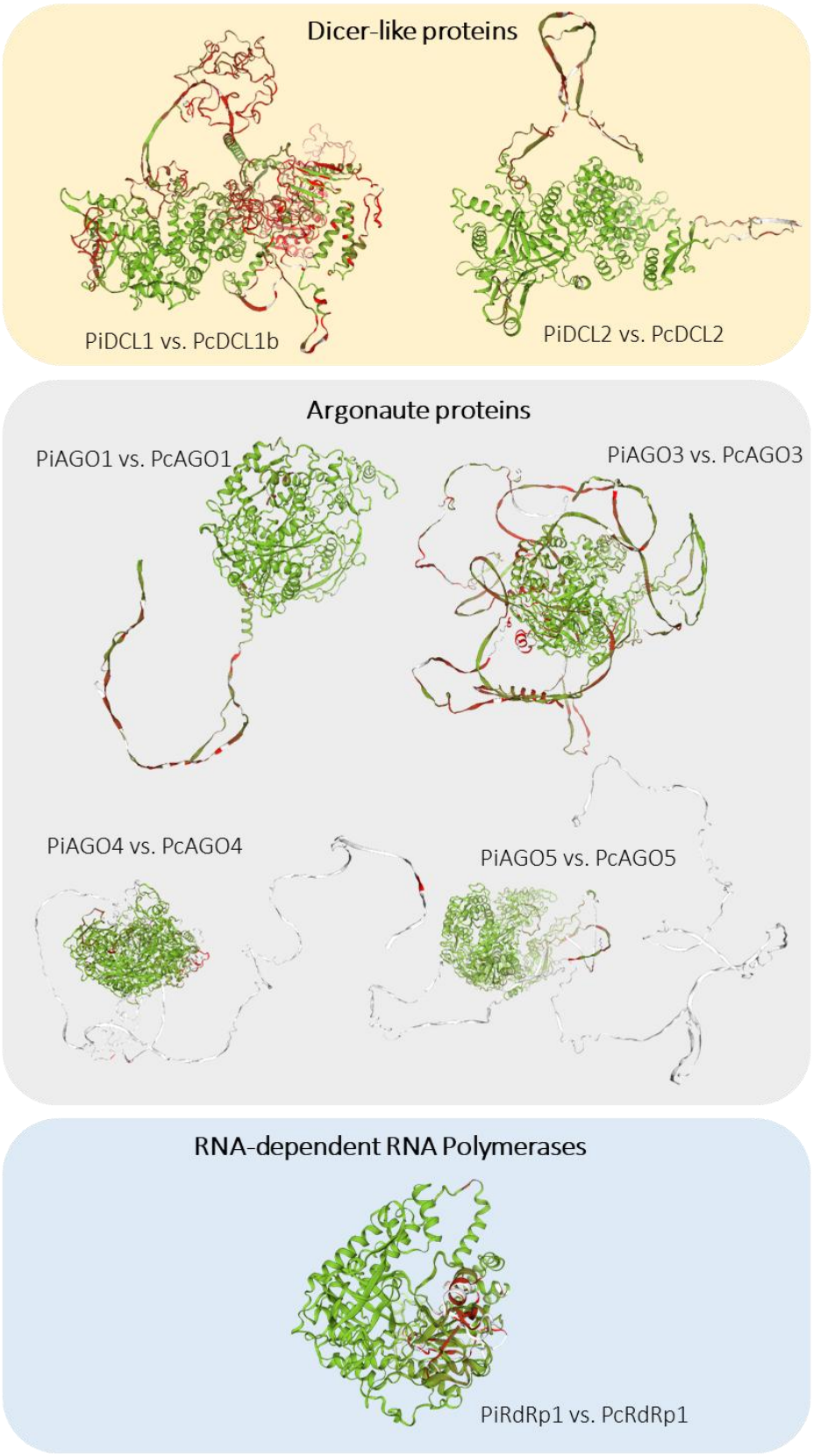

Figure 30. Comparative analysis of the 3D structures of the proteins of *P. infestans* and *P. cinnamomi*: DCL, AGO and RdRp. The 3D structures of the *P. cinnamomi* RNAi proteins were found to be highly similar to their orthologues in *P. infestans*. Individual structures were predicted using SWISS-MODEL and compared using the structure comparison tool. Regions in green indicate good structural alignment between the proteins and red regions signify areas of poor alignment or significant structural differences between the proteins.

In conclusion, *in silico* analysis demonstrated that *P. cinnamomi* possesses the components of canonical gene silencing pathways similar to those of other eukaryotes, including two DCL, four AGO, and one RdRp. Protein domain and structure analysis indicated that these proteins may be functional in the RNAi pathway, suggesting that *P. cinnamomi* possesses the complete RNAi machinery and may therefore be susceptible to control by SIGS technology. It seems that *Phytophthora* genus has at least two distinct small RNA pathways, which can be distinguished by DCL, AGO and RdRp diversification, as well as small RNA size. Given the high degree of structural homology, it can be reasonably assumed that the RNAi machinery identified in *P. cinnamomi* is functional and capable of producing sRNAs of at least 21 and 25 nt via PcDCL1 and PcDCL2. The presence of PcDCL1 in *P. cinnamomi* appears to facilitate the generation of 21-nt sRNAs from dsRNAs, thereby initiating the mechanism of post-transcriptional silencing by SIGS. PcAGO proteins appear to be involved in binding sRNAs of varying sizes; however, it is currently unclear which of these proteins may be directly involved in SIGS silencing. Similarly, the function of RdRp has not yet been characterized in the genus *Phytophthora*, thus further research is necessary to confirm the function of all these RNAi proteins identified in the present study in *P. cinnamomi* in an analogous manner to that described for the proteins of *F. circinatum*.

1.2. Limited uptake of dsRNA molecules has been observed in *Phytophthora cinnamomi*-infecting structures (sporangia and zoospores)

The efficacy of SIGS control is contingent upon the successful delivery of externally applied dsRNA molecules to the pathogen (Qiao *et al.*, 2021). The pathogen can internalize the silencing molecules in two ways: directly, by capturing the dsRNAs directly from the environment; and indirectly, through the plant.

Unlike the assays performed for *F. circinatum*, where fluorescein-labeled dsRNA was used due to equipment availability, experimental setup, and the research group's prior experience with fluorescein in fungal pathogen uptake assays (Qiao *et al.*, 2021), the uptake assay for *P. cinnamomi* was conducted using Cy3-labeled dsRNA. Cy3 offers several advantages, including a high molar extinction coefficient and strong brightness. Its excitation/emission profile around 550-570 nm helps reduce overlap with autofluorescence. Moreover, Cy3 labeling does not interfere with the internalization or processing of dsRNA (Fletcher *et al.*, 2025). This experiment was carried out at the University of Queensland (Brisbane, Australia), where Cy3 labeling and confocal imaging resources were already established and optimized for this fluorophore, having been successfully applied in previous uptake studies (Degnan *et al.*, 2022). Considering that the infection structures of *Phytophthora* spp. are the

zoospores produced in sporangia, we evaluated dsRNA uptake in both these infective structures and the mycelium. This approach follows established protocols in *P. infestans* (Kalyandurg *et al.*, 2021) and other pathogens such as *Austropuccinia psidii* (Degnan *et al.*, 2022) and *Clonostachys rosea* (Piombo *et al.*, 2024).

Our results indicated that exposure of *P. cinnamomi* to labeled dsRNA for varying periods did not result in detectable fluorescence within zoospores or sporangia, and only faint fluorescence was observed in some mycelial structures, indicating a very limited dsRNA uptake under the tested conditions (Figure 31). Although fluorescence was not detected within the zoospores or sporangia and was only faintly observed in the mycelium, a clear fluorescent signal was consistently observed around the periphery of the cells. This signal likely corresponds to Cy3-labeled dsRNA retained at the cell wall level, indicating that while the labeled molecules were successfully applied and visualized using CLSM, they were not internalized by the pathogen under the tested conditions. These results are consistent with those observed in other *Phytophthora* species, such *as P. infestans*, where Qiao *et al.* (2021) reported a low dsRNA uptake efficiency, which ultimately resulted in the failure to inhibit pathogen virulence. Similarly, Cheng *et al.* (2022) observed no or very weak fluorescent signals in *P. capsici* germinated cysts and hyphae when labeled-dsRNA was applied, indicating a very poor uptake of these molecules. Although there are exceptions, such as the study by Kalyandurg *et al.* (2021), which did observe uptake of dsRNA by *P. infestans*. The limited uptake efficiency of double-stranded RNA (dsRNA) restricts its application against the notorious oomycete genus *Phytophthora*. Nevertheless, the potential of carriers is being explored to enhance the direct uptake of dsRNAs in oomycetes. The use of dsRNA-carbon dots (CDs) has been demonstrated to strongly enhance cellular uptake in *P. capsici*, and CDs showed to facilitate dsRNA delivery also in plants (Wang *et al.*, 2023b). Furthermore, Wang *et al.* (2023b) demonstrated that CDs enhanced the efficacy of dsRNA in controlling the infection of *P. infestans*, *P. sojae*, and *P. capsici*, thereby reducing the incidence of infection in comparison to the use of naked dsRNAs. Similarly, spraying dsRNAs along with nanoclay carriers has been proved effective against *P. infestans* for management of potato late blight (Sundaresha *et al.,* 2022). Despite the observed limitation in the uptake of dsRNAs in several *Phytophthora* species, including the present study on *P. cinnamomi*, recent reports indicate that *P. capsici* could effectively uptake siRNAs (Cheng *et al.*, 2022). This may be attributed to the characteristics of siRNAs, namely their low molecular weight and ready delivery. Using siRNAs may be a useful approach to evaluate uptake ability on *Phytophthora* spp. and may facilitate future uptake experiments on *P. cinnamomi*. Nevertheless, the utilization of siRNAs is not the ideal approach for SIGS experiments, as they are more susceptible to degradation, have

a shorter durability, and dsRNAs permit the targeting of multiple genes with a single molecule (Wang *et al.*, 2013). The efficiency of dsRNA internalization varies considerably among different plant pathogens. Nevertheless, it has been demonstrated in numerous studies that the vast majority of fungi are capable of internalizing dsRNAs from the surrounding medium, leading to the silencing of pathogen genes (Qiao *et al.*, 2023; Wang *et al.*, 2016). The reason for the limited uptake in oomycetes such as *Phytophthora* spp. is currently unknown. However, oomycetes diverge from fungi in that they possess a very tough cellulose-rich cell wall ranging from 0.1 to several µm in thickness, which may pose a physical barrier to biomolecule delivery. Indeed, Whisson *et al.* (2005) evaluated dsRNA uptake in *P. infestans* protoplasts and observed fluorescence within them, confirming that *P. infestans* protoplasts (lacking the cell wall) were able to uptake labeled-dsRNAs. Nevertheless, the mechanism of cellular uptake of dsRNA and strategies to enhance this process remain largely unknown and require further investigation.

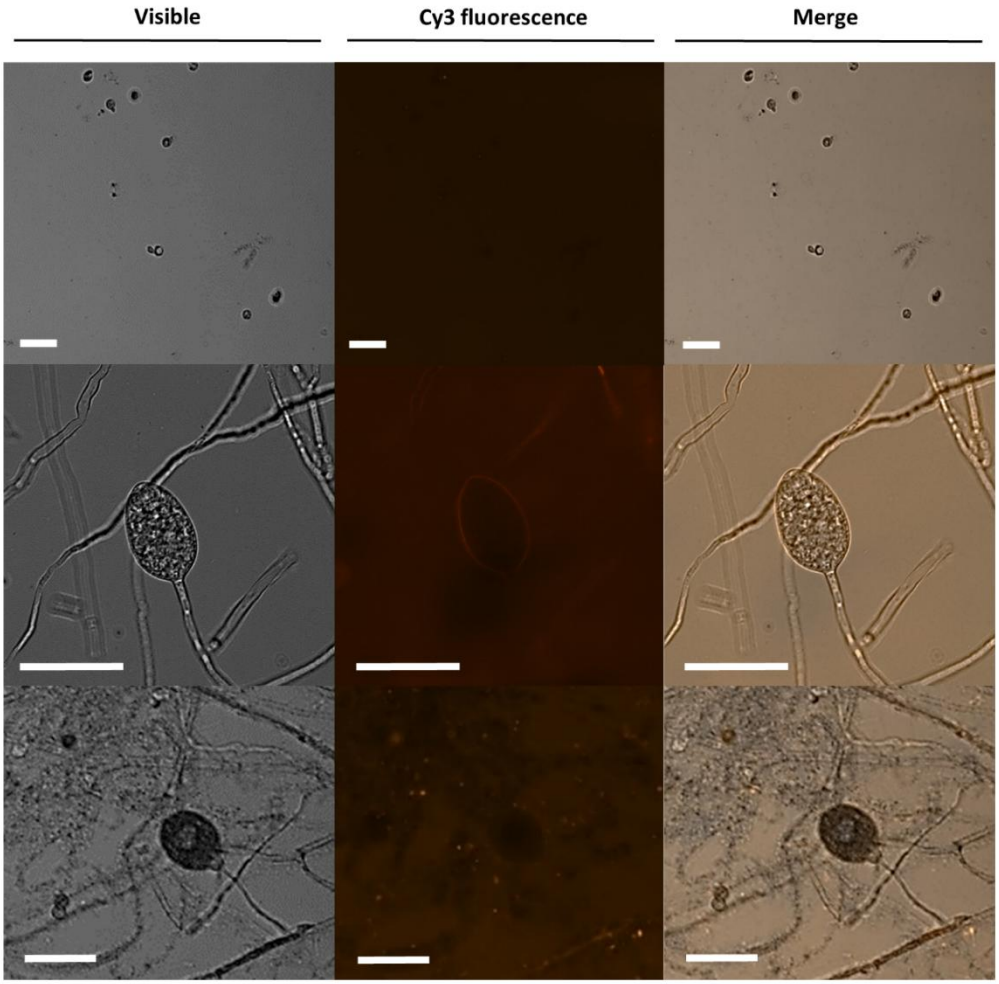

Figure 31. Cy3-labeled dsRNA is not internalized by the infecting structures of the oomycete *P. cinnamomi*, indicating limited uptake by the pathogen. Cy3-labeled dsRNA was applied to *P. cinnamomi* zoospores, sporangia and mycelium, and samples were visualized by CLSM at 6-8 h and 24 h post-incubation. No intracellular fluorescence signal was detected in any structure at either time point, suggesting the dsRNA was not internalized. Some fluorescence was observed associated with the cell surface, possibly retained in the cell wall. The first row of images shows zoospores, the second row shows a sporangium with the zoospores inside, and the third row shows *P. cinnamomi* mycelium and sporangia. Scale bars represent 50 µm.

2. Preliminary assays to validate *Phytophthora cinnamomi* target genes for SIGS-based control

Prior to the assessment of the dsRNA in one of the main hosts of *P. cinnamomi*, *Q. ilex*, preliminary trials were conducted in model plants. The use of model plants allowed faster and more controlled testing of dsRNA efficacy and pathogen response, given their ease of handling, rapid growth, and extensive molecular characterization. Thus, this system allowed us to test initial hypotheses under controlled conditions before transferring them to more complex hosts. *L. angustifolius* and *N. benthamiana* were selected for these assays due to their known susceptibility to *P. cinnamomi* (Allardyce *et al.*, 2012; Kharel, 2020; Kharel *et al.*, 2025; Kirby and Grand, 1975; Serrano *et al.*, 2011). *Lupinus* spp. are known hosts for various *Phytophthora* spp., and *L. angustifolius* in particular has long been used as a bait plant for isolating *Phytophthora* spp. from soil (Chee and Newhook, 1965). *P. cinnamomi* symptoms observed in lupins, both in artificial inoculations and in the field, include sudden wilting, yellowing, root rot, and plant death (Serrano *et al.*, 2011). In parallel, *N. benthamiana* has been frequently used in RNAi-based studies involving *Phytophthora* species (Park *et al.*, 2023b; Park *et al.*, 2023a). This plant provides a model system for studying the interaction between the roots of a susceptible host and *P. cinnamomi* and remain valuable model organisms for plant-pathology research. In *N. benthamiana*, the pathogen induces characteristic symptoms such as brown necrotic lesions extending to the stem, severe chlorosis, pronounced wilting, and extensive root necrosis (Kharel *et al.*, 2025).

Despite *P. cinnamomi* being a soil-borne pathogen that primarily invades through the root tips, most studies employing *N. benthamiana* as a host have focused predominantly on leaf-based assays (Belisle *et al.*, 2019; He *et al.*, 2024). However, root inoculation is critical for accurately reflecting the biology of *P. cinnamomi*, a root-invading pathogen, and provides a more realistic approximation of its natural infection process (Allardyce *et al.*, 2012). In this study, we wanted to evaluate the earliest symptoms, those that occur at the root. To achieve this, and despite the inherent challenges posed by the inaccessibility of the root system, we performed inoculations and applied dsRNA treatments directly to the roots of the model plants using a hydroponic setup. Hydroponic culture has been previously utilized in research experiments involving *P. cinnamomi* and other *Phytophthora* species (Crone *et al.*, 2013a; Rodríguez-Padrón *et al.*, 2018), demonstrating its effectiveness as a controlled system for studying pathogen-plant interactions. This approach provides a reliable environment for assessing disease progression, pathogen virulence, and the efficacy of potential treatments. It allows direct exposure of plant roots to both the pathogen and treatments and enables the observation of early infection

dynamics while minimizing external variables present in soil-based systems. Accordingly, and given the complexity and number of variables in our experimental setup, this previously established approach was adopted.

This work was conducted at the University of Queensland (Brisbane, Australia), and some of the results presented in this subsection were obtained during a stay under the supervision of Prof. Anne Sawyer. Her research group is actively developing RNA "vaccines" to protect plants from fungal and oomycete pathogens, including *P. cinnamomi*, which severely affects economically important species in Australia, such as avocado and pineapple.

To explore the potential of the dsRNA molecules produced in Chapter 1 for controlling *P. cinnamomi*, a series of assays were conducted in different plants. The treatments applied across these experiments are summarized in Table 12.

Table 12. Summary of treatments used for SIGS efficacy assessment against *P. cinnamomi*

Treatment name	*P. cinnamomi* inoculation (+/-)	dsRNA application (300 ng/µl)
Non-inoculated	-	(-) ddH_2O
PH2003	+	(-) ddH_2O
Mock control	+	YFP-dsRNA (non-specific dsRNA)
PcDCL-dsRNA	+	PcDCL-dsRNA
PcDDS-dsRNA	+	PcDDS-dsRNA
PcPTP-dsRNA	+	PcPTP-dsRNA

2.1. dsRNA molecules showed protective effects against *Phytophthora cinnamomi* in model plants

An initial experiment was conducted to optimize the application method of dsRNA in 3-day-old *L. angustifolius* seedlings under hydroponic conditions. A series of delivery strategies were meticulously evaluated to ascertain the most suitable approach for ensuring reliable infection and effective dsRNA uptake. dsRNA treatment was applied using four different methods: (A) by immersing the plant roots directly in the dsRNA solution prior to pathogen inoculation; (B) by soaking *P. cinnamomi* mycelial plugs in the dsRNA solution prior to plant inoculation; (C) by spraying the dsRNA onto the aerial parts of the seedlings; and (D) by diluting the dsRNA in the hydroponic growth medium for root uptake. The experiments were conducted under hydroponic conditions, and the percentage of root necrosis of the seedlings was assessed. PcDCL-dsRNA molecule was used for this test, since *dcl* genes have already been successfully used by SIGS to prevent other plant diseases (Haile *et al.*, 2021; Qiao *et al.*, 2021; Wang *et al.*, 2016; Werner *et al.*, 2020). dsRNA was applied at a concentration of 300 ng/µL (as previously used on *F. circinatum*), and treatment effects were compared with PH2003 control, consisting of plants inoculated with *P. cinnamomi* in the absence of dsRNA treatment.

The results obtained with methodology A, soaking plant roots for 24 hours in dsRNA, prior to pathogen inoculation, PcDCL-dsRNA treatment showed a clear trend toward reduced root necrosis in comparison to PH2003 control (Figure 32A, Table S8). Although the difference was not statistically significant at the conventional threshold (*p*-value = 0.068), the observed decrease in necrosis suggests a potential biological effect. This trend, while not conclusive, highlights the potential of the dsRNA application approach and underscores the need for further experiments with larger sample sizes to increase statistical power. Other studies have demonstrated the efficacy of dsRNA application via root soaking, resulting in efficient gene silencing in the target organism (Jiang *et al.*, 2014; Li *et al.*, 2015). More recently, root soaking has been found to be more effective than dsRNA spraying in *Nicotiana* spp. model plants against viral diseases, providing a strong preventive effect (Xu *et al.*, 2023). Similarly, Qiao *et al.* (2021) applied dsRNA directly to plant roots by dipping *Arabidopsis* roots in dsRNA against the root pathogen *Verticillium dahliae,* resulting in reduced disease symptoms in treated plants. Moreover, the pre-application of dsRNA prior to pathogen challenge has been reported to enhance protection (Zheng *et al.*, 2025), which supports our approach of soaking the roots in dsRNA 24 hours before P. cinnamomi inoculation.

Methodologies B, C, and D did not result in any discernible effect on the virulence of the pathogen (Figure 32A, Table S8). The percentage of necrosis in roots was comparable between the treatment and control group, with considerable variability in the data. With regard to methodology B, which involved soaking the pathogen in a solution of dsRNA, this outcome is consistent with the previous findings regarding its limited dsRNA uptake ability. Our observations indicated that *P. cinnamomi* exhibits minimal direct uptake of dsRNA from the external environment. Consequently, when the treatment is applied directly to the pathogen, it may be unable to take up the dsRNA, rendering the SIGS technique ineffective. This has been observed by Qiao *et al.* (2021), who evaluated the direct uptake ability of different pathogens and found that those that did not efficiently uptake dsRNA failed to suppress infection. Indeed, one of the pathogens evaluated in the study was *P. infestans*, which demonstrated a low efficiency in the uptake of dsRNA. Consequently, the topical application of dsRNA was unsuccessful in inhibiting the virulence (Qiao *et al.*, 2021).

Strategies C, and D, like A approach, facilitate an indirect uptake of dsRNA by the plant, which would subsequently deliver it to the pathogen. However, the results of methodology C, which involved spraying the treatment, and methodology D, which involved adding dsRNA to the growth media, showed no effect on the protection against the pathogen (Figure 32A, Table S8). In C approach, this may be due to the fact that since the infection is localized in the root, the

dsRNA is unable to translocate at a sufficient rate to induce gene silencing at the point of infection. There is growing evidence that externally applied dsRNAs and siRNAs can be absorbed by plant tissues and subsequently transported through the vascular system to distal parts of the plant, where they may exert their gene-silencing effects. For instance, Koch *et al*. (2016) demonstrated the systemic movement of dsRNA in barley (*Hordeum vulgare*) following foliar application, leading to protection against *F. graminearum* in distal leaves. Similarly, Mitter *et al*. (2017) showed that clay nanosheets loaded with dsRNA allowed for prolonged protection and systemic transport in *Nicotiana tabacum* against cucumber mosaic virus (CMV). Konakalla *et al*. (2016a) reported systemic gene silencing following spray-induced RNAi targeting *Tobacco mosaic virus* (TMV) in *N. tabacum*. Finally, in tomato, exogenously applied dsRNA molecules were shown to move rapidly from treated leaves to systemic tissues, conferring protection against insect pests and mites (Gogoi *et al.*, 2017). However, it is important to note that most of this movement was observed toward especially young developing tissues (Zheng *et al.*, 2025), but not toward roots. Although downward transport cannot be completely dismissed, its efficiency remains unclear, which may help to explain the limited efficacy observed in our assays when dsRNA was sprayed onto leaves. The long-distance movement of a silencing signal between different plant organs requires loading into the vascular system, subsequent transport, and eventual discharge into the recipient tissue or cells, a process that takes place over days (Melnyk *et al.*, 2011). In our case study, the dsRNA must be transported from the leaves, where the dsRNA is applied, to the root tip, which is the entry point for *P. cinnamomi*. As the infection caused by this pathogen progresses rapidly, this method of dsRNA application may not be sufficiently effective in reducing symptoms. Additionally, we did not include organosilicon-based adjuvants in our foliar applications. These compounds are known to enhance uptake and facilitate apoplastic movement, and their absence may have limited the translocation efficiency of dsRNA treatments in our experimental conditions.

In the case of methodology D, this involves an indirect uptake through the plant via the root, thus obviating the necessity for the dsRNA to move long distances. Nevertheless, this method has not demonstrated efficacy in reducing the virulence of the pathogen. This may be attributed to the dilution of dsRNA in the hydroponic growth medium, which may not be at a sufficient concentration to reduce the virulence of the pathogen. The effect of SIGS is dependent on the dose or concentration applied; therefore, it is essential to utilize a sufficient amount of dsRNA that will result in a reduction in growth and transcript silencing (Mcloughlin *et al.*, 2018). However, due to the high volume of media in which the plants are placed to grow, it is not possible to increase the concentration of dsRNA sufficiently, given the current limitations of dsRNA

production method used in this study. Moreover, increasing dsRNA concentration is not necessarily beneficial, as higher dsRNA concentrations may hinder molecular uptake due to increased solution osmolarity. Additionally, when dsRNAs are formulated with certain carriers, their application at high concentrations has been associated with phytotoxic effects (Tang *et al.*, 2024).

In summary, our results demonstrate that among the various dsRNA delivery methods tested, root soaking (approach A) emerged as the most promising strategy for reducing *P. cinnamomi* infection in *L. angustifolius*. This method provided localized delivery at the site of pathogen entry and avoided the limitations associated with foliar translocation or limited pathogen uptake. Although statistical significance was not achieved, the consistent trend of reduced necrosis supports the biological relevance of this approach. A wide range of techniques have been reported in the literature for delivering dsRNAs, siRNAs, or hpRNAs to plants, with the effectiveness of each method depending on the specific plant-pathogen system and experimental context (Das and Sherif, 2020). Given these considerations, root soaking approach (A) was therefore employed in the following experiments to evaluate the effectiveness of all designed dsRNA molecules in both *L. angustifolius* and *N. benthamiana* model plants.

The dsRNA molecules PcDCL-dsRNA, PcDDS-dsRNA, and PcPTP-dsRNA were then tested against *P. cinnamomi* using hydroponic assays in *L. angustifolius* and *N. benthamiana*. Each trial included a non-inoculated, PH2003 and mock control. The roots were soaked in dsRNA solutions 24 hours prior to infection, after which the plants were inoculated with mycelial plugs of *P. cinnamomi*. The disease symptoms were assessed at 7 dpi.

In *L. angustifolius,* root necrosis was evaluated as a measure of disease severity. This disease rating has been previously employed in studies of *P. cinnamomi* across various hosts (Kharel *et al.*, 2025; Ploetz and Schaffer, 1987), including *L. angustifolius* (Allardyce *et al.*, 2012). Although no statistically significant differences were found between treatments (p-value > 0.05), plants treated with PcDCL-dsRNA, PcDDS-dsRNA, and PcPTP-dsRNA exhibited reduced levels of necrosis compared to both the mock control and PH2003 (Figure 32B, Table S9). Specifically, necrosis was reduced by 38%, 35%, and 53%, respectively, relative to mock control, and by 39%, 35%, and 53% when compared to *P. cinnamomi*-control. Despite considerable variability between individuals, some plants exhibited complete protection: 5 plants in the PcDCL-dsRNA group, 4 in the PcDDS-dsRNA group, and 5 in the PcPTP-dsRNA group showed no visible root necrosis. In contrast, only one plant in the mock control group remained free of root damage. *P. cinnamomi* typically caused necrotic lesions of varying lengths extending from the root tip.

Among the treatments, PcPTP-dsRNA, which targets genes associated with the signal transduction pathway, yielded the most pronounced protective effect, with results approaching statistical significance. Plants receiving this treatment exhibited an overall healthier appearance, with more developed and vigorous root systems and visibly reduced necrotic tissue relative to inoculated controls. Additionally, infected plants showed a noticeable decline in secondary root formation and exhibited thinner, less resilient roots (Figure 32B).

Overall, the dsRNA treatments tested in *L. angustifolius* demonstrated a consistent trend toward reducing disease symptoms caused by *P. cinnamomi*, despite the lack of statistically significant differences. Notably, the severity of root necrosis observed in the mock control and the PH2003-inoculated control groups was comparable, indicating that both served as reliable baselines for evaluating the efficacy of the dsRNA molecules.

In *N. benthamiana*, plants infected with *P. cinnamomi* displayed disease symptoms, including reduced root and shoot growth, smaller, less vigorous leaves, and noticeable wilting. To quantify disease severity, the canopy area was measured at 7 dpi. Plants treated with the mock control exhibited pronounced symptoms, with an average canopy area of just 1.03 cm^2, reflecting reduced vegetative development and leaf collapse (Figure 32C, Table S10). Among the dsRNA treatments, PcPTP-dsRNA produced the most significant protective effect, with treated plants showing a significantly larger average canopy area (2.89 cm^2) compared to the mock control (p-value < 0.001). Notably, several plants exhibited no apparent symptoms of infection and displayed enhanced root development, including the emergence of secondary roots. Leaf wilting was rarely observed in this group (Figure 32C). PcDCL-dsRNA treatment showed a trend toward reduced disease severity, with an average canopy area of 1.73 cm^2, indicating partial protection, although the effect was not statistically significant (p-value > 0.05). In contrast, PcDDS-dsRNA treatment did not appear to have any effect on the protection of *N. benthamiana* seedlings, with results comparable to those of the mock control (canopy mean = 1.08 cm^2) (Figure 32C, Table S10).

Taken together, these results underscore the potential of PcPTP-dsRNA as the most effective molecule, showing consistent protection in both model systems tested. However, while all dsRNA treatments showed a trend toward reduced infection in *L. angustifolius*, their efficacy varied significantly in *N. benthamiana*. Notably, PcDDS-dsRNA failed to confer any observable protection in this species. These findings highlight the possibility of species-specific responses to SIGS-based strategies, underscoring the importance of validating candidate dsRNA molecules across multiple host systems to account for differences in RNA uptake, mobility, or processing.

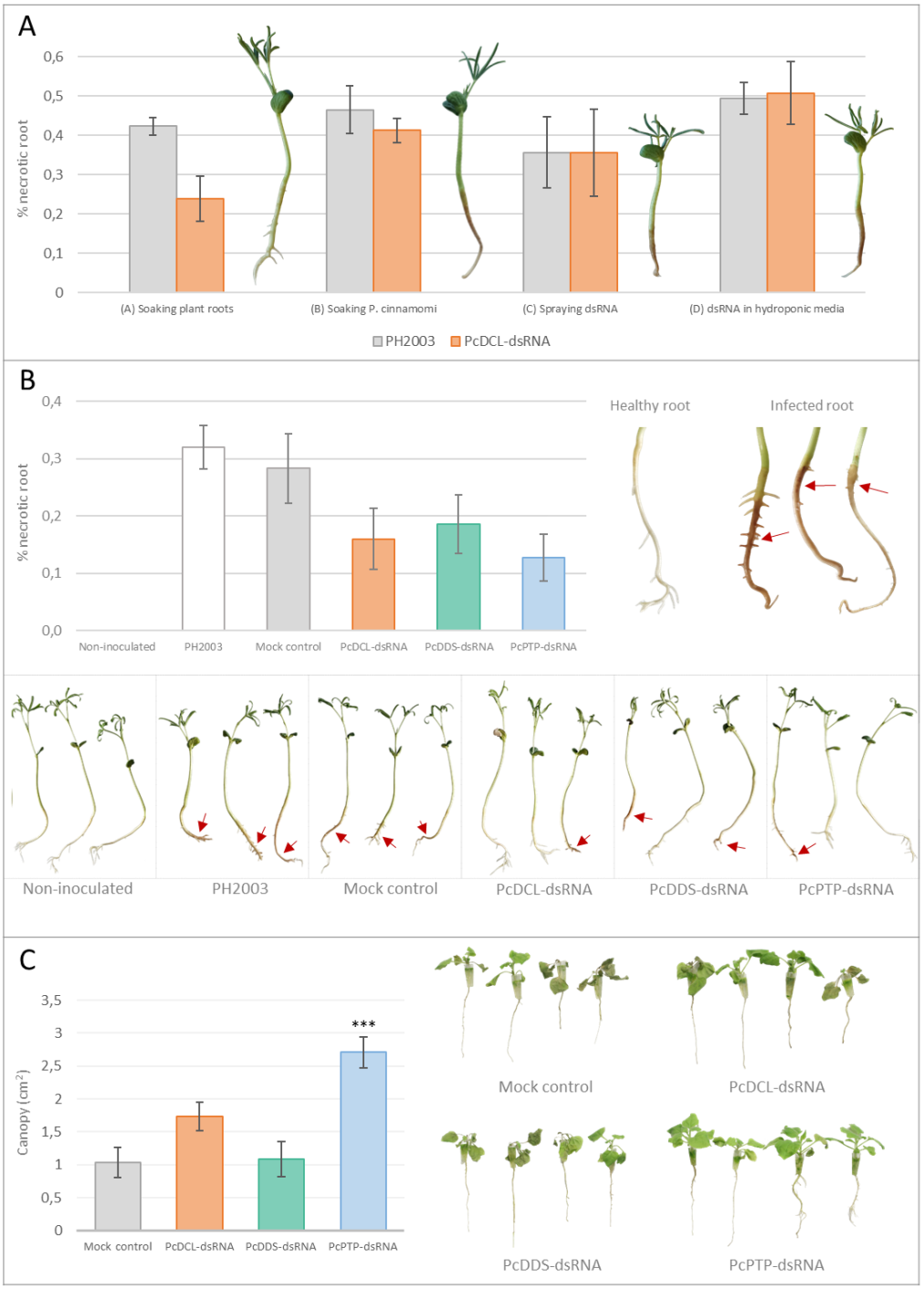

Figure 32. Evaluation of different dsRNA delivery methods and dsRNA molecules protective effects against *P. cinnamomi* in model plants. A. Comparison of four dsRNA application methods in *L. angustifolius* using PcDCL-dsRNA: (A) root soaking, (B) soaking *P. cinnamomi* mycelial plugs, (C) foliar spraying, and (D) dsRNA diluted in hydroponic media. Bar graph shows the percentage of necrotic root in response to various dsRNA delivery methodologies. Error bars represent the standard error between biological replicates. Plants treated by root soaking exhibited reduced necrosis, although not statistically significant. **B.** Efficacy of PcDCL-dsRNA, PcDDS-dsRNA, and PcPTP-dsRNA in *L. angustifolius* using root soaking. Bar graph shows the percentage of necrotic root in the various treatments. Error bars represent the standard error between biological replicates. All treatments showed a trend toward reduced root necrosis compared to PH2003 and mock control. The right panel illustrates healthy and infected roots, highlighting characteristic symptoms of root necrosis (indicated by red arrows). The lower panel presents representative seedlings from each treatment group included in the trial. **C.** Evaluation of canopy development in *N. benthamiana* seedlings treated with dsRNA molecules. Bar graph shows the percentage of necrotic root in the different treatments. Error bars represent the standard error between biological *replicates*. PcPTP-*dsRNA* treatment resulted in a statistically significant increase in canopy area compared to the mock control. Statistical analysis was performed

using Kruskal-Wallis and Wilcoxon rank-sum tests with Holm's correction (***p-value < 0.001). Photographs on the right display phenotypic differences across treatments, highlighting better overall plant vigor in PcPTP-dsRNA–treated plants.

In conclusion, the preliminary assays conducted in *L. angustifolius* and *N. bethamiana* demonstrate that both species represent valuable systems for early-stage validation of RNA-based control strategies of *P. cinnamomi*. Its rapid growth, stable infection and compatibility with hydroponic systems make them well-suited for evaluating root rot severity. The measurable reductions in disease severity obtained through root-based delivery in both model systems demonstrate that the designed molecules are biologically active and capable of modulating pathogen virulence. However, the primary challenge appears to lie not in the efficacy of the molecules themselves, but in the delivery method due to the limited uptake ability of the pathogenic oomycete.

The pre-treatment approach, applying dsRNA 24 hours prior to inoculation, likely allowed sufficient time for uptake, processing into siRNAs, and activation of RNAi mechanisms in the plant, contributing to the observed effects infection (Park *et al.*, 2023b). Although the dsRNA was not directly applied to the pathogen, the reduction in infection suggests that gene silencing may have occurred indirectly, possibly via plant-mediated delivery. These findings align with previous studies showing enhanced protection following dsRNA pre-treatment (Yoon *et al.*, 2021). This approach may be particularly effective for pathogens that do not efficiently uptake dsRNA molecules by themselves, such as *P. cinnamomi*. However, it should be noted that this limits the potential for using SIGS technique to eradicate the pathogen once established, making it a preventive rather than a curative method.

The efficiency of sRNA uptake from the plant may be influenced by stomatal density and leaf architecture, as these factors can represent barriers to dsRNA penetration. Stomatal opening has been hypothesized to facilitate passive entry of sprayed RNAs into plant tissues (Rank and Koch, 2021). Therefore, future investigations of the group could explore the use of formulations, such as adjuvants that promote stomatal opening or increase leaf permeability, as a means to enhance dsRNA uptake from foliar sprays and potentially improve the efficacy of the SIGS approach. Moreover, the differing results observed between both model plants underscore the critical importance of validating dsRNA molecules across multiple host systems, particularly when aiming to develop cross-species or field-applicable SIGS strategies.

Overall, this work lays the foundation for further testing in the primary host, *Q. ilex*, and provided evidence of the effect of dsRNAs designed and produced against *P. cinnamomi* in this study.

3. SIGS mediated control of *Phytophthora cinnamomi* in the host *Quercus ilex*

The dsRNA molecules (PcDCL-dsRNA, PcDDS-dsRNA, and PcPTP-dsRNA) were tested in *Q. ilex* to evaluate their effectiveness in controlling the disease in the main host. Similarly, to the experiments in pines included in Chapter 2, *Q. ilex* plants for these experiments require a considerable period of time to germinate and reach maturity. In these experiments, plants of a five-month-old age were utilized. Considering the significant time required for these assays and the inherent instability of RNA in environmental conditions, we undertook a dual approach, conducting detached leave assays and seedlings assays on *Q. ilex*.

3.1. Challenges in establishing effective *Phytophthora cinnamomi* infection in *Quercus ilex* seedlings for *in planta* assessment of dsRNAs

To more accurately replicate the natural conditions of infection, two experimental systems were tested for establishing *P. cinnamomi* infection in *Q. ilex*: (1) 5-month-old seedlings grown in substrate, and (2) 1-month-old seedlings cultivated in hydroponic systems.

In the first approach, 5-month-old *Q. ilex* seedlings grown on substrate in greenhouses were subjected to several inoculation aimed at mimicking natural soil-borne infection. These included: (A) placing mycelial plugs of *P. cinnamomi* within the substrate, to promote progressive colonization and root infection; (B) irrigating with a mycelial suspension, to simulate pathogen dissemination through contaminated water sources; and (C) saturating the substrate with inoculated water to recreate waterlogging conditions favorable to oomycete spread. Despite these efforts, infections were inconsistent and generally failed to produce reproducible disease symptoms (Figure 33A). As an alternative approach (D), a wound inoculation method involving stem cutting and direct application of *P. cinnamomi* mycelium was tested. This method has previously demonstrated efficacy in other woody hosts (Aloi *et al.*, 2021). However, this strategy also yielded variable outcomes, likely influenced by a combination of factors, including plant species, developmental stage, environmental conditions, and differences in pathogen virulence. Consequently, these inconsistencies hindered a proper evaluation of SIGS efficacy in greenhouse-grown holm oak seedlings.

To address these challenges, a second approach involved younger, 1-month-old *Q. ilex* seedlings grown under hydroponic conditions. *Q. ilex* seedlings were inoculated following a similar protocol to the one used in the *L. angustifolius* and *N. benthamiana* assays. This system allowed direct root-pathogen contact in a water-saturated environment, which aligns closely with the natural infection biology of *P. cinnamomi* (Sánchez-Cuesta *et al.*, 2021). Furthermore,

this method would enable the direct application of dsRNA treatments to the roots of plants, a technique that had proven effective in our preliminary trials in *L. angustifolius* and *N. benthamiana*. Although hydroponic methodology had been previously employed in inoculation trials of *P. cinnamomi* on *Quercus* plants (Garay *et al.*, 2023), this hydroponic system also failed to produce consistent infections in our experimental context. Some morphological differences were observed between inoculated and non-inoculated seedlings, such as reduced growth or fewer lateral roots, but these symptoms were mild and inconsistent (Figure 33B). Thus, infection levels were not reproducible or strong enough to support reliable SIGS efficacy assays in this system. This suggests that additional factors, such as inoculum concentration, exposure time, or plant physiological state, may influence the success of infection under hydroponic conditions. Further optimization of the inoculation protocol may be necessary to improve pathogen establishment and ensure reproducible results in future studies.

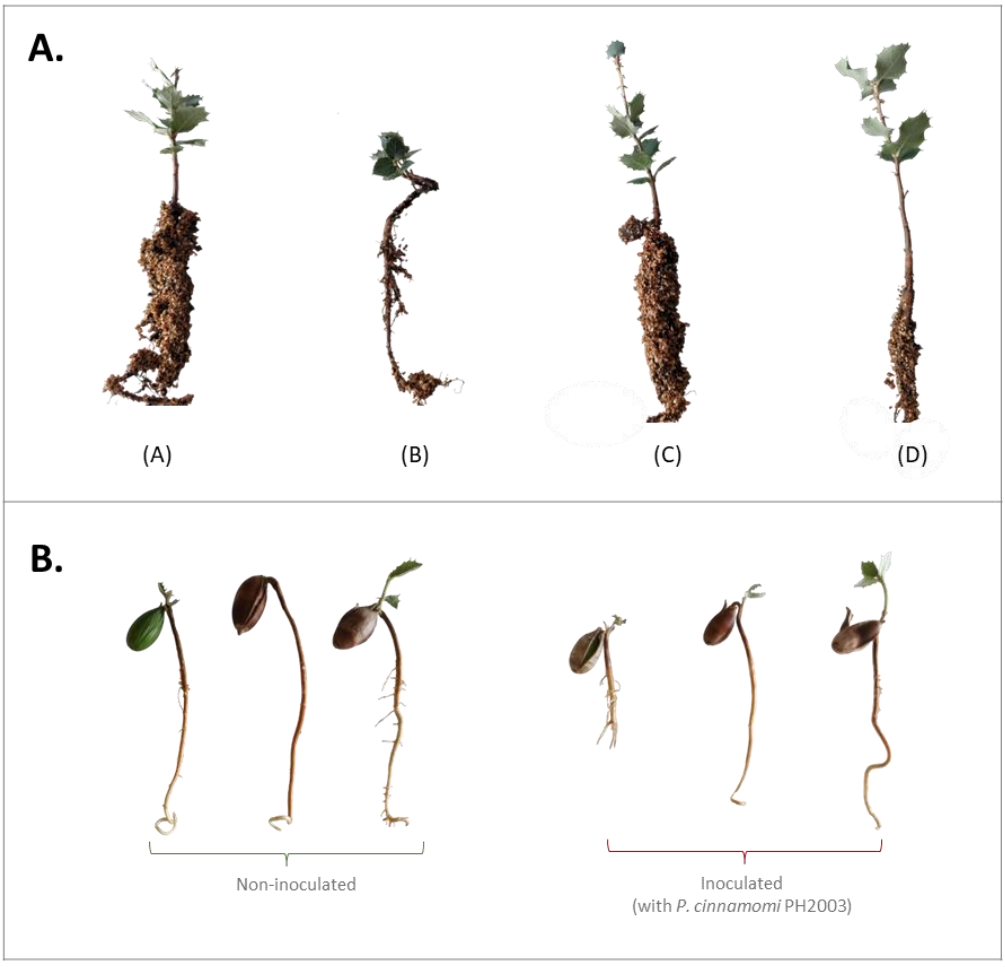

Figure 33. Evaluation of *P. cinnamomi* infection in *Q. ilex* using different inoculation approaches. A. Representative images of 5-month-old *Q. ilex* seedlings grown in substrate, subjected to various inoculation strategies, including (A) mycelial plug placement on the substrate, (B) irrigation with mycelial suspension, (C) substrate saturation, and (D) wound inoculation. None of the approaches consistently resulted in robust and reproducible infections under greenhouse conditions. **B.** Representative images of one-month-old *Q. ilex* seedlings grown hydroponically and inoculated with *P. cinnamomi*. While some morphological differences were observed between inoculated and non-inoculated seedlings, the infection levels were not sufficiently consistent or reproducible to support SIGS efficacy testing.

In conclusion, despite numerous attempts using various methodologies, a stable and consistent infection of *Q. ilex* seedlings with *P. cinnamomi* could not be achieved. The lack of reproducibility may be attributed to several factors. First, *P. cinnamomi* is a root pathogen and may require specific environmental conditions or host interactions to successfully infect and colonize its target. The artificial setups used in this study, such as hydroponics and vermiculite-based systems, may not have adequately replicated the natural conditions of soil-borne infections. Additionally, the physiological state of the seedlings and the type or quantity of inoculum may have influenced the pathogen's ability to establish infection. Zoospores, for example, require precise conditions for germination and host penetration, which may not have been met in the experimental setups. The lack of clear and reproducible infection symptoms limited our ability to evaluate the impact of the dsRNA treatments under controlled conditions. Without a stable pathogen presence, it was impossible to measure reductions in virulence or pathogen biomass that would indicate dsRNA efficacy. This highlights the importance of refining infection protocols and developing reliable systems for pathogen-host interactions in future studies. Altogether, these outcomes highlight the complexity of establishing reliable *P. cinnamomi* infections in *Q. ilex* and emphasize the need for further optimization of experimental conditions to enable robust testing of SIGS-based strategies in this challenging woody host.

3.2. Application of SIGS to detached *Quercus ilex* leaves reduced *Phytophthora cinnamomi* infection

In light of the challenges in establishing consistent and measurable *P. cinnamomi* infections in *Q. ilex* seedlings, a detached leaf assay was employed as an alternative approach to evaluate the efficacy of dsRNA treatments. Additionally, considering that *P. cinnamomi* primarily infects through the roots, and that dsRNAs applied via irrigation in substrate-grown plants are more susceptible to environmental degradation, it was likely that such factors could compromise any potential protective effects. The detached leaf approach provided a more controlled environment, enabling rapid and reliable evaluation of dsRNA treatments efficacy directly in host tissue.

In this experiment, dsRNA treatments were sprayed onto the abaxial side of young, detached *Q. ilex* leaves 24 h before inoculation, following the same pre-treatment strategy that proved effective in model plant assays. Non-inoculated, PH2003 and mock control were included in the assays. Disease progression was assessed by measuring the necrotic area and calculating relative necrosis in relation to total leaf area at 2, 3 and 4 dpi.

The most pronounced differences between treatments were observed at 3 dpi, as shown in the results presented below (Figure 34). The necrotic lesions observed and measured in PH2003 and mock control groups were found to be similar. Consequently, no significant differences were detected between these two treatments (*p*-value = 0.66). Meanwhile, the necrotic lesions observed in the three treatments were smaller than those observed in PH2003 (Figure 34B, Table S11). Pathogen virulence was significantly impaired in leaves treated with PcPTP-dsRNA, which achieved a necrosis reduction of 37% at 3 dpi (*p*-value < 0.01) compared to PH2003. A significant reduction of 31% in pathogen virulence was also observed with the application of PcDDS-dsRNA treatment with respect to PH2003 (*p*-value < 0.01). While PcDCL-dsRNA treatment did not produce statistically significant reductions, an observable treatment effect was noted at 3 dpi, with reductions of 20%. These reductions approached the threshold for statistical significance (*p*-value < 0.10).

These findings align with the results obtained in model plants, where PcPTP-dsRNA molecule exhibited the most pronounced reduction in virulence. The application of the three designed molecules demonstrated potential for reducing infection and necrosis on the leaf surface, although the observed effect was not significant in all three cases. These results indicate that the designed molecules have an effect against *P. cinnamomi* on its main host, with differences among them.

To provide further confirmation of the reduction of *P. cinnamomi* virulence resulting from dsRNA application by SIGS in this assay, we conducted a biomass analysis of the pathogen using qPCR. This analysis was carried out using RNA extracted at 3 dpi from infected leaf samples that had been pre-treated with dsRNA. qPCR was conducted using *ef1α* as a reference for pathogen biomass and *gadph* as the housekeeping gene for *Q. ilex*.

The results of the relative quantification analysis are shown in Figure 34C (Table S12). All dsRNA treatments led to a significant reduction in the biomass of *P. cinnamomi* in *Q. ilex* detached leaves at 3 dpi, as inferred from the transcript levels of pathogen target genes. Plants treated with PcDCL-dsRNA and PcDDS-dsRNA showed the strongest reduction in pathogen biomass, with relative quantification (RQ) values of 0.098 (*p*-value = 0.004) and 0.128 (*p*-value = 0.003), respectively, compared to the PH2003-inoculated control (RQ = 1). These results indicate that in these samples, the expression of *ef1α* was approximately ten times lower than in the reference control, suggesting a substantial decrease in *P. cinnamomi* presence. PcPTP-dsRNA also resulted in a significant decrease in pathogen gene expression (RQ = 0.265; *p*-value = 0.018), although to a lesser extent than the other two treatments. These results indicate that the

application of dsRNA molecules designed in this study effectively reduced *P. cinnamomi* colonization in holm oak leaves. This aligns with earlier observations showing decreased necrotic lesions in all leaves treated with the dsRNAs designed in this study.

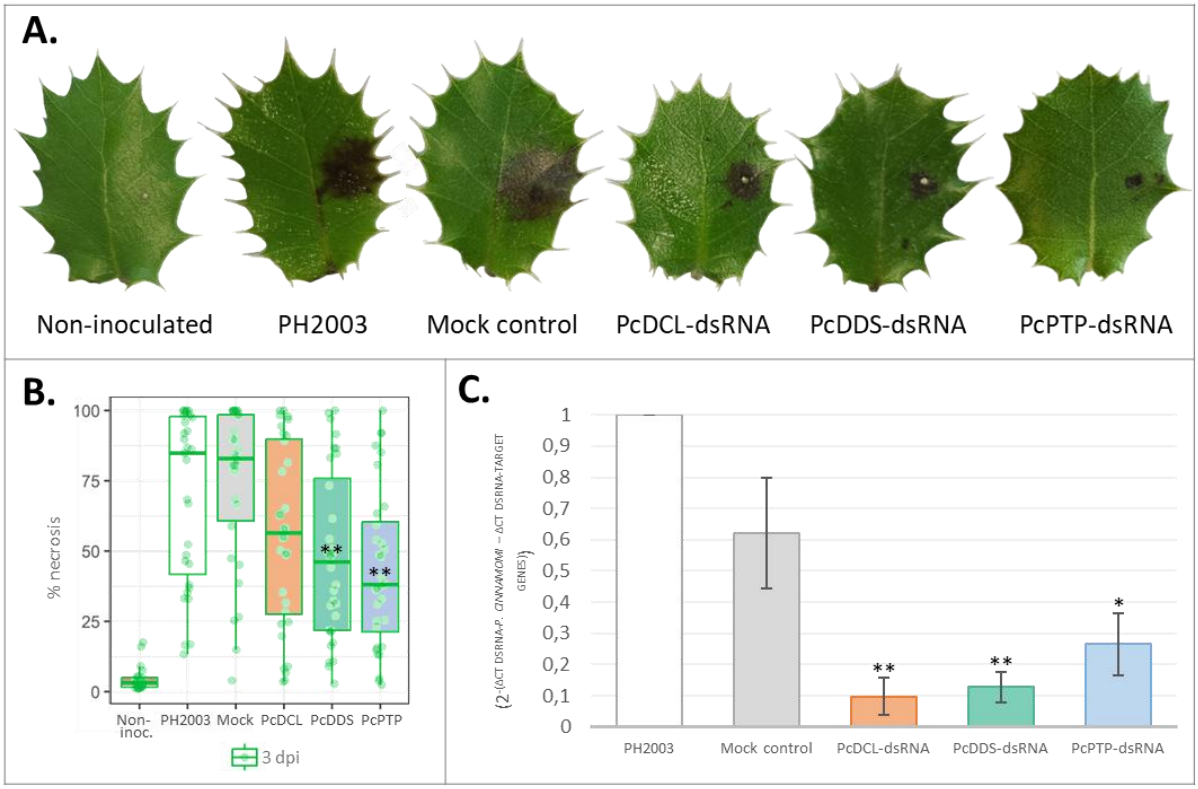

Figure 34. dsRNA treatments reduce *P. cinnamomi* biomass in *Q. ilex* leaves. A. Representative images of *Q. ilex* leaves at 3 dpi show the visual impact of dsRNA treatments on lesion size following *P. cinnamomi* infection. Leaves treated with dsRNAs exhibited smaller necrotic areas compared to PH2003 and mock control, indicating a potential protective effect. **B.** Quantification of leaf necrosis. Boxplot representation of percentage of necrotic leaf area at 3 dpi across different treatments. Significant reductions in necrosis were observed in leaves treated with PcPTP-dsRNA and PcDDS-dsRNA compared to the PH2003 control. Each dot represents a biological replicate. Statistical analysis was performed using Kruskal-Wallis and Wilcoxon rank-sum tests with Holm's correction (**: *p*-value < 0.01). **C.** Reduction of *P. cinnamomi* biomass in *Q. ilex* leaves following dsRNA treatment. Bar graph represents the relative pathogen biomass in each treatment as determined by RT-qPCR. Error bars represent exponentially transformed standard error between biological replicates. All dsRNA treatments significantly reduced biomass compared to PH2003 control, with PcDCL-dsRNA and PcDDS-dsRNA having the strongest effect, and PcPTP-dsRNA showing moderate reduction. Statistical analysis was performed using Kruskal-Wallis and Wilcoxon rank-sum tests with Holm's correction (*: *p*-value < 0.05, **: *p*-value < 0.01).

Although PcPTP-dsRNA showed the most pronounced reduction in leaf necrosis at 3 dpi, indicating a strong phenotypic protection effect, PcDCL-dsRNA and PcDDS-dsRNA were the most effective in reducing *P. cinnamomi* biomass, as revealed by qPCR quantification of *ef1α* transcripts. This divergence between visual symptom assessment and molecular detection suggests that different dsRNA molecules may influence distinct aspects of the infection process. One possible explanation is that PcDCL-dsRNA and PcDDS-dsRNA may effectively suppress early pathogen colonization or biomass accumulation without completely preventing the onset of visible symptoms. Conversely, PcPTP-dsRNA may delay or limit the symptoms more

effectively, possibly by interfering with host–pathogen interaction pathways that modulate defense responses or cell death, rather than drastically reducing pathogen biomass. These findings underscore the importance of using multiple, complementary analysis when evaluating dsRNA efficacy. They also highlight that symptom suppression does not always correlate directly with reduced pathogen biomass. Further investigations into the specific mode of action of each dsRNA, including time-course expression analyses and target gene silencing efficiency, would help clarify these differences.

The results from these trials demonstrated a potential effect of the dsRNA treatments designed against *P. cinnamomi* in reducing its virulence in the primary host, *Q. ilex*. However, SIGS implementation against this pathogen faces several challenges, notably its limited ability for direct dsRNA uptake. It has been observed that dsRNA-mediated SIGS occur in *P. cinnamomi*; however, it has yet to be demonstrated whether this gene silencing is the result pathogen dsRNA processing through direct uptake or plant dsRNA processing trough indirect uptake. Further analysis, including sRNA sequencing from the dsRNA-sprayed leaves, could prove whether the plant RNA silencing machinery is processing the sprayed dsRNAs (Çalışır *et al.*, 2022). Additionally, immunoprecipitation-based sequencing approaches, which use antibodies targeting key RNAi proteins to pull down associated small RNAs, could confirm whether exogenous dsRNAs are loaded into silencing complexes.

Detached leaf assays provided a practical and controlled framework for testing SIGS efficacy, even though they are not ideal given the root-infecting nature of *P. cinnamomi*. Nevertheless, they serve as a valuable tool for preliminary evaluation of treatment effectiveness under standardized conditions in the host. Similar assays have been conducted for SIGS evaluation in other *Phytophthora* spp. (Kalyandurg *et al.,* 2021). The consistent reduction in both necrosis and pathogen biomass across treated samples supports the biological activity of the designed dsRNAs. These results suggest that SIGS can trigger a protective response in *Q. ilex*. However, for SIGS to be a viable strategy against root-infecting pathogens, it is essential to overcome key challenges, including the translocation of dsRNA from aerial parts to roots and the limited uptake efficiency by the pathogen.

Future research should focus on enhancing systemic movement of dsRNA, potentially through the use of adjuvants that facilitate apoplastic or symplastic transport, or by employing targeted nanoparticle-based delivery systems. Additionally, optimizing dsRNA formulations to improve uptake efficiency remains a priority. Some nanocarriers have shown to improve cellular uptake and systemic movement of dsRNA inside the plant, leading to enhanced protection. One

promising option for use against *P. cinnamomi* could be CDs, which have already demonstrated improved cellular uptake in other *Phytophthora* species (Wang *et al.*, 2023b). Additionally, LDH nanoparticles and AVs could also be valuable alternatives, as studies have shown they can significantly increase the protective effect of SIGS, in some cases even doubling disease suppression (Niño-Sánchez *et al.,* 2022; Qiao *et al.,* 2023).

Alternative delivery strategies, such as soil application of dsRNA, should also be explored. However, this approach poses challenges, notably the rapid degradation of naked RNA in the soil, which can significantly reduce its efficacy (Bachman *et al.*, 2020). Encapsulation technologies offer a promising solution by protecting dsRNA from degradation, thereby enhancing its stability and prolonging its protective effect (Mosquera *et al.*, 2025).

Addressing these limitations will be critical for advancing the use of SIGS against *P. cinnamomi* and similar soil-borne pathogens. These efforts will help refine the use of SIGS for managing tree diseases and extend its applicability as a sustainable, environmentally friendly plant protection strategy.

General discussion, contribution to knowledge and future directions

About the design and production of dsRNA

Our initial hypotheses and experimental approach were based on the assumption that silencing efficiency can be enhanced through the careful and optimized design of dsRNA molecules, considering molecular characteristics that influence the functionality of the RNAi machinery. This work presents a thoroughly optimized process for selecting target genes and designing dsRNA molecules, taking into account multiple factors known to affect silencing efficiency. The dsRNA molecules developed and produced in this study were designed to target multiple genes, specifically between three and four each, within an essential metabolic pathway for the pathogen. While previous studies have successfully silenced multiple genes with a single dsRNA molecule, these have typically involved paralogous genes (Haile *et al.,* 2021; Koch *et al.,* 2019; Wang et al., 2016). In contrast, our approach targeted up to four distinct genes at different points within the same metabolic pathway, a strategy that, to our knowledge, has only been previously attempted by Qiao *et al.* (2021), who targeted three different genes simultaneously within a pathway using a single dsRNA molecule. This innovative approach increases the likelihood of disrupting a pathway and strengthens the silencing effect, contributing to more robust disease control outcomes. Furthermore, the dsRNA molecules designed in this study ranged in size from approximately 500 to 800 base pairs. The use of molecules up to 800 bp that targeted up to four genes was shown to be effective against target pathogens and yielded promising results. Although it would have been possible to include more target genes, this would have significantly increased the overall length of the molecules. The decision to limit the size to no more than 800 bp was based on previous findings by Degnan *et al.* (2022) and Höfle *et al.* (2020), which reported a decline in silencing efficiency with excessively long dsRNA constructs. This balance between the number of targets and molecule length aimed to optimize both efficacy and stability. Furthermore, this study represents the first time that target mRNA accessibility has

been considered in the design of dsRNA molecules. By analyzing and selecting regions of the mRNA that are more likely to be exposed and accessible to RISC, the likelihood of effective gene silencing was enhanced. Consequently, the comprehensive design and production optimization carried out in this study has contributed to enhancing silencing efficiency, making this strategy more viable and sustainable in forest disease management.

The metabolic pathways selected for dsRNA design in this study were essential for pathogen development, with a focus on cell wall biogenesis, signal transduction, vesicle trafficking, and the RNAi machinery. The target genes were chosen based on previous literature, aiming to disrupt key biological functions in the pathogens (Cheng *et al.,* 2015; Fahlgren *et al.,* 2013; Qiao *et al.,* 2021; Yu *et al.,* 2014). While this literature-guided strategy proved effective, future efforts to identify optimal gene targets could benefit from experimental approaches that exploit the concept of cross-kingdom RNAi, which involves the movement of miRNAs from the host plant into the pathogen to silence essential genes (Wang *et al.,* 2016; Weiberg *et al.,* 2013). This would provide information on which genes are naturally silenced. By studying highly tolerant plant–pathogen interactions, it may be possible to identify endogenous miRNAs that are naturally translocated into the pathogen and contribute to host resistance. Functional validation of such miRNAs would involve deleting or silencing them in the host plant and observing whether susceptibility to the pathogen increases, providing evidence of their protective function. Once identified, bioinformatic analyses and advanced sequencing technologies, such as degradome sequencing, could be used to determine their targets within the pathogen transcriptome. These experiments are currently underway in our laboratory and could help discover naturally effective targets, improve specificity of dsRNA molecules and reduce the likelihood of off-target effects, further improving the accuracy and efficacy of SIGS-based control methods by mimicking or enhancing natural defense mechanisms.

SIGS against the fungal pathogen *Fusarium circinatum*

In this study, we established a proof of concept for the use of SIGS in the pine-*F. circinatum* pathosystem. Utilizing confocal microscopy, the present study has provided novel insights into the cellular uptake of dsRNA by *F. circinatum*, which is essential for achieving high silencing efficiency (Qiao *et al.,* 2021). The application of dsRNAs by SIGS in pines led to a substantial reduction in PPC symptoms, ranging from approximately 29% to 42% depending on the treatment. These are highly encouraging results, especially considering the aggressive nature of this vascular and canker pathogenic fungus and the limited availability of effective disease management options for PPC disease. The observed levels of disease suppression demonstrate

the strong protective potential of the dsRNA molecules developed in this study. It is also worth noting that the protective effect of the dsRNA treatments significantly diminished between 25 and 35 dpi. This decline suggests that SIGS strategy is, for now, primarily preventive, offering protection during the early stages of infection rather than acting as a long-term curative measure. This could be due to one of the main limitations of SIGS approach: the instability and easy degradation of naked dsRNA under ambient conditions (Bachman *et al.*, 2020). Numerous studies applying naked dsRNA report a small protection window post spray (5–10 days, usually one week), with the efficacy of dsRNA decreasing over time (Koch *et al.*, 2016; Mitter *et al.*, 2017; Qiao *et al.*, 2021; Song *et al.*, 2018b; Wang *et al.*, 2016). Thus, this observation was consistent with most studies on SIGS, which report primarily preventive effects (Niu *et al.,* 2021). However, Degnan *et al.* (2023) stands out as the only study to date that has successfully demonstrated a curative effect of the disease using periodic SIGS treatments.

Thus, the temporary nature of the protective effect observed with SIGS in this study highlights the need for strategies such as repeated applications or improved formulations to prolong protection against forest pathogens. In this way, as a vascular pathogen, the timing and method of dsRNA application are critical to achieving disease suppression. Future studies of SIGS against *F. circinatum* should consider two key intervention points: during seed germination in nurseries and in mature forest stands. For nurseries, seed coating with dsRNA molecules could provide a practical and effective preventive strategy, protecting seedlings at their most vulnerable stage. For established forest stands, however, a potential application alternative to prolong the protective effect could be the delivery of dsRNAs via trunk injection (Wise *et al.,* 2022). This approach would represent a major leap from small-scale laboratory or greenhouse bioassays to field-scale applications in forest trees.

Importantly, SIGS application method should be adapted to several factors to success, such as the biology of the pathogen and infection strategy, the developmental stage of the host plant, and the phase of the infection. Therefore, future research should focus on understanding dsRNA translocation dynamics within the plant, evaluating host uptake and processing mechanisms, and determining how factors like tree phenology, plant age, and environmental conditions influence dsRNA persistence and silencing efficacy. Tailoring the SIGS approach to these variables will be essential for its successful use in forest ecosystems.

SIGS against the pathogenic oomycete *Phytophthora cinnamomi*

Our working hypothesis assumed that *P. cinnamomi* would be capable of taking up dsRNA either directly or indirectly. However, our experimental results revealed limited evidence

of direct dsRNA uptake in *P. cinnamomi, which* could limit the effectiveness of the technology. This is consistent with previous observations in other *Phytophthora* species (Cheng *et al.,* 2022; Qiao *et al.,* 2021). This disparity in uptake ability can be attributed to structural differences in cell walls of oomycetes and fungi (Whisson *et al.,* 2005), as well as other potential biological or physiological factors. Regardless of the underlying cause, future efforts should focus on assessing uptake under varying conditions (temperature, pH, dsRNA length…) to better understand these limitations. Despite the lack of confirmed direct uptake, the observed reduction in disease symptoms in both plants and detached-leaf assays strongly suggests that *P. cinnamomi* is capable of taking up and processing dsRNA indirectly via the host plant. To provide experimental evidence for this assumption, future studies should include uptake assays on plant material as well as studies of dsRNA movement within the plant.

The application of SIGS treatments in model plants and detached leaves of *Q. ilex* demonstrated a measurable reduction in the symptoms caused by *P. cinnamomi*. Specifically, the results showed a clear decrease in necrotic lesions and pathogen biomass in treated *Q. ilex* leaves, with necrosis reduced by up to 37% compared to controls, offering valuable insight into the protective potential of SIGS in the host. Although *P. cinnamomi* is a pathogen of significant concern in both agricultural and forest ecosystems, there is a notable lack of studies exploring the use of SIGS for its control. This work therefore represents one of the first applications of this technology against *P. cinnamomi* in a woody host, setting a foundation for future improvements *in planta* assays and point toward the feasibility of deploying SIGS in forest trees against oomycete pathogens.

An important area for improvement in our experiments lies in having more thoroughly accounted for the biology of *P. cinnamomi*, which presents a root-based infection strategy. This characteristic poses a significant challenge for SIGS, which has shown greater efficacy when applied via foliar sprays, due to easier delivery and uptake through leaves (Yan *et al.,* 2020). In contrast, root-targeted delivery is hindered by the rapid degradation of dsRNA in the soil (Bachman *et al.*, 2020) and the limited uptake ability of *P. cinnamomi* showed in this study. Although this was taken into account in the design of hydroponics trials, further research is needed to determine the applicability of SIGS to soil-borne pathogens when ideal treatment conditions cannot be achieved. Furthermore, the use of adjuvants to enhance dsRNA penetration and stability could have improved treatments efficiency in this work, as demonstrated in other studies using organosilicon surfactants, which improve foliar uptake and prolong dsRNA persistence (Bennet *et al.,* 2020; Degnan *et al.,* 2022). Another main limitation of this study was the difficulty in establishing a reliable and reproducible assay methodology for

evaluating dsRNA treatments in *Q. ilex* seedlings. This inconsistency impeded a comprehensive evaluation of SIGS efficacy in living plants of the primary hosts, and not only in detached leaves. Developing a standardized and sensitive infection model for *Q. ilex* remains essential to fully validate dsRNA-based approaches in this species and will be a key focus for future work.

These considerations open up valuable avenues for research, including the exploration of nanoparticle-based formulations with a threefold objective: protecting the dsRNA from environmental degradation, improving cellular uptake facilitating its delivery to the target pathogen and systemic movement inside the plant, and ensuring treatment optimal release (Mosquera *et al.,* 2025). Several nanocarrier formulations have shown some promising results, notably LDH nanocarriers (Niño-Sánchez *et al.,* 2022) and AVs (Qiao *et al.,* 2023), which even double the protection times in other plant pathogens. Thus, future efforts should focus on enhancing *P. cinnamomi* uptake efficiency and optimizing treatment delivery methods through exploring encapsulation technologies, and improving infection models *in Q. ilex*. Addressing these limitations will be essential for translating the promising outcomes of SIGS into robust, field-applicable strategies for managing soil-borne pathogens in forest ecosystems.

SIGS in forestry

This study represents the first attempt to explore the potential of SIGS as a control strategy against forest pathogens, a field where its application remains largely unexplored compared to agricultural crops. This work lays the groundwork for future research on forest pathogens by highlighting both the challenges associated with applying SIGS in complex pathosystems and the practical insights gained throughout the study. It identifies effective strategies as well as those that proved less successful, offering valuable lessons for refining SIGS approaches in subsequent studies. The findings demonstrate that SIGS can provide protective effects against two biologically distinct forest pathogens, highlighting its versatility. The specificity and rapid adaptability of SIGS strategy to new targets make it a particularly promising solution in an era marked by the rapid emergence of phytopathological threats. Continued research and investment in the development and optimization of SIGS could offer innovative and sustainable solutions to safeguard the health and resilience of forest ecosystems under growing environmental pressures. Ultimately, this thesis contributes to the development of innovative and sustainable disease control methods in forestry, paving the way for more targeted and efficient use of RNA-based technologies in the protection of forest ecosystems.

Conclusions

This thesis successfully advances the application of SIGS as a disease control strategy for forest pathogens by achieving the objectives outlined in this thesis. We can conclude that:

I. The efficiency of SIGS was enhanced through careful optimization of dsRNA design and production. Target genes essential for survival and virulence were selected in *F. circinatum* and *P. cinnamomi*, with a strategic focus on key biological pathways such as cell wall biosynthesis, signal transduction, RNA interference machinery, and vesicle trafficking. The dsRNA molecules were meticulously designed to maximize silencing efficacy while minimizing off-target effects. Furthermore, a cost-effective and scalable method for dsRNA synthesis was established, ensuring sufficient yield and quality for subsequent applications in experimental assays.

II. SIGS technology was successfully applied to the forest pathogenic fungus *F. circinatum*. Through initial screening in plant material and subsequent assays in the natural host *P. radiata*, the results demonstrated that dsRNA treatments could reduce disease progression and fungal biomass. These treatments showed strong preventive potential, delaying symptom development significantly. The outcomes validate the efficacy of SIGS against this important fungal pathogen and provide a foundation for future optimization in conifer hosts.

III. SIGS was evaluated as a tool to control the forest oomycete *P. cinnamomi*. The experiments highlighted both the promise and the challenges of applying SIGS to oomycete pathogens. Although *P. cinnamomi* showed limited direct uptake of dsRNA, indirect uptake through the host plant appears to enable gene silencing, leading to measurable reductions in disease symptoms and pathogen biomass in model plants. Detached leaf assays in *Quercus ilex* further confirmed the effectiveness of dsRNA molecules in the host. However, challenges encountered in these experiments underscore the need for further refinement of delivery strategies, particularly those targeting root tissues.

IV. Overall, the findings of this thesis demonstrate that SIGS is a viable and adaptable strategy for forest systems, offering a promising path forward for sustainable disease management in the face of increasing pathogenic threats.

Bibliography

Abubakar, Y.S., Sadiq, I.Z., Aarti, A., Wang, Z. & Zheng, W. (2023) Interplay of transport vesicles during plant-fungal pathogen interaction. *Stress biology*, 3, 35. https://doi.org/10.1007/s44154-023-00114-0.

Ahmar, S., Ballesta, P., Ali, M. & Mora-Poblete, F. (2021) Achievements and Challenges of Genomics-Assisted Breeding in Forest Trees: From Marker-Assisted Selection to Genome Editing. *International Journal of Molecular Sciences*, 22, 10583. https://doi.org/10.3390/ijms221910583.

Allardyce, J.A., Rookes, J.E. & Cahill, D.M. (2012) Defining Plant Resistance to Phytophthora cinnamomi: A Standardized Approach to Assessment. *Journal of Phytopathology*, 160, 269–276. https://doi.org/10.1111/j.1439-0434.2012.01895.x.

Aloi, F., Zamora-Ballesteros, C., Martín-García, J., Diez, J.J. & Cacciola, S.O. (2021) Co-Infections by Fusarium circinatum and Phytophthora spp. on Pinus radiata: Complex Phenotypic and Molecular Interactions. *Plants 2021, Vol. 10, Page 1976*, 10, 1976. https://doi.org/10.3390/PLANTS10101976.

Awan, H.U.M. & Asiegbu, F.O. (2021) Interspecific interactions within fungal communities associated with wood decay and forest trees. Forest Microbiology. Elsevier, pp. 75–108.

Axtell, M.J. (2013) Classification and Comparison of Small RNAs from Plants. *Annual Review of Plant Biology*, 64, 137–139.

Bachman, P., Fischer, J., Song, Z., Urbanczyk-Wochniak, E. & Watson, G. (2020) Environmental Fate and Dissipation of Applied dsRNA in Soil, Aquatic Systems, and Plants. *Frontiers in Plant Science*, 11, 508351. https://doi.org/10.3389/FPLS.2020.00021/BIBTEX.

Bartoszewski, R. & Sikorski, A.F. (2019) Editorial focus: understanding off-target effects as the key to successful RNAi therapy. *Cellular & Molecular Biology Letters*, 24, 69. https://doi.org/10.1186/s11658-019-0196-3.

Baum, J.A., Bogaert, T., Clinton, W., Heck, G.R., Feldmann, P., Ilagan, O., *et al.* (2007) Control of coleopteran insect pests through RNA interference. *Nature Biotechnology*, 25, 1322–1326. https://doi.org/10.1038/nbt1359.

Bel, L.M. Del & Brill, J.A. (2018) Sac1, a lipid phosphatase at the interface of vesicular and nonvesicular transport. *Traffic*, 19, 301–318. https://doi.org/10.1111/TRA.12554.

Belisle, R.J., McKee, B., Hao, W., Crowley, M., Arpaia, M.L., Miles, T.D., *et al.* (2019) Phenotypic Characterization of Genetically Distinct Phytophthora cinnamomi Isolates from Avocado. *Phytopathology*, 109, 384–394. https://doi.org/10.1094/PHYTO-09-17-0326-R.

Bennett, M., Deikman, J., Hendrix, B. & Iandolino, A. (2020) Barriers to Efficient Foliar Uptake of dsRNA and Molecular Barriers to dsRNA Activity in Plant Cells. *Frontiers in Plant Science*, 11. https://doi.org/10.3389/fpls.2020.00816.

Bernhart, S.H., Mückstein, U. & Hofacker, I.L. (2011) RNA Accessibility in cubic time. *Algorithms for Molecular Biology*, 6, 1–7. https://doi.org/10.1186/1748-7188-6-3/FIGURES/4.

Biedenkopf, D., Will, T., Knauer, T., Jelonek, L., Furch, A.C.U., Busche, T., *et al.* (2020) Systemic spreading of exogenous applied rna biopesticides in the crop plant hordeum vulgare. *ExRNA*, 2, 1–10. https://doi.org/10.1186/S41544-020-00052-3/FIGURES/7.

Biraghi, A. (1946) Il cancro del castagno causato da Endothia parasitica. *Ital. Agric.*, 7, 1–9.

Bocos-Asenjo, I.T., Amin, H., Mosquera, S., Díez-Hermano, S., Ginésy, M., Diez, J.J., *et al.* (2024) Spray-induced gene silencing (SIGS) as a tool for the management of Pine Pitch Canker forest disease. *Plant disease*. https://doi.org/10.1101/2024.03.05.583474.

Bocos-Asenjo, I.T., Niño-Sánchez, J., Ginésy, M. & Diez, J.J. (2022) New Insights on the Integrated Management of Plant Diseases by RNA Strategies: Mycoviruses and RNA Interference. *International Journal of Molecular Sciences*, 23, 9236. https://doi.org/10.3390/IJMS23169236.

Bohula, E.A., Salisbury, A.J., Sohail, M., Playford, M.P., Riedemann, J., Southern, E.M., *et al.* (2003a) The efficacy of small interfering RNAs targeted to the type 1 insulin-like growth factor receptor (IGF1R) is influenced by secondary structure in the IGF1R transcript. *The Journal of biological chemistry*, 278, 15991–15997. https://doi.org/10.1074/JBC.M300714200.

Bollmann, S.R., Fang, Y., Press, C.M., Tyler, B.M. & Grünwald, N.J. (2016) Diverse Evolutionary Trajectories for Small RNA Biogenesis Genes in the Oomycete Genus Phytophthora. *Frontiers in Plant Science*, 7, 284. https://doi.org/10.3389/FPLS.2016.00284.

Bonello, P. (2010) *Potential of Induced Resistance as a Tool for the Management of Pathogens and Insects in Trees-an Ecological Viewpoint †*.

Bonifacino, J.S. & Hierro, A. (2011) Transport according to GARP: Receiving retrograde cargo at the trans-Golgi network. *Trends in Cell Biology*, 21, 159–167. https://doi.org/10.1016/j.tcb.2010.11.003.

Borg, R., Farrugia Wismayer, M., Bonavia, K., Farrugia Wismayer, A., Vella, M., Joke, J.F., *et al.* (2021) Genetic analysis of ALS cases in the isolated island population of Malta. *European Journal of Human Genetics*, 29, 604–614. https://doi.org/10.1038/s41431-020-00767-9.

Borg, R., Herrera, P., Purkiss, A., Cacciottolo, R. & Cauchi, R.J. (2023) Reduced levels of ALS gene DCTN1 induce motor defects in Drosophila. *Frontiers in Neuroscience*, 17, 1–10. https://doi.org/10.3389/fnins.2023.1164251.

Bowman, S.M. & Free, S.J. (2006) The structure and synthesis of the fungal cell wall. *BioEssays*, 28, 799–808. https://doi.org/10.1002/BIES.20441.

Boyd, I.L., Freer-Smith, P.H., Gilligan, C.A. & Godfray, H.C.J. (2013) The consequence of tree pests and diseases for ecosystem services. *Science*, 342.

Bramlett, M., Plaetinck, G. & Maienfisch, P. (2020) RNA-Based Biocontrols—A New Paradigm in Crop Protection. *Engineering*, 6, 522–527. https://doi.org/10.1016/j.eng.2019.09.008.

Brasier, C.M. (1979) Dual origin of recent Dutch elm disease outbreaks in Europe. *Nature*, 281, 78–80.

Brasier, C.M. & Webber, J.F. (2019) Is there evidence for post-epidemic attenuation in the Dutch elm disease pathogen Ophiostoma novo-ulmi? *Plant Pathology*, 68, 921–929. https://doi.org/10.1111/ppa.13022.

Burley, S.K. (1996) The TATA box binding protein. *Current Opinion in Structural Biology*, 6, 69–75.

Cai, Q., He, B., Kogel, K.H. & Jin, H. (2018a) Cross-kingdom RNA trafficking and environmental RNAi — nature's blueprint for modern crop protection strategies. *Current Opinion in Microbiology*, 46, 58–64. https://doi.org/10.1016/J.MIB.2018.02.003.

Cai, Q., Qiao, L., Wang, M., He, B., Lin, F.M., Palmquist, J., *et al.* (2018b) Plants send small RNAs in extracellular vesicles to fungal pathogen to silence virulence genes. *Science*, 360, 1126–1129. https://doi.org/10.1126/SCIENCE.AAR4142.

Çalışır, K., Krczal, G. & Uslu, V.V. (2022) Small RNA-seq dataset of wild type and 16C Nicotiana benthamiana leaves sprayed with naked dsRNA using the high-pressure spraying technique. *Data in Brief*, 45, 108706. https://doi.org/10.1016/j.dib.2022.108706.

Camarero, J.J. & Gazol, A. (2022) Climate change and forest health: Detecting dieback hotspots. Forest Microbiology: Volume 2: Forest Tree Health. Elsevier, pp. 99–106.

Caruthers, J.M. & McKay, D.B. (2002) Helicase structure and mechanism. *Current Opinion in Structural Biology*, 12, 123–133. https://doi.org/10.1016/S0959-440X(02)00298-1.

Caseys, C., Muhich, A.J., Vega, J., Ahmed, M., Hopper, A., Kelly, D., *et al.* (2024) Leaf abaxial and adaxial surfaces differentially affect plant-fungal pathogen interactions. *bioRxiv*. https://doi.org/10.1101/2024.02.13.579726.

Catalanotto, C., Pallotta, M., ReFalo, P., Sachs, M.S., Vayssie, L., Macino, G., *et al.* (2004) Redundancy of the Two Dicer Genes in Transgene-Induced Posttranscriptional Gene Silencing in Neurospora crassa. *Molecular and Cellular Biology*, 24, 2536–2545. https://doi.org/10.1128/MCB.24.6.2536-2545.2004.

Chang, S.-S., Zhang, Z. & Liu, Y. (2012) RNA Interference Pathways in Fungi: Mechanisms and Functions. *Annual Review of Microbiology*, 66, 305–323. https://doi.org/10.1146/annurev-micro-092611-150138.

Chee, K. & Newhook, F.J. (1965) Improved methods for use in studies on Phytophtohora cinnamomi Rands and other Phytophthora species. *New Zealand Journal of Agricultural Research*, 8, 88–95. https://doi.org/10.1080/00288233.1965.10420024.

Chen, D.H. & Ronald, P.C. (1999) A Rapid DNA Minipreparation Method Suitable for AFLP and Other PCR Applications. *Plant Molecular Biology Reporter*, 17, 53–57. https://doi.org/10.1023/A:1007585532036.

Chen, W., Kastner, C., Nowara, D., Oliveira-Garcia, E., Rutten, T., Zhao, Y., *et al.* (2016) Host-induced silencing of Fusarium culmorum genes protects wheat from infection. *Journal of Experimental Botany*, 67, 4979–4991. https://doi.org/10.1093/JXB/ERW263.

Chen, Y., Gao, Q., Huang, M., Liu, Y., Liu, Z., Liu, X., *et al.* (2015) Characterization of RNA silencing components in the plant pathogenic fungus Fusarium graminearum. *Scientific Reports*, 5, 12500. https://doi.org/10.1038/srep12500.

Cheng, W., Lin, M., Chu, M., Xiang, G., Guo, J., Jiang, Y., *et al.* (2022) RNAi-Based Gene Silencing of RXLR Effectors Protects Plants Against the Oomycete Pathogen Phytophthora capsici. *Molecular Plant-Microbe Interactions*, 35, 444–449. https://doi.org/10.1094/MPMI-12-21-0295-R.

Cheng, W., Song, X.S., Li, H.P., Cao, L.H., Sun, K., Qiu, X.L., *et al.* (2015) Host-induced gene silencing of an essential chitin synthase gene confers durable resistance to Fusarium head blight and seedling blight in wheat. *Plant Biotechnology Journal*, 13, 1335–1345. https://doi.org/10.1111/PBI.12352.

Choi, G.H. & Nuss, D.L. (1992) Hypovirulence of Chestnut Blight Fungus Conferred by an Infectious Viral cDNA. *Science*, 257, 800–803. https://doi.org/10.1126/science.1496400.

Christiaens, O., Whyard, S., Vélez, A.M. & Smagghe, G. (2020) Double-Stranded RNA Technology to Control Insect Pests: Current Status and Challenges. *Frontiers in Plant Science*, 11.

Ciechanowska, K., Pokornowska, M. & Kurzyńska-Kokorniak, A. (2021) Genetic insight into the domain structure and functions of dicer-type ribonucleases. *International Journal of Molecular Sciences*, 22, 1–18.

Cogoni, C. & Macino, G. (1999) Gene silencing in Neurospora crassa requires a protein homologous to RNA-dependent RNA polymerase. *Nature 1999 399:6732*, 399, 166–169. https://doi.org/10.1038/20215.

Cogoni, C. & Macino, G. (2000) Post-transcriptional gene silencing across kingdoms. *Current Opinion in Genetics & Development*, 10, 638–643. https://doi.org/10.1016/S0959-437X(00)00134-9.

Collar, U. (1995) Informe de la reunión del grupo de trabajo de laboratorios de diagnóstico y prospecciones fitosanitarias. Almería.

Conibear, E., Cleck, J.N. & Stevens, T.H. (2003) Vps51p Mediates the Association of the GARP (Vps52/ 53/54) Complex with the Late Golgi t-SNARE Tlg1p. *Molecular Biology of the Cell*, 14, 1610–1623. https://doi.org/10.1091/mbc.E02-10.

Corcobado, T., Solla, A., Madeira, M.A. & Moreno, G. (2013) Combined effects of soil properties and Phytophthora cinnamomi infections on Quercus ilex decline. *Plant and Soil*, 373, 403–413. https://doi.org/10.1007/s11104-013-1804-z.

Correll, J.C., Gordon, T.R., McCain, A.H., Fox, J.W., Koehler, C.S., Wood, D.L., *et al.* (1991) Pitch Canker Disease in California: Pathogenicity, Distribution, and Canker Development on Monterey Pine (Pinus radiata). *Plant Disease*, 75, 676. https://doi.org/10.1094/PD-75-0676.

Cortes Generales. Informe de la Ponencia de Estudio sobre la protección del ecosistema de la dehesa (543/000009). BOCG del Senado. 2010.

Crone, M, Mccomb, J.A., O'brien, P.A., & Hardy, G.E.S.J. (2013a) Assessment of Australian native annual/herbaceous perennial plant species as asymptomatic or symptomatic hosts of Phytophthora cinnamomi under controlled conditions. *Forest Pathology*, 43, 245–251. https://doi.org/10.1111/efp.12027.

Crone, M, McComb, J.A., O'Brien, P.A. & Hardy, G.E.S.J. (2013b) Survival of Phytophthora cinnamomi as oospores, Stromata, And thick-walled chlamydospores in roots of symptomatic and asymptomatic annual and herbaceous perennial plant species. *Fungal Biology*, 117, 112–123. https://doi.org/10.1016/j.funbio.2012.12.004.

Das, P.R. & Sherif, S.M. (2020) Application of Exogenous dsRNAs-induced RNAi in Agriculture: Challenges and Triumphs. *Frontiers in Plant Science*, 11, 542801. https://doi.org/10.3389/FPLS.2020.00946/BIBTEX.

Dasgupta, S., Fernandez, L., Kameyama, L., Inada, T., Nakamura, Y., Pappas, A., *et al.* (1998) Genetic uncoupling of the dsRNA-binding and RNA cleavage activities of the Escherichia coli endoribonuclease RNase III — the effect of dsRNA binding on gene expression. *Molecular Microbiology*, 28, 629–640. https://doi.org/10.1046/J.1365-2958.1998.00828.X.

Deacon, S.W., Serpinskaya, A.S., Vaughan, P.S., Lopez Fanarraga, M., Vernos, I., Vaughan, K.T., *et al.* (2003) Dynactin is required for bidirectional organelle transport. *Journal of Cell Biology*, 160, 297–301. https://doi.org/10.1083/JCB.200210066.

Degnan, R.M., McTaggart, A.R., Shuey, L.S., Jane Pame, L.S., Smith, G.R., Gardiner, D.M., *et al.* (2022) Exogenous double-stranded RNA inhibits the infection physiology of rust fungi to reduce symptoms in planta. *Mol Plant Pathol*, 24, 191–207. https://doi.org/10.1111/mpp.13286.

Degnan, R.M., Shuey, L.S., Radford-Smith, J., Gardiner, D.M., Carroll, B.J., Mitter, N., *et al.* (2023) Double-stranded RNA prevents and cures infection by rust fungi. *Communications Biology*, 6, 1234. https://doi.org/10.1038/s42003-023-05618-z.

Delgado-Martín, J., Delgado-olidén, A. & Velasco, L. (2022) Carbon Dots Boost dsRNA Delivery in Plants and Increase Local and Systemic siRNA Production. *International Journal of Molecular Sciences*, 23. https://doi.org/10.3390/ijms23105338.

Delgado-Martín, J. & Velasco, L. (2021) An efficient dsRNA constitutive expression system in Escherichia coli. *Applied Microbiology and Biotechnology*, 105, 6381–6393. https://doi.org/10.1007/S00253-021-11494-6.

Der, C., Courty, P.E., Recorbet, G., Wipf, D., Simon-Plas, F. & Gerbeau-Pissot, P. (2024) Sterols, pleiotropic players in plant–microbe interactions. *Trends in Plant Science*, 29, 524–534. https://doi.org/10.1016/J.TPLANTS.2024.03.002.

Drenkhan, R., Ganley, B., Martín-García, J., Vahalík, P., Adamson, K., Adamčíková, K., *et al.* (2020) Global Geographic Distribution and Host Range of Fusarium circinatum, the Causal Agent of Pine Pitch Canker. *Forests*, 11, 724. https://doi.org/10.3390/f11070724.

Dunker, F., Trutzenberg, A., Rothenpieler, J.S., Kuhn, S., Pröls, R., Schreiber, T., *et al.* (2020) Oomycete small RNAs bind to the plant RNA-induced silencing complex for virulence. *eLife*, 9. https://doi.org/10.7554/eLife.56096.

Durán, A., Gryzenhout, M., Slippers, B., Ahumada, R., Rotella, A., Flores, F., *et al.* (2008) Phytophthora pinifolia sp. nov. associated with a serious needle disease of Pinus radiata in Chile. *Plant Pathology*, 57, 715–727. https://doi.org/10.1111/j.1365-3059.2008.01893.x.

Eggers, J., Juzwik, J., Bernick, S. & Mordaunt, L. (2005) Evaluation of propiconazole operational treatments of oaks for oak wilt control. *Res. Note NC-390 USDA Forest Service*

Elbashir, S.M., Harborth, J., Lendeckel, W., Yalcin, A., Weber, K. & Tuschl, T. (2001) Duplexes of 21-nucleotide RNAs mediate RNA interference in cultured mammalian cells. *Nature*, 411, 494–498. https://doi.org/10.1038/35078107.

Elliott, K.J. & Swank, W.T. (2008) Long-term changes in forest composition and diversity following early logging (1919-1923) and the decline of American chestnut (Castanea dentata). *Plant Ecology*, 197, 155–172. https://doi.org/10.1007/s11258-007-9352-3.

EPPO (2019). EPPO Reporting Service – No. 08 – 2019. EPPO, Num. article: 2019/169. https://gd.eppo.int/reporting/article-6599 (*Accessed on Jul 10, 2025*).

EPPO (2025a) EPPO A2 List. https://www.eppo.int/ACTIVITIES/plant_quarantine/A2_list *(Accessed on Feb 25, 2025)*.

EPPO (2025b) Fusarium circinatum. EPPO datasheets on pests recommended for regulation. Available online. https://gd.eppo.int (*Accessed on Jul 10, 2025*).

Eschen-Lippold, L., Landgraf, R., Smolka, U., Schulze, S., Heilmann, M., Heilmann, I., *et al.* (2012) Activation of defense against Phytophthora infestans in potato by down-regulation of syntaxin gene expression. *New Phytologist*, 193, 985–996. https://doi.org/10.1111/j.1469-8137.2011.04024.x.

Fahlgren, N., Bollmann, S.R., Kasschau, K.D., Cuperus, J.T. & Press, C.M. (2013) Phytophthora Have Distinct Endogenous Small RNA Populations That Include Short Interfering and microRNAs. *PLoS ONE*, 8, 77181. https://doi.org/10.1371/journal.pone.0077181.

FAO (2020). Global Forest Resources Assessment 2020 – Key findings. Rome. https://doi.org/10.4060/ca8753en

FAO (2024). The State of the World's Forests 2024 – Forest-sector innovations towards a more sustainable future. Rome. https://doi.org/10.4060/cd1211en

Fernandes, C., Gow, N.A.R. & Gonçalves, T. (2016) The importance of subclasses of chitin synthase enzymes with myosin-like domains for the fitness of fungi. *Fungal Biology Reviews*, 30, 1–14. https://doi.org/10.1016/J.FBR.2016.03.002.

Fernandes, P., Colavolpe, M.B., Serrazina, S. & Costa, R.L. (2022) European and American chestnuts: An overview of the main threats and control efforts. *Frontiers in Plant Science*, 13. https://doi.org/10.3389/fpls.2022.951844.

Ferreira, P., Chahed, A., Estevinho, L.M., Seixas, N., Costa, R. & Choupina, A. (2023) Post-Transcriptional Gene Silencing of Glucanase Inhibitor Protein in Phytophthora cinnamomi. *Plants*, 12, 3821. https://doi.org/10.3390/plants12223821.

Fire, A., Xu, S., Montgomery, M.K., Kostas, S.A., Driver, S.E. & Mello, C.C. (1998) Potent and specific genetic interference by double-stranded RNA in Caenorhabditis elegans. *Nature*, 391, 806–811. https://doi.org/10.1038/35888.

Fire, A.Z. & Mello, C.C. (2006) The Nobel Prize in Physiology or Medicine 2006. *Available online: http://www.nobelprize.org/nobel_prizes/medicine/laureates/2006/ (accessed on 18 April 2025)*.

Firon, A. & D'Enfert, C. (2002) Identifying essential genes in fungal pathogens of humans. *Trends in Microbiology*, 10, 456–462. https://doi.org/10.1016/S0966-842X(02)02442-3.

Fletcher, S.J., Bardossy, E.S., Tomé-Poderti, L., Moss, T., Mongelli, V., Frangeul, L., *et al.* (2025) Hsc70-4: An unanticipated mediator of dsRNA internalization in Drosophila. *Science Advances*, 11. https://doi.org/10.1126/sciadv.adv1286.

Forster, H. & Shuai, B. (2020) Exogenous siRNAs against chitin synthase gene suppress the growth of the pathogenic fungus Macrophomina phaseolina. *Mycologia*, 112, 699–710. https://doi.org/10.1080/00275514.2020.1753467.

Forzieri, G., Girardello, M., Ceccherini, G., Spinoni, J., Feyen, L., Hartmann, H., *et al.* (2021) Emergent vulnerability to climate-driven disturbances in European forests. *Nature Communications 2021*, 12, 1–12. https://doi.org/10.1038/s41467-021-21399-7.

Fu, C., Zhang, X., Veri, A.O., Iyer, K.R., Lash, E., Xue, A., *et al.* (2021) Leveraging machine learning essentiality predictions and chemogenomic interactions to identify antifungal targets. *Nature Communications 2021*, 12, 1–18. https://doi.org/10.1038/s41467-021-26850-3.

Gaffar, F.Y., Imani, J., Karlovsky, P., Koch, A. & Kogel, K.H. (2019) Different Components of the RNA Interference Machinery Are Required for Conidiation, Ascosporogenesis, Virulence, Deoxynivalenol Production, and Fungal Inhibition by Exogenous Double-Stranded RNA in the Head Blight Pathogen Fusarium graminearum. *Frontiers in Microbiology*, 10. https://doi.org/10.3389/fmicb.2019.01662.

Galli, M., Feldmann, F., Vogler, U.K. & Kogel, K.H. (2024) Can biocontrol be the game-changer in integrated pest management? A review of definitions, methods and strategies. *Journal of Plant Diseases and Protection*, 131, 265–291.

Garay, A.G., Manzanera, J.A., Campo, R. del & López, B.P. (2023) Evaluation of Bacillus amyloliquefaciens as a biocontrol agent against oak decline disease in Quercus trees. *Forest systems*, 32, 1–68.

Garbelotto, M. & Hayden, K.J. (2012) Sudden oak death: Interactions of the exotic oomycete Phytophthora ramorum with naïve North American hosts. *Eukaryotic Cell*, 11, 1313–1323.

Garbelotto, M., Schmidt, D.J. & Harnik, T.Y. (2007) Phosphite Injections and Bark Application of Phosphite + PentrabarkTM Control Sudden Oak Death in Coast Live Oak. *Arboriculture & Urban Forestry*, 33, 309–317. https://doi.org/10.48044/jauf.2007.035.

Garcia-Rubio, R., Oliveira, H.C. de, Rivera, J. & Trevijano-Contador, N. (2020) The Fungal Cell Wall: Candida, Cryptococcus, and Aspergillus Species. *Frontiers in Microbiology*, 10. https://doi.org/10.3389/fmicb.2019.02993.

Geoghegan, I., Steinberg, G. & Gurr, S. (2017) The Role of the Fungal Cell Wall in the Infection of Plants. *Trends in Microbiology*, 25, 957–967. https://doi.org/10.1016/J.TIM.2017.05.015.

Ghelardini, L., Santini, A. & Luchi, N. (2022) Globalization, invasive forest pathogen species, and forest tree health. Forest *Microbiology: Volume 2: Forest Tree Health*. Elsevier, pp. 61–76. https://doi.org/10.1016/B978-0-323-85042-1.00035-5.

Goded, S., Ekroos, J., Domínguez, J., Azcárate, J.G., Guitián, J.A. & Smith, H.G. (2019) Effects of eucalyptus plantations on avian and herb species richness and composition in North-West Spain. *Global Ecology and Conservation*, 19, e00690. https://doi.org/10.1016/J.GECCO.2019.E00690.

Gogoi, A., Sarmah, N., Kaldis, A., Perdikis, D. & Voloudakis, A. (2017) Plant insects and mites uptake double-stranded RNA upon its exogenous application on tomato leaves. *Planta*, 246, 1233–1241. https://doi.org/10.1007/s00425-017-2776-7.

Gómez, P. & Ortuño, S.F. (2022) La España rural: retos y oportunidades de futuro. *Mediterráneo económico*, 35, 123–141.

Gordon, T.R., Storer, A.J. & Wood, D.L. (2001) The Pitch Canker Epidemic in California. *Plant Disease*, 85, 1128–1139. https://doi.org/10.1094/PDIS.2001.85.11.1128.

Greslebin, A.G., Hansen, E.M. & Sutton, W. (2007) Phytophthora austrocedrae sp. nov., a new species associated with Austrocedrus chilensis mortality in Patagonia (Argentina). *Mycological Research*, 111, 308–316. https://doi.org/10.1016/j.mycres.2007.01.008.

Guégan, J.F., Thoisy, B. de, Gomez-Gallego, M. & Jactel, H. (2023) World forests, global change, and emerging pests and pathogens. *Current Opinion in Environmental Sustainability*, 61.

Haile, Z.M., Gebremichael, D.E., Capriotti, L., Molesini, B., Negrini, F., Collina, M., *et al.* (2021) Double-Stranded RNA Targeting Dicer-Like Genes Compromises the Pathogenicity of Plasmopara viticola on Grapevine. *Frontiers in Plant Science*, 12, 1–7. https://doi.org/10.3389/fpls.2021.667539.

Haller, S., Widmer, F., Siegfried, B.D., Zhuo, X. & Romeis, J. (2019) Responses of two ladybird beetle species (Coleoptera: Coccinellidae) to dietary RNAi. *Pest Management Science*, 75, 2652–2662. https://doi.org/10.1002/PS.5370.

Hamby, R., Wang, M., Qiao, L. & Jin, H. (2020) Synthesizing fluorescently labeled dsRNAs and sRNAs to visualize fungal RNA uptake. *Methods in Molecular Biology*, 2166, 215–225. https://doi.org/10.1007/978-1-0716-0712-1_12/FIGURES/2.

Hammond, S.M., Bernstein, E., Beach, D. & Hannon, G.J. (2000) An RNA-directed nuclease mediates post-transcriptional gene silencing in Drosophila cells. *Nature*, 404, 293–296. https://doi.org/10.1038/35005107.

Hardham, A.R. (2006) Cell biology of plant-oomycete interactions. *Cellular Microbiology*, 9, 31–39. https://doi.org/10.1111/J.1462-5822.2006.00833.X.

He, B., Cai, Q., Qiao, L., Huang, C.-Y., Wang, S., Miao, W., *et al.* (2021) RNA-binding proteins contribute to small RNA loading in plant extracellular vesicles. *Nature Plants*, 7, 342–352. https://doi.org/10.1038/s41477-021-00863-8.

He, B., Wang, H., Liu, G., Chen, A., Calvo, A., Cai, Q., *et al.* (2023) Fungal small RNAs ride in extracellular vesicles to enter plant cells through clathrin-mediated endocytosis. *Nature Communications 2023 14:1*, 14, 1–15. https://doi.org/10.1038/s41467-023-40093-4.

He, H., Xu, T., Cao, F., Xu, Y., Dai, T. & Liu, T. (2024) PcAvh87, a virulence essential RxLR effector of Phytophthora cinnamomi suppresses host defense and induces cell death in plant nucleus. *Microbiological Research*, 286, 127789. https://doi.org/10.1016/j.micres.2024.127789.

Hepting, G.H. & Roth, E.R. (1946) Pitch canker, a new disease of some Southern Pines. *Journal of Forestry*, 44, 742–744.

Hernandez-Escribano, L., Iturritxa, E., Elvira-Recuenco, M., Berbegal, M., Campos, J.A., Renobales, G., *et al.* (2018) Herbaceous plants in the understory of a pitch canker-affected Pinus radiata plantation are endophytically infected with Fusarium circinatum. *Fungal Ecology*, 32, 65–71. https://doi.org/10.1016/j.funeco.2017.12.001.

Hernandez-Escribano, L., Visser, E.A., Iturritxa, E., Raposo, R. & Naidoo, S. (2020) The transcriptome of Pinus pinaster under Fusarium circinatum challenge. *BMC Genomics*, 21, 28. https://doi.org/10.1186/s12864-019-6444-0.

Höck, J. & Meister, G. (2008) The Argonaute protein family. *Genome Biology*, 9, 210. https://doi.org/10.1186/GB-2008-9-2-210.

Höfle, L., Biedenkopf, D., Werner, B., Jelonek, L. & Koch, A. (2020) Study on the efficiency of dsRNAs with increasing length in RNA-based silencing of the Fusarium CYP51 genes. https://doi.org/10.1080/15476286.2019.1700033.

Hou, Y., Zhai, Y., Feng, L., Karimi, H.Z., Rutter, B.D., Zeng, L., *et al.* (2019) A Phytophthora Effector Suppresses Trans-Kingdom RNAi to Promote Disease Susceptibility. *Cell Host & Microbe*, 25, 153-165.e5. https://doi.org/10.1016/j.chom.2018.11.007.

Hu, D., Chen, Z.Y., Zhang, C. & Ganiger, M. (2020) Reduction of Phakopsora pachyrhizi infection on soybean through host- and spray-induced gene silencing. *Molecular Plant Pathology*, 21, 794–807. https://doi.org/10.1111/MPP.12931.

Huang, G., Allen, R., Davis, E.L., Baum, T.J. & Hussey, R.S. (2006) Engineering broad root-knot resistance in transgenic plants by RNAi silencing of a conserved and essential root-knot nematode parasitism gene. *Proceedings of the National Academy of Sciences*, 103, 14302–14306. https://doi.org/10.1073/pnas.0604698103.

Idnurm, A. & Howlett, B.J. (2001) Pathogenicity genes of phytopathogenic fungi. *Molecular Plant Pathology*, 2, 241–255. https://doi.org/10.1046/J.1464-6722.2001.00070.X.

Iwakawa, H. & Tomari, Y. (2022) Life of RISC: Formation, action, and degradation of RNA-induced silencing complex. *Molecular Cell*, 82, 30–43. https://doi.org/10.1016/j.molcel.2021.11.026.

Jain, R.G., Fletcher, S.J., Manzie, N., Robinson, K.E., Li, P., Lu, E., *et al.* (2022) Foliar application of clay-delivered RNA interference for whitefly control. *Nature Plants*, 8, 535–548. https://doi.org/10.1038/s41477-022-01152-8.

Jassim, H.K., Foster, H.A. & Fairhurst, C.P. (1990) Biological control of Dutch elm disease: Larvicidal activity of Trichoderma harzianum, T. polysporum and Scytalidium lignicola in Scolytus scolytus and S. multistriatus reared in artificial culture. *Annals of Applied Biology*, 117, 187–196. https://doi.org/10.1111/j.1744-7348.1990.tb04206.x.

Ji, H., Mao, H., Li, S., Feng, T., Zhang, Z., Cheng, L., *et al.* (2021) Fol -milR1, a pathogenicity factor of Fusarium oxysporum, confers tomato wilt disease resistance by impairing host immune responses. *New Phytologist*, 232, 705–718. https://doi.org/10.1111/nph.17436.

Jiang, L., Ding, L., He, B., Shen, J., Xu, Z., Yin, M., *et al.* (2014) Systemic gene silencing in plants triggered by fluorescent nanoparticle-delivered double-stranded RNA. *Nanoscale*, 6, 9965–9969. https://doi.org/10.1039/C4NR03481C.

Jung, T. & Blaschke, M. (2004) Phytophthora root and collar rot of alders in Bavaria: distribution, modes of spread and possible management strategies. *Plant Pathology*, 53, 197–208. https://doi.org/10.1111/j.0032-0862.2004.00957.x.

Kalyandurg, P.B., Sundararajan, P., Dubey, M., Ghadamgahi, F., Zahid, M.A., Whisson, S.C., *et al.* (2021) Spray-Induced Gene Silencing as a Potential Tool to Control Potato Late Blight Disease. *Phytopathology*, 111, 2168–2175. https://doi.org/10.1094/PHYTO-02-21-0054-SC.

Kamoun, S., Furzer, O., Jones, J.D.G., Judelson, H.S., Ali, G.S., Dalio, R.J.D., *et al.* (2015) The Top 10 oomycete pathogens in molecular plant pathology. *Molecular Plant Pathology*, 16, 413–434. https://doi.org/10.1111/mpp.12190.

Karami, J., Kavosi, M.R., Babanezhad, M. & Kiapasha, K. (2018) Integrated management of the charcoal disease by silviculture, chemical and biological methods in forest parks. *Journal of Sustainable Forestry*, 37, 429–444. https://doi.org/10.1080/10549811.2017.1416642.

Kasanen, R., Awan, H.U.M., Zarsav, A., Sun, H. & Asiegbu, F.O. (2022) Forest tree disease control and management. *Forest Microbiology*. Elsevier, pp. 425–462.

Kharel, A. (2020) Role of elicitins of Phytophthora cinnamomi in interactions with Lupinus angustifolius. *(Doctoral dissertation, Deakin University)*.

Kharel, A., Ziemann, M., Rookes, J. & Cahill, D. (2025) Modulation of key sterol-related genes of Nicotiana benthamiana by phosphite treatment during infection with Phytophthora cinnamomi. *Functional Plant Biology*, 52. https://doi.org/10.1071/FP24251.

Kim, S., Lee, R., Jeon, H., Lee, N., Park, J., Moon, H., *et al.* (2023) Identification of Essential Genes for the Establishment of Spray-Induced Gene Silencing-Based Disease Control in Fusarium graminearum. *Cite This: J. Agric. Food Chem*, 71. https://doi.org/10.1021/acs.jafc.3c04557.

King, F.J., Yuen, E.L.H. & Bozkurt, T.O. (2024) Border Control: Manipulation of the Host-Pathogen Interface by Perihaustorial Oomycete Effectors. *Molecular Plant-microbe Interactions: MPMI*, 37, 220–226. https://doi.org/10.1094/MPMI-09-23-0122-FI.

Kirby, H.W. & Grand, L.F. (1975) Susceptibility of Pinus strobus and Lupinus spp. to Phytophthora cinnamomi. *Phytopathology*, 65, 693–695.

Koch, A., Biedenkopf, D., Furch, A., Weber, L., Rossbach, O., Abdellatef, E., *et al.* (2016) An RNAi-Based Control of Fusarium graminearum Infections Through Spraying of Long dsRNAs Involves a Plant Passage and Is Controlled by the Fungal Silencing Machinery. *PLOS Pathogens*, 12, e1005901. https://doi.org/10.1371/JOURNAL.PPAT.1005901.

Koch, A., Höfle, L., Werner, B.T., Imani, J., Schmidt, A., Jelonek, L., *et al.* (2019) SIGS vs HIGS: a study on the efficacy of two dsRNA delivery strategies to silence Fusarium FgCYP51 genes in infected host and non-host plants. *Molecular Plant Pathology*, 20, 1636–1644. https://doi.org/10.1111/MPP.12866.

Koch, A. & Wassenegger, M. (2021) Host-induced gene silencing – mechanisms and applications. *New Phytologist*, 231, 54–59. https://doi.org/10.1111/nph.17364.

Koch, J.L. (2010) Beech Bark Disease: The Oldest "New" Threat to American Beech in the United States. *Outlooks on Pest Management*, 21, 64–68. https://doi.org/10.1564/21apr03.

Konakalla, N.C., Kaldis, A., Berbati, M., Masarapu, H. & Voloudakis, A.E. (2016) Exogenous application of double-stranded RNA molecules from TMV p126 and CP genes confers resistance against TMV in tobacco. *Planta*, 244, 961–969. https://doi.org/10.1007/s00425-016-2567-6.

Kretschmer-Kazemi Far, R. & Sczakiel, G. (2003) The activity of siRNA in mammalian cells is related to structural target accessibility: a comparison with antisense oligonucleotides. *Nucleic acids research*, 31, 4417–4424. https://doi.org/10.1093/NAR/GKG649.

Kück, U. (2022) Special Issue "Signal Transductions in Fungi." *Journal of Fungi 2022, Vol. 8, Page 528*, 8, 528. https://doi.org/10.3390/JOF8050528.

Kwak, P.B. & Tomari, Y. (2012) The N domain of Argonaute drives duplex unwinding during RISC assembly. *Nature Structural & Molecular Biology 2012 19:2*, 19, 145–151. https://doi.org/10.1038/nsmb.2232.

Latgé, J.P. (2007) The cell wall: a carbohydrate armour for the fungal cell. *Molecular microbiology*, 66, 279–290. https://doi.org/10.1111/J.1365-2958.2007.05872.X.

Lau, P.W., Guiley, K.Z., De, N., Potter, C.S., Carragher, B. & MacRae, I.J. (2012) The Molecular Architecture of Human Dicer. *Nature structural & molecular biology*, 19, 436. https://doi.org/10.1038/NSMB.2268.

Li, H., Guan, R., Guo, H. & Miao, X. (2015) New insights into an RNAi approach for plant defence against piercing-sucking and stem-borer insect pests. *Plant, cell & environment*, 38, 2277–2285. https://doi.org/10.1111/PCE.12546.

Li, M., Hieno, A., Motohashi, K., Suga, H. & Kageyama, K. (2021) Pythium intermedium, a species complex consisting of three phylogenetic species found in cool-temperate forest ecosystems. *Fungal Biology*, 125, 1017–1025. https://doi.org/10.1016/j.funbio.2021.07.004.

Liang, Y.T., Luo, H., Lin, Y. & Gao, F. (2024) Recent advances in the characterization of essential genes and development of a database of essential genes. *iMeta*, 3, e157. https://doi.org/10.1002/IMT2.157.

Lierop, P. van, Lindquist, E., Sathyapala, S. & Franceschini, G. (2015) Global forest area disturbance from fire, insect pests, diseases and severe weather events. *Forest Ecology and Management*, 352, 78–88. https://doi.org/10.1016/J.FORECO.2015.06.010.

Lingel, A., Simon, B., Izaurralde, E. & Sattler, M. (2003) Structure and nucleic-acid binding of the Drosophila Argonaute 2 PAZ domain. *Nature 2003 426:6965*, 426, 465–469. https://doi.org/10.1038/nature02123.

Liu, J., Carmell, M.A., Rivas, F. V., Marsden, C.G., Thomson, J.M., Song, J.-J., *et al.* (2004) Argonaute2 Is the Catalytic Engine of Mammalian RNAi. *Science*, 305, 1437–1441. https://doi.org/10.1126/science.1102513.

Liu, J., Chang, W., Pan, L., Liu, X., Su, L., Zhang, W., *et al.* (2018) An Improved Method of Preparing High Efficiency Transformation Escherichia coli with Both Plasmids and Larger DNA Fragments. *Indian Journal of Microbiology*, 58, 448–456. https://doi.org/10.1007/S12088-018-0743-Z/FIGURES/3.

Liu, Q., Feng, Y. & Zhu, Z. (2009) Dicer-like (DCL) proteins in plants. *Functional and Integrative Genomics*, 9, 277–286. https://doi.org/10.1007/S10142-009-0111-5/FIGURES/6.

Liu, S., Wu, B., Lv, S., Shen, Z., Li, R., Yi, G., *et al.* (2019) Genetic Diversity in FUB Genes of Fusarium oxysporum f. sp. cubense Suggests Horizontal Gene Transfer. *Front. Plant Sci*, 10, 1069. https://doi.org/10.3389/fpls.2019.01069.

Livak, K.J. & Schmittgen, T.D. (2001) Analysis of Relative Gene Expression Data Using Real-Time Quantitative PCR and the 2−ΔΔCT Method. *Methods*, 25, 402–408. https://doi.org/10.1006/METH.2001.1262.

Loo, J.A. (2009) Ecological impacts of non-indigenous invasive fungi as forest pathogens. *Biological Invasions*, 11, 81–96.

López-Berges, M.S., Rispail, N., Prados-Rosales, R.C. & Pietro, A. di (2010) A nitrogen response pathway regulates virulence functions in Fusarium oxysporum via the protein kinase TOR and the bZIP protein MeaB. *Plant Cell*, 22, 2459–2475. https://doi.org/10.1105/tpc.110.075937.

Lorenz, R., Wolfinger, M.T., Tanzer, A. & Hofacker, I.L. (2016) Predicting RNA secondary structures from sequence and probing data. *Methods*, 103, 86–98. https://doi.org/10.1016/J.YMETH.2016.04.004.

Lucas, J.A., Hawkins, N.J. & Fraaije, B.A. (2015) The Evolution of Fungicide Resistance. pp. 29–92.

Lück, S., Kreszies, T., Strickert, M., Schweizer, P., Kuhlmann, M. & Douchkov, D. (2019) siRNA-Finder (si-Fi) Software for RNAi-Target Design and Off-Target Prediction. *Frontiers in Plant Science*, 10, 1–12. https://doi.org/10.3389/fpls.2019.01023.

Luo, L., Hannemann, M., Koenig, S., Hegermann, J., Ailion, M., Cho, M.K., *et al.* (2011) The Caenorhabditis elegans GARP complex contains the conserved Vps51 subunit and is required to maintain lysosomal morphology. *Molecular Biology of the Cell*, 22, 2564. https://doi.org/10.1091/MBC.E10-06-0493.

Ma, J.B., Ye, K. & Patel, D.J. (2004) Structural basis for overhang-specific small interfering RNA recognition by the PAZ domain. *Nature 2004 429:6989*, 429, 318–322. https://doi.org/10.1038/nature02519.

Mann, C.W.G., Sawyer, A., Gardiner, D.M., Mitter, N., Carroll, B.J. & Eamens, A.L. (2023) RNA-Based Control of Fungal Pathogens in Plants. *International Journal of Molecular Sciences*, 24, 12391. https://doi.org/10.3390/ijms241512391.

Mao, Y.B., Cai, W.J., Wang, J.W., Hong, G.J., Tao, X.Y., Wang, L.J., *et al.* (2007) Silencing a cotton bollworm P450 monooxygenase gene by plant-mediated RNAi impairs larval tolerance of gossypol. *Nature Biotechnology*, 25, 1307–1313. https://doi.org/10.1038/nbt1352.

Martín, J.A., Sobrino-Plata, J., Rodríguez-Calcerrada, J., Collada, C. & Gil, L. (2019) Breeding and scientific advances in the fight against Dutch elm disease: Will they allow the use of elms in forest restoration? *New Forests*, 50, 183–215. https://doi.org/10.1007/s11056-018-9640-x.

Martín, J.A., Solla, A., Venturas, M., Collada, C., Domínguez, J., Miranda, E., *et al.* (2014) Seven ulmus minor clones tolerant to Ophiostoma novo-ulmi registered as forest reproductive material in Spain. *IForest*, 8, 172–180. https://doi.org/10.3832/ifor1224-008.

Martín-Rodrigues, N., Espinel, S., Sanchez-Zabala, J., Ortíz, A., González-Murua, C. & Duñabeitia, M.K. (2013) Spatial and temporal dynamics of the colonization of Pinus radiata by Fusarium circinatum, of conidiophora development in the pith and of traumatic resin duct formation. *New Phytologist*, 198, 1215–1227. https://doi.org/10.1111/nph.12222.

Martins, L., Castro, J., Macedo, W., Marques, C. & Abreu, C. (2007) Assessment of the spread of chestnut ink disease using remote sensing and geostatistical methods. *European Journal of Plant Pathology*, 119, 159–164. https://doi.org/10.1007/s10658-007-9155-3.

McKinley, D.C., Ryan, M.G., Birdsey, R.A., Giardina, C.P., Harmon, M.E., Heath, L.S., *et al.* (2011) A synthesis of current knowledge on forests and carbon storage in the United States. *Ecological Applications*, 21, 1902–1924. https://doi.org/10.1890/10-0697.1.

Mcloughlin, A.G., Wytinck, N., Walker, P.L., Girard, I.J., Rashid, K.Y., Kievit, T. De, *et al.* (2018) Identification and application of exogenous dsRNA confers plant protection against Sclerotinia sclerotiorum and Botrytis cinerea OPEN. *Scientific RepoRts* |, 8, 7320. https://doi.org/10.1038/s41598-018-25434-4.

McRae, A.G., Taneja, J., Yee, K., Shi, X., Haridas, S., LaButti, K., *et al.* (2023) Spray-induced gene silencing to identify powdery mildew gene targets and processes for powdery mildew control. https://doi.org/10.1111/mpp.13361.

Mello, C.C. & Conte, D. (2004) Revealing the world of RNA interference. *Nature*, 431, 338–342. https://doi.org/10.1038/nature02872.

Melnyk, C.W., Molnar, A. & Baulcombe, D.C. (2011) Intercellular and systemic movement of RNA silencing signals. *EMBO Journal*, 30, 3553–3563. https://doi.org/10.1038/EMBOJ.2011.274.

Mistry, J., Chuguransky, S., Williams, L., Qureshi, M., Salazar, G.A., Sonnhammer, E.L.L., *et al.* (2021) Pfam: The protein families database in 2021. *Nucleic Acids Research*, 49. https://doi.org/10.1093/nar/gkaa913.

Mittempergher, L. & Santini, A. (2004) The history of elm breeding. *Forest Systems*, 13, 161–177.

Mitter, N., Worrall, E.A., Robinson, K.E., Li, P., Jain, R.G., Taochy, C., *et al.* (2017) Clay nanosheets for topical delivery of RNAi for sustained protection against plant viruses. *Nature Plants 2017 3:2*, 3, 1–10. https://doi.org/10.1038/nplants.2016.207.

Morales-Rodríguez, C., Vannini, A., Scanu, B., González-Moreno, P., Turco, S., Drais, M.I., *et al.* (2025) Challenges to Mediterranean Fagaceae ecosystems affected by Phytophthora cinnamomi and Climate Change: Integrated Pest Management perspectives. *Current Forestry Reports*, 11. https://doi.org/10.1007/s40725-024-00237-1.

Mora-Sala, B., León, M., Pérez-Sierra, A. & Abad-Campos, P. (2022) New Reports of Phytophthora Species in Plant Nurseries in Spain. *Pathogens*, 11. https://doi.org/10.3390/pathogens11080826.

Mosquera, S., Ginésy, M., Bocos-Asenjo, I.T., Amin, H., Diez-Hermano, S., Diez, J.J., *et al.* (2025) Spray-induced gene silencing to control plant pathogenic fungi: A step-by-step guide. *Journal of Integrative Plant Biology*.

Mukherjee, S., Beligala, G., Feng, C. & Marzano, S.Y.L. (2024) Double-stranded RNA targeting white mold Sclerotinia sclerotiorum argonaute 2 for disease control via spray-induced gene silencing. *https://doi.org/10.1094/PHYTO-11-23-0431-R*. https://doi.org/10.1094/PHYTO-11-23-0431-R.

Mumbanza, F.M., Kiggundu, A., Tusiime, G., Tushemereirwe, W.K., Niblett, C. & Bailey, A. (2013) In vitro antifungal activity of synthetic dsRNA molecules against two pathogens of banana, Fusarium oxysporum f. sp. cubense and Mycosphaerella fijiensis. *Pest management science*, 69, 1155–1162. https://doi.org/10.1002/ps.3480.

Muzika, R.M. (2017) Opportunities for silviculture in management and restoration of forests affected by invasive species. *Biological Invasions*, 19, 3419–3435. https://doi.org/10.1007/s10530-017-1549-3.

Nakayashiki, H., Kadotani, N. & Mayama, S. (2006) Evolution and Diversification of RNA Silencing Proteins in Fungi. *Journal of Molecular Evolution*, 63, 127–135. https://doi.org/10.1007/s00239-005-0257-2.

Napoli, C., Lemieux, C. & Jorgensen, R. (1990) Introduction of a Chimeric Chalcone Synthase Gene into Petunia Results in Reversible Co-Suppression of Homologous Genes in trans. *The Plant Cell*, 2, 279. https://doi.org/10.2307/3869076.

Nerva, L., Sandrini, M., Gambino, G. & Chitarra, W. (2020) Double-Stranded RNAs (dsRNAs) as a Sustainable Tool against Gray Mold (Botrytis cinerea) in Grapevine: Effectiveness of Different Application Methods in an Open-Air Environment. *Biomolecules*, 10, 200. https://doi.org/10.3390/biom10020200.

Niño-Sánchez, J., Chen, L.-H., Souza, J.T. De, Mosquera, S. & Stergiopoulos, I. (2021) Targeted Delivery of Gene Silencing in Fungi Using Genetically Engineered Bacteria. *J. Fungi*, 7. https://doi.org/10.3390/jof7020125.

Niño-Sánchez, J., Sambasivam, P.T., Sawyer, A., Hamby, R., Chen, A., Czislowski, E., *et al.* (2022) BioClay™ prolongs RNA interference-mediated crop protection against Botrytis cinerea. *Journal of Integrative Plant Biology*, 64, 2187–2198. https://doi.org/10.1111/JIPB.13353/SUPPINFO.

Niu, D., Hamby, R., Sanchez, J.N., Cai, Q., Yan, Q. & Jin, H. (2021) RNAs — a new frontier in crop protection. *Current Opinion in Biotechnology*, 70, 204–212. https://doi.org/10.1016/J.COPBIO.2021.06.005.

Nowara, D., Gay, A., Lacomme, C., Shaw, J., Ridout, C., Douchkov, D., *et al.* (2010) HIGS: Host-Induced Gene Silencing in the Obligate Biotrophic Fungal Pathogen Blumeria graminis. *The Plant Cell*, 22, 3130–3141. https://doi.org/10.1105/tpc.110.077040.

Nowicki, M., Foolad, M.R., Nowakowska, M. & Kozik, E.U. (2012) Potato and Tomato Late Blight Caused by Phytophthora infestans: An Overview of Pathology and Resistance Breeding. *Plant disease*, 96, 4–17. https://doi.org/10.1094/PDIS-05-11-0458.

Obbard, D.J., Gordon, K.H.J., Buck, A.H. & Jiggins, F.M. (2009) The evolution of RNAi as a defence against viruses and transposable elements. *Philosophical Transactions of the Royal Society B: Biological Sciences*, 364, 99–115. https://doi.org/10.1098/rstb.2008.0168.

Okorski, A., Pszczółkowska, A., Oszako, T. & Nowakowska, J.A. (2015) Current possibilities and prospects of using fungicides in forestry. *Forest Research Papers*, 76, 191–206. https://doi.org/10.1515/frp-2015-0019.

Oliveira-Garcia, E. & Deising, H.B. (2013) Infection Structure–Specific Expression of β-1,3-Glucan Synthase Is Essential for Pathogenicity of Colletotrichum graminicola and Evasion of β-Glucan–Triggered Immunity in Maize. *The Plant Cell*, 25, 2356–2378. https://doi.org/10.1105/TPC.112.103499.

Olivoto, T. (2022) Lights, camera, pliman! An R package for plant image analysis. *Methods in Ecology and Evolution*, 13, 789–798. https://doi.org/10.1111/2041-210X.13803.

Ouyang, S.Q., Ji, H.M., Feng, T., Luo, S.J., Cheng, L. & Wang, N. (2023) Artificial trans-kingdom RNAi of FolRDR1 is a potential strategy to control tomato wilt disease. *PLOS Pathogens*, 19, e1011463. https://doi.org/10.1371/JOURNAL.PPAT.1011463.

Pant, P. & Kaur, J. (2023) Spray-Induced Gene Silencing of SsOah1 and SsCyp51 confers protection to Nicotiana benthamiana and Brassica juncea against Sclerotinia sclerotiorum. *Physiological and Molecular Plant Pathology*, 127, 102109. https://doi.org/10.1016/J.PMPP.2023.102109.

Pardo-Medina, J., Dahlmann, T.A., Nowrousian, M., Limón, M.C. & Avalos, J. (2024) The RNAi Machinery in the Fungus Fusarium fujikuroi Is Not Very Active in Synthetic Medium and Is Related to Transposable Elements. *Non-Coding RNA*, 10, 31. https://doi.org/10.3390/ncrna10030031.

Park, M., Kweon, Y., Eom, J., Oh, M. & Shin, C. (2023a) Development of multi-target dsRNAs targeting PcNLP gene family to suppress Phytophthora capsici infection in Nicotiana benthamiana. *Applied Biological Chemistry*, 66, 69. https://doi.org/10.1186/s13765-023-00828-9.

Park, M., Kweon, Y., Lee, D. & Shin, C. (2023b) Suppression of Phytophthora capsici using double-stranded RNAs targeting NLP effector genes in Nicotiana benthamiana. *Applied Biological Chemistry*, 66, 5. https://doi.org/10.1186/s13765-023-00768-4.

Parker, J.S. (2010) How to slice: snapshots of Argonaute in action. *Silence*, 1, 3. https://doi.org/10.1186/1758-907X-1-3.

Pascoal-Ferreira, P., Chahed, A., Costa, R., Branco, I. & Choupina, A. (2023) Use of iRNA in the post-transcriptional gene silencing of necrosis-inducing Phytophthora protein 1(NPP1) in Phytophthora cinnamomi. *Molecular Biology Reports*, 50, 6493–6504. https://doi.org/10.1007/s11033-023-08562-7.

Pautasso, M., Schlegel, M. & Holdenrieder, O. (2015) Forest Health in a Changing World. *Microbial ecology*, 69, 826–842. https://doi.org/10.1007/s00248-014-0545-8.

Pérez-Victoria, F.J., Schindler, C., Magadán, J.G., Mardones, G.A., Delevoye, C., Romao, M., *et al.* (2010) A Highlights from MBoC Selection: Ang2/Fat-Free Is a Conserved Subunit of the Golgi-associated Retrograde Protein Complex. *Molecular Biology of the Cell*, 21, 3386. https://doi.org/10.1091/MBC.E10-05-0392.

Piombo, E., Kelbessa, B.G., Sundararajan, P., Whisson, S.C., Vetukuri, R.R. & Dubey, M. (2023) RNA silencing proteins and small RNAs in oomycete plant pathogens and biocontrol agents. *Frontiers in Microbiology*, 14, 1–17. https://doi.org/10.3389/fmicb.2023.1076522.

Piombo, E., Vetukuri, R.R., Konakalla, N.C., Kalyandurg, P.B., Sundararajan, P., Jensen, D.F., *et al.* (2024) RNA silencing is a key regulatory mechanism in the biocontrol fungus Clonostachys rosea-wheat interactions. *BMC Biology*, 22, 219. https://doi.org/10.1186/s12915-024-02014-9.

Ploetz, R.C. & Schaffer, B. (1987) Effects of flooding and Phytophthora root rot on photosynthetic characteristics of avocado. Proc. *Fla. State Hort. Soc.* 100, 290–294

Postma, J. & Goossen-van de Geijn, H. (2016) Twenty-four years of Dutch Trig® application to control Dutch elm disease. *BioControl*, 61, 305–312. https://doi.org/10.1007/s10526-016-9731-6.

Pratt, J.E., Niemi, M. & Sierota, Z.H. (2000) Comparison of Three Products Based on Phlebiopsis gigantea for the Control of Heterobasidion annosum in Europe. *Biocontrol Science and Technology*, 10, 467–477. https://doi.org/10.1080/09583150050115052.

Qian, X., Hamid, F.M., Sahili, A. El, Darwis, D.A., Wong, Y.H., Bhushan, S., *et al.* (2016) Functional evolution in orthologous cell-encoded RNA-dependent RNA polymerases. *Journal of Biological Chemistry*, 291, 9295–9309. https://doi.org/10.1074/jbc.M115.685933.

Qiao, L., Lan, C., Capriotti, L., Ah-Fong, A., Niño-Sánchez, J., Hamby, R., *et al.* (2021) Spray-induced gene silencing for disease control is dependent on the efficiency of pathogen RNA uptake. *Plant Biotechnology Journal*, 19, 1756–1768. https://doi.org/10.1111/PBI.13589.

Qiao, L., Niño-Sánchez, J., Hamby, R., Capriotti, L., Chen, A., Mezzetti, B., *et al.* (2023) Artificial nanovesicles for dsRNA delivery in spray-induced gene silencing for crop protection. *Plant Biotechnology Journal*, 21, 854–865. https://doi.org/10.1111/PBI.14001.

Quilez-Molina, A.I., Niño-Sánchez, J. & Merino, D. (2024) The role of polymers in enabling RNAi-based technology for sustainable pest management. *Nature Communications*, 15, 9158. https://doi.org/10.1038/s41467-024-53468-y.

R Core Team. (2024) R: The R Project for Statistical Computing. *R Foundation for Statistical Computing, Vienna, Austria*. URL: https://www.R-project.org/

Ray, P., Sahu, D., Aminedi, R., & Chandran, D. (2022). Concepts and considerations for enhancing RNAi efficiency in phytopathogenic fungi for RNAi-based crop protection using nanocarrier-mediated dsRNA delivery systems. *Frontiers in fungal biology*, 3, 977502. https://doi.org/10.3389/ffunb.2022.977502.

RedPAC. (2020). El Ministerio de Agricultura, Pesca y Alimentación inicia un programa de mejora genética de la encina. https://redpac.es/noticia/el-ministerio-agricultura-pesca-y-alimentacion-inicia-un-programa-mejora-genetica-la-encina (*Accessed on Jul 10, 2025*).

Rabiey, M., Hailey, L.E., Roy, S.R., Grenz, K., Al-Zadjali, M.A.S., Barrett, G.A., *et al.* (2019) Endophytes vs tree pathogens and pests: can they be used as biological control agents to improve tree health? *European Journal of Plant Pathology*, 155, 711–729. https://doi.org/10.1007/s10658-019-01814-y.

Rammuki, B.M. (2024) Molecular characterisation of RNA interference in Fusarium circinatum. *Doctoral dissertation, University of Pretoria*.

Ramsfield, T.D., Bentz, B.J., Faccoli, M., Jactel, H. & Brockerhoff, E.G. (2016) Forest health in a changing world: effects of globalization and climate change on forest insect and pathogen impacts. *Forestry*, 89, 245–252. https://doi.org/10.1093/forestry/cpw018.

Redondo, M.Á., Pérez-Sierra, A., Abad-Campos, P., Torres, L., Solla, A., Reig-Armiñana, J., *et al.* (2015) Histology of Quercus ilex roots during infection by Phytophthora cinnamomi. *Trees*, 29, 1943–1957. https://doi.org/10.1007/s00468-015-1275-3.

Reeser, P. (2013) Phytophthora pluvialis, a new species from mixed tanoak-Douglas-fir forests of western Oregon, U.S.A. *North American Fungi*, 1–8. https://doi.org/10.2509/naf2013.008.007.

Reggiori, F., Wang, C.W., Stromhaug, P.E., Shintani, T. & Klionsky, D.J. (2003) Vps51 is part of the yeast Vps fifty-three tethering complex essential for retrograde traffic from the early endosome and Cvt vesicle completion. *The Journal of biological chemistry*, 278, 5009–5020. https://doi.org/10.1074/JBC.M210436200.

Robin, C., Piou, D., Feau, N., Douzon, G., Schenck, N. & Hansen, E.M. (2011) Root and aerial infections of Chamaecyparis lawsoniana by Phytophthora lateralis: a new threat for European countries. *Forest Pathology*, 41, 417–424. https://doi.org/10.1111/j.1439-0329.2010.00688.x.

Rodrigues, M.L. (2018) The multifunctional fungal ergosterol. *mBio*, 9. https://doi.org/10.1128/MBIO.01755-18/ASSET/8D6513B2-F099-46A0-8E03-2070037BC0E7/ASSETS/GRAPHIC/MBO0041840720001.JPEG.

Rodrigues, M.L., Godinho, R.M.C., Zamith-Miranda, D. & Nimrichter, L. (2015) Traveling into Outer Space: Unanswered Questions about Fungal Extracellular Vesicles. *PLOS Pathogens*, 11, e1005240. https://doi.org/10.1371/JOURNAL.PPAT.1005240.

Rodríguez-Padrón, C., Siverio, F., Pérez-Sierra, A. & Rodríguez, A. (2018) Isolation and pathogenicity of Phytophthora species and Phytopythium vexans recovered from avocado orchards in the Canary Islands, including Phytophthora niederhauserii as a new pathogen of avocado. *Phytopathologia Mediterranea*, 57, 89–106. https://doi.org/10.14601/PHYTOPATHOL_MEDITERR-22022.

Rolando, C., Gaskin, R., Horgan, D., Williams, N. & Bader, M.K.-F. (2014) The use of adjuvants to improve uptake of phosphorous acid applied to Pinus radiata needles for control of foliar Phytophthora diseases. *New Zealand Journal of Forestry Science*, 44, 8. https://doi.org/10.1186/s40490-014-0008-5.

Romano, N. & Macino, G. (1992) Quelling: transient inactivation of gene expression in Neurospora crassa by transformation with homologous sequences. *Molecular Microbiology*, 6, 3343–3353. https://doi.org/10.1111/j.1365-2958.1992.tb02202.x.

Romero-Rodríguez, M.C., Archidona-Yuste, A., Abril, N., Gil-Serrano, A.M., Meijón, M. & Jorrín-Novo, J. V. (2018) Germination and early seedling development in quercus ilex recalcitrant and non-dormant seeds: Targeted transcriptional, hormonal, and sugar analysis. *Frontiers in Plant Science*, 871, 403376. https://doi.org/10.3389/FPLS.2018.01508/BIBTEX.

Rothstein, S.J., DiMaio, J., Strand, M. & Rice, D. (1987) Stable and heritable inhibition of the expression of nopaline synthase in tobacco expressing antisense RNA. *Proceedings of the National Academy of Sciences*, 84, 8439–8443. https://doi.org/10.1073/pnas.84.23.8439.

Ruiz Gómez, F.J., Pérez-de-Luque, A., Sánchez-Cuesta, R., Quero, J.L. & Navarro Cerrillo, R.M. (2018) Differences in the Response to Acute Drought and Phytophthora cinnamomi Rands Infection in Quercus ilex L. Seedlings. *Forests*, 9, 634. https://doi.org/10.3390/f9100634.

Ruiz-Jiménez, L., Polonio, Á., Vielba-Fernández, A., Pérez-García, A. & Fernández-Ortuño, D. (2021) Gene mining for conserved, non-annotated proteins of podosphaera xanthii identifies novel target candidates for controlling powdery mildews by spray-induced gene silencing. *Journal of Fungi*, 7. https://doi.org/10.3390/jof7090735.

Saito, H., Sakata, N., Ishiga, T. & Ishiga, Y. (2022) Efficacy of RNA-spray-induced silencing of Phakopsora pachyrhizi chitin synthase genes to control soybean rust. *Journal of General Plant Pathology*, 88, 203–206. https://doi.org/10.1007/S10327-022-01061-W/FIGURES/2.

Sakamoto, J.M. & Gordon, T.R. (2006) Factors influencing infection of mechanical wounds by *Fusarium circinatum* on Monterey pines (*Pinus radiata*). *Plant Pathology*, 55, 130–136. https://doi.org/10.1111/j.1365-3059.2005.01310.x.

Sambrook, J. & Russell, D.W. (2006) Preparation and Transformation of Competent E. coli Using Calcium Chloride . *Cold Spring Harbor Protocols*, 2006, pdb.prot3932. https://doi.org/10.1101/PDB.PROT3932.

Sampaio e Paiva Camilo-Alves, C. de, Clara, M.I.E. da & Almeida Ribeiro, N.M.C. de (2013) Decline of Mediterranean oak trees and its association with Phytophthora cinnamomi: A review. *European Journal of Forest Research*, 132, 411–432.

Sánchez, F., Rodríguez, R., Rojo, A., Álvarez, J.G., López, C., Gorgoso, J., *et al.* (2003) Crecimiento y tablas de producción de Pinus radiata D. Don en Galicia. *Agrar.: Sist. Recur. For*, 12, 65–83.

Sánchez-Cuesta, R., Ruiz-Gómez, F.J., Duque-Lazo, J., González-Moreno, P. & Navarro-Cerrillo, R.M. (2021) The environmental drivers influencing spatio-temporal dynamics of oak defoliation and mortality in dehesas of Southern Spain. *Forest Ecology and Management*, 485, 118946. https://doi.org/10.1016/J.FORECO.2021.118946.

Schneider, C.A., Rasband, W.S. & Eliceiri, K.W. (2012) NIH Image to ImageJ: 25 years of image analysis. *Nature Methods 2012 9:7*, 9, 671–675. https://doi.org/10.1038/nmeth.2089.

Scott, P.M. (2014) Phytophthora diseases in New Zealand forests. *NZ Journal of Forestry*, 59, 14–21.

Šečić, E. & Kogel, K.H. (2021) Requirements for fungal uptake of dsRNA and gene silencing in RNAi-based crop protection strategies. *Current Opinion in Biotechnology*, 70, 136–142. https://doi.org/10.1016/J.COPBIO.2021.04.001.

Sena, K., Crocker, E., Vincelli, P. & Barton, C. (2018) Phytophthora cinnamomi as a driver of forest change: Implications for conservation and management. *Forest Ecology and Management*, 409, 799–807.

Seringhaus, M., Paccanaro, A., Borneman, A., Snyder, M. & Gerstein, M. (2006) Predicting essential genes in fungal genomes. *Genome Research*, 16, 1126–1135. https://doi.org/10.1101/GR.5144106.

Serrano, M.S., Fernández-Rebollo, P., Vita, P. De, Carbonero, M.D. & Sánchez, M.E. (2011) The role of yellow lupin (Lupinus luteus) in the decline affecting oak agroforestry ecosystems. *Forest Pathology*, 41, 382–386. https://doi.org/10.1111/j.1439-0329.2010.00694.x.

Serrano, Y., Iturritxa, E., Elvira-Recuenco, M. & Raposo, R. (2017) Survival of Fusarium circinatum in soil and Pinus radiata needle and branch segments. *Plant Pathology*, 66, 934–940. https://doi.org/10.1111/PPA.12648.

Shabalina, S.A. & Koonin, E. V. (2008) Origins and evolution of eukaryotic RNA interference. *Trends in ecology & evolution*, 23, 578. https://doi.org/10.1016/J.TREE.2008.06.005.

Shapira, R., Choi, G.H. & Nuss, D.L. (1991) Virus-like genetic organization and expression strategy for a double-stranded RNA genetic element associated with biological control of chestnut blight. *The EMBO Journal*, 10, 731–739. https://doi.org/10.1002/j.1460-2075.1991.tb08004.x.

Shearer, B.L. & Crane, C.E. (2009) Influence of site and rate of low-volume aerial phosphite spray on lesion development of Phytophthora cinnamomi and phosphite persistence in Lambertia inermis var. inermis and Banksia grandis. *Australasian Plant Pathology*, 38, 288. https://doi.org/10.1071/AP09005.

Shvidenko, A., Barber, C.V., Lead, R.P., Gonzalez, P., Hassan, R., Lakyda, P., *et al.* (2005) Forest and Woodland Systems. In: Hassan, R.; S.R., A.N. (Ed.) Ecosystems and human well-being: current state and trends. Washington: Island Press.

Sicard, A., Zeilinger, A.R., Vanhove, M., Schartel, T.E., Beal, D.J., Daugherty, M.P., *et al.* (2025) Xylella fastidiosa: Insights into an Emerging Plant Pathogen. *Annual Review of Phytopathology Downloaded from www.annualreviews.org. Guest*, 8, 0. https://doi.org/10.1146/annurev-phyto-080417.

Sigova, A., Rhind, N. & Zamore, P.D. (2004a) A single Argonaute protein mediates both transcriptional and posttranscriptional silencing in Schizosaccharomyces pombe. *Genes & Development*, 18, 2359–2367. https://doi.org/10.1101/gad.1218004.

Sniezko, R.A., Koch, J., Liu, J.-J. & Romero-Severson, J. (2023) Will Genomic Information Facilitate Forest Tree Breeding for Disease and Pest Resistance? *Forests*, 14, 2382. https://doi.org/10.3390/f14122382.

Son, H., Ran, A., 2¤, P., Lim, J.Y., Shin, C. & Lee, Y.-W. (2017) Genome-wide exonic small interference RNA-mediated gene silencing regulates sexual reproduction in the homothallic fungus Fusarium graminearum. *PLoS Genetics*, 13, e1006595. https://doi.org/10.1371/journal.pgen.1006595.

Song, X.S., Gu, K.X., Duan, X.X., Xiao, X.M., Hou, Y.P., Duan, Y.B., *et al.* (2018a) A myosin5 dsRNA that reduces the fungicide resistance and pathogenicity of Fusarium asiaticum. *Pesticide Biochemistry and Physiology*, 150, 1–9. https://doi.org/10.1016/j.pestbp.2018.07.004.

Song, X.S., Gu, K.X., Duan, X.X., Xiao, X.M., Hou, Y.P., Duan, Y.B., *et al.* (2018b) Secondary amplification of siRNA machinery limits the application of spray-induced gene silencing. *Molecular Plant Pathology*, 19, 2543–2560. https://doi.org/10.1111/MPP.12728.

Sturm, Á., Saskoï, É., Tibor, K., Weinhardt, N. & Vellai, T. (2018) Highly efficient RNAi and Cas9-based auto-cloning systems for C. elegans research. *Nucleic Acids Research*, 46, e105–e105. https://doi.org/10.1093/NAR/GKY516.

Sturrock, R.N., Frankel, S.J., Brown, A. V., Hennon, P.E., Kliejunas, J.T., Lewis, K.J., *et al.* (2011) Climate change and forest diseases. *Plant Pathology*, 60, 133–149. https://doi.org/10.1111/j.1365-3059.2010.02406.x.

Sun, Q., Choi, G.H. & Nuss, D.L. (2009) A single Argonaute gene is required for induction of RNA silencing antiviral defense and promotes viral RNA recombination. *Proceedings of the National Academy of Sciences of the United States of America*, 106, 17927–17932. https://doi.org/10.1073/PNAS.0907552106/SUPPL_FILE/0907552106SI.PDF.

Sundaresha, S., Sharma, S., Bairwa, A., Tomar, M., Kumar, R., Bhardwaj, V., *et al*. (2022). Spraying of dsRNA molecules derived from Phytophthora infestans, along with nanoclay carriers as a proof of concept for developing novel protection strategy for potato late blight. *Pest management science*, *78*, 3183-3192. https://doi.org/10.1002/ps.6949.

Swett, C.L. & Gordon, T.R. (2009) Colonization of corn (Zea mays) by the pitch canker pathogen, Fusarium circinatum: Insights into the evolutionary history of a pine pathogen. *Phytopathology*, 99, 126–127.

Swett, C.L. & Gordon, T.R. (2015) Endophytic association of the pine pathogen Fusarium circinatum with corn (Zea mays). *Fungal Ecology*, 13, 120–129. https://doi.org/10.1016/j.funeco.2014.09.003.

Swett, C.L. & Gordon, T.R. (2012) First Report of Grass Species (Poaceae) as Naturally Occurring Hosts of the Pine Pathogen Gibberella circinata. *Plant disease*, 96, 908.

Swett, C.L., Porter, B., Fourie, G., Steenkamp, E.T., Gordon, T.R. & Wingfield, M.J. (2014) Association of the pitch canker pathogen Fusarium circinatum with grass hosts in commercial pine production areas of South Africa. *Southern Forests: a Journal of Forest Science*, 76, 161–166. https://doi.org/https://doi.org/10.2989/20702620.2014.916087.

Tabara, H., Grishok, A. & Mello, C.C. (1998) RNAi in C. elegans: Soaking in the Genome Sequence. *Science*, 282, 430–431. https://doi.org/10.1126/science.282.5388.430.

Tang, X., Jiang, X., Chen, Q. & Lin, X. (2024) Amphiphilic layered double hydroxides enhance plant-mediated delivery of dsRNAs to phloem-feeding planthoppers. *Chemical Engineering Journal*, 491, 151953. https://doi.org/10.1016/j.cej.2024.151953.

Taning, C.N., Arpaia, S., Christiaens, O., Dietz-Pfeilstetter, A., Jones, H., Mezzetti, B., *et al.* (2020) RNA-based biocontrol compounds: current status and perspectives to reach the market. *Pest Management Science*, 76, 841–845. https://doi.org/10.1002/ps.5686.

Teichert, S., Wottawa, M., Schönig, B. & Tudzynski, B. (2006) Role of the Fusarium fujikuroi TOR kinase in nitrogen regulation and secondary metabolism. *Eukaryotic Cell*, 5, 1807–1819. https://doi.org/10.1128/EC.00039-06/FORMAT/EPUB.

Tenllado, F., Martínez-García, B., Vargas, M. & Díaz-Ruíz, J.R. (2003) Crude extracts of bacterially expressed dsRNA can be used to protect plants against virus infections. *BMC Biotechnology*, 3, 3. https://doi.org/10.1186/1472-6750-3-3.

Thines, M. (2014) Phylogeny and evolution of plant pathogenic oomycetes-a global overview. *European Journal of Plant Pathology*, 138, 431–447. https://doi.org/10.1007/s10658-013-0366-5.

Timmons, L., Court, D.L. & Fire, A. (2001) Ingestion of bacterially expressed dsRNAs can produce specific and potent genetic interference in Caenorhabditis elegans. *Gene*, 263, 103–112. https://doi.org/10.1016/S0378-1119(00)00579-5.

Timmons, L. & Fire, A. (1998) Specific interference by ingested dsRNA. *Nature*, 395, 854–854. https://doi.org/10.1038/27579.

Tretiakova, P., Voegele, R.T., Soloviev, A. & Link, T.I. (2022) Successful Silencing of the Mycotoxin Synthesis Gene TRI5 in Fusarium culmorum and Observation of Reduced Virulence in VIGS and SIGS Experiments. *Genes*, 13, 395. https://doi.org/10.3390/GENES13030395/S1.

Valli, A.A., Santos, B.A.C.M., Hnatova, S., Bassett, A.R., Molnar, A., Chung, B.Y., *et al.* (2016) Most microRNAs in the single-cell alga Chlamydomonas reinhardtii are produced by Dicer-like 3-mediated cleavage of introns and untranslated regions of coding RNAs. *Genome Research*, 26, 519–529. https://doi.org/10.1101/GR.199703.115.

Vangalis, V., Markakis, E.A., Knop, M., Pietro, A. Di, Typas, M.A. & Papaioannou, I.A. (2023) Components of TOR and MAP kinase signaling control chemotropism and pathogenicity in the fungal pathogen Verticillium dahliae. *Microbiological research*, 271. https://doi.org/10.1016/J.MICRES.2023.127361.

Vannini, A., Natili, G., Thomidis, T., Belli, C. & Morales-Rodríguez, C. (2021) Anthropogenic and landscape features are associated with ink disease impact in Central Italy. *Forest Pathology*, 51, e12722.

Vasiliauskas, R., Larsson, E., Larsson, K.-H. & Stenlid, J. (2005) Persistence and long-term impact of Rotstop biological control agent on mycodiversity in Picea abies stumps. *Biological Control*, 32, 295–304. https://doi.org/10.1016/j.biocontrol.2004.10.008.

Vettraino, A.M., Morel, O., Perlerou, C., Robin, C., Diamandis, S. & Vannini, A. (2005) Occurrence and distribution of Phytophthora species in European chestnut stands, and their association with Ink Disease and crown decline. *European Journal of Plant Pathology*.

Vetukuri, R.R., Åsman, A.K.M., Tellgren-Roth, C., Jahan, S.N., Reimegård, J., Fogelqvist, J., *et al.* (2012) Evidence for Small RNAs Homologous to Effector-Encoding Genes and Transposable Elements in the Oomycete Phytophthora infestans. *PLOS ONE*, 7, e51399. https://doi.org/10.1371/JOURNAL.PONE.0051399.

Vetukuri, R.R., Avrova, A.O., Grenville-Briggs, L.J., West, P. Van, Söderbom, F., Savenkov, E.I., *et al.* (2011) Evidence for involvement of Dicer-like, Argonaute and histone deacetylase proteins in gene silencing in Phytophthora infestans. *Molecular Plant Pathology*, 12, 772–785. https://doi.org/10.1111/J.1364-3703.2011.00710.X.

Vickers, T.A., Koo, S., Bennett, C.F., Crooke, S.T., Dean, N.M. & Baker, B.F. (2003) Efficient reduction of target RNAs by small interfering RNA and RNase H-dependent antisense agents. A comparative analysis. *Journal of Biological Chemistry*, 278, 7108–7118. https://doi.org/10.1074/jbc.M210326200.

Wang, H., Zhang, X., Liu, J., Kiba, T., Woo, J., Ojo, T., *et al.* (2011) Deep sequencing of small RNAs specifically associated with Arabidopsis AGO1 and AGO4 uncovers new AGO functions. *Plant Journal*, 67, 292–304. https://doi.org/10.1111/j.1365-313X.2011.04594.x.

Wang, J., Wu, M., Wang, B. & Han, Z. (2013) Comparison of the RNA interference effects triggered by dsRNA and siRNA in Tribolium castaneum. *Pest management science*, 69, 781–786. https://doi.org/10.1002/PS.3432.

Wang, M. & Dean, R.A. (2020) Movement of small RNAs in and between plants and fungi. *Molecular Plant Pathology*, 21, 589–601. https://doi.org/10.1111/mpp.12911.

Wang, M. & Jin, H. (2017) Spray-Induced Gene Silencing: a Powerful Innovative Strategy for Crop Protection. *Trends in Microbiology*, 25, 4–6. https://doi.org/10.1016/j.tim.2016.11.011.

Wang, M., Weiberg, A., Dellota, E., Yamane, D. & Jin, H. (2017) Botrytis small RNA Bc-siR37 suppresses plant defense genes by cross-kingdom RNAi. *RNA Biology*, 14, 421–428. https://doi.org/10.1080/15476286.2017.1291112.

Wang, M., Weiberg, A., Lin, F.M., Thomma, B.P.H.J., Huang, H. Da & Jin, H. (2016) Bidirectional cross-kingdom RNAi and fungal uptake of external RNAs confer plant protection. *Nature Plants 2016 2:10*, 2, 1–10. https://doi.org/10.1038/nplants.2016.151.

Wang, S., He, B., Wu, H., Cai, Q., Ramírez-Sánchez, O., Abreu-Goodger, C., *et al.* (2024) Plant mRNAs move into a fungal pathogen via extracellular vesicles to reduce infection. *Cell Host & Microbe*, 32, 93-105.e6. https://doi.org/10.1016/j.chom.2023.11.020.

Wang, W., Liu, X. & Govers, F. (2021) The mysterious route of sterols in oomycetes. *PLoS Pathogens*, 17. https://doi.org/10.1371/JOURNAL.PPAT.1009591.

Wang, W., Zhang, F., Zhang, S., Xue, Z., Xie, L., Govers, F., *et al.* (2022) Phytophthora capsici sterol reductase PcDHCR7 has a role in mycelium development and pathogenicity. https://doi.org/10.1098/rsob.210282.

Wang, Y., Yan, Q., Lan, C., Tang, T., Wang, K., Shen, J., *et al.* (2023a) Nanoparticle carriers enhance RNA stability and uptake efficiency and prolong the protection against Rhizoctonia solani. *Phytopathology Research*, 5, 1–11. https://doi.org/10.1186/s42483-023-00157-1.

Wang, Z., Li, Yu, Zhang, Borui, Gao, Xiang, Shi, Mengru, Zhang, Sicong, *et al.* (2023b) Functionalized Carbon Dot-Delivered RNA Nano Fungicides as Superior Tools to Control Phytophthora Pathogens through Plant RdRP1 Mediated Spray-Induced Gene Silencing. https://doi.org/10.1002/adfm.202213143.

Wang, Z.G., Chen, R.Y., Jiang, Y.K., Wang, Z.W., Wang, J.J. & Niu, J. (2023c) Investigation of potential non-target effects to a ladybeetle Propylea japonica in the scenario of RNAi-based pea aphid control. *Entomologia Generalis*, 43, 79. https://doi.org/10.1127/ENTOMOLOGIA/2022/1748.

Waring, K.M. & O'Hara, K.L. (2005) Silvicultural strategies in forest ecosystems affected by introduced pests. *Forest Ecology and Management*, 209, 27–41. https://doi.org/10.1016/j.foreco.2005.01.008.

Waterhouse, A., Bertoni, M., Bienert, S., Studer, G., Tauriello, G., Gumienny, R., *et al.* (2018) SWISS-MODEL: Homology modelling of protein structures and complexes. *Nucleic Acids Research*, 46, W296–W303. https://doi.org/10.1093/nar/gky427.

Watson, J.E.M., Evans, T., Venter, O., Williams, B., Tulloch, A., Stewart, C., *et al.* (2018) The exceptional value of intact forest ecosystems. *Nature Ecology & Evolution 2018 2:4*, 2, 599–610. https://doi.org/10.1038/s41559-018-0490-x.

Watt, M.S., Kriticos, D.J., Alcaraz, S., Brown, A. V. & Leriche, A. (2009) The hosts and potential geographic range of Dothistroma needle blight. *Forest Ecology and Management*, 257, 1505–1519. https://doi.org/10.1016/j.foreco.2008.12.026.

Wei, K.F., Wu, L.J., Chen, J., Chen, Y.F. & Xie, D.X. (2012) Structural Evolution and Functional Diversification Analyses of Argonaute Protein. *J. Cell. Biochem*, 113, 2576–2585. https://doi.org/10.1002/jcb.24133.

Weiberg, A., Wang, M., Lin, F.M., Zhao, H., Zhang, Z., Kaloshian, I., *et al.* (2013) Fungal Small RNAs Suppress Plant Immunity by Hijacking Host RNA Interference Pathways. *Science*, 342, 118–123. https://doi.org/10.1126/science.1239705.

Werner, B.T., Gaffar, F.Y., Schuemann, J., Biedenkopf, D. & Koch, A.M. (2020) RNA-Spray-Mediated Silencing of Fusarium graminearum AGO and DCL Genes Improve Barley Disease Resistance. *Frontiers in Plant Science*, 11, 483792. https://doi.org/10.3389/FPLS.2020.00476/BIBTEX.

Westerhout, E.M. & Berkhout, B. (2007) A systematic analysis of the effect of target RNA structure on RNA interference. *Nucleic Acids Research*, 35, 4322–4330. https://doi.org/10.1093/NAR/GKM437.

Westlund, A. & Nohrstedt, H.-Ö. (2000) Effects of Stump-treatment Substances for Root-rot Control on Ground Vegetation and Soil Properties in a *Picea abies* forest in Sweden. *Scandinavian Journal of Forest Research*, 15, 550–560. https://doi.org/10.1080/028275800750173519.

Whangbo, J.S. & Hunter, C.P. (2008) Environmental RNA interference. *Trends in Genetics*, 24, 297–305. https://doi.org/10.1016/j.tig.2008.03.007.

Whisson, S.C., Avrova, A.O., West, P. Van & Jones, J.T. (2005) A method for double-stranded RNA-mediated transient gene silencing in Phytophthora infestans. *Molecular Plant Pathology*, 6, 153–163. https://doi.org/10.1111/J.1364-3703.2005.00272.X.

Wilson, R.C. & Doudna, J.A. (2013) Molecular Mechanisms of RNA Interference. *Annual Review of Biophysics*, 42, 217–239. https://doi.org/10.1146/annurev-biophys-083012-130404.

Wingfield, M.J., Hammerbacher, A., Ganley, R.J., Steenkamp, E.T., Gordon, T.R., Wingfield, B.D., *et al.* (2008) Pitch canker caused by Fusarium circinatum - A growing threat to pine plantations and forests worldwide. *Australasian Plant Pathology*, 37, 319–334. https://doi.org/10.1071/AP08036/METRICS.

Wise, J. C., Wise, A. G., Rakotondravelo, M., Vandervoort, C., Seeve, C., & Fabbri, B. (2022). Trunk injection delivery of dsRNA for RNAi-based pest control in apple trees. *Pest Management Science*, 78, 3528-3533. https://doi.org/10.1002/ps.6993.

Woodward, S., Amin, H., Martín-García, J., Solla, A., Díaz-Vázquez, C., Romeralo, C., *et al.* (2025) Host-Pathogen Interactions in the Pine-Fusarium circinatum Pathosystem and the Potential for Resistance Deployment in the Field. *Forest Pathology*, 55, e70020. https://doi.org/10.1111/efp.70020.

Wytinck, N., Manchur, C.L., Li, V.H., Whyard, S. & Belmonte, M.F. (2020) dsRNA Uptake in Plant Pests and Pathogens: Insights into RNAi-Based Insect and Fungal Control Technology. *Plants*, 9, 1780. https://doi.org/10.3390/plants9121780.

Xie, H., Li, B., Chang, Y., Hou, X., Zhang, Y., Guo, S., *et al.* (2021) Selection and Validation of Reference Genes for RT-qPCR Analysis in Spinacia oleracea under Abiotic Stress. *BioMed research international*, 2021. https://doi.org/10.1155/2021/4853632.

Xu, X., Jiao, Y., Shen, L., Li, Y., Mei, Y., Yang, W., *et al.* (2023) Nanoparticle-dsRNA Treatment of Pollen and Root Systems of Diseased Plants Effectively Reduces the Rate of Tobacco Mosaic Virus in Contemporary Seeds. *ACS Applied Materials & Interfaces*, 15, 29052–29063. https://doi.org/10.1021/acsami.3c02798.

Xu, Y. Bin, Li, H.P., Zhang, J.B., Song, B., Chen, F.F., Duan, X.J., *et al.* (2010) Disruption of the chitin synthase gene CHS1 from Fusarium asiaticum results in an altered structure of cell walls and reduced virulence. *Fungal Genetics and Biology*, 47, 205–215. https://doi.org/10.1016/J.FGB.2009.11.003.

Yan, S., Ren, B., Zeng, B., & Shen, J. (2020). Improving RNAi efficiency for pest control in crop species. *BioTechniques*, 68, 283-290. https://doi.org/10.2144/btn-2019-0171.

Yang, C., Hamel, C., Vujanovic, V. & Gan, Y. (2011) Fungicide: Modes of Action and Possible Impact on Nontarget Microorganisms. *ISRN Ecology*, 2011, 1–8. https://doi.org/10.5402/2011/130289.

Yang, P., Yi, S.Y., Nian, J.N., Yuan, Q.S., He, W.J., Zhang, J.B., *et al.* (2021a) Application of Double-Strand RNAs Targeting Chitin Synthase, Glucan Synthase, and Protein Kinase Reduces Fusarium graminearum Spreading in Wheat. *Frontiers in Microbiology*, 12, 660976. https://doi.org/10.3389/FMICB.2021.660976/BIBTEX.

Yang, X., Jiang, X., Yan, W., Huang, Q., Sun, H., Zhang, X., *et al.* (2021b) The Mevalonate Pathway Is Important for Growth, Spore Production, and the Virulence of Phytophthora sojae. *Frontiers in microbiology*, 12. https://doi.org/10.3389/FMICB.2021.772994.

Ye, X., Paroo, Z. & Liu, Q. (2007) Functional anatomy of the Drosophila microRNA-generating enzyme. *Journal of Biological Chemistry*, 282, 28373–28378. https://doi.org/10.1074/jbc.M705208200.

Yoon, J., Fang, M., Lee, D., Park, M., Kim, K.H. & Shin, C. (2021) Double-stranded RNA confers resistance to pepper mottle virus in Nicotiana benthamiana. *Applied Biological Chemistry*, 64. https://doi.org/10.1186/S13765-020-00581-3.

Younessi-Hamzekhanlu, M. & Gailing, O. (2022) Genome-Wide SNP Markers Accelerate Perennial Forest Tree Breeding Rate for Disease Resistance through Marker-Assisted and Genome-Wide Selection. *International Journal of Molecular Sciences*, 23, 12315. https://doi.org/10.3390/ijms232012315.

Yu, F., Gu, Q., Yun, Y., Yin, Y., Xu, J.R., Shim, W.B., *et al.* (2014) The TOR signaling pathway regulates vegetative development and virulence in Fusarium graminearum. *New Phytologist*, 203, 219–232. https://doi.org/10.1111/NPH.12776.

Yu, R., Huo, L., Huang, H., Yuan, Y., Gao, B., Liu, Y., *et al.* (2022) Early detection of pine wilt disease tree candidates using time-series of spectral signatures. *Frontiers in Plant Science*, 13. https://doi.org/10.3389/fpls.2022.1000093.

Yu, R., Luo, Y., Li, H., Yang, L., Huang, H., Yu, L., *et al.* (2021) Three-Dimensional Convolutional Neural Network Model for Early Detection of Pine Wilt Disease Using UAV-Based Hyperspectral Images. *Remote Sensing*, 13, 4065. https://doi.org/10.3390/rs13204065.

Zamora, P., Martín, A.B., San Martín, R., Martínez-Álvarez, P. & Diez, J.J. (2014) Control of chestnut blight by the use of hypovirulent strains of the fungus Cryphonectria parasitica in northwestern Spain. *Biological Control*, 79, 58–66. https://doi.org/10.1016/j.biocontrol.2014.08.005.

Zamora-Ballesteros, C., Diez, J.J., Martín-García, J., Witzell, J., Solla, A., Ahumada, R., *et al.* (2019) Pine Pitch Canker (PPC): Pathways of Pathogen Spread and Preventive Measures. *Forests*, 10, 1158. https://doi.org/10.3390/f10121158.

Zamora-Ballesteros, C., Martín-García, J., Fernández-Fernández, M.M. & Diez, J.J. (2022) Pine pitch canker (PPC): An introduction, an overview. https://doi.org/10.1016/B978-0-323-85042-1.00005-7.

Zamora-Ballesteros, C., Pinto, G., Amaral, J., Valledor, L., Alves, A., Diez, J.J., *et al.* (2021) Dual rna-sequencing analysis of resistant (Pinus pinea) and susceptible (pinus radiata) hosts during fusarium circinatum challenge. *International Journal of Molecular Sciences*, 22. https://doi.org/10.3390/ijms22105231.

Zamora-Ballesteros, C., Wingfield, B.D., Wingfield, M.J., Martín-García, J. & Diez, J.J. (2020) Residual Effects Caused by a Past Mycovirus Infection in Fusarium circinatum. *Forests*, 12, 11. https://doi.org/10.3390/f12010011.

Zand Karimi, H., Baldrich, P., Rutter, B.D., Borniego, L., Zajt, K.K., Meyers, B.C., *et al.* (2022) Arabidopsis apoplastic fluid contains sRNA- and circular RNA–protein complexes that are located outside extracellular vesicles. *The Plant Cell*, 34, 1863–1881. https://doi.org/10.1093/plcell/koac043.

Zeglen, S., Pronos, J. & Merler, H. (2010) Silvicultural management of white pines in western North America. *Forest Pathology*, 40, 347–368. https://doi.org/10.1111/j.1439-0329.2010.00662.x.

Zhang, B., Yu, Q., Jia, C., Wang, Y., Xiao, C., Dong, Y., *et al.* (2015) The actin-related protein Sac1 is required for morphogenesis and cell wall integrity in Candida albicans. *Fungal Genetics and Biology*, 81, 261–270. https://doi.org/10.1016/j.fgb.2014.12.007.

Zhang, C. & Ruvkun, G. (2012) New insights into siRNA amplification and RNAi. *RNA Biology*, 9, 1045–1049. https://doi.org/10.4161/rna.21246.

Zhang, H., Kolb, F.A., Jaskiewicz, L., Westhof, E. & Filipowicz, W. (2004) Single processing center models for human Dicer and bacterial RNase III. *Cell*, 118, 57–68. https://doi.org/10.1016/j.cell.2004.06.017.

Zhang, K., Wei, J., Huff Hartz, K.E., Lydy, M.J., Moon, T.S., Sander, M., *et al.* (2020) Analysis of RNA Interference (RNAi) Biopesticides: Double-Stranded RNA (dsRNA) Extraction from Agricultural Soils and Quantification by RT-qPCR. *Cite This: Environ. Sci. Technol*, 54, 4902. https://doi.org/10.1021/acs.est.9b07781.

Zhang, S., Khalid, A.R., Guo, D., Zhang, J., Xiong, F. & Ren, M. (2021) TOR Inhibitors Synergistically Suppress the Growth and Development of Phytophthora infestans, a Highly Destructive Pathogenic Oomycete. *Frontiers in Microbiology*, 12, 596874. https://doi.org/10.3389/FMICB.2021.596874/FULL.

Zhang, T., Zhao, Y.L., Zhao, J.H., Wang, S., Jin, Y., Chen, Z.Q., *et al.* (2016) Cotton plants export microRNAs to inhibit virulence gene expression in a fungal pathogen. https://doi.org/10.1038/NPLANTS.2016.153.

Zheng, Y., Moorlach, B., Jakobs-Schönwandt, D., Patel, A., Pastacaldi, C., Jacob, S., *et al.* (2025) Exogenous dsRNA triggers sequence-specific RNAi and fungal stress responses to control Magnaporthe oryzae in Brachypodium distachyon. *Communications Biology*, 8, 121. https://doi.org/10.1038/s42003-025-07554-6.

Zimmermann, G.R., Lehár, J. & Keith, C.T. (2007) Multi-target therapeutics: when the whole is greater than the sum of the parts. *Drug Discovery Today*, 12, 34–42. https://doi.org/10.1016/J.DRUDIS.2006.11.008.

Żółciak, A., Sikora, K., Wrzosek, M., Damszel, M. & Sierota, Z. (2020) Why Does Phlebiopsis gigantea not Always Inhibit Root and Butt Rot in Conifers? *Forests*, 11, 129. https://doi.org/10.3390/f11020129.

Supplementary material

Table S1. Structural alignment analysis of compared proteins in *F. circinatum*. Low RMSD values and high MatchAlign scores indicate good structural similarity.

Alignment	RMSD	MatchAlign	Atoms aligned
FgDCL1 vs. FcDCL1b	0.270	4663.500	10064
FgDCL2 vs. FcDCL2	0.354	4182.500	9622
FgAGO1 vs. FcAGO1	0.780	2828.000	6205
FgAGO2 vs. FcAGO2	0.072	4270.000	7420
FgAGO1 vs. FcAGO3	33.304	1365.500	5868
FgAGO2 vs. PcAGO3	19.501	724.000	5525
FcAGO1 vs. FcAGO3	14.453	1487.500	6033
FcAGO3 vs. PcAGO3	12.066	764.000	5604
FgRdRP1 vs. FcRdRP1	0.235	7897.000	14362
FgRdRP2 vs. FcRdRP2	0.869	3758.000	7984
FgRdRP3 vs. FcRdRP3	0.400	4950.000	9385
FgRdRP5 vs. FcRdRP4	0.057	4432.000	8632

Table S2. Statistical summary corresponding to figure 24B

Centrality and dispersion estimations			
Treatment	**Relative lesion area**	**SD**	**SE**
FcCHS-dsRNA	0.66	0.42	0.05
FcPTP-dsRNA	0.67	0.49	0.07
FcVDS-dsRNA	0.58	0.68	0.07
Statistical analysis			
Comparison	**N**	**Mean diff**	**p-value**
FcCHS-dsRNA vs FC072V	62 vs 94	-0.43	<0.001
FcPTP-dsRNA vs FC072V	50 vs 94	-0.33	<0.001
FcVDS-dsRNA vs FC072V	93 vs 94	-0.37	<0.001

Table S3. Statistical summary corresponding to figure 24C

Centrality and dispersion estimations			
Treatment	**RQ**	**SD**	**SE**
FcCHS-dsRNA	0.37	0.26	0.11
FcPTP-dsRNA	0.40	0.26	0.11
FcVDS-dsRNA	0.47	0.22	0.11
Statistical analysis			
Comparison	**N**	**Mean diff**	**p-value**
FcCHS-dsRNA vs FC072V	6 vs 6	-0.63	0.015
FcPTP-dsRNA vs FC072V	6 vs 6	-0.59	0.015
FcVDS-dsRNA vs FC072V	4 vs 4	-0.53	0.06

Table S4. Centrality and dispersion estimations corresponding to figure 25

Week	Method	Treatment	count	mean	SD	median	IQR
2	Drop	Non-inoculated	5	0.00	0.00	0.00	0.00
2	Drop	FC072V	4	2.00	0.00	2.00	0.00
2	Drop	Mock control	5	2.00	1.00	2.00	2.00
2	Drop	FcCHS-dsRNA	5	2.00	0.71	2.00	0.00
2	Drop	FcPTP-dsRNA	5	1.40	0.55	1.00	1.00
2	Drop	FcVDS-dsRNA	5	1.60	0.55	2.00	1.00
2	Spray	Non-inoculated	5	0.00	0.00	0.00	0.00
2	Spray	FC072V	4	1.75	0.50	2.00	0.25
2	Spray	Mock control	5	1.40	0.55	1.00	1.00
2	Spray	FcCHS-dsRNA	5	1.20	0.45	1.00	0.00
2	Spray	FcPTP-dsRNA	5	2.00	0.71	2.00	0.00
2	Spray	FcVDS-dsRNA	5	1.60	0.55	2.00	1.00
2	Drop+Spray	Non-inoculated	5	0.00	0.00	0.00	0.00
2	Drop+Spray	FC072V	4	2.00	0.00	2.00	0.00
2	Drop+Spray	Mock control	5	2.40	0.55	2.00	1.00
2	Drop+Spray	FcCHS-dsRNA	5	0.60	0.55	1.00	1.00
2	Drop+Spray	FcPTP-dsRNA	5	1.60	0.55	2.00	1.00
2	Drop+Spray	FcVDS-dsRNA	5	1.20	0.45	1.00	0.00
3	Drop	Non-inoculated	5	0.00	0.00	0.00	0.00
3	Drop	FC072V	4	2.38	0.25	2.50	0.12
3	Drop	Mock control	5	2.40	0.42	2.50	0.50
3	Drop	FcCHS-dsRNA	5	2.30	0.76	2.50	1.50
3	Drop	FcPTP-dsRNA	5	2.40	0.82	2.00	1.00
3	Drop	FcVDS-dsRNA	5	2.10	0.55	2.00	0.00
3	Spray	Non-inoculated	5	0.00	0.00	0.00	0.00
3	Spray	FC072V	4	2.38	0.25	2.50	0.12
3	Spray	Mock control	5	2.00	0.35	2.00	0.00
3	Spray	FcCHS-dsRNA	5	2.00	0.71	2.50	1.00
3	Spray	FcPTP-dsRNA	5	2.40	0.65	2.50	1.00
3	Spray	FcVDS-dsRNA	5	2.10	0.42	2.00	0.50
3	Drop+Spray	Non-inoculated	5	0.00	0.00	0.00	0.00
3	Drop+Spray	FC072V	4	2.38	0.25	2.50	0.12
3	Drop+Spray	Mock control	5	2.30	0.27	2.50	0.50
3	Drop+Spray	FcCHS-dsRNA	5	1.40	0.42	1.50	0.50
3	Drop+Spray	FcPTP-dsRNA	5	2.40	0.42	2.50	0.50
3	Drop+Spray	FcVDS-dsRNA	5	1.90	0.42	2.00	0.50
4	Drop	Non-inoculated	5	0.00	0.00	0.00	0.00
4	Drop	FC072V	4	2.75	0.50	3.00	0.25
4	Drop	Mock control	5	2.70	0.27	2.50	0.50
4	Drop	FcCHS-dsRNA	5	2.60	0.74	2.50	0.50
4	Drop	FcPTP-dsRNA	5	2.90	0.65	2.50	0.50

4	Drop	FcVDS-dsRNA	5	2.40	0.55	2.50	0.00
4	Spray	Non-inoculated	5	0.00	0.00	0.00	0.00
4	Spray	FC072V	4	2.88	0.25	3.00	0.12
4	Spray	Mock control	5	2.50	0.35	2.50	0.00
4	Spray	FcCHS-dsRNA	5	2.40	0.82	3.00	1.50
4	Spray	FcPTP-dsRNA	5	2.60	0.74	2.50	0.50
4	Spray	FcVDS-dsRNA	5	2.30	0.45	2.00	0.50
4	Drop+Spray	Non-inoculated	5	0.00	0.00	0.00	0.00
4	Drop+Spray	FC072V	4	2.75	0.50	3.00	0.25
4	Drop+Spray	Mock control	5	2.50	0.35	2.50	0.00
4	Drop+Spray	FcCHS-dsRNA	5	1.80	0.27	2.00	0.50
4	Drop+Spray	FcPTP-dsRNA	5	2.60	0.55	2.50	0.00
4	Drop+Spray	FcVDS-dsRNA	5	2.10	0.42	2.00	0.50
5	Drop	Non-inoculated	5	0.00	0.00	0.00	0.00
5	Drop	FC072V	4	3.25	0.29	3.25	0.50
5	Drop	Mock control	5	3.20	0.27	3.00	0.50
5	Drop	FcCHS-dsRNA	5	2.90	0.42	3.00	0.50
5	Drop	FcPTP-dsRNA	5	3.20	0.57	3.00	0.50
5	Drop	FcVDS-dsRNA	5	3.30	0.84	3.50	1.00
5	Spray	Non-inoculated	5	0.00	0.00	0.00	0.00
5	Spray	FC072V	4	3.38	0.25	3.50	0.12
5	Spray	Mock control	5	2.80	0.27	3.00	0.50
5	Spray	FcCHS-dsRNA	5	3.20	0.91	3.50	1.50
5	Spray	FcPTP-dsRNA	5	3.20	0.57	3.00	0.50
5	Spray	FcVDS-dsRNA	5	3.20	0.45	3.00	0.00
5	Drop+Spray	Non-inoculated	5	0.00	0.00	0.00	0.00
5	Drop+Spray	FC072V	4	3.25	0.29	3.25	0.50
5	Drop+Spray	Mock control	5	3.10	0.42	3.00	0.50
5	Drop+Spray	FcCHS-dsRNA	5	2.50	0.35	2.50	0.00
5	Drop+Spray	FcPTP-dsRNA	5	3.30	0.57	3.50	0.50
5	Drop+Spray	FcVDS-dsRNA	5	2.90	0.42	3.00	0.50

Table S5. Statistical analysis corresponding to figure 25 (*p*-value)

Drop				
Treatment	**vsFC072V_Week2**	**vsFC072V_Week3**	**vsFC072V_Week4**	**vsFC072V_Week5**
Mock control	1.000	1.000	1.000	1.000
FcCHS-dsRNA	1.000	1.000	1.000	0.477
FcPTP-dsRNA	0.202	1.000	1.000	1.000
FcVDS-dsRNA	0.355	0.594	0.594	1.000
Treatment	**vsMock_Week2**	**vsMock_Week3**	**vsMock_Week4**	**vsMock_Week5**
FcCHS-dsRNA	0.576	0.914	1.000	0.385
FcPTP-dsRNA	0.547	0.914	1.000	1.000
FcVDS-dsRNA	0.576	0.469	0.604	1.000

Spray				
Treatment	**VsFC72V_Week2**	**vsFC072V_Week3**	**vsFC072V_Week4**	**vsFC072V_Week5**
Mock control	0.594	0.280	0.210	0.072
FcCHS-dsRNA	0.315	0.561	0.558	0.602
FcPTP-dsRNA	0.768	0.651	0.558	0.602
FcVDS-dsRNA	0.766	0.507	0.177	0.507
Treatment	**vsMock _Week2**	**vsMock_Week3**	**vsMock_Week4**	**vsMock_Week5**
FcCHS-dsRNA	0.901	1	1.000	1
FcPTP-dsRNA	1.000	1	1.000	1
FcVDS-dsRNA	1.000	1	0.651	1
Drop+spray				
Treatment	**vsFC072V_Week2**	**vsFC072V_Week3**	**vsFC072V_Week4**	**vsFC072V_Week5**
Mock control	0.936	0.766	0.359	0.687
FcCHS-dsRNA	0.026	0.046	0.072	0.061
FcPTP-dsRNA	0.237	0.766	0.359	0.687
FcVDS-dsRNA	0.051	0.174	0.147	0.358
Treatment	**vsMock_Week2**	**vsMock_Week3**	**vsMock_Week4**	**vsMock_Week5**
FcCHS-dsRNA	0.015	0.027	0.032	0.094
FcPTP-dsRNA	0.038	0.678	0.593	0.778
FcVDS-dsRNA	0.019	0.146	0.175	0.507

Table S6. Statistical summary corresponding to figure 26

Centrality and dispersion estimations					
Treatment	**Dpi**	**Mean**	**SD**	**Median**	**IQR**
Non-inoculated	25	0	0	0	0
FC072V	25	2.39	0.49	2.5	0.75
Mock control	25	2.54	0.57	2.5	1
FcCHS-dsRNA	25	1.49	0.77	1.5	1
FcPTP-dsRNA	25	1.67	0.80	2	1
FcVDS-dsRNA	25	2.01	0.84	2	1
Fcmix-dsRNA	25	1.80	0.80	2	1.5
Non-inoculated	35	0.00	0.00	0	0
FC072V	35	3.74	0.67	4	0.75
Mock control	35	3.77	0.61	4	0.5
FcCHS-dsRNA	35	2.90	0.57	3	0.75
FcPTP-dsRNA	35	3.07	0.73	3	0.5
FcVDS-dsRNA	35	3.21	0.85	3.5	1.37
Fcmix-dsRNA	35	3.24	0.72	3.5	0.5
Statistical analysis					
Comparison	**N**	**Mean diff**	**lwr.ci**	**upr.ci**	**p-value**
25 dpi FC072V vs Mock control	35 vs 35	0.16	-0.28	0.60	0.83
25 dpi FC072V vs FcCHS-dsRNA	35 vs 35	-0.90	-1.34	-0.46	2e-6
25 dpi FC072V vs FcPTP-dsRNA	35 vs 35	-0.71	-1.15	-0.28	0.0002
25 dpi FC072V vs FcVDS-dsRNA	35 vs 35	-0.37	-0.81	0.07	0.013

25 dpi FC072V vs Fcmix-dsRNA	35 vs 35	-0.59	-1.02	-0.15	0.004
25 dpi Mock vs FcCHS-dsRNA	35 vs 35	-1.06	-1.50	-0.62	2e-8
25 dpi Mock vs FcPTP-dsRNA	35 vs 35	-0.87	-1.31	-0.43	4.8e-6
25 dpi Mock vs FcVDS-dsRNA	35 vs 35	-0.53	-0.97	-0.09	0.013
25 dpi Mock vs Fcmix-dsRNA	35 vs 35	-0.74	-1.18	-0.30	0.0001
35 dpi FC072V vs Mock control	35 vs 35	0.03	-0.39	0.45	0.99
35 dpi FC072V vs FcCHS-dsRNA	35 vs 35	-0.84	-1.26	-0.42	3.9e-6
35 dpi FC072V vs FcPTP-dsRNA	35 vs 35	-0.67	-1.09	-0.25	0.0003
35 dpi FC072V vs FcVDS-dsRNA	35 vs 35	-0.54	-0.96	-0.11	0.007
35 dpi FC072V vs Fcmix-dsRNA	35 vs 35	-0.50	-0.92	-0.08	0.013
35 dpi Mock vs FcCHS-dsRNA	35 vs 35	-0.87	-1.29	-0.45	2.5e-6
35 dpi Mock vs FcPTP-dsRNA	35 vs 35	-0.70	-1.12	-0.28	0.0001
35 dpi Mock vs FcVDS-dsRNA	35 vs 35	-0.57	-0.99	-0.14	0.004
35 dpi Mock vs Fcmix-dsRNA	35 vs 35	-0.53	-0.95	-0.11	0.007

Table S7. Structural alignment analysis of compared proteins in *P. cinnamomi*. Low RMSD values and high MatchAlign scores indicate good structural similarity

Alignment	RMSD	MatchAlign	Atoms aligned
PiDCL1 vs. PcDCL1b	0.116	4887.000	8351
PiDCL2 vs. PcDCL2	0.021	3858.500	6906
PiAGO1 vs. PcAGO1	0.052	3954.500	6859
PiAGO3 vs. PcAGO3	0.367	4508.000	7170
PiAGO4 vs. PcAGO4	0.475	3645.500	6265
PiAGO5 vs. PcAGO5	0.672	3965.000	6352
PiRdRP1 vs. PcRdRP1	0.150	3303.500	5928

Table S8. Statistical summary corresponding to figure 32A

Application method	Treatment	count	mean	sd	se	t	p-value
(A) Soaking plant roots	PH2003	5	0.42	0.10	0.04	2.11	0.068
	PcDCL-dsRNA	5	0.24	0.17	0.08		
(B) Soaking P. cinnamomi	PH2003	5	0.47	0.05	0.02	0.85	0.422
	PcDCL-dsRNA	5	0.41	0.13	0.06		
(C) Spraying dsRNA	PH2003	5	0.36	0.12	0.06	0.02	0.983
	PcDCL-dsRNA	5	0.36	0.06	0.03		
(D) dsRNA solution diluted in hydroponic media	PH2003	5	0.49	0.19	0.09	1.20	0.265
	PcDCL-dsRNA	5	0.51	0.24	0.11		

Table S9. Statistical summary corresponding to figure 32B

Centrality and dispersion estimations				
Treatment	**count**	**mean**	**SD**	**SE**
Non- inoculated	11	0.00	0.00	0.00
PH2003	6	0.32	0.09	0.04
Mock control	11	0.28	0.20	0.06
PcDCL-dsRNA	12	0.16	0.18	0.05
PcDDS-dsRNA	12	0.19	0.18	0.05
PcPTP-dsRNA	12	0.13	0.14	0.04
Statistical analysis				
Treatment	**Wilcoxon statistic**	**Raw p-value**	**Holm-adjusted p-value**	**Significant**
PH2003 vs mock control	0.91	0.37	0.41	False
PH2003 vs PcDCL-dsRNA	1.87	0.06	0.18	False
PH2003 vs PcDDS-dsRNA	1.26	0.21	0.41	False
PH2003 vs PcPTP-dsRNA	2.44	0.02	0.06	False

Table S10. Statistical summary corresponding to figure 32C

Centrality and dispersion estimations				
Treatment	**Count**	**Mean**	**SD**	**SE**
Mock control	16	1.03	0.91	0.23
PcDCL-dsRNA	16	1.73	0.86	0.21
PcDDS-dsRNA	16	1.08	1.07	0.27
PcPTP-dsRNA	16	2.89	0.54	0.14
Statistical analysis				
Treatment	**Wilcoxon statistic**	**Raw p-value**	**Holm-adjusted p-value**	**Significant**
Mock control vs PcDCL-dsRNA	2.04	0.04	0.08	False
Mock control vs PcDDS-dsRNA	0.09	0.92	0.92	False
Mock control vs PcPTP-dsRNA	3.86	<0.001	<0.001	True

Table S11. Statistical summary corresponding to figure 34B

Centrality and dispersion					
Treatment	**dpi**	**Mean**	**SD**	**Median**	**IQR**
Non-inoculated	3	4.47	4.35	3.25	3.35
PH2003	3	69.58	30.26	84.91	56.09
Mock control	3	74.06	28.38	82.98	37.72
PcDCL-dsRNA	3	55.72	32.67	56.56	62.25
PcDDS-dsRNA	3	48.10	30.03	46.22	54.02
PcPTP-dsRNA	3	43.60	28.30	38.16	39.18
Statistical analysis					
comparison	**dpi**	**mediandiff**	**lwr.ci**	**upr.ci**	***p*-value**
Mock control vs PH2003	3	1.93	-37.44	13.83	0.66
PcDCL-dsRNA vs PH2003	3	28.35	-10.69	44.61	0.09
PcEDS-dsRNA vs PH2003	3	38.69	0.32	57.59	0.009
PcPTP-dsRNA vs PH2003	3	46.75	4.89	59.66	0.003

Table S12. Statistical summary corresponding to figure 34C

Centrality and dispersion				
Treatment	**Mean ΔΔCt vs PH2003**	**RQ**	**SD**	**transformed SE**
PH2003	0	1		
Mock control	0.68	0.62	3.13	0.18
PcDCL-dsRNA	3.34	0.10	1.29	0.06
PcDDS-dsRNA	2.96	0.13	2.40	0.05
PcPTP-dsRNA	1.92	0.26	2.47	0.10
Statistical analysis				
Comparison			**t**	**p-value**
Mock control vs PH2003			-2.13	0.166
PcDCL-dsRNA vs PH2003			-15.38	0.004
PcEDS-dsRNA vs PH2003			-17.75	0.003
PcPTP-dsRNA vs PH2003			-7.45	0.018